

Adaptations of small intestinal nutrient absorption during pregnancy in mice

Teunis Sebastian Overduin, BSc (Hons)

Robinson Research Institute,

Vagal Afferent Research Group, South Australian Health and Medical Research Institute,

And,

School of Biomedicine

Faculty of Health and Medical Sciences

University of Adelaide

South Australia

Thesis submitted to the University of Adelaide for fulfilment of the requirements for
admission to the degree of Doctor of Philosophy (PhD)

December 2023



THE UNIVERSITY
of ADELAIDE

Table of Contents

List of tables.....	8
List of figures.....	9
Abstract.....	11
Statement of Originality and Authenticity	13
Acknowledgements	14
List of abbreviations in text	16
Manuscripts arising from PhD	22
Work directly related to this thesis:	22
Other manuscripts published during PhD:.....	22
Conference abstracts arising from PhD.....	23
1. Chapter 1: introduction	24
1.1. Pregnancy.....	24
1.1.1. Overview.....	24
1.1.2. Weight gain.....	25
1.1.3. Maternal adaptations.....	27
1.1.4. Placental growth, development and function	28
1.1.5. Food intake	30
1.2. Importance of nutrition during pregnancy	33
1.2.1. Overview.....	33
1.2.2. Impacts of maternal global undernutrition during pregnancy	34
1.2.3. Over-nutrition, obesity and pregnancy outcomes	46
1.2.4. Excess carbohydrate intake	56
1.2.5. Excess lipid intake.....	59
1.2.6. Protein supplementation and excess protein intake in adequately and malnourished subjects.....	62
1.2.7. Low protein intake and protein restriction	68
1.2.8. Multi-factorial poor diet quality.....	72
1.2.9. Micronutrients	77

1.3.	Gastrointestinal tract	80
1.3.1.	Overview.....	80
1.3.2.	Gastric and SI anatomy.....	81
1.3.3.	Neural innervation of the upper GIT	87
1.3.3.1.	Intrinsic innervation: the enteric nervous system (ENS)	88
1.3.3.2.	Extrinsic innervation	89
1.3.3.3.	Vagal innervation	89
1.3.3.4.	Spinal innervation	90
1.3.4.	Small intestinal nutrient catabolism	91
1.4.	Nutrient absorption.....	92
1.4.1.	Overview.....	92
1.4.2.	Carbohydrates	93
1.4.3.	Amino acids	95
1.4.4.	Lipids	100
1.4.5.	Micronutrients	101
1.5.	Thesis Aims	105
2.	Chapter 2: Scoping review protocol.....	106
2.1.	Overview	106
2.2.	Statement of authorship - Adaptations in gastrointestinal nutrient absorption and its determinants during pregnancy in monogastric mammals: a scoping review protocol	107
2.3.	Abstract.....	109
2.4.	Introduction	109
2.5.	Review question:.....	111
2.6.	Inclusion criteria	111
2.6.1.	Participants	111
2.6.2.	Concept	111
2.6.3.	Context	112
2.6.4.	Types of studies.....	112
2.7.	Methods	112

2.7.1.	Search strategy.....	112
2.7.2.	Study selection.....	113
2.7.3.	Data extraction.....	113
2.7.4.	Data analysis and presentation	113
2.8.	Appendix I: Search strategy	114
2.9.	Appendix II: Data extraction instrument.....	115
3.	Chapter 3: Scoping review	116
3.1.	Overview	116
3.2.	Statement of authorship - Adaptations in gastrointestinal nutrient absorption and its determinants during pregnancy in monogastric mammals: a scoping review.....	117
3.3.	Abstract.....	119
3.4.	Introduction	119
3.5.	Methods	121
3.5.1.	Protocol and search strategy.....	121
3.5.2.	Eligibility criteria	121
3.5.3.	Study selection.....	121
3.5.4.	Data extraction and synthesis	122
3.6.	Results.....	122
3.6.1.	Characteristics of published literature.....	122
3.6.2.	Macronutrient uptake – carbohydrates	125
3.6.3.	Macronutrient uptake – amino acids.....	128
3.6.4.	Macronutrient uptake – lipids	128
3.6.5.	Micronutrient uptake – minerals	129
3.6.5.1.	Calcium.....	129
3.6.5.2.	Iron	130
3.6.5.3.	Zinc.....	130
3.6.5.4.	Others.....	130
3.6.6.	Micronutrient uptake – vitamins.....	131
3.6.6.1.	Vitamin B ₁₂	131

3.6.6.2.	Vitamin B ₉	131
3.6.7.	Gastric emptying	131
3.6.8.	Gastrointestinal and SI motility	133
3.6.9.	Whole SI anatomy.....	136
3.6.10.	Region-specific SI anatomy	137
3.6.11.	Nutrient transporter expression – macronutrients	139
3.6.11.1.	Carbohydrates	139
3.6.11.2.	Peptides and amino acids	139
3.6.11.3.	Lipids	139
3.6.12.	Nutrient transporter expression – micronutrients	140
3.6.12.1.	Calcium.....	140
3.6.12.2.	Iron	141
3.6.12.3.	Others.....	141
3.6.13.	Gallbladder emptying.....	148
3.6.14.	Expression and activity of digestive enzymes	150
3.6.14.1.	Carbohydrate digestion	150
3.6.14.2.	Protein digestion	152
3.6.14.3.	Others.....	152
3.7.	Discussion.....	153
3.8.	Supplementary table S3.1 – search string for each database.....	159
3.9.	Supplementary table S3.2 Main characteristics and key results for studies investigating changes in nutrient absorption and its determinants during pregnancy	162
4.	Chapter 4: Active glucose transport varies by small intestinal region and oestrous cycle stage in C57BL/6 mice	258
4.1.	Overview	258
4.2.	Statement of authorship - Active glucose transport varies by small intestinal region and oestrous cycle stage in C57BL/6 mice	259
4.3.	Abstract.....	261
4.4.	Introduction	262
4.5.	Materials and Methods	263

4.5.1.	Ethics approval	263
4.5.2.	Mice	263
4.5.3.	Tissue preparation and Ussing chamber conditions	263
4.5.4.	Study 1 - Region-specific glucose dose response	264
4.5.5.	Study 2 - SGLT1 inhibition	265
4.5.6.	Study 3 - Oestrous cycle	265
4.5.7.	Statistical analysis.....	265
4.6.	Results.....	266
4.6.1.	Study 1 – Region-specific glucose dose response	266
4.6.2.	Study 2 – SGLT1 inhibition.....	266
4.6.3.	Study 3 – Oestrous cycle	270
4.7.	Discussion.....	272
5.	Chapter 5: Differential changes in anatomical, molecular and functional determinants of intestinal glucose absorption during murine pregnancy	275
5.1.	Overview	275
5.2.	Statement of authorship - Differential changes in anatomical, molecular and functional determinants of intestinal glucose absorption during murine pregnancy ..	276
5.3.	Abstract.....	279
5.4.	Introduction	280
5.5.	Methods	281
5.5.1.	Ethics.....	281
5.5.2.	Study 1 – Animals	281
5.5.3.	Study 1 - Small intestine histology.....	282
5.5.4.	Study 1 – Gene expression	282
5.5.4.1.	Taqman assays.....	284
5.5.4.2.	SYBR green assays.....	284
5.5.5.	Study 2 – Animals	284
5.5.6.	Study 2 – <i>Ex vivo</i> active glucose transport	285
5.5.7.	Statistics	285
5.6.	Results.....	286

5.6.1.	Study 1 - mouse and SI characteristics	286
5.6.2.	Study 1 - SI morphology.....	286
5.6.3.	Study 1 - Nutrient transporter gene expression	289
5.6.3.1.	Carbohydrate transporters	289
5.6.3.2.	Amino acid transporters	291
5.6.3.3.	Fatty acid transporters	291
5.6.4.	Study 2 – mouse characteristics and SI gross morphology	294
5.6.5.	Study 2 - Active glucose transport.....	294
5.7.	Discussion.....	297
5.8.	Conclusion	300
6.	Chapter 6: general discussion	301
6.1.	Introduction	301
6.2.	Strengths, weaknesses and limitations of studies presented in this thesis	306
6.3.	Conclusion	307
	References	309
	Appendices	333
	Appendix 1 Adaptations in gastrointestinal nutrient absorption and its determinants during pregnancy in monogastric mammals: a scoping review protocol	333
	Appendix 2 Active glucose transport varies by intestinal region and oestrous cycle stage in mice	334
	Appendix 3 Endocrine disruptor compounds – a cause of impaired immune tolerance driving inflammatory disorders of pregnancy?.....	335

LIST OF TABLES

Table 1.1 Under-nutrition, low GWG and pregnancy outcomes: Evidence from human observational studies.....	36
Table 1.2 Pre-pregnancy low BMI and pregnancy outcomes: Evidence from human observational studies.....	42
Table 1.3 Global under-nutrition and pregnancy outcomes: Evidence from intervention-based animal studies.....	44
Table 1.4 High GWG and pregnancy outcomes: Evidence from human observational studies.....	47
Table 1.5 Pre-pregnancy high BMI and pregnancy outcomes: Evidence from human observational studies.....	51
Table 1.6 Global over-nutrition and pregnancy outcomes: Evidence from intervention studies in sheep.....	54
Table 1.7 Maternal high sugar (HS) diet consumption and pregnancy outcomes: Evidence from rodent models.....	57
Table 1.8 Maternal excess lipid (HF) diet consumption and pregnancy outcomes: Evidence from NHP and rodent models.....	60
Table 1.9 Dietary protein supplementation and pregnancy outcomes: Evidence from human intervention-based studies.....	63
Table 1.10 Dietary protein supplementation and pregnancy outcomes: Evidence from NHP and rodent models.....	66
Table 1.11 Dietary protein deficiency during pregnancy and adverse outcomes: Evidence from observational human studies.....	69
Table 1.12 Maternal protein restriction and pregnancy outcomes: Evidence from animal models (NHP, pig and rodent).....	70
Table 1.13 Maternal high fat-high sugar (HFHS) consumption and pregnancy outcomes: Evidence from NHPs and rodent models.....	74
Table 1.14 Dietary micronutrient deficiency and pregnancy outcomes: Evidence from observational human studies.....	78
Table 1.15 Human SI brush border and basolateral membrane amino acid transporters.....	98
Table 1.16 SI absorption of micronutrients and their associated transporters.....	102
Table 3.1 Expression of mineral micronutrient transporters during pregnancy.....	143
Supplementary table S3.1 Search string for each database.....	159
Supplementary table S3.2 Main characteristics and key results for studies investigating changes in nutrient absorption and its determinants during pregnancy.....	162
Table 5.1 Information for gene targets assessed by qRT-PCR study.....	283
Table 5.2 Study 1 mouse characteristics.....	287
Table 5.3 Study 2 mouse characteristics.....	295

LIST OF FIGURES

Figure 1.1 Changes in maternal, fetal and placental weight and food intake during pregnancy in humans and mice.....	26
Figure 1.2 Schematic representations of human and mouse placenta.....	29
Figure 1.3 Daily energy intake during pregnancy in humans, and food intake during pregnancy in mice and rats.....	32
Figure 1.4 Overview of the gastrointestinal tract and its individual components.....	80
Figure 1.5 Schematic representation of anatomical boundaries and transition zones along the SI axis in mice.....	83
Figure 1.6 Transverse schematic view of the duodenum.....	84
Figure 1.7 Region-specific villi length along the SI oral-aboral axis in humans, rats, mice and shrews.....	85
Figure 1.8 Abundance and distribution of different cell types in the SI epithelium.....	86
Figure 1.9 Satiety and incretin hormone release by enteroendocrine cells native to the SI epithelium.....	87
Figure 1.10 Gastric and SI vagal afferent innervation.....	89
Figure 1.11 Uptake of glucose and fructose by SI enterocytes.....	94
Figure 1.12 Brush border and basolateral membrane amino acid transport systems.....	96
Figure 1.13 Uptake of medium and long-chain fatty acids, monoglycerides and cholesterol by SI enterocytes.....	101
Figure 3.1 PRISMA flow diagram.....	123
Figure 3.2 Characteristics of published literature.....	124
Figure 3.3 <i>In vivo</i> glucose uptake during pregnancy.....	126
Figure 3.4 Changes in arterial and portal vein glucose following a meal test in dogs.....	128
Figure 3.5 Gastric emptying of liquids and solids during pregnancy.....	133
Figure 3.6 Changes in gastrointestinal motility during pregnancy.....	135
Figure 3.7 Changes in absolute SI wet weight and length during pregnancy.....	136
Figure 3.8 Changes in region-specific SI anatomy during pregnancy.....	138
Figure 3.9 Changes in gallbladder volume and emptying during human pregnancy.....	149
Figure 3.10 Changes in activity of carbohydrate-digesting enzymes sucrase, lactase and maltase during pregnancy in rat and pig.....	151
Figure 3.11 Changes in nutrient uptake and its determinants during pregnancy in monogastric mammals.....	154
Figure 4.1 Glucose dose-response.....	267
Figure 4.2 Glucose and carbachol responses to DMSO.....	268
Figure 4.3 Efficacy of SGLT1-antagonist phlorizin.....	269
Figure 4.4 Active glucose uptake varies across the oestrous cycle in mice.....	271

Figure 5.1 SI region-specific changes in morphology during pregnancy in mice.....	288
Figure 5.2 SI region-specific changes in relative transcript expression of carbohydrate transporters during pregnancy in mice.....	290
Figure 5.3 SI region-specific changes in relative transcript expression of amino acid transporters during pregnancy in mice.....	292
Figure 5.4 SI region-specific changes in relative transcript expression of fatty acid transporters during pregnancy in mice.....	293
Figure 5.5 SI region-specific changes in active glucose transport in late-pregnant and non-pregnant mice	296
Figure 6.1 Thesis graphical abstract.....	302

ABSTRACT

Mammalian pregnancy represents a natural state of increased maternal nutrient demand due to conceptus nutrient and energy requirements, and to prepare for lactation post parturition. To permit increased nutrient absorption, the maternal small intestine (SI), which is the main site of nutrient absorption, needs to adapt to permit increased nutrient absorption throughout pregnancy. However, the timing, size and regional localisation of SI adaptations are unclear. We therefore investigated how SI nutrient absorption and its determinants adapt during pregnancy in mice.

To identify gaps in existing knowledge of maternal gut adaptations during pregnancy in monogastric mammals, a scoping review was undertaken (Chapters 2 and 3) which uncovered gaps in knowledge regarding timing, size and regional localisation of SI adaptations. Furthermore, available evidence was inconsistent across species, strains and pregnancy stages for outcomes including macro- and micro-nutrient absorption, nutrient transporter and digestive enzyme expression and region-specific anatomical changes. Most studies did not investigate SI adaptations at early- and mid- pregnancy.

To enable characterisation of active glucose transport during pregnancy, we conducted several experiments to optimise Ussing chamber measures of SI active glucose transport *ex vivo* (Chapter 4). Once optimised, active glucose transport via sodium-dependent glucose transporter 1 (SGLT1) throughout the jejunum (region of peak nutrient absorption) was characterised across the murine oestrous cycle. Food intake changes during the ovarian cycle in rodents and humans, with a nadir during the pre-ovulatory phase and a peak during the luteal phase. However, whether SI glucose absorption also changes remains unknown. We hypothesised that active glucose transport would decrease at oestrus (equivalent to the follicular phase of the human menstrual cycle) based on blood glucose data following a 50 g glucose preload obtained during the luteal and follicular phases of the menstrual cycle. SGLT1-dependent glucose transport decreased at oestrus, providing the first direct evidence of oestrous-stage dependent changes in SI active glucose transport in mice. Once optimised, the Ussing chamber method was utilised to study changes in SI active glucose transport in late- compared to non-pregnant control mice.

In Chapter 5, we characterised concurrent SI anatomical, molecular and functional in C57BL/6 mice at early (gestational day, GD6.5), mid (GD12.5) and late-pregnancy (GD17.5) compared to non-pregnant controls using routine histological methods, quantitative real-time polymerase chain reaction and functional studies using Ussing chambers. Despite greater SI villi length and augmented expression of carbohydrate

transporter transcripts at late pregnancy, SGLT1-dependent glucose transport per unit area was similar to non-pregnant mice. This suggests other mechanisms beyond SGLT1-dependent transport may take on a greater role in apical glucose absorption.

Data presented in this thesis support the hypothesis that adaptations of SI nutrient uptake occur across the oestrous cycle and pregnancy, the latter possibly in response to altered nutrient demand. Further studies are required to elucidate the role(s) of other mechanisms involved in SI glucose uptake and mechanisms driving SI anatomical and molecular adaptations during pregnancy, such as food intake and hormone abundance. Further studies are also required to address gaps in knowledge regarding adaptations which occur at early- and mid-pregnancy.

STATEMENT OF ORIGINALITY AND AUTHENTICITY

I certify that this work contains no material which has been accepted for the award of any other degree or diploma in my name, in any university or other tertiary institution, and, to the best of my knowledge and belief, contains no material previously published or written by another person, except where due reference has been made in the text. In addition, I certify that no part of this work will, in the future, be used in a submission in my name, for any other degree or diploma in any university or tertiary institution without prior approval of the University of Adelaide and where applicable, any partner institution responsible for the joint award of this degree.

The author acknowledges that copyright of published works contained within the thesis resides with the copyright holder(s) of those works.

I give permission for the digital version of my thesis to be made available on the web, via the University's digital research repository, the Library Search and also through web search engines, unless permission has been granted by the University to restrict access for a period of time.

I acknowledge the support I have received for my research through the provision of an Australian Government Research Training Program Scholarship.

ACKNOWLEDGEMENTS

I would like to start by thanking my supervisory panel; primary supervisor Associate Professor Kathy Gafford, co-supervisors Associate Professor Richard Young and Professor Amanda Page. I feel extremely lucky and privileged to have been supervised by all three, and I am forever grateful for all the help, guidance and advice provided by each of my supervisors over the course of my candidature. All of my supervisors sat through many hours of poster and oral presentation practice sessions, watching me slowly improve my public speaking skills. Public speaking is something I have struggled with my entire life, and was actually one of the reasons why I was hesitant about undertaking a PhD in the first place. As Kathy told me many times, “as a research scientist, you need to be able to talk about and present your work in a public setting”. Aside from nurturing my presentation and speaking skills, my supervisors displayed extraordinary patience with me, something I am also extremely grateful for. I will forever be indebted to their patience, and there is no denying I have been challenging to work with. I do not dare to think how my candidature would have transpired with a different supervisory team.

I would like to thank my parents, family and friends for supporting me throughout my PhD journey, in particular my mum who moved back to the Netherlands shortly after I commenced my candidature. Her continued enthusiasm and interest in my project motivated me to keep going during the tougher times of my PhD, particularly during the final 18 months.

I would like to thank all members of the Vagal Afferent Research Group, both past and present, for their help and support throughout my candidature. In particular, I would like to thank Dr Hui Li and Dr Georgia Clarke for helping me troubleshoot some of the issues I faced during my lab work. Georgia also generated tissue samples which I would go on to use as part of my own project. I would like to thank Dr Hannah Wardill for teaching me how to use the Ussing chamber equipment, which unbeknownst to me at the time would become the backbone of my PhD work. Lastly, I would also like to say a special thank you to all the Bioresources facility staff members, both past and present, for providing and maintaining the animals which were used as part of my Ussing chamber work.

Lastly, I am thankful I received travel grants from the Faculty of Health and Medical Sciences and the Society for Reproductive Biology during the third year of my candidature which enabled me to travel to a major international conference in New Zealand to present some of the work undertaken during the 2nd and 3rd year of my candidature, and visit the lab of one of our collaborators who are also based in New Zealand. The experiences and insights gained from attending the conference and subsequent lab visit will stay with me

for years to come. I was also able to attend and present at numerous local conferences which allowed me to network and build on my professional skills.

The following manuscripts from this work have been published/accepted for publication:

Overduin TS, Page AJ, Young RL, Gatford KL. Adaptations in gastrointestinal nutrient absorption and its determinants during pregnancy in monogastric mammals: a scoping review protocol. *JBIE Evidence Synthesis* 2022 Feb;20(2):640-646. doi: 10.11124/JBIES-21-00025. PMID: 35165214.

Overduin TS, Wardill HR, Young RL, Page AJ, Gatford KL. Active glucose transport varies by small intestinal region and oestrous cycle stage in mice. *Exp Physiol*. 2023 Jun;108(6):865-873. doi: 10.1113/EP091040. Epub 2023 Apr 6. PMID: 37022128.

Signed,

Teunis Sebastian Overduin

LIST OF ABBREVIATIONS IN TEXT

5-HT	serotonin	<i>CD36</i>	CD36 (cluster of differentiation 36, also known as FAT – fatty acid translocase)
<i>ABCC1</i>	ATP-binding cassette subfamily C member 1 (MRP1 - multidrug-resistance protein 1)	<i>CD98</i>	CD98 (cluster of differentiation 98)
AC	abdominal circumference	<i>Cldn2</i>	CLDN2 (claudin 2)
Ad lib	ad libitum	<i>Cldn9</i>	CLDN9 (claudin 9)
<i>AMN</i>	amniotless	CNS	central nervous system
ATP	adenosine triphosphate	CRBP	cellular retinol binding protein
<i>Atp1a3</i>	ATPase Na ⁺ /K ⁺ Transporting Family Member alpha 3 (Na ⁺ /K ⁺ -ATPase subunit)	C-sect	caesarean section
<i>Atp1b4</i>	ATPase Na ⁺ /K ⁺ Transporting Family Member beta 4 (Na ⁺ /K ⁺ -ATPase subunit)	<i>CUBN</i>	cubulin
<i>ATP2B1</i>	PMCA1b (plasma membrane Ca ²⁺ -ATPase)	<i>Dcytb</i>	duodenal cytochrome b (ferriductase)
AU	arbitrary units	DEI	daily energy intake
AUC	area under curve	DMSO	dimethyl sulfoxide
<i>B2M</i>	β2 microglobulin	<i>ECAC1</i>	TRPV5 (transient receptor potential cation channel subfamily V member 5 subunit)
BL	body length	<i>ECAC2</i>	TRPV6 (transient receptor potential cation channel subfamily V member 6 subunit)
<i>BK-α</i>	big potassium channel	E-DII	energy-adjusted dietary inflammation index
BMI	body mass index	EEC	enteroendocrine cell
BW	body weight	EMG	electromyography
CaBP	calcium binding protein	ENS	enteric nervous system
<i>CACNA1D</i>	Ca _v 1.3 (calcium channel, voltage-dependent, L-type, α-1D subunit)	EP	early pregnant
<i>CALB1</i>	calbindin D28K		
CCK	cholecystokinin		

F ₁	First generation	HS	high sugar
F ₂	Second generation	IF	intrinsic factor
<i>FABP1</i>	FABP1 (fatty acid binding protein 1)	IF-Cbl	intrinsic factor-cobalamin
<i>FABP2</i>	FABP2 (fatty acid binding protein 2)	IGLE	intraganglionic laminar ending
<i>FABP4</i>	FABP4 (fatty acid binding protein 4)	IMA	intramuscular array
<i>FABP5</i>	FABP5 (fatty acid binding protein 5)	IOM	Institute of Medicine
<i>FATP1</i>	FATP1 (fatty acid transporter protein 1)	IU	international units
<i>FATP4</i>	FATP4 (fatty acid transporter protein 4)	IUGR	intrauterine growth restriction
FITC	fluorescein isothiocyanate	IQR	inter-quartile range
FR	food restriction	IRE	iron-responsive element
<i>GAPDH</i>	glyceraldehyde-3-phosphate dehydrogenase	<i>Ireg1</i>	iron regulated transporter 1 (FPN)
GD	gestational day	<i>I_{sc}</i>	short-circuit current
GDM	gestational diabetes mellitus	IVGTT	intravenous glucose tolerance test
GIP	glucose-dependent insulinotropic polypeptide	KRB	Krebb-Ringer bicarbonate
GIT	gastrointestinal tract	LBW	low birth weight
GLP-1	glucagon like peptide-1	LCFA	long-chain fatty acid
GWG	gestational weight gain	LGA	large for gestational age
HDP	hypertensive disorders of pregnancy	LP	late pregnant
HF	high fat	MCFA	medium-chain fatty acid
<i>Hp</i>	hephaestin (ferroxidase)	MP	mid pregnant
<i>HRPT</i>	hypoxanthine phosphoribosyltransferase 1	NHP	non-human primate
		Non-rand exp	non-randomised experimental study
		NP	non pregnant
		<i>NPC1L1</i>	Niemann-Pick C1 like-1

N/S	not stated	SGA	small for gestational age
Nsd	no significant difference	SI	small intestine
NW	normal weight	SLC	solute carrier family
OB	obese	<i>SLC1A1</i>	solute carrier family 1 member 1 (EAAC3 excitatory amino acid transporter 3)
OGTT	oral glucose tolerance test		
OW	overweight		
PE	preeclampsia	<i>SLC1A5</i>	solute carrier family 1 member 5 (ASCT2 - neutral amino acid transporter B(0))
PIH	pregnancy-induced hypertension		
PND	postnatal day	<i>SLC2A1</i>	solute carrier family 2 member 1 (GLUT1 - glucose transporter 1)
PPH	postpartum haemorrhage		
<i>PPIA</i>	peptidylprolyl isomerase A	<i>SLC2A2</i>	solute carrier family 2 member 2 (GLUT2 - glucose transporter 2)
PPM	parts per million		
Prosp cohort	prospective cohort study	<i>SLC2A5</i>	solute carrier family 2 member 5 (GLUT5 - glucose transporter 5)
PR	protein restriction		
PROM	premature rupture of membranes	<i>SLC3A1</i>	solute carrier family 3 member 1 (rBAT - neutral and basic amino acid transporter)
PTD	preterm delivery		
PYY	peptide YY		
Pz	phlorizin	<i>SLC5A1</i>	solute carrier family 5 member 1 (SGLT1 - sodium-dependent glucose transporter 1)
Rand double-blinded	randomised double-blinded study		
Rand exp	randomised experimental study	<i>SLC5A6</i>	solute carrier family 5 member 5 (SMVT - sodium-dependent multivitamin transporter)
RFU	relative fluorescent units		
RT-PCR	real time polymerase chain reaction	<i>SLC6A6</i>	solute carrier family 6 member 6 (TAUT - sodium/chloride-dependent taurine transporter)
<i>S100g</i>	calbindin-D9K		
SCFA	short-chain fatty acid		

<i>SLC6A9</i>	solute carrier family 6 member 9 (GLYT1 – sodium/chloride-dependent glycine transporter 1)		type amino acid transporter 1)
<i>SLC6A14</i>	solute carrier family 6 member 14 (ATB ^{0,+} - sodium/chloride-dependent neutral and basic amino acid transporter)	<i>SLC8A1</i>	solute carrier family 8 member 1 (NCX1 - sodium-calcium exchanger 1)
<i>SLC6A19</i>	solute carrier family 6 member 19 (B ⁰ AT1 - sodium-dependent neutral amino acid transporter)	<i>SLC9A3</i>	solute carrier family 9 member 3 (NHE3 – sodium/hydrogen exchanger 3)
<i>SLC6A20</i>	solute carrier family 6 member 20 (IMINO - sodium/chloride-dependent imino acid transporter 1)	<i>SLC10A2</i>	solute carrier family 10 member 2 (ASBT - apical sodium-dependent bile transporter)
<i>SLC7A1</i>	solute carrier family 7 member 1 (CAT1 – cationic amino acid transporter 1)	<i>SLC11A2</i>	solute carrier family 11 member 2 (DMT1 - divalent metal transporter 1)
<i>SLC7A6</i>	solute carrier family 7 member 6 (y ⁺ LAT2 – y ⁺ L amino acid transporter 2)	<i>SLC13A1</i>	solute carrier family 13 member 1 (NAS1 - sodium-dependent sulphate transporter 1)
<i>SLC7A7</i>	solute carrier family 7 member 7 (y ⁺ LAT1 – y ⁺ L amino acid transporter 1)	<i>SLC15A1</i>	solute carrier family 15 member 1 (PEPT1 - peptide transporter 1)
<i>SLC7A8</i>	solute carrier family 7 member 8 (LAT2- large neutral amino acid transporter small subunit 2)	<i>SLC19A1</i>	solute carrier family 19 member 1 (FOLT1 - folate transporter 1)
<i>SLC7A9</i>	solute carrier family 7 member 9 (b ^{0,+} AT - b(0,+)- type amino acid transporter)	<i>SLC19A2</i>	solute carrier family 19 member 2 (THTR1 - thiamine transporter 1)
<i>SLC7A10</i>	solute carrier family 7 member 10 (ASC1 - ASC-	<i>SLC19A3</i>	solute carrier family 19 member (THTR2 - thiamine transporter 2)
		<i>SLC23A1</i>	solute carrier family 23 member 1 (SVCT1 - sodium-dependent ascorbate cotransporter 1)

<i>SLC23A2</i>	solute carrier family 23 member 3 (SVCT2 - sodium-dependent ascorbate cotransporter 2)	<i>SLC36A1</i>	solute carrier family 36 member 1 (PAT1 - H ⁺ -coupled amino acid transporter 1)
<i>SLC26A1</i>	solute carrier family 26 member 1 (SAT1 - sodium-independent sulphate transporter 1)	<i>SLC36A4</i>	solute carrier family 36 member 4 (PAT4 - H ⁺ -coupled amino acid transporter 4)
<i>SLC26A2</i>	solute carrier family 26 member 2 (DSDST - diastrophic dysplasia sulphate transporter)	<i>SLC38A2</i>	solute carrier family 38 member 2 (SNAT2 - sodium-dependent neutral amino acid transporter 2)
<i>SLC26A3</i>	solute carrier family 26 member 3 (chloride/anion exchanger 3)	<i>SLC38A3</i>	solute carrier family 38 member 3 (SNAT3 - sodium-dependent neutral amino acid transporter 3)
<i>SLC27A4</i>	solute carrier family 27 member 4 (FATP4 - long-chain fatty acid transporter 4)	<i>SLC38A5</i>	solute carrier family 38 member 5 (SNAT5 - sodium-dependent neutral amino acid transporter 5)
<i>SLC30A1</i>	solute carrier family 30 member 1 (ZnT1 - zinc transporter 1)	<i>SLC39A4</i>	solute carrier family 39 member 4 (ZIP4 - zinc transporter protein 4)
<i>SLC30A2</i>	solute carrier family 30 member 2 (ZnT2 - zinc transporter 2)	<i>SLC39A5</i>	solute carrier family 39 member 5 (ZIP5 - zinc transporter protein 5)
<i>SLC30A4</i>	solute carrier family 30 member 4 (ZnT4 - zinc transporter 4)	<i>SLC40A1</i>	solute carrier family 40 member 1 (FPN - ferroportin 1)
<i>SLC31A1</i>	solute carrier family 31 member 1 (CRT1 - copper transporter 1)	<i>SLC46A1</i>	solute carrier family 46 member 1 (HCP1 – H ⁺ -coupled folate transporter 1)
<i>SLC34A2</i>	solute carrier family 34 member 2 (NaPi-IIB - sodium-dependent phosphate transporter 2B)	<i>SLC52A1</i>	solute carrier family 52 member 1 (RFVT1 - riboflavin transporter 1)

<i>SLC52A2</i>	solute carrier family 52 member 2 (RFVT2 - riboflavin transporter 2)
Tri	trimester
TRIG	triglyceride
<i>TRPM6</i>	TRPM6 (transient receptor potential cation channel subfamily M member 6)
<i>TRPM7</i>	TRMP7 (transient receptor potential cation channel subfamily M member 7)
Wnt	Wingless and Int-1
<i>ZO-1</i>	TJP1 (tight junction protein 1, also known as zona occludens 1)

MANUSCRIPTS ARISING FROM PHD

Work directly related to this thesis:

Published manuscripts:

Overduin TS, Page AJ, Young RL, Gatford KL. Adaptations in gastrointestinal nutrient absorption and its determinants during pregnancy in monogastric mammals: a scoping review protocol. *JB Evidence Synthesis* 2022 Feb;20(2):640-646. doi: 10.11124/JBIES-21-00025. PMID: 35165214. (Appendix 1)

Overduin TS, Wardill HR, Young RL, Page AJ, Gatford KL. Active glucose transport varies by small intestinal region and oestrous cycle stage in mice. *Exp Physiol*. 2023 Jun;108(6):865-873. doi: 10.1113/EP091040. Epub 2023 Apr 6. PMID: 37022128.

Editorial: Taylor V. Still searching for the female norm: a GLUT of knowledge remains to be revealed. *Exp Physiol*. 2023 Jun;108(6):799-801. doi: 10.1113/EP091204. Epub 2023 May 2. PMID: 37130067.

Submitted manuscript:

Overduin TS, Page AJ, Young RL, Gatford KL. Adaptations in gastrointestinal nutrient absorption and its determinants during pregnancy in monogastric mammals: a scoping review. Submitted to *J Gastroenterol*, JOGA-D-23-01736, 14th of December 2023

Other manuscripts published during PhD:

Schjenken JE, Green ES, **Overduin TS**, Mah CY, Russell DL, Robertson SA. Endocrine disruptor compounds - a cause of impaired immune tolerance driving inflammatory disorders of pregnancy? *Front Endocrinol (Lausanne)*. 2021 Apr 12;12:607539. PMID: 33912131.

CONFERENCE ABSTRACTS ARISING FROM PHD

Overduin, T.S., Clarke, G.S., Li, H., Page, A.J., Young, R.L., Gatford, K.L. (2021) Determinants of nutrient absorption across pregnancy in mice. Poster presentation – 2021 ASMR SA meeting, Adelaide, South Australia

Overduin, T.S., Clarke, G.S., Li, H., Page, A.J., Young, R.L., Gatford, K.L. (2021) Determinants of nutrient absorption across pregnancy in mice. Poster presentation – 2021 SAHMRI Research Showcase, Adelaide, South Australia

Overduin, T.S., Page, A.J., Young, R.L., Gatford, K.L. (2021) Changes in anatomical and functional determinants of nutrient absorption during pregnancy in mice. Oral Presentation – Barossa Valley Conference, Novotel Retreat, South Australia

Overduin, T.S., Wardill, H.R., Young, R.L., Page, A.J., Gatford, K.L. (2022) Characterising small intestinal glucose absorption across the oestrous cycle in mice – 2022 Florey Postgraduate Conference, Adelaide, South Australia

Overduin, T.S., Page, A.J., Young, R.L., Gatford, K.L. (2022) Evidence for changing mechanisms of small intestinal glucose absorption during the oestrous cycle in mice – 2022 ASMR SA meeting, Adelaide, South Australia

Overduin, T.S., Page, A.J., Young, R.L., Gatford, K.L. (2022) Small intestinal glucose absorption across the oestrous cycle in mice – 2022 ESA-SRB Conference, Christchurch, New Zealand

1. CHAPTER 1: INTRODUCTION

How and when nutrient absorption by the small intestine (SI), and its determinants, change during pregnancy is a research enquiry that has spanned the last eight decades. Despite these efforts, many questions remain regarding the precise timing and nature of these adaptations. There is a growing body of evidence from observational human and intervention-based animal studies indicating that maternal malnutrition during pregnancy worsens maternal and fetal outcomes, resulting in short and long-term health complications and future disease burdens [1-3]. A better understanding of how and when SI adaptations emerge throughout pregnancy will inform new strategies aimed at optimising maternal nutrition for pregnancy, as well as maternal and fetal outcomes. This will in turn reduce the risk of short-term complications and future disease burden.

The demand for nutrients increases during pregnancy to support increased maternal energy expenditure, adipose tissue deposition and fetal growth and development [4, 5]. To meet this increased demand, maternal food intake increases, particularly towards the end of pregnancy when fetal growth is rapid. In addition, the SI, which is the primary site of nutrient absorption for humans and rodents, adapts rapidly to changes in nutrient supply and demand during pregnancy. The scope of this introduction is to provide an overview of changes in maternal physiology, food intake and weight gain during pregnancy in monogastric mammals. A summary of the consequences of variable maternal nutrition during pregnancy on maternal and fetal outcomes is also provided. The introduction concludes with an overview of the gastrointestinal tract and its components, SI anatomy and function and mechanisms of nutrient uptake, providing context to maternal SI adaptations in nutrient uptake during pregnancy.

1.1. Pregnancy

1.1.1. Overview

Pregnancy results from the fusion of male and female gametes to create a zygote [6]. Following fertilisation, the zygote undergoes multiple rounds of cell division to establish the blastocyst, comprised of two distinctive cell lineages. The inner cell mass contains cells that develop into the embryo while the trophoblast epithelium develops into the placenta [7]. This period is also referred to as the pre-implantation stage, and lasts around 5-7 days in humans [7]. Next, the inner cell mass differentiates into two distinct cell lineages; epiblast and primitive endoderm, which occurs immediately prior to implantation. Implantation occurs around 5-7 days post fertilisation in humans and around gestational day (GD) 4.5 in mice [8, 9]. Following implantation, the human embryonic period encompasses week 3-10 from the last menstrual period; characterised by the development

of embryonic organs and remodelling of the uterine environment to support pregnancy [9]. The fetal period then extends from 9-10 weeks from the last menstrual period until parturition at ~280 days. In contrast, the embryonic period in mice and rats spans GD4.5-14.5, while the fetal period spans GD14.5 until GD19-22, depending on individual strains [10].

Energy and nutrient demands are significantly increased during pregnancy to meet maternal and fetal energy and nutrient needs. The following sections describe the timing and composition of weight gain during pregnancy, some of the key maternal adaptations to support pregnancy, development and function of the placenta, and finally, current knowledge on changes in food intake during pregnancy.

1.1.2. Weight gain

Women with a normal body mass index (BMI, 18.5-24.9 kg/m²) typically gain between 11.5-16 kg during pregnancy. This includes a 3.8 kg fetus, 690 g placenta and ~3-4 kg of adipose tissue at parturition [4, 11, 12]. In contrast, litter-bearing species such as mice [13, 14] and rat [15, 16] typically undergo bodyweight increases of 50-100% by parturition, depending on the size of the litter. The marked difference in relative pregnancy weight gain between humans and litter-bearing species such as rodents relates to the different contributions of conceptus weight (weight of fetus and placenta) to pregnancy weight gain. In humans, the fetal/maternal weight ratio at parturition is 6% compared to 25% in rat [17]. In mice, weight of the gravid uterus accounts for ≥ 60% of total pregnancy weight gain at GD19 (term = 19.5 days, [18, 19]).

Maternal weight gain during the first trimester in humans equates to an increase of 0.18 kg/week (Fig. 1.1, [4]). This modest weight gain mostly reflects maternal adipose tissue deposition rather than conceptus growth and development, as the first 8 weeks are characterised by preimplantation and embryonic periods [4, 20]. Second trimester weight gain equates to 0.54 kg/week and is attributable to accelerated conceptus growth concurrent with continuing deposition of maternal adipose tissue and increases in blood volume and extravascular fluid [4, 21].

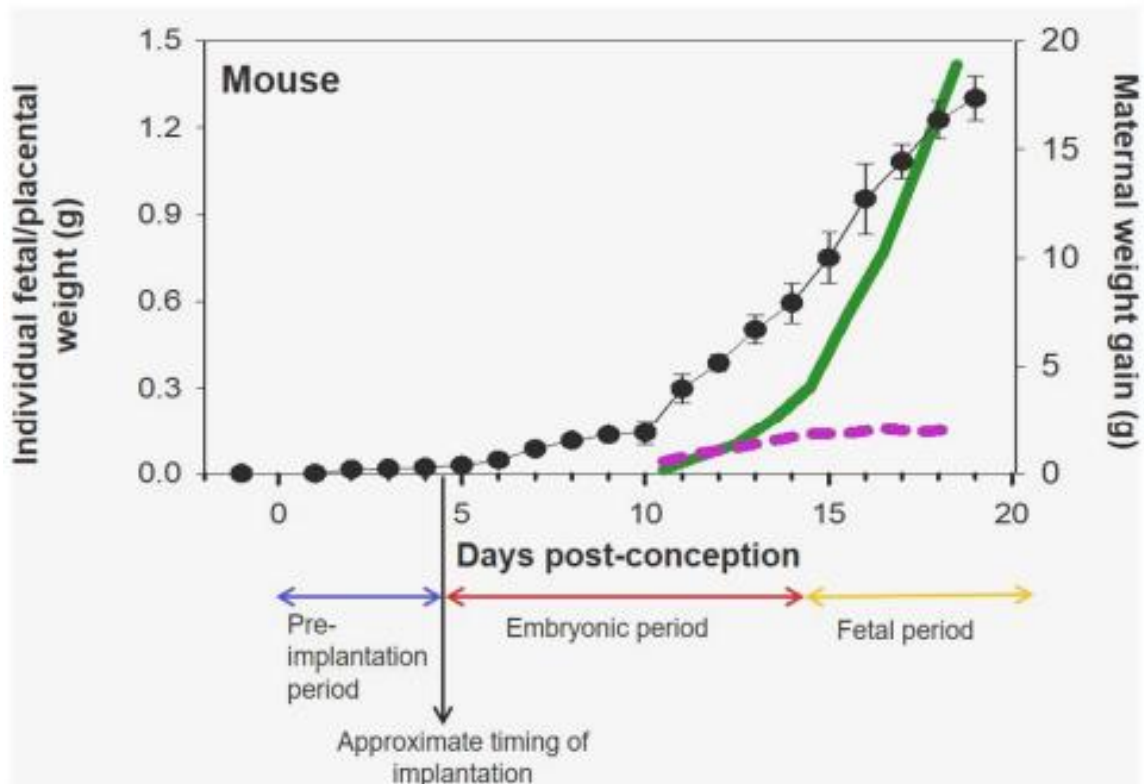
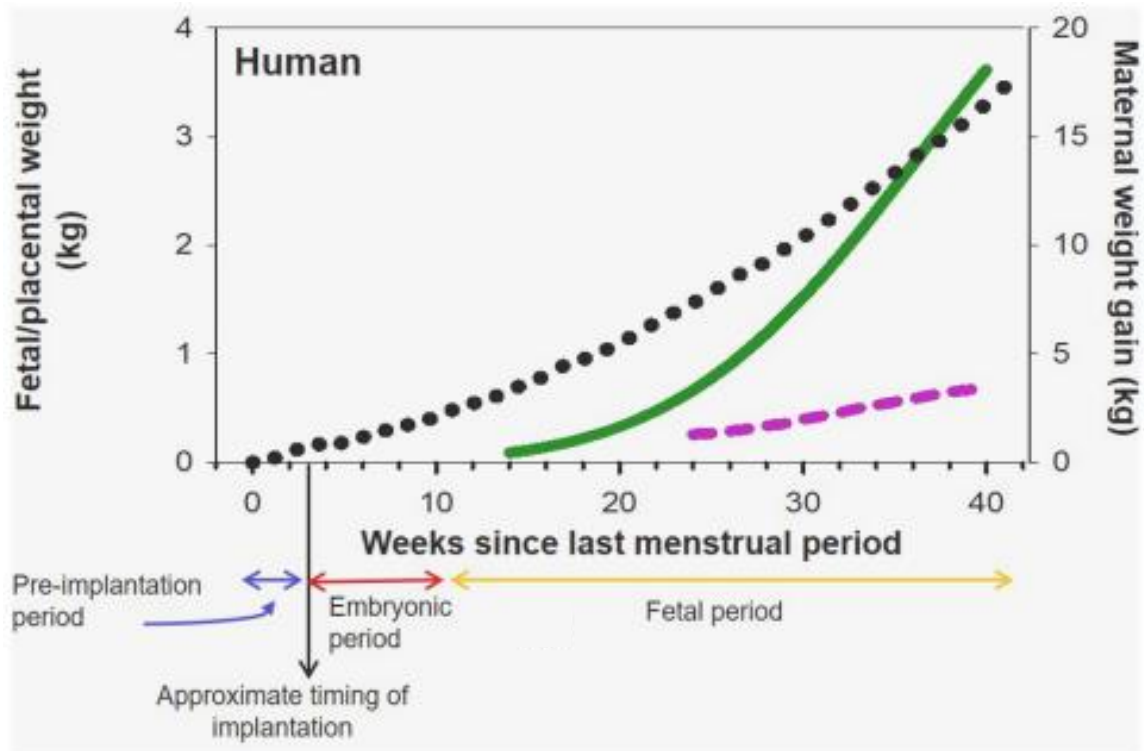


Figure 1.1 Changes in maternal, fetal and placental weight during pregnancy in humans and mice, reproduced from Kaur et al. 2021 [22]. Solid black circles represent maternal weight gain, solid green line represents fetal weight and placental weight is represented by the dashed purple line. Range and units differ on both x axes. Mouse data are based on individual fetal/placental weights, not litter totals.

The rate of adipose tissue deposition in support of post-parturition lactation and accumulation of adipose tissue stores peaks towards the end of the 2nd trimester [23, 24], and accounts for 3-4 kg of maternal weight gain in a typical human pregnancy [4]. During the third trimester, maternal weight gain equates to 0.49 kg/week, characterised by rapid fetal growth and development and ongoing expansion of maternal blood and extravascular fluid volumes [4, 21]. The human placenta increases in size and weight concurrent with fetal growth and development, exemplified by a 13.5-fold increase in placental weight between week 10-12 gestation (51 g) and term (680 g, [4]). Placental volume concurrently increases 2.5-fold from 200 cm³ at 21 weeks gestation to 500 cm³ at term [4, 20]. These placental changes are needed to meet the increase in nutrient demand of the conceptus over the course of gestation [21].

A similar pattern of maternal weight gain across pregnancy is observed in mice (Fig. 1.1, bottom panel, solid black circles), characterised by limited weight gain during the first week before acceleration of fetal weight gain in the second and third week following implantation and commencement of placental blood flow around GD9.5 (Fig. 1.1, bottom panel, dashed purple line, [13]). In rats, there is a continuous increase in maternal adipose tissue content until GD19 (term = 22 days) at which point adipose tissue content has increased by ~80% from time of mating [25]. At parturition, maternal adipose tissue content declines slightly, but is still ~60% greater than pre-pregnancy levels [25].

1.1.3. Maternal adaptations

Anatomical and physiological adaptations occur concurrently to support conceptus growth and development in human pregnancy. These include increased function of cardiovascular, pulmonary and renal systems, which act in concert to effectively supply nutrients to maternal tissues and the conceptus, and remove waste from the fetal circulation.

Maternal blood volume increases progressively during human pregnancy, driven by an increase in plasma volume of 50-60% from pre-pregnancy to the end of the third trimester [21]. As a result, maternal blood volume peaks at ~145% of pre-pregnancy volume at term, and is accompanied by a 40% increase in cardiac output [21]. Kidney function is also augmented in concert with the increase in blood volume, with glomerular filtration rate and renal plasma flow rate increased by 50 and 85%, respectively, over the course of pregnancy [26]. As a consequence of the 15% increase in metabolic rate resulting from increased cardiac output and kidney function, oxygen consumption increases by 20% towards the end of pregnancy compared to non-pregnant controls [21]. Additionally, the metabolically active placenta consumes as much as 40% of the oxygen supplied to the

feto-placental unit to enable active nutrient transport as well as endogenous protein synthesis [27]. Together, these anatomical and physiological adaptations protect feto-placental substrate supply. Fasting glucose concentrations decline progressively over the course of pregnancy, while fasting insulin concentrations increase ~2-fold by late-pregnancy [28, 29]. This decrease in fasting glucose concentrations may parallel increased glucose utilisation by maternal and fetal tissues and organs. Fasting blood glucose changes parallel a 30% increase in hepatic glucose production [30], a ~50% decrease in insulin sensitivity and 3- to 3.5-fold increase in insulin secretion assessed by intravenous glucose tolerance tests by late-pregnancy [29].

Pregnant rodents undergo similar anatomical and physiological changes to humans. Cardiac output increases by 48-64% at late-stage pregnancy in mice [31, 32], concurrent with a 27% increase in plasma volume [32]. In contrast to humans, fasting glucose concentrations progressively increase during pregnancy in mice, rising to ~130% of basal concentration on GD8 and ~120% on GD16 [33, 34]. As with humans, fasting insulin concentration increases ~2-fold from basal concentration, whilst hepatic glucose production increases 4-fold at late-pregnancy in C57BL/6 mice [34]; insulin sensitivity is also reduced at GD16 but similar at GD19 compared to non-pregnant controls [34]. In naked mole rats, both metabolic rate and oxygen use increase ~1.5-fold between the second week of pregnancy until the end of the 10 week gestation period [35]. The increase in metabolic rate in naked mole rats is accompanied by an increase in energy requirement equivalent to 1300 kJ above basal energy requirements over the course of a single breeding cycle [35].

1.1.4. Placental growth, development and function

Nutrients and gases are supplied to the fetus via the placenta during pregnancy, which acts as an exchange interface between the maternal and fetal circulation (Fig. 1.2, [36]). To enhance the rate of exchange, the epithelial barrier between maternal and fetal blood is very thin. In addition, the distance between the maternal blood space and fetal capillaries progressively thins to further increase the rate of exchange between maternal and fetal circulation [36]. Although functionally similar, there are anatomical differences between the human and murine placenta. The human placenta resembles a villous “tree”, while the murine placenta comprises two distinct zones; the junctional zone and labyrinth zone (Fig. 1.2). The junctional zone has endocrine functions whereas the labyrinth zone is the site of nutrient and gas exchange between maternal and fetal blood [36].

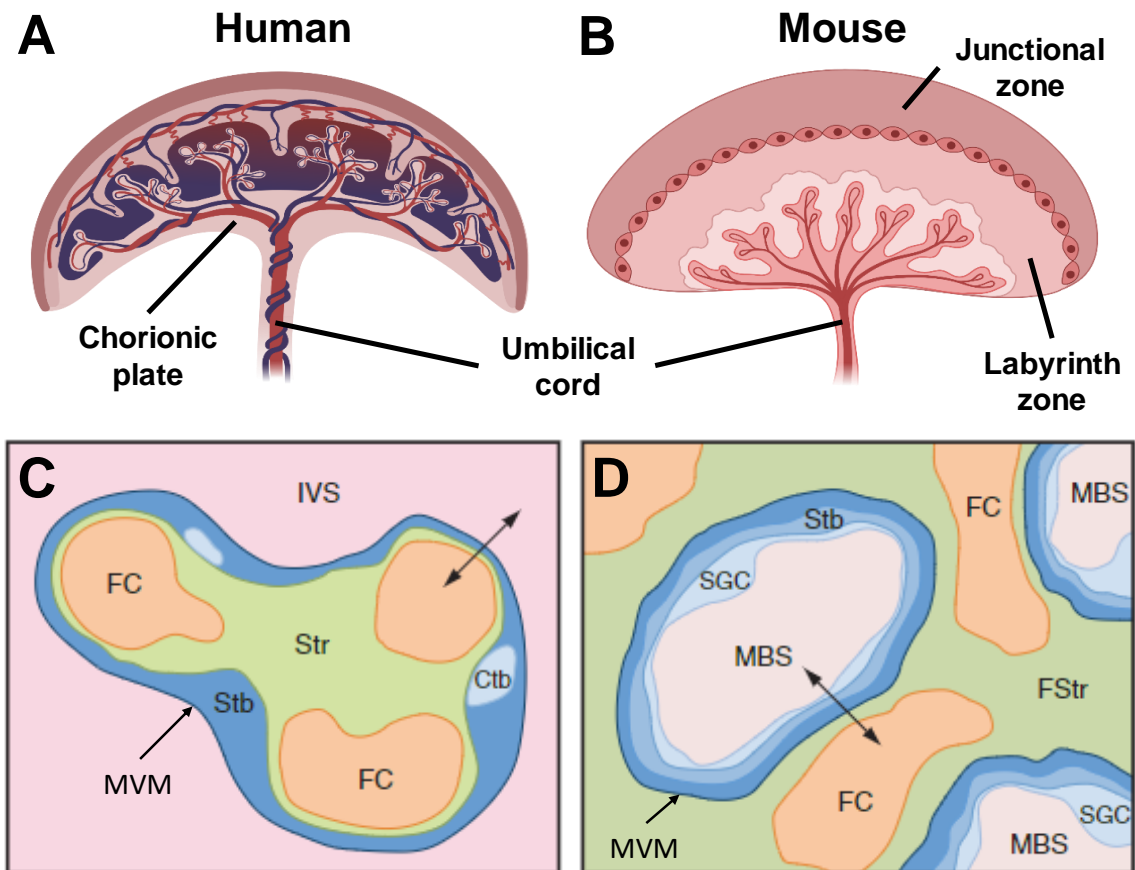


Figure 1.2 Schematic representation (not drawn to scale) of human (A) and mouse (B) placenta. In human placenta (C), fetal capillaries (FC) within the stromal core (Str) are covered by a single layer of epithelium comprised of syncytiotrophoblast (Stb) cells, which are derived from cytotrophoblast (Ctb) cells. The Stb cells together with the stroma form the barrier between fetal circulation and the intervillous space (IVS) where nutrient and gas exchange take place as indicated by double headed arrow. In mouse placenta (D), the maternal blood space (MBS) infiltrates the fetal stroma (FStr) of the labyrinth zone. Unlike human placenta, the MBS is covered by two layers of epithelium, comprised of inner sinusoidal giant cells (SGC) and Stb cells. MVM = microvillus plasma membrane. Panels A and B were created in Biorender.com and panels C and D were reproduced from Burton et al. 2016 [37].

The rate of nutrient transport across the placenta depends on several factors including vascular density, the surface area available for nutrient transport, the molecular properties of the nutrient being transported, (size and lipid solubility), nutrient transporter density, and the concentration gradient between the maternal and fetal circulation [36, 38]. Small lipophilic molecules, such as respiratory gases, can diffuse directly across the apical lipid bilayers of the syncytiotrophoblast microvillus plasma membrane (Fig. 1.2), while larger and less lipid-soluble molecules, cross the MVM with the aid of specific transporter proteins [39].

To facilitate nutrient delivery to the fetus, specific transporters of macronutrients - carbohydrates [39], amino acids [40, 41], and lipids [42, 43] - and of micronutrients such as calcium [44, 45] are expressed in human, mouse and rat placenta. As glucose is the

primary substrate for fetal energy metabolism, placental expression of glucose transporter 1 (GLUT1) increases progressively across pregnancy in humans [46], in parallel with fetal growth and development. The rate of transport of glucose, and some other specific nutrients, across the placenta depends on multiple factors such as the rate of blood flow, available surface area and number of nutrient transporters [36]. The characteristics of, and differences between, passive and active nutrient transport are further explored in the nutrient absorption section (section 1.4). There is evidence that maternal diet and the presence of gestational diabetes can directly influence placental glucose and fatty acid transporter gene expression in humans [47] and mice [48], reflecting the sensitivity of the placenta to nutrient availability and substrate concentrations in the uterine environment.

Another factor affecting nutrient transport across the placenta is the difference in substrate concentration between the maternal and fetal circulation, and the resulting concentration gradients. The maternofetal transfer of glucose via GLUT1 occurs down a concentration gradient, and therefore requires higher glucose concentrations in the maternal than fetal circulation [36]. In contrast, some neutral amino acids such as alanine, glycine and serine are transported across the placenta by carrier proteins against an electrochemical gradient established by Na^+/K^+ ATPase. This exchange complex is situated at the basolateral membrane of syncytiotrophoblast MVM and requires ATP to exchange Na^+ and K^+ from the circulation to generate a low intracellular Na^+ concentration [36].

1.1.5. Food intake

Adequate maternal food intake is important to ensure optimal pregnancy outcomes; however, such nutrition may not always be available depending on dietary habits and food availability. Towards the end of the 3rd trimester in humans, and the 3rd week of pregnancy in mice and rat, daily food intake has increased by ~15% [4, 49, 50] and 50% [14, 51] respectively (Fig. 1.3). This marked increase in food intake parallels demand for energy and nutrients associated with adipose tissue deposition, increased metabolic rate and conceptus growth and development. The difference in effects of pregnancy maternal food intake between humans, mice and rat could at least, in part, be attributable to differences in the ratio of fetal to maternal weight between humans and rodents [17]. Although there is less data available regarding changes in daily energy or food intake in humans compared to mice and rats, there is a pattern of increased daily energy- and food intake over the course of pregnancy compared to non-pregnant controls [5, 14, 51-59]. In humans, Goldberg and colleagues reported a 14% increase in daily energy intake compared to non-pregnant controls at 18- and 24-weeks' gestation, in contrast to Kopp-Hoolihan, who reported no significant change in daily energy intake compared to non-pregnant controls, despite their 9% higher daily energy-intake at 36 weeks (Fig. 1.3A, [23,

49]). It also should be noted that a considerable degree of variation between individual subjects, combined with small sample sizes, means results from these studies needs to be interpreted with a degree of caution. Li and colleagues and Makarova and colleagues reported significant increases in daily food intake from pre-pregnancy intake in GD8.5 mice until parturition, while Ladyman and colleagues reported a similar increase from GD13 until parturition (Fig. 1.3B, [14, 52, 53]). These increases coincide with the onset of blood flow from the placenta to the fetus and the fetal period, respectively, during which rapid fetal growth and development occur. There are equivocal reports on effects of pregnancy on food intake in rats, possibly due to the different strains used (Fig. 3C, [51, 54-58]). While some report significant increases in daily food intake in pregnant Wistar from GD1 until parturition [57] and in Sprague-Dawley rats from GD4 until parturition [51], compared to age-matched controls, other studies reported no differences in food intake over the course of pregnancy [54-56, 58].

Improved understanding of how food intake changes across a healthy pregnancy has the potential to yield new strategies and treatment methods to optimise pregnancy diets for women who are under or overweight, display poor dietary habits or do not have access to adequate or optimal nutrition. Section 1.2 addresses the importance of adequate maternal nutrition and summarises the impacts of maternal malnutrition during pregnancy on maternal, fetal and pregnancy outcomes.

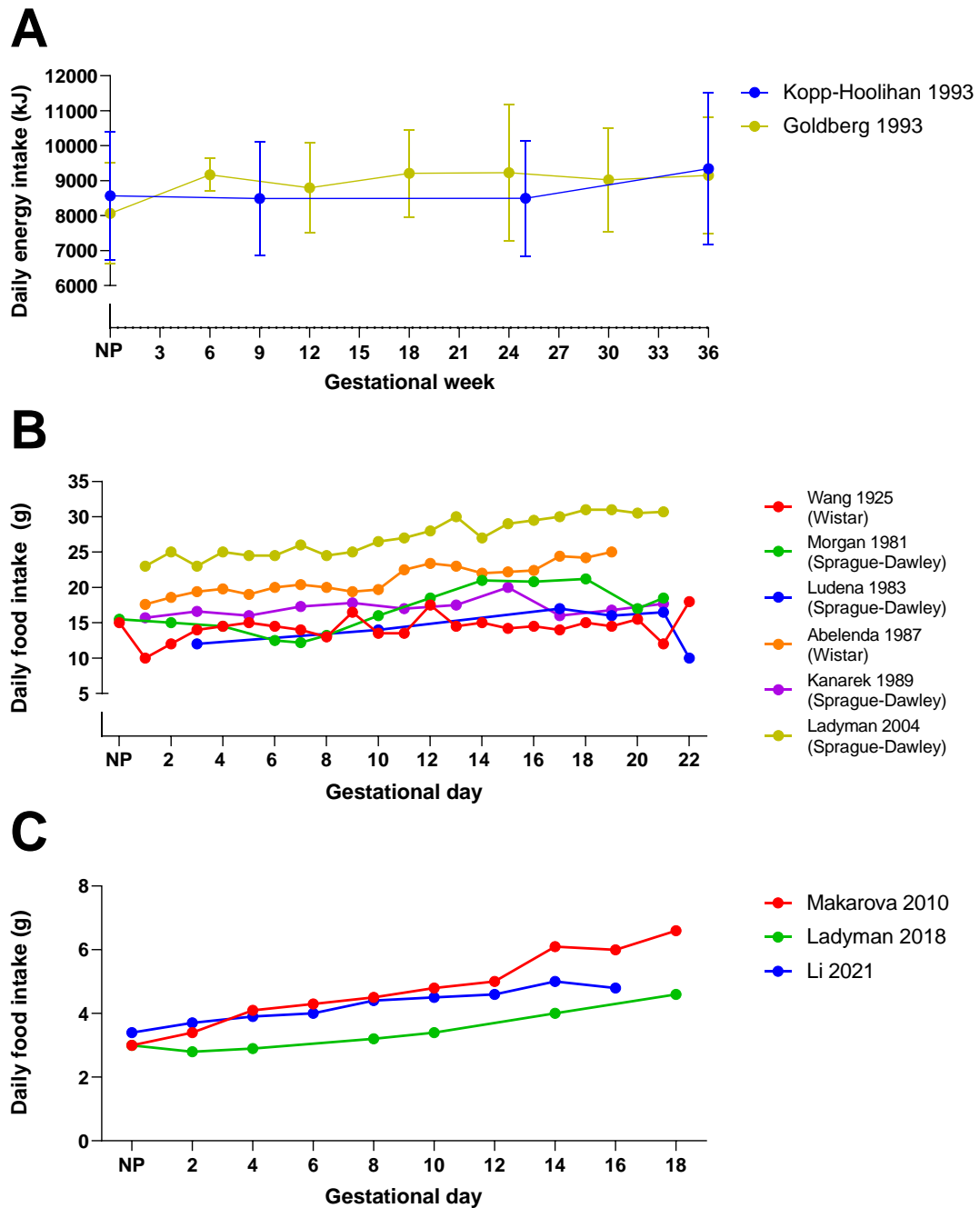


Figure 1.3 Daily energy intake (kJ) in humans during pregnancy (A, [23, 49]), and food intake (g) during pregnancy in rats (B, [51, 54-58]) and mice (C, [14, 52, 53]). NP = non-pregnant.

1.2. Importance of nutrition during pregnancy

1.2.1. Overview

Pregnancy is a state of increased nutrient demand; however, maternal nutrition must remain balanced. Global under-nutrition and over-nutrition, as well as individual macro- and micronutrient malnutrition during the perinatal period, can result in acute and chronic pregnancy complications. It is also emerging that inadequate maternal nutrition and related changes in the uterine environment increase the risk of developmental perturbations in progeny that extend to subsequent generations, in part, due to epigenetic re-programming [60-62].

To help guide women on gestational weight gain (GWG), a series of guidelines was developed by the Institute of Medicine (IOM) in 1990 based on evidence from population studies examining weight gain, maternal, fetal and pregnancy outcomes. These guidelines were updated in 2009 to encompass changing population dynamics, such as the increased prevalence of maternal obesity [20]. Based on the IOM guidelines, women with a BMI less than 18.5 kg/m² at the time of conception are classed as underweight and advised to achieve a GWG of between 12.5-18 kg over the course of their pregnancy [20]. Recent observational studies have reported that the proportion of Asian women with pre-pregnancy low BMI at conception who achieved recommended GWG below, within and above IOM guidelines were 44.4-76.3%, 21-46.6% and 2.3-9.4% respectively [63, 64]. In contrast, the proportion of American women with pre-pregnancy low BMI at conception who achieved GWG below, within and above IOM guidelines were 19.5%, 36.8% and 43.7% respectively [65].

Based on IOM guidelines, women with a BMI between 25-29.9 kg/m² and BMI \geq 30 kg/m² at conception are classed as overweight and obese, respectively. These women are advised to achieve a GWG of 7-11.5 and 5-9 kg over the course of pregnancy [20]. Adverse maternal, fetal and pregnancy outcomes resulting from high and low GWG are summarised in sections 1.2.2 and 1.2.3. Recent observational studies reported that the proportion of Asian women with pre-pregnancy high BMI (>25 kg/m²) at conception who achieved recommended GWG below, within and above IOM guidelines were 13.1-43.2%, 34-46.4% and 23-52.5% [63, 64]. In contrast, the average proportion of American women with pre-pregnancy high BMI (>25 kg/m²) at conception who achieved GWG below, within and above IOM guidelines were 9.1%, 11.9% and 79% [65].

Carbohydrates such as glucose are the primary substrate utilised during the perinatal period for fetal energy metabolism, fuelling fetal growth and development [46]. Lipids are required for fetal lipogenesis and adipogenesis, while amino acids are involved in

formation of tissues such as muscle and the central nervous system, but also serve functional roles in hormone synthesis, cell signalling and nutrient transport [66-69]. There has been a contemporary increase in use of vegetarian or vegan style diets [70], which can lack key animal-derived macro- and micro-nutrients such as certain amino acids, iron, calcium, iodine, omega-3 fatty acids and vitamin B₁₂ [70, 71]. Adverse maternal, fetal and pregnancy outcomes resulting from carbohydrate, lipid and protein malnutrition are summarised in sections 1.2.4-1.2.7.

1.2.2. Impacts of maternal global undernutrition during pregnancy

Under-nutrition during pregnancy can be caused by acute changes resulting from hyperemesis gravidum, short-term changes in food availability due to seasonal variations such as wet and dry seasons, and longer-lasting phenomena such as famine (Table 1.1). Acute under-nutrition resulting from hyperemesis gravidum, is associated with adverse maternal and fetal outcomes such as weight-loss, dehydration, micronutrient deficiencies, low birth weight and preterm birth [72, 73]. Under-nutrition caused by seasonal variations in food availability is associated with decreased GWG and an increased risk of low birth weight (Table 1.1, [74, 75]). Long-term under-nutrition can be caused by natural disasters such as flooding, draught and crop failure, but also by human-made circumstances such as global and localised civil unrest and conflict (Table 1.1 [76, 77]). The Great Chinese Famine of 1959-1961 is regarded as one of the most severe famines in recent history caused by natural disasters, and was the result of devastating country-wide crop failures. The resulting famine caused an estimated 30 million deaths, and the loss of 33 million pregnancies [78]. Furthermore, adult women who were exposed to famine *in utero* are 30% more likely to suffer a stillbirth in their own pregnancies [78]. Although scarce records exist regarding daily energy intake during this time, it is estimated that the daily energy intake was ≤ 1500 kcal per day due to nation-wide food rationing [79, 80]. Recent research examining the long-term health complications of infants born during the famine reported that they are at greater risk of developing obesity, metabolic syndrome [81] and hypertension [82]. Interestingly, females who were born during the famine period were reported to be 20-30% more likely to suffer loss of pregnancy due to stillbirth compared to unexposed females. The Dutch Hunger Winter of 1944-1945 during World War II is another well-studied example of human-made famine, caused by severe country-wide food shortages due to an embargo on the transport of food supplies by Allied forces imposed by the German occupying forces. This led to food rationing, which consisted almost exclusively of bread and potatoes by April 1945, and provided an estimated daily energy intake of 500 kcal (Table 1.1, [76]). Pregnancies which occurred throughout the famine period were characterised by a near 5-fold reduction in 3rd trimester GWG, a 4-fold

increase in the prevalence of pre-term delivery in parallel with a 10% decrease in birthweight, and a 2.5-fold increase in the prevalence of small for gestational age infants compared to unexposed pregnancies (Table 1.1).

Low GWG, defined as GWG below recommended IOM guidelines, provides another marker of maternal undernutrition during pregnancy. In observational human studies, acute and chronic undernutrition during pregnancy have been associated with a range of adverse maternal and fetal outcomes (Table 1.1). These include increased risk of hypertensive disorders of pregnancy such as preeclampsia and pregnancy-induced hypertension, gestational diabetes mellitus, preterm birth, small for gestational age and low birthweight offspring (Table 1.1). Furthermore, findings of a greater risk of hypertensive disorders of pregnancy in women with low GWG, including preeclampsia and pregnancy-induced hypertension, are consistent across available studies and pre-pregnancy BMI weight categories (Table 1.1). It should be noted that the risk of preterm birth and SGA associated with low GWG is observed globally across different ethnic population groups [2].

Table 1.1 Under-nutrition, low GWG and pregnancy outcomes: Evidence from human observational studies

Context	Exposure group(s)	Comparison group	Outcomes compared to comparison group		
			Maternal	Pregnancy	Fetal/neonate/ newborn
Under-nutrition during pregnancy					
Dutch Hunger Winter [76]	Singleton births between Aug 1 st 1944 and Apr 15 th 1946 (famine exposed). DEI <1000 kcal/day by Jan 1945, <500 kcal/day by Apr 1945.	Singleton births before Feb 1 st 1945 and after Dec 31 st 1945.	3 rd trimester GWG ▼4.8-fold (0.05 kg/week vs 0.24 kg/week) between August 1944 and April 1946	PTD prevalence ▲4-fold when exposed to famine at any stage of pregnancy vs unexposed pregnancy	BW and crown-heel length ▼10%, ▲2.5-fold in prevalence of SGA when exposed to famine during the 3 rd trimester
Dutch Hunger Winter [77]	Births between Feb 1 st 1945 and Mar 31 st 1946. DEI <1000 kcal/day by Jan 1945, <500 kcal/day by Apr 1945.	Births between 1943 and 1947 whose mothers were not exposed to famine at any stage of pregnancy	Not assessed	◀▶ prevalence of miscarriage, abortion, neonatal mortality or PTD	▼ BW (male 5%, female 4%)
Rural Gambia (Dec 1978 – Nov 1979) [74]	Males born from 1976-1980 during seasonal periods of lower energy intake (wet season, 1200-1400 kcal/day) and higher physical activity level	Males born from 1976-1980 during seasonal periods of adequate energy intake (dry season, 1500-1600 kcal/day).	Not assessed	Not assessed	BW ▼10% during periods of reduced energy intake and increased physical activity level (1200-1400 kcal/day)

Rural Gambia 1977 [75]	Women in the 3 rd trimester of pregnancy during the wet season (Jun-Sep: average DEI 1435 kcal/43 g protein per day)	Women in the 3 rd trimester of pregnancy during the dry season (Feb-May: average DEI 1524 kcal/49 g protein per day)	3 rd trimester GWG ▼8-fold during wet season vs dry season	Not assessed	Increased risk of LBW (<2500 g) when 3 rd trimester DEI <1600 kcal/day
---------------------------	--	--	---	--------------	--

Low GWG during pregnancy (outcomes sub-divided according to pre-pregnancy BMI)

Retrospective cohort study – Taiwan [64]	GWG < IOM guidelines	GWG within IOM guidelines	UW: PE and GDM risk ▲1.7- fold	UW: PROM risk ▲1.3- fold	UW: LBW risk ▲2.4- fold, SGA risk ▲2.2- fold
			NW: PE risk ▲1.1-fold, GDM risk ▲1.5-fold	NW: PROM risk ◀▶	NW: LBW risk ▲1.7- fold, SGA risk ▲1.6- fold
			OW/OB: PE risk ◀▶, GDM risk ▲1.8-fold	OW/OB: PROM risk ▲7-fold	OW/OB: LBW risk ▲2.3-fold, SGA risk ▲1.3-fold

Retrospective cohort study – Japan [63]

GWG < IOM guidelines

GWG within IOM guidelines

UW: PIH risk ◀▶, GDM risk ▲1.7-fold

UW: PTD risk ▲3.9-fold, PROM risk ▲3.4-fold

UW: SGA risk ▲2.1-fold

NW: PIH risk ◀▶, GDM risk ▲1.8-fold

NW: PTD risk ▲3-fold, PROM risk ▲2.9-fold

NW: SGA risk ▲1.8-fold

OW: PIH risk ◀▶, GDM risk ▲1.7-fold

OW: PTD risk ▲2.4-fold, PROM risk ▲2.2-fold

OW: SGA risk ▲1.5-fold

OB: PIH risk ◀▶, GDM risk ▲1.7-fold

OB: PTD risk ▲1.5-fold, PROM risk ▲1.3-fold

OB: SGA risk ▲1.6-fold

Retrospective cohort study – China [83]

GWG < IOM guidelines

GWG within IOM guidelines

UW: GDM & PIH risk ◀▶

UW: PTD risk ▲1.4-fold, C-sect risk ◀▶

UW: LBW risk ▲1.5-fold, SGA risk ▲2.2-fold

NW: GDM risk ▲1.3-fold, PIH risk ▲1.1-fold

NW: PTD risk ▲1.5-fold, C-sect risk ◀▶

NW: LBW risk ▲1.2-fold, SGA risk ▲1.5-fold

OW: GDM risk ▲1.8-fold, PIH risk ◀▶

OW: PTD risk ▲1.7-fold, C-sect risk ▲1.3-fold

OW: LBW risk ▲1.2-fold, SGA risk ◀▶

OB: GDM risk ◀▶, PIH risk ▲6.6-fold

OB: PTD risk ▲2.5-fold, C-sect risk ▲1.8-fold

OB: LBW risk ▲3.9-fold, SGA risk ▲1.2-fold

Retrospective cohort study – USA [65]	GWG < IOM guidelines	GWG within IOM guidelines	UW: PE risk ▲2.5-fold, PIH risk ◀▶	UW: PTD risk ▲1.2-fold, C-sect risk ◀▶	UW: SGA risk ▲1.6-fold
			NW: PE risk ▲1.3-fold, PIH risk ◀▶	NW: PTD risk ▲2-fold, C-sect risk ◀▶	NW: SGA risk ▲1.3-fold
			OW: PE and PIH risk ◀▶	OW: PTD and C-sect risk ◀▶	OW: SGA risk ◀▶
			OB: PE risk ▲1.1-fold, PIH risk ◀▶	OB: PTD and C-sect risk ◀▶	OB: SGA risk ▲1.7-fold
Retrospective cohort study – European, North American & Australian cohorts [84]	GWG < IOM guidelines	GWG within IOM guidelines	UW: PE & PIH risk ◀▶, GDM risk ▲1.4-fold	UW: PTD risk ▲1.8-fold	UW: SGA risk ▲3.1-fold
			NW: PE, PIH & GDM risk ◀▶	NW: PTD risk ▲1.2-fold	NW: SGA risk ▲1.8-fold
			OW: PE risk ▲1.9-fold, PIH risk ▲1.5-fold, GDM risk ▲1.9-fold	OW: PTD risk ▲1.2-fold	OW: SGA risk ▲1.2-fold
			OB: PE risk ▲3.5-fold, PIH risk ▲3.1-fold, GDM risk ▲4.4-fold	OB: PTD risk ▲1.4-fold	OB: SGA risk ◀▶

Retrospective cohort study – Brazil [85]	GWG < IOM guidelines	GWG within IOM guidelines	UW: HDP and GDM risks ◀▶	UW: C-sect risk ◀▶	Not assessed
			NW: HDP and GDM risks ◀▶	NW: C-sect risk ◀▶	
			OW: HDP and GDM risks ◀▶	OW: C-sect risk ◀▶	
			OB: HDP and GDM risks ◀▶	OB: C-sect risk ◀▶	

BMI = body mass index, BW = body weight, DEI = daily energy intake, GDM = gestational diabetes mellitus, GWG = gestational weight gain, HDP = hypertensive disorders of pregnancy, IOM = Institute of Medicine guidelines 2009, LBW = low birth weight, NW = normal weight (BMI = 18.5-24.9 kg/m²), OB = obese (BMI ≥ 30 kg/m²), OW = overweight (BMI = 25-29.9 kg/m²), PAL = physical activity level, PE = preeclampsia, PIH = pregnancy-induced hypertension, PROM = premature rupture of membranes, PTD = preterm delivery, SGA = small for gestational age, UW = underweight (BMI ≤18.5 kg/m²)

The availability of nutrients to support pregnancy depends at least partially on maternal nutritional status entering pregnancy, reflected by pre-pregnancy BMI. Interestingly, a pre-pregnancy low BMI (<18.5 kg/m²) does not increase the risk of pregnancy-induced hypertension, preeclampsia or gestational diabetes mellitus compared to normal BMI (18.5-24.9 kg/m²), while effects on the risk of preterm delivery varies between studies (Table 1.2, [63, 64, 83, 84, 86]). There was however an increased risk of small for gestational age offspring identified in the pre-pregnancy low compared to pre-pregnancy normal BMI groups (Table 1.2) [63, 64, 83, 84, 86]. In a cohort of Chinese women with pre-pregnancy low BMI, 3rd trimester systolic and diastolic blood pressure, in addition to the incidence of caesarean delivery and preterm delivery, were lower than those in women with pre-pregnancy normal BMI [83]. Conversely, the incidence of small for gestational age and low birth weight infants were higher in women with pre-pregnancy low BMI compared to women with pre-pregnancy normal BMI (Table 1.2). It is important to note that pre-pregnancy low BMI may not reflect maternal diet throughout pregnancy, which may improve based on primary care nutritional advice at pregnancy care visits. Furthermore, challenges assessing the impact of any dietary change during pregnancy (relative to pre-pregnancy) on maternal outcomes is a limitation of observational studies, where diet composition pre-pregnancy is often not determined.

Table 1.2 Pre-pregnancy low BMI and pregnancy outcomes: Evidence from human observational studies

Context	Exposure group	Comparison group	Outcomes relative to comparison group		
			Maternal	Pregnancy	Fetal/neonate/ newborn
Retrospective cohort study – Taiwan [64]	Pre-pregnancy BMI <18.5 kg/m ²	Pre-pregnancy BMI 18.5-24.9 kg/m ²	PE & GDM risks ◀▶	PTD risk ◀▶	SGA risk ▲2-fold
Retrospective cohort study – Japan [63]	Pre-pregnancy BMI <18.5 kg/m ²	Pre-pregnancy BMI 18.5-24.9 kg/m ²	PIH & GDM risks ◀▶	PTD risk ▲1.2-fold, C-sect & PPH with C-sect risk ◀▶	SGA risk ▲1.7-fold
Retrospective cohort study – China [83]	Pre-pregnancy BMI <18.5 kg/m ²	Pre-pregnancy BMI 18.5-23.9 kg/m ²	3 rd trimester systolic BP: 105 vs 108, diastolic BP: 67 vs 69	Incidence of C-sect: 55.1% vs 63.1%, PTD: 2.6% vs 2.9%	Incidence of SGA: 15.5% vs 9%, LBW: 2.9% vs 2%
Retrospective cohort study – European, North American & Australian cohorts [84]	Pre-pregnancy BMI <18.5 kg/m ²	Pre-pregnancy BMI 18.5-23.9 kg/m ²	PIH, PE & GDM risks ◀▶	PTD risk ▲1.2-fold	SGA risk ▲1.7-fold
Retrospective cohort study – Australia [86]	Pre-pregnancy BMI <18 kg/m ²	Pre-pregnancy BMI 19-24 kg/m ²	PIH & GDM risks ◀▶	C-sect risk ◀▶	SGA risk ▲1.8-fold, LBW risk ▲1.7-fold

BMI = body mass index, BP = blood pressure (mmHg), C-sect = caesarean section, GDM = gestational diabetes mellitus, GWG = gestational weight gain, LBW = low birth weight (<2500 g), PE = preeclampsia, PIH = pregnancy-induced hypertension, PPH = postpartum haemorrhage, PTD = preterm delivery, SGA = small for gestational age

Animal models of food restriction before and/or throughout pregnancy have been used to study the effects of acute and chronic food restriction on maternal, fetal and pregnancy outcomes. Acute and chronic food restriction result in lower GWG, increased risk of spontaneous abortion and fetal growth restriction in rats, mice and guinea pigs (Table 1.3). Interestingly, the effect of similar levels of maternal food restriction during pregnancy on fetal birth weight differs between humans and rodents. In humans, mild to moderate maternal food restriction reduces birthweight 5-10%, compared to a 60% reduction in Wistar rats (Table 1.3). A possible reason for this difference may relate to the difference in the ratio of maternal to fetal weight at birth which is an indicator of maternal load [17].

In addition to effects on pregnancy and progeny, maternal malnutrition also causes adverse fetal outcomes beyond the first generation in mice. For example, in a study of undernutrition in late pregnancy, Jimenez-Chillaron et al. fed F₀ dams 50% of the food eaten by controls, from GD12.5-GD18.5. When their F₁ female offspring (termed intrauterine calorie restricted mice) were fed *ad libitum* from birth until weaning and then mated with malnourished F₁ males, F₂ generation birth weights were reduced by 4% compared to birth weights in litters from F₁ females born to control F₀ dams *ad libitum* fed from birth until weaning and mated with control F₁ males [87]. Total body fat mass and serum leptin concentrations of F₂ males born to F₁ malnourished females were both increased by > 1.5-fold at 4 months of age compared to F₂ males born to control F₁ females [87]. Furthermore, the same F₂ males were glucose intolerant and insulin resistant, based on elevated blood glucose and insulin concentrations following intraperitoneal tolerance tests at 6 months of age, and had >2-fold higher plasma insulin concentrations (hyperinsulinaemia) than control F₂ males at 8 months of age [87].

Table 1.3 Global under-nutrition and pregnancy outcomes: Evidence from intervention studies in non-human animals

Species, strain (term)	Intervention/exposure group(s)	Control group	Outcomes compared to control group		
			Maternal	Pregnancy	Fetal/neonate/newborn
Guinea pig, N/S (70 d) [88]	Mild FR (85% <i>ad libitum</i> food intake/kg BW 4 weeks prior to and throughout pregnancy) or moderate FR (70% <i>ad libitum</i> food intake per kg/BW) 4 weeks prior to mating until GD35, then 90% <i>ad libitum</i> food intake until term	<i>Ad libitum</i> fed 4 weeks prior to mating and throughout pregnancy	15 & 30% FR: GWG ▼20% at GD63	Moderate FR: 2 cases of spontaneous abortion at GD50-55	15% FR: BW ▼10% (both sexes), AC ▼10% (males only), 30% FR: BW & BL ▼10% (males only) at birth
Rat, Wistar (22 d) [89]	FR (75% of control <i>ad libitum</i> food intake) throughout pregnancy	<i>Ad libitum</i> fed throughout pregnancy	GWG ▼60% at term	Not assessed	BW ◀▶ at PND1

Mouse, C57BL/6 (19 d) [90]	FR (50% of control <i>ad libitum</i> food intake) from GD10-18.5	<i>Ad libitum</i> fed throughout pregnancy	placental weight ▼60%, placental GLUT3 protein expression ▼50%, placental SNAT1&2 expression ▲2.5-3 fold, intra and trans-placental glucose transfer ▼50-70%, intra- and trans-placental leucine transfer ▼40-60% at GD18.5	Not assessed	BW ▼50% at GD18.5
Mouse, ICR (19-21 d) [91]	FR (50%) GD12.5-18.5	<i>Ad libitum</i> fed throughout pregnancy	Not assessed	Not assessed	BW ▼40% at GD16.5 and birth

BL = body length, BW = body weight, FR = food restriction, GD = gestational day, GLUT3 = glucose transporter 3, GWG = gestational weight gain, IUGR = intrauterine growth restriction, N/S = not stated, PND = postnatal day, SNAT1&2 = sodium-dependent neutral amino acid transporter 1 and 2

1.2.3. Over-nutrition, obesity and pregnancy outcomes

In humans, high GWG (i.e. GWG exceeding IOM guidelines [4]) is associated with adverse maternal and fetal outcomes such as an increased risk of pregnancy-induced hypertension, preeclampsia, caesarean delivery, postpartum haemorrhage after caesarean delivery, preterm delivery, macrosomia (birthweight > 4000 g) and large for gestational age infants, irrespective of pre-pregnancy BMI (Table 1.4). However, despite similar GWG, an increased risk of adverse outcomes was apparent in some studies but not all (Table 1.4). Nonetheless, it should be noted that the overall greater risk of caesarean delivery, large for gestational age (LGA) infants and macrosomia associated with high GWG was not confined to a single population, ethnic group or geographic region [2].

Table 1.4 High GWG and pregnancy outcomes: Evidence from human observational studies

Context	Exposure group	Comparison group	Outcomes relative to comparison group		
			Maternal	Pregnancy	Fetal/neonate/newborn
Retrospective cohort study – Taiwan [64]	GWG > IOM guidelines	GWG within IOM guidelines	UW: PE risk ▲4.6-fold, GDM risk ◀▶	UW: C-sect risk ▲2.3-fold, PTD risk ▲1.2-fold	UW: LGA risk ▲2.6-fold, macrosomia risk ▲5.7-fold
			NW: PE risk ▲3.7-fold, GDM risk ◀▶	NW: C-sect risk ▲1.4-fold, PTD risk ◀▶	NW: LGA risk ▲1.8-fold, macrosomia risk ▲2.2-fold
			OW/OB: PE risk ▲1.2-fold, GDM risk ◀▶	OW/OB: C-sect risk ▲1.3-fold, PTD risk ◀▶	OW/OB: LGA risk ▲1.3-fold, macrosomia risk ▲2.5-fold
Retrospective cohort study – Japan [63]	GWG > IOM guidelines	GWG within IOM guidelines	UW: PIH risk ▲2.4-fold, GDM & PTD risks ◀▶	UW: C-sect risk ▲1.2-fold, PPH with C-sect risk ▲1.4-fold, PTD risk ◀▶	UW: LGA risk ▲1.4-fold, macrosomia risk ▲5.3-fold
			NW: PIH risk ▲1.9-fold, GDM risk ▲1.5-fold, PTD risk ◀▶	NW: C-sect risk ▲1.4-fold, PPH with C-sect risk ▲1.4-fold, PTD risk ◀▶	NW: LGA risk ▲1.7-fold, macrosomia risk ▲2.7-fold
			OW: PIH risk ▲1.5-fold, GDM and PTD risk ◀▶	OW: C-sect risk ▲1.2-fold, PPH with C-sect risk ▲1.1-fold, PTD risk ◀▶	OW: LGA risk ▲1.7-fold, macrosomia risk ▲3.1-fold
			OB: GDM and PIH risk ◀▶	OB: PPH with C-sect risk ▲1.5-fold, C-sect and PTD risk ◀▶	OB: LGA risk ▲1.5-fold, macrosomia risk ▲1.6-fold

Retrospective cohort study – China [83]	GWG > IOM guidelines	GWG within IOM guidelines	<p>UW: GDM & PIH risks ◀▶</p> <p>NW: GDM risk ◀▶, PIH risk ▲1.4-fold</p> <p>OW: GDM risk ▲1.6-fold, PIH risk ▲2.4-fold</p> <p>OB: GDM risk ▲2.2-fold, PIH risk ▲6-fold</p>	<p>UW: C-sect risk ▲1.2-fold, PTD risk ◀▶</p> <p>NW: C-sect risk ▲1.3-fold, PTD risk ◀▶</p> <p>OW: C-sect risk ▲1.9-fold, PTD risk ◀▶</p> <p>OB: C-sect risk ▲2.9-fold, PTD risk ▲1.5-fold</p>	<p>UW: LGA & macrosomia risks ◀▶</p> <p>NW: LGA & macrosomia risks ▲1.9-fold</p> <p>OW: LGA risk ▲2.6-fold, macrosomia risk ▲2.7-fold</p> <p>OB: LGA risk ▲4-fold, macrosomia risk ▲4.1-fold</p>
Retrospective cohort – USA [65]	GWG > IOM guidelines	GWG within IOM guidelines	<p>UW: PIH risk ▲2-fold, PE risk ▲3.6-fold</p> <p>NW: PIH risk ▲1.5-fold, PE risk ▲2.5-fold</p> <p>OW: PIH risk ▲1.4-fold, PE risk ▲4.2-fold</p> <p>OB: PIH risk ▲1.2-fold, PE risk ▲1.9-fold</p>	<p>UW: C-sect risk ▲1.3-fold, PTD risk ◀▶</p> <p>NW: C-sect risk ▲1.6-fold, PTD risk ◀▶</p> <p>OW: C-sect risk ▲1.8-fold, PTD risk ▲1.2-fold</p> <p>OB: C-sect risk ▲1.1-fold, PTD risk ▲1.3-fold</p>	<p>UW: LGA risk ▲2.5-fold</p> <p>NW: LGA risk ▲1.7-fold</p> <p>OW: LGA risk ▲2.5-fold</p> <p>OB: LGA risk ▲1.9-fold</p>
Retrospective cohort – Poland [101]	GWG > IOM guidelines	GWG within IOM guidelines	<p>GDM risk ▲1.7-fold, PIH risk ▲5.9-fold</p>	<p>C-sect risk ▲2.7-fold</p>	<p>Macrosomia risk ▲6.9-fold</p>

Retrospective cohort study – European, North American & Australian cohorts [84]	GWG > IOM guidelines	GWG within IOM guidelines	<p>UW: PIH, PE & GDM risks ◀▶</p> <p>NW: PIH risk ▲1.4-fold, PE risk ▲1.2-fold, GDM risk ▲1.3-fold</p> <p>OW: PIH risk ▲2.7-fold, PE risk ▲2.5-fold, GDM risk ▲3.5-fold</p> <p>OB: PIH risk ▲4.5-fold, PE risk ▲4.6-fold, GDM risk ▲7.8-fold</p>	<p>UW: PTD risk ◀▶</p> <p>NW: PTD risk ▲1.3-fold</p> <p>OW: PTD risk ▲1.5-fold</p> <p>OB: PTD risk ▲2.1-fold</p>	<p>UW: LGA risk ◀▶</p> <p>NW: LGA risk ▲2.3-fold</p> <p>OW: LGA risk ▲3.5-fold</p> <p>OB: LGA risk ▲4.8-fold</p>
Retrospective cohort study – Brazil [85]	GWG > IOM guidelines	GWG within IOM guidelines	<p>UW: HDP and GDM risks ◀▶</p> <p>NW: HDP risk ▲3.6-fold, GDM risk ◀▶</p> <p>OW: HDP risk ▲2.4-fold, GDM risk ◀▶</p> <p>*OB: HDP risk ▲2.5-fold, GDM risk ◀▶</p>	<p>UW: C-sect risk ◀▶</p> <p>NW: C-sect risk ▲1.8-fold</p> <p>OW: C-sect risk ▲1.8-fold</p> <p>*OB: C-sect risk ▲1.9-fold</p>	Not assessed

BMI = body mass index, CS = caesarean section, GDM = gestational diabetes mellitus, GWG = gestational weight gain, IOM = Institute of Medicine 2009 guidelines [20], HDP = hypertensive disorders of pregnancy, LGA = large for gestational age, macrosomia = birthweight >4000 g, NW = normal weight (BMI 18.5-24.9 kg/m²), OB = obese (BMI ≥30 kg/m²), OW = overweight (BMI 25-29.9 kg/m²), PE = preeclampsia, PIH = pregnancy-induced hypertension, PPH = postpartum haemorrhage, PTD = preterm delivery, UW = underweight (BMI ≤18.5 kg/m²)

In 2016, 1.9 billion adults globally were overweight, while 650 million adults were obese (World Health Organization, [102]). In recent decades, the prevalence of maternal obesity has increased in developed countries including the USA, Australia and the UK [103, 104]. The prevalence of maternal obesity amongst adults aged 20 years or older increased from 26% in 2016 to 29% in 2019 in the USA [105]. In 2006, more than a third of Australian women aged 25-35 were overweight or obese [104]. In 2021, 28% and 24% of Australian mothers who gave birth were overweight and obese, respectively [106]. In England, the prevalence of maternal obesity was 19% in the early 2000s [104]. A key driver behind the increase in obesity prevalence is the habitual over-consumption of diets containing highly processed foods, which typically contain high concentrations of sodium, fats and carbohydrates, termed the 'Western' or 'Cafeteria'-style diet (WSD, [71]). The WSD also lacks certain amino acids, minerals and vitamins which are derived predominantly from plant products such as fruits, nuts, leafy green vegetables, and dairy products. To study the risk of adverse outcomes associated with over-nutrition and obesity before and during pregnancy, animal models have utilised experimental diets enriched with fat, carbohydrate, or both, which mimic a WSD.

Pre-pregnancy high BMI is an important indicator of nutritional status to consider when studying adverse pregnancy outcomes such as a higher risk of gestational diabetes, preeclampsia, hypertension, preterm and caesarean delivery, macrosomia, and large for gestational age progeny compared to outcomes in women with a normal pre-pregnancy BMI (Table 1.5).

Table 1.5 Pre-pregnancy high BMI and pregnancy outcomes: Evidence from human observational studies

Context	Exposure group	Comparison group	Outcomes relative to comparison group		
			Maternal	Pregnancy	Fetal/neonate/ newborn
Retrospective cohort study – Taiwan [64]	Pre-pregnancy BMI 25-29.9 kg/m ²	Pre-pregnancy BMI 18.5-24.9 kg/m ²	PE risk ▲3.7-fold, GDM risk ▲2.2 fold	PTD risk ▲1.1-fold	LGA risk ▲1.9-fold, macrosomia risk ▲1.8-fold
	Pre-pregnancy BMI >30 kg/m ²		PE risk ▲7.9-fold, GDM risk ▲3.8 fold	PTD risk ▲1.9-fold	LGA risk ▲2.3-fold, macrosomia risk ▲2.5-fold
Retrospective cohort study – Japan [63]	Pre-pregnancy BMI 25-29.9 kg/m ²	Pre-pregnancy BMI 18.5-24.9 kg/m ²	PIH risk ▲2.4-fold, GDM risk ▲2.9-fold	PTD risk ▲1.1-fold, CS risk ▲1.5-fold, PPH with CS risk ▲1.5-fold	LGA risk ▲2-fold, macrosomia risk ▲2.6-fold
	Pre-pregnancy BMI >30 kg/m ²		PIH risk ▲3.7-fold, GDM risk ▲6.6-fold	PTD risk ▲1.2-fold, CS risk ▲2-fold, PPH with CS risk ▲1.9-fold	LGA risk ▲2.7-fold, macrosomia risk ▲4.6-fold
Retrospective cohort study – China [83]	Pre-pregnancy BMI 24-27.9 kg/m ²	Pre-pregnancy BMI 18.5-23.9 kg/m ²	3 rd trimester systolic BP: 112 vs 108, diastolic BP: 72 vs 69	Incidence of CS: 75.3% vs 63.1%, PTD: 3.4% vs 2.9%	Incidence of LGA: 14.9% vs 9.1%, macrosomia: 14.1% vs 8.6%
	Pre-pregnancy BMI >28 kg/m ²		3 rd trimester systolic BP: 116 vs 108, diastolic BP: 75 vs 69	Incidence of CS: 83.6% vs 63.1%, PTD: 4.9% vs 2.9%	Incidence of LGA: 22.6% vs 5.1%, macrosomia: 20.0% vs 8.6%

Retrospective cohort study – European, North American & Australian cohorts [84]	Pre-pregnancy BMI 25-29.9 kg/m ²		PIH risk ▲2-fold, PE risk ▲2-fold, GDM risk ▲2.2-fold	PTD risk ▲1.1-fold	LGA risk ▲1.6-fold
	Pre-pregnancy BMI >30 kg/m ²	Pre-pregnancy BMI 18.5-24.9 kg/m ²	PIH risk ▲3.3- to 5.4-fold, PE risk ▲3.2- to 6.5-fold, GDM risk ▲4- to 7.6-fold	PTD risk ▲1.3- to 1.5-fold	LGA risk ▲2.2- to 3.1-fold
Retrospective cohort study – Australia [86]	Pre-pregnancy BMI 25-29 kg/m ²		PIH risk ▲2-fold, GDM risk ▲2-2-fold	CS risk ▲1.3-fold	LGA risk ▲1.6-fold, macrosomia risk ▲1.5-fold
	Pre-pregnancy BMI >30 kg/m ²	Pre-pregnancy BMI 19-24 kg/m ²	PIH risk ▲3.4- to 8.9-fold, GDM risk ▲3.5- to 7.8-fold	CS risk ▲1.8- to 2.7-fold	LGA risk ▲2- to 2.7-fold, macrosomia risk ▲1.5- to 1.9-fold

BMI = body mass index, CS = caesarean section, GWG = gestational weight gain, LGA = large for gestational age, macrosomia = birthweight >4000 g, NW = normal weight (BMI 18.5-24.9 kg/m²), OB = obese (BMI ≥30 kg/m²), OW = overweight (BMI 25-29.9 kg/m²), PE = preeclampsia, PIH = pregnancy-induced hypertension, GDM = gestational diabetes mellitus, PTD = preterm delivery, PPH = postpartum haemorrhage, UW = underweight

Animal models of over-nutrition during pregnancy and high GWG report similar adverse maternal, fetal and progeny outcomes across different species. For example, progeny of obese sheep fed 150% of their nutritional requirement (1.5x ration of recommended energy requirement based on bodyweight) prior to and throughout pregnancy are heavier, while plasma glucose, insulin, cholesterol and triglycerides are elevated at mid- and late-gestation compared to progeny from sheep fed a normal diet (Table 1.6, [92-95, 107]). Weight and crown-rump length were similar at birth, but plasma glucose and cortisol remained elevated. Furthermore, ewes born to over-fed obese sheep displayed increased appetite, growth rate, insulin resistance and plasma leptin in adulthood. Maternal obesity and/or over-nutrition during pregnancy is also associated with an increased risk of maternal dyslipidaemia, insulin resistance and hypertension in rodents and rabbits [96, 97]; while their offspring were at greater risk of cardiovascular and chronic kidney disease [97-99]. More detailed overview summaries of evidence from animal models detailing the consequences of chronic maternal over-nutrition on maternal, progeny and pregnancy outcomes and proposed mechanisms involved are available elsewhere [3, 100].

Table 1.6 Global over-nutrition and pregnancy outcomes: Evidence from intervention studies in sheep

Species, strain (term)	Intervention/ exposure group(s)	Control group	Outcomes compared to control group		
			Maternal	Pregnancy	Fetal/neonate/ newborn
Sheep (150 d) [93]	Over-nutrition (150% of control diet) 60 days prior to, and throughout pregnancy	Control diet throughout pregnancy	Insulin AUC ▲3.5-fold following OGTT at GD75	Not assessed	BW ▲1.3-fold, adiposity ▲1.6-fold, heart weight ▲1.3-fold, brain weight ▲1.4-fold, kidney & liver weight ▲1.5-fold, pancreas weight ▲3.4-fold at GD75
Sheep (150 d) [94]	Over-nutrition (150% of control diet) 60 days prior to, and throughout pregnancy	Control diet throughout pregnancy	BW ▲1.4-fold at GD75, ▲1.6-fold at GD135, plasma cholesterol ▲1.2-fold, leptin ▲2.9-fold at GD75, plasma cholesterol ▲1.3-fold, leptin 1.4-fold at GD135	Placental FATP1, FATP4 & CD36 gene expression ▲1.2-2 fold at GD75, ▲1.7-2.3 fold at GD135. Placental FATP1 & FATP4 protein content ▲1.3-1.5 fold at GD75, FATP4 protein content ▲1.3-fold at GD135	Plasma cholesterol & triglyceride ▲1.2-fold at GD75, plasma cholesterol ▲1.4-fold at GD135
Sheep (150 d) [107]	Over-nutrition (150% of control diet) 60 days prior to, and throughout pregnancy	Control diet throughout pregnancy	Following IVGTT, plasma glucose AUC ▲1.3-fold, plasma insulin AUC ▲2.5-fold at GD75, plasma glucose AUC ▲1.3-fold, plasma	Not assessed	Not assessed

			insulin AUC ▲2.4- fold at GD135	
Sheep (150 d) [108]	Over-nutrition (150% of control diet) 60 days prior to, and throughout pregnancy	Control diet throughout pregnancy	BW ▲1.3-fold at GD135	BW ◀▶ at GD135, sub-cutaneous adipose tissue CD36, FATP1, FATP4, GLUT4, FABP1, FABP4 & FABP5 gene expression ▲3-16 fold at GD135

AUC = area under curve, BW = body weight, CD36 = cluster of differentiation 36, FABP1 = fatty acid binding protein 1, FABP4 = fatty acid binding protein 4, FABP5 = fatty acid binding protein 5, FATP1 = fatty acid transporter 1, FATP4 = fatty acid transporter 4, GD = gestational day, GLUT4 = glucose transporter 4, IVGTT = intravenous glucose tolerance test, OGTT = oral glucose tolerance test,

The sections below (1.2.4-1.2.7) describe consequences of macronutrient malnutrition. Due to ethical constraints associated with performing dietary-intervention studies in humans, animal models utilising experimental diets are instead used to interrogate the consequences of maternal macronutrient malnutrition. Whilst experimental diets aim to mimic the Western/cafeteria-style diet consumed particularly in developed countries, these diets have limitations due to their macronutrient composition. Therefore, adverse maternal, pregnancy and fetal outcomes may arise due to relative protein restriction if high fat and/or high sugar diet(s) are isocaloric, or caloric overconsumption if the high fat and/or high sugar diet(s) are non-isocaloric, relative to the control diet. These factors are important and need to be considered when interpreting preclinical findings.

1.2.4. Excess carbohydrate intake

Evidence is accumulating that excess intake of individual macronutrients, such as carbohydrate, exerts detrimental consequences on maternal, placental, fetal and progeny health. Current knowledge regarding excess maternal carbohydrate intake is primarily derived from diet intervention studies in animals. In these studies, animals are fed a high sugar (HS) diet enriched in carbohydrates in the form of sucrose, glucose, and fructose at over 60% of caloric content, before and/or throughout pregnancy. This HS diet contrasts with the typical composition of carbohydrates in control diets which are derived predominantly from di- and polysaccharides. As a result, this diet partly models WSDs consumed in developed countries [109].

Adverse outcomes associated with maternal consumption of a HS diet in rats prior to and/or throughout pregnancy include high GWG and maternal metabolic dysfunction characterised by impaired glucose tolerance and insulin sensitivity, increased adiposity, increased plasma lipids such as non-esterified fatty acids, and lower fetal body and organ weights at birth (Table 1.6, [110-113]). However, while reports of adverse outcomes are equivocal, there are inconsistencies between studies regarding the specific adverse outcomes identified.

Table 1.7 Maternal high sugar/carbohydrate (HS) diet consumption and pregnancy outcomes: Evidence from rodent models

Species, strain (term)	Intervention/exposure group(s)	Control group	Outcomes compared to control group(s)		
			Maternal	Pregnancy	Fetal/neonate/newborn
Rat, Wistar (22 d) [110]	HS diet (10% w/v sugar-sweetened beverage sweetened with high fructose corn syrup-55 or sucrose, 1.8 kJ·mL ⁻¹) 4 weeks prior to, and throughout pregnancy	Control diet (14 kJ·g ⁻¹) before and throughout pregnancy	Blood glucose ▲ 1.3-fold (10 min peak glucose concentration) after intraperitoneal glucose tolerance test in sucrose-fed dams (pre-pregnancy time-point), adiposity ▲ 1.6-fold in sucrose dams, plasma insulin ▲ 1.8-fold, non-esterified fatty acids ▼ 0.6-fold in high fructose corn syrup-55 fed dams	Not assessed	BW ◀▶, liver weight (% BW) ▼ 0.9-fold (pups from high fructose corn syrup-55-fed dams), adrenal gland weight (% BW) ▼ 0.8-fold (pups from sucrose-fed dams)
Rat, Wistar (22 d) [111]	HS diet – high glucose (53.76% of carbohydrates, 14.4 kJ·g ⁻¹) or high fructose (54.35% of carbohydrates, 14.4 kJ·g ⁻¹) throughout pregnancy	Control diet (starch 35.4%, sucrose 4.64% of carbohydrates, 14.2 kJ·g ⁻¹) throughout pregnancy	GWG ▼ 9% at GD15 – FRU dams	Not assessed	BW ▼ 7-11% (glucose and fructose groups respectively)

Rat, Wistar (22 d) [112]	HS diet (64% carbohydrates mainly from sucrose/fructose/glucose 2:1:1, 24% protein, 12% fat, 15.8 kJ g ⁻¹), fed for 6 weeks prior to, and throughout pregnancy	Control diet (64% carbohydrates (mainly from polysaccharides), 12% fat, 24% protein) 6 weeks prior to, and throughout pregnancy	GWG ◀▶	Not assessed	BW ▼ at PND3
Mouse, C57BL/6 (19 d) [113]	HS diet (70% carbohydrate, 20% protein, 10% fat, 16.1 kJ g ⁻¹) throughout pregnancy	HF diet (20% carbohydrate and protein, 60% fat, 21.9 kJ g ⁻¹) throughout pregnancy	GWG ▲ 1.2-fold in dams of the HF group (1 st pregnancy)	Not assessed	Adiposity ▲ 1.2-fold, liver weight (% BW) ▼ 10-30% in pups from HF compared to HS dams (1 st pregnancy), liver TRIG content ▼ 40-50% at birth in pups from HF to HS dams across 3 consecutive pregnancies

BW = bodyweight, GWG = gestational weight gain, HF = high fat, HS = high sugar, GLU = glucose, PND = postnatal day, TRIG = triglyceride

1.2.5. Excess lipid intake

Maternal excess lipid consumption also exerts detrimental consequences on maternal, placental, fetal and progeny health. Intake of a high-fat diet (HF, 40-60% kcal fat) before and/or throughout pregnancy is used to model excess fat intake during pregnancy in animals. These diets also model the excess fat composition of Western/cafeteria-style diets as consumed in developed countries [109].

Adverse outcomes associated with maternal consumption of a HF diet in non-human primate (NHP) and rodents before and/or throughout pregnancy include high GWG, maternal metabolic dysfunction characterised by impaired glucose tolerance and insulin sensitivity, increased maternal adiposity and circulating lipids, increased placental lipid content, placental dysfunction characterised by reduced placental weight and nutrient transporter transcript expression, reduced placental and uterine artery blood flows and fetal organ weights [113-118]. HF diet effects on birthweight, however, are inconsistent across available studies, with reports of no change, increased or decreased birthweight (Table 1.7).

Table 1.8 Maternal excess lipid consumption and pregnancy outcomes: Evidence from non-human primate and rodent models

Species, strain (term)	Intervention/exposure group(s)	Control group	Outcomes compared to control group(s)		
			Maternal	Pregnancy	Fetal/neonate/newborn
Japanese Macaque (175 d) [114]	HF diet (32% fat, isocaloric) for at least 4 years prior to and throughout pregnancy	Control diet (14% fat, isocaloric) for at least 4 years prior and throughout pregnancy	GWG ▲1.5-fold, plasma insulin ▲10.5-fold, plasma leptin ▲5.8-fold, total plasma triglycerides ▲1.4-fold at GD130	placental volume blood flow ▼40%, uterine artery volume blood flow ▼60%, placental true triglyceride content ▲1.2-fold at GD130	BW ◀▶ at GD130
Japanese Macaque (175 d) [115]	HF diet (14.9% fat, 55.5% carbohydrate, 17.1% protein, 12 kJ·g ⁻¹ , isocaloric) 2-4 years prior to, and throughout pregnancy	Control diet (5.5% fat, 70.8% carbohydrate, 20.6% protein, 15.9 kJ·g ⁻¹ , isocaloric) throughout pregnancy	GWG ◀▶, insulin AUC ▲3-fold following intraperitoneal insulin tolerance test, plasma leptin ▲2.2-fold, plasma glycerol ▲1.7-fold on GD130	Not assessed	BW ▼10%, plasma total triglyceride ▲1.8-fold, plasma glycerol ▲2-fold, liver triglycerides ▲3-fold at GD130.
Rhesus Macaque, N/S (168 d) [116]	HF diet (36% fat) for at least 3.5 years prior to and throughout pregnancy	Control diet (15% fat) for at least 4 years prior and throughout pregnancy	GWG ◀▶, adiposity ▲2-fold at term	Placental weight ◀▶, placental GLUT1 expression ▼40%, GLUT9 expression ▲1.8-fold	BW ◀▶

Rat, N/S (22 d) [117]	HF diet (cafeteria-style, includes food-items such as chips, cookies, biscuits and chocolate) 4 weeks prior to and throughout pregnancy	Control diet (17.9% protein, 7% fat, 57.8% carbohydrate, 16.1 kJ·g ⁻¹) 4 weeks prior to and throughout pregnancy	GWG ◀▶, adiposity ◀▶ both before pregnancy and after lactation	Not assessed	BW ◀▶ at PND3
Rat, N/S (22 d) [118]	HF diet (cafeteria-style, includes food-items such as jelly bean, cookies, biscuits and chocolate) throughout pregnancy	Control diet (55% carbohydrate, 22% protein, 4% fat) throughout pregnancy	Adiposity ▲ 1.8-fold, plasma insulin ▲ 1.9-fold, leptin ▲ 1.6-fold, triglycerides ▲ 1.4-fold	Not assessed	Litter weight ▲ 1.1-fold
Mouse, C57BL/6 (19 d) [113]	HS diet (70% carbohydrate, 20% protein, 10% fat, 16.1 kJ·g ⁻¹) or HF diet (20% carbohydrate and protein, 60% fat) throughout pregnancy	None	GWG ▲ 1.2-fold in dams of the HF group (1 st pregnancy)	Not assessed	Adiposity ▲ 1.2-fold, liver weight (% BW) ▼ 10-30% in pups from HF compared to HS dams (1 st pregnancy), liver TRIG content ▼ 40-50% at birth in pups from HF to HS dams across 3 consecutive pregnancies

AUC = area under curve, BW = bodyweight, GD = gestational day, GWG = gestational weight gain, GLUT1 = glucose transporter 1, GLUT9 = glucose transporter 9, HF = high fat, HS = high sugar, N/S = not stated, PND = postnatal day, TRIG = triglyceride

1.2.6. Protein supplementation and excess protein intake in adequately and malnourished subjects

Adequate protein intake during human pregnancy equates to 10-25% of total daily caloric intake and is derived from both animal and plant sources [119]. An important difference between animal and plant-derived protein is the availability of essential amino acids such as lysine and threonine; animal sources of protein contain all 9 essential amino acids whereas plant sources can be deficient in one or more such amino acid [119].

Although no human studies of protein-overconsumption during pregnancy have been reported, presumably due to ethical constraints, several observational studies have reported the effect of protein-supplementation during pregnancy in adequately nourished and malnourished women (Table 1.8). When malnourished women received a protein supplement daily from 28-38 weeks gestation, total GWG increased, but there was no difference in placental weight or birthweight compared to women who did not receive the protein supplement [120]. Furthermore, adequately nourished women who received the same supplement daily from 18-38 weeks gestation did not experience an increase in GWG, although birthweight increased (Table 1.8, [120]). Interestingly, infant birthweights of adequately nourished women who received a daily high protein bulk supplement, placebo or zinc gluconate were 10% lower compared to women who received a low bulk protein supplement (Table 1.8, [121]).

Table 1.9 Dietary protein supplementation and pregnancy outcomes: Evidence from human intervention studies

Context	Intervention/ exposure group(s)	Comparison group	Outcomes compared to comparison group		
			Maternal	Pregnancy	Fetal/neonate/ newborn
Protein supplementation during pregnancy [120]	Malnourished mothers - daily PrEnVi supplement from 18-38 weeks gestation	Malnourished mothers – daily Vi or EnVi supplement from 18-38 weeks gestation	<p>18-28 weeks: weekly GWG ▲ 1.3-fold compared to Vi supplement, ◀▶ compared to EnVi supplement.</p> <p>28-38 weeks: weekly GWG ◀▶ between supplement regimes</p>	Placental weight ◀▶	BW ◀▶

Protein supplementation during pregnancy [122]	Malnourished and adequately nourished mothers – daily PrEnVi supplement from 28-38 weeks gestation	Malnourished and adequately nourished mothers – daily Vi or EnVi supplement from 28-38 weeks gestation	Malnourished mothers: 3 rd trimester weekly GWG ▲1.6-fold when receiving PrEnVi supplement vs Vi or EnVi supplement Adequately nourished mothers: 3 rd trimester weekly GWG ◀▶ between supplement groups	Length of gestation and placental weight ◀▶ in both malnourished and adequately nourished mothers between supplementation regimes	Malnourished mothers: BW ▲1.1-fold when receiving PrEnVi supplement vs Vi or EnVi supplement. BL ◀▶ between supplement groups. Adequately nourished mothers: BW ▼1.1-fold when receiving PrEnVi supplement compared to Vi or EnVi supplement. BL ▼3% when receiving PrEnVi supplement compared to Vi or EnVi supplement.
Protein supplementation during pregnancy [121]	Adequately nourished mothers – High (53 g protein) or low (49 g protein) bulk supplement daily from 20 weeks gestation until term	Adequately nourished mothers – placebo or 30-90 mg zinc gluconate daily from 20 weeks gestation until term	GWG ◀▶ between all 4 groups	Not assessed	BW ▼1.1-fold when mothers received placebo, zinc gluconate or high bulk supplement compared to low bulk supplement

BL = birth length, BW = bodyweight, EnVi = vitamin supplement containing 3 mg iron and 30 mg Vitamin C in flavoured carbonated liquid glucose drink (369 ml) providing 273 kcal/day, PrEnVi = protein, energy and vitamin supplement containing 3 mg iron and 30 mg Vitamin C in flavoured carbonated liquid glucose drink (1/3rd bottle) + chocolate flavoured skimmed-milk powder (26 g daily) providing 11% protein, Vi = vitamin supplement containing 3 mg iron and 30 mg Vitamin C in flavoured carbonated water (369 ml)

When Sprague-Dawley rats were fed a protein-restricted diet from mating until GD17, then switched to a protein-supplemented diet from GD17 until term, or fed a protein-supplemented diet throughout pregnancy, both of these interventions resulted in elevated maternal adiposity, placental, fetal body and brain weights at term compared to control progeny (Table 1.9, [123]). Interestingly, when C57BL/6 mice were fed a protein supplement throughout pregnancy, placental expression of amino acid, fatty acid and carbohydrate transporter transcripts was higher, but placental and fetal body weight did not change (Table 1.9, [124]). Furthermore, when intrauterine calorie-restricted (ICR) mice were fed a protein-restricted diet supplemented with specific amino acids for two weeks before and throughout pregnancy, offspring bodyweight was similar at PND3 compared to offspring from dams fed a low-protein diet (Table 1.9, [125]). This suggests amino acid supplementation may improve fetal outcomes, in addition to potentially reversing adverse placental impacts in the setting of maternal low-protein consumption.

Table 1.10 Dietary protein supplementation and pregnancy outcomes: Evidence from studies in non-human primate and rodent models.

Species, strain (term)	Intervention/exposure group(s)	Control group	Outcomes compared to control group		
			Maternal	Pregnancy	Fetal/neonate/newborn
Protein supplementation of control diet					
Mouse, C57BL/6 (19 d) [124]	20% casein + 0.5% proline	20% casein	Not assessed	Placental amino acid (SNAT2, B(0)+, PAT4), fatty acid (FATP4) and glucose (GLUT1&3) transporter gene expression ▲1.2- to1.7-fold at GD12.5. Placental weight ◀▶ at term	Litter size & BW ◀▶ at birth
Protein supplementation of a low protein diet					
Mouse, ICR (19-21 d) [125]	10% protein + 2% branched-chain amino acids And 10% protein+ 2% alanine, fed 2 weeks prior to and throughout pregnancy	10% protein (-ve control) and 20% protein (+ve control), diets fed 2 weeks prior to and throughout pregnancy	Compared to low protein (10%) diet: branched-chain amino acids group adiposity ▲2.7-fold at term Compared to control (20%) diet: adiposity ▲2.4 to 3.2-fold, serum glucose ▼55% at term	Not assessed	Compared to low protein (10%) diet: BW ◀▶ at PND3 Compared to control (20%) diet: BW ▼50% at PND3

Rat, Sprague-Dawley (22 d) [123]	5% casein from mating until GD17, then 25% casein + 2.5% DL-methionine from GD17-20 (supplemented) or 25% casein + 2.5% DL-methionine throughout pregnancy	5% casein throughout pregnancy	Compared to supplemented diet: adiposity ▲ 1.5-fold at GD22	Compared to supplemented diet: placental weight ▲ 1.2-fold at GD22	Compared to supplemented diet: BW ▲ 1.3-fold, brain weight ▲ 1.1-fold at GD22
			Compared to 25% casein + 2.5% DL-methionine: adiposity ▲ 2.1-fold at GD22	Compared to 25% casein + 2.5% DL-methionine: placental weight ▲ 1.3-fold at GD22	Compared to 25% casein + 2.5% DL-methionine: BW ▲ 1.4-fold, brain weight ▲ 1.3-fold at GD22

B(0)⁺ = sodium/chloride-dependent neutral and basic amino acid transporter, BW = bodyweight, FATP4 = long-chain fatty acid transporter 4, GD = gestational day, GLUT1 = glucose transporter 1, GLUT3 = glucose transporter 3, PAT4 = proton-coupled amino acid transporter 4, PND = postnatal day, SNAT2 = sodium-dependent neutral amino acid transporter

1.2.7. Low protein intake and protein restriction

A moderate to severe deficiency in dietary protein intake ($\leq 50\%$ of recommended daily intake of >55 g/day) due to low diet quality throughout pregnancy in humans increased the incidence of preeclampsia, preterm delivery, stillbirth, miscarriage and neonatal mortality, as well as inducing sex-specific decreases in birth weight and length (Table 1.10, [126-128]). Reports of adverse outcomes such as risk of preeclampsia are consistent amongst available studies, although the number of available studies is insufficient to draw definitive conclusions [126-128]. Interestingly, a single study of maternal protein deficiency reported a gender-specific effect on birthweight, wherein birthweight reduction was 3-fold greater in female compared to male offspring [126]. Furthermore, another study of moderate maternal protein deficiency arising from poor diet quality throughout pregnancy reported compromised postnatal immunity in the first 6 months after birth, characterised by a higher incidence of common colds, tetanus, rickets and neonatal mortality, compared to offspring from mothers who consumed at least the recommended daily protein intake [128].

Preclinical models of protein restriction during pregnancy are used widely to model pregnancy consequences of low maternal protein intake ($\leq 50\%$ of control). Protein restriction during pregnancy in rodents, NHPs and pigs resulted in reduced maternal GWG, maternal metabolic dysfunction (characterised by impaired glucose tolerance and decreased insulin sensitivity), impaired placental function characterised by reduced umbilical blood flow, impaired fetal pancreatic development (characterised by smaller islet area and β -cell mass) and fetal growth restriction (Table 1.11, [125, 129-135]).

Table 1.11 Dietary protein deficiency during pregnancy and adverse outcomes: Evidence from observational human studies

Context	Intervention/ exposure group(s)	Control group	Outcomes compared to comparison group		
			Maternal	Pregnancy	Fetal/neonate/ newborn
Low dietary protein consumption [126]	Dietary protein consumption <45 g·d ⁻¹ throughout pregnancy	Dietary protein consumption ≥55 g/day throughout pregnancy	Not assessed	Not assessed	▼ BW (male 10%, female 30%), ▼ BL (both sexes, 10%)
Low dietary protein consumption [127]	Dietary protein consumption 42.5-55 g/day during second half of pregnancy	Dietary protein consumption ≥55 g/day during second half of pregnancy	PE incidence ▲ 1.3-2.1-fold, GWG ◀▶	PTD incidence ◀▶	Neonatal mortality ▲ 2.1-2.8-fold
Low dietary protein consumption [128]	Dietary protein consumption 56-62 g/day throughout pregnancy	Dietary protein consumption 81-92 g/day throughout pregnancy	PE risk ◀▶	PTD incidence ▲ 2.7-fold, stillbirth ▲ 5.7-fold, miscarriage ▲ 5-fold	During first 6 months of life: incidence of frequent colds ▲ 4.5-fold, rickets ▲ 6.1-fold, tetanus ▲ 4.2-fold, neonatal mortality ▲ 3-fold

BL = birth length, BW = bodyweight, PE = preeclampsia, PTD = preterm delivery

Table 1.12 Maternal protein restriction and pregnancy outcomes: Evidence from animal models (NHP, pig and rodent)

Species, strain (term)	Intervention/exposure group(s)	Control group	Outcomes compared to control group		
			Maternal	Pregnancy	Fetal/neonate/newborn
Rhesus Macaque, N/S (168 d) [129]	13.5% protein diet throughout pregnancy	26.8% protein diet throughout pregnancy	Fasting glucagon ▼60%, fasting leptin ▲1.1-fold, insulin sensitivity at GD120	Increased pregnancy loss (3/10 vs 1/9)	Not assessed
Rhesus Macaque, N/S (168 d) [136]	13% protein diet throughout pregnancy	26% protein diet throughout pregnancy	GWG ▼10% at GD85, GWG ▼20% at GD135, umbilical artery pulsatility index ▼30% at GD135	Not assessed	AC ▼10% at GD85 & GD135
Pig, Chester White x Landrace x Large white x Yorkshire (115 d) [130]	0.5% protein diet GD1-63	13% protein diet throughout pregnancy	Not assessed	Not assessed	Liver, kidney & placenta weights ▼20% at GD63
Pig, Yorkshire (115 d) [131]	0.5% protein diet throughout pregnancy	18% protein diet throughout pregnancy	Not assessed	Not assessed	BW ▼30%, organ weight (brain, liver) ▼10-50% at birth
Rat, Wistar (22 d) [132]	8% protein diet throughout pregnancy	20% protein diet throughout pregnancy	GWG ▼20%	Not assessed	Total weight of litter ▼30%
Rat, Wistar (22 d) [133]	8% protein diet throughout pregnancy	20% protein diet throughout pregnancy	Not assessed	Not assessed	BW ▼10%, ▼ islet area and β -cell mass, apoptotic islet cells (% total islet cells) ▲3-fold at birth

Rat, Wistar (22 d) [134]	8% protein diet throughout pregnancy	20% protein diet throughout pregnancy	GWG ▼10% at GD21.5	Not assessed	BW ▼10%, pancreatic head islet size (μm^2) ▼30% at birth
Mouse, ICR (21 d) [125]	10% protein 2 weeks prior to and throughout pregnancy	20% protein 2 weeks prior to and throughout pregnancy	Adiposity ◀▶, serum glucose ▼63% at term	Not assessed	BW ▼30% at PND3
Mouse, C57BL/6 (19 d) [135]	6% protein diet throughout pregnancy	22% protein diet throughout pregnancy	Not assessed	Not assessed	BW ▼40%, BL ▼30%, lung mass ▼50% at PND1

AC = abdominal circumference, BL = body length, BW = birth weight, GD = gestational day, GWG = gestational weight gain, PND = postnatal day, BW = bodyweight, PR = protein restriction

1.2.8. Multi-factorial poor diet quality

The effects of excess carbohydrate intake on maternal, fetal and pregnancy outcomes have been extensively investigated in observational human studies and preclinical studies in rodents. A recent (2022) systematic review and meta-analysis that examined associations between maternal diet consumption throughout pregnancy, fetal and neonatal outcomes in humans reported that consumption of diets with a high caloric density, i.e., a “WSD” or unhealthy diet, was associated with high GWG [137]. Another systematic review and meta-analysis (2021) that examined the association between maternal dietary patterns and the risk of developing preeclampsia in low- and middle-income countries reported that adequate consumption of fruits and vegetables reduced the risk of developing preeclampsia by 51-82% compared to a diet poor in fruits and vegetables [138]. An observational study examining pregnancy outcomes following high carbohydrate and low protein intake in early and late pregnancy in humans reported a negative association with birth- and placental weights. Birth- and placental weights were 3% and 2% lower, respectively, when carbohydrate intake during early pregnancy exceeded 340 g/day [139]. Furthermore, birth- and placental weights were 2% and 7% lower, respectively, in women with low late-pregnancy dairy and meat protein intakes, respectively, after adjustment for adequate carbohydrate intake (340 g/day) in early pregnancy [139].

Poor diet quality has been reported to affect maternal cardio-metabolic health and inflammatory markers. Diet quality can be assessed using an energy-adjusted dietary inflammatory index (E-DII) and used “to quantify the inflammatory potential of an individual’s diet, measured through inflammatory markers such as Interleukin-1 and C-reactive protein” [140], such that a higher E-DII diet score indicates a more proinflammatory diet. Maternal high E-DII was associated with higher maternal BMI and elevated maternal plasma lipids between early- and late-pregnancy in humans [140]. In addition, maternal high E-DII was reported to be associated with higher diastolic blood pressure at early- but not late-pregnancy, while there was no association between E-DII and systolic blood pressure at early- or late-pregnancy [140].

A “WSD” is an example of a diet with multi-factor poor diet quality due to factors described earlier. Evidence from NHPs and mice show that maternal consumption of a HFHS diet prior to and/or throughout pregnancy results in high maternal GWG, maternal dyslipidaemia, elevated adiposity, plasma lipids, insulin and glucose, placental macronutrient transfer and gene expression, and lower fetal bodyweight (Table 1.12, [18, 19, 141, 142]). It is also emerging that maternal HFHS diet consumption causes intergenerational harm to progeny. A recent review and meta-analysis of obesogenic diets

in rodents found that both single and intergenerational exposure to obesogenic diets resulted in elevated bodyweight, dyslipidaemia, glucose intolerance and insulin insensitivity in the F₁ and F₂ generations [143]. Several causal mechanisms have been proposed for intergenerational metabolic programming following maternal HFHS consumption, including effects of specific nutrient deficiencies on tissues such as adipose tissue, and organs such as the pancreas, liver, kidneys and the reproductive tract. Other proposed mechanisms include impaired placental function and placental remodelling [144, 145], epigenetic programming through altered DNA methylation [146], effects of glucocorticoids and accelerated cellular aging [146, 147].

Table 1.13 Maternal high fat-high sugar (HFHS) consumption and pregnancy outcomes: Evidence from NHPs and rodent models

Species, strain (term)	Intervention/exposure group(s)	Control group	Outcomes compared to control group(s)		
			Maternal	Pregnancy	Fetal/neonate/newborn
Japanese Macaque (175 d) [141]	HFHS diet (36% fat, 50% carbohydrate) for at least 1 year prior to and throughout pregnancy	Control diet (14.7% fat) for at least 1 year prior and throughout pregnancy	Plasma leptin ▲2-fold, insulin ▲1.3-fold, glucose AUC ▼9%, insulin AUC ▲1.5-fold at GD127	Not assessed	Not assessed
Mouse, C57BL/6 (19 d) [142]	HFHS diet – HF pellet (43% carbohydrate, 40% fat, 17% protein) and 20% sucrose solution supplemented with vitamins and minerals 4-6 weeks prior to and throughout pregnancy	Control diet (72.6% carbohydrate, 10.6% fat, 16.8% protein) 4-6 weeks prior to, and throughout pregnancy	GWG ▲1.1-fold, plasma cholesterol ▲1.4-fold, plasma triglyceride ▲1.5-fold, ▲ plasma leptin 2.2-fold, insulin sensitivity ▼75% on PND21	Not assessed	Not assessed

<p>Mouse, C57BL/6 (19 d) [18]</p>	<p>HFHS diet (30% fat, 17% protein, 53% carbohydrate) throughout pregnancy</p>	<p>Control diet (11% fat, 26% protein, 62% carbohydrate) throughout pregnancy</p>	<p>Adiposity ▲1.3-fold at GD16, ▲1.4-fold at GD19</p>	<p>Placental weight ▼10% at GD16 and GD19, absolute placental transfer of methyl aminoisobutyric acid (non-metabolisable radioactive amino acid tracer) and methyl D- glucose (glucose tracer) ▲1.5-fold, transfer per mm² of labyrinth zone surface area and fetal accumulation of methyl aminoisobutyric acid and methyl D-glucose ▲1.5- to 1.6-fold at GD16, placental Glut3 and SLC38A2 gene expression ▲1.4-1.5- fold at GD16, FATP gene expression ▲1.5- fold at GD19</p>	<p>BW ▼10% at GD16, ◀▶ BW at GD19</p>
---------------------------------------	--	---	---	--	---

Mouse, C57BL/6 (19 d) [19]	HFHS diet (30% fat, 17% protein, 53% carbohydrate) throughout pregnancy	Control diet (11% fat, 26% protein, 62% carbohydrate) throughout pregnancy	Plasma cholesterol ▲ 1.6-fold, plasma insulin ▲ 2.2-fold and serum leptin ▲ 3.4-fold, placental weight ▼ 10% at GD16, plasma non-esterified fatty acids ▼ 40%, liver and placental weight ▼ 10%, adiposity ▲ 1.4-fold, fed state and 6h fasted blood glucose ▲ 1.1-1.2-fold, AUC ▲ 2-fold after intraperitoneal glucose tolerance test on GD19	Not assessed	BW ▼ 10% at GD16, ◀▶ BW at GD19
----------------------------	---	--	--	--------------	---------------------------------

AUC = area under curve, BW = bodyweight, DHA = docosahexaenoic acid, FATP = fatty acid transporter protein, GD = gestational day, GLUT1 = glucose transporter 1, GLUT3 = glucose transporter 3, GLUT9 = glucose transporter 9, GWG = gestational weight gain, NHP = Non-human primate, SNAT = sodium-dependent neutral amino acid transporter, TRIG = triglyceride

1.2.9. Micronutrients

Micronutrients are critically important for fetal growth and development during the perinatal period and to ensure healthy pregnancy outcomes for mother and newborn. Low intake of key micronutrients such as iron, calcium, zinc, folate, vitamin A, vitamin B₂, B₃, B₆, B₁₂ and vitamin D increase the risk of a wide range of adverse maternal and fetal outcomes in humans (Table 1.13). Common adverse maternal and fetal outcomes associated with micronutrient malnutrition include greater risks of developing hypertensive disorders of pregnancy such as preeclampsia, pre-term delivery, congenital birth defects and low birth weight (Table 1.13, [70, 119, 148-153]).

As this thesis is focussed on maternal SI adaptations and macronutrient absorption during pregnancy, the consequences of impaired micronutrient intake and absorption during pregnancy, or their consequences in preclinical models have not been reviewed in detail. More information on these topics can be found in recent reviews [70, 119, 148-154].

Table 1.14 Dietary micronutrient deficiency and pregnancy outcomes: Evidence from observational human studies

Micronutrient	Outcomes relative to controls/comparison group		
	Maternal	Pregnancy	Fetal/neonate/newborn
Iron	Not reported	▲ risk of preterm delivery, placental hypertrophy	▲ risk of low birth weight, neonatal mortality, impaired brain development
Calcium	▲ risk of osteopenia, preeclampsia and hypertension	▲ risk of preterm delivery	▲ risk of low birth weight and delayed growth
Zinc	▲ risk of hypertension	▲ risk of IUGR, prolonged labour, pre- and post-term birth	▲ risk of low birth weight
Magnesium	▲ risk of reduction in cognitive capacity	Not reported	Not reported
Selenium	▲ risk of reduced immune system activity (innate and adaptive)	Not reported	Not reported
Folate	▲ risk of preeclampsia	▲ risk of placental rupture, preterm delivery, spontaneous abortion and stillbirth	▲ risk of low birth weight, neural tube defects
Iodine	▲ of iodine deficiency disorders (i.e. hypothyroidism)	▲ risk of impaired placental morphology	▲ risk of impaired brain development
Vitamin A	▲ risk of night blindness	▲ risk of preterm delivery and stillbirth	▲ risk of low birth weight
Vitamin B ₂ (Riboflavin)	▲ risk of preeclampsia	Not assessed	▲ risk of low birth weight, congenital heart defects
Vitamin B ₃ (Niacin)	Not assessed	Not assessed	▲ risk of congenital birth defects

Vitamin B ₆ (Pyroxidine)	▲ risk of preeclampsia	Not assessed	Not assessed
Vitamin B ₁₂ (Cyanocobalamin)	Not assessed	▲ risk of preterm delivery	▲ risk of low birth weight, neural tube defects
Vitamin C (Ascorbic acid)	▲ risk of preeclampsia	▲ risk of premature rupture of membranes	Not assessed
Vitamin D	▲ risk of preeclampsia and gestational diabetes mellitus	▲ risk of preterm delivery	▲ risk of low birth weight and small for gestational age infants
Vitamin E	▲ risk of preeclampsia	▲ risk of premature placental detachment and preterm delivery	▲ risk of low birth weight
Vitamin K	Not assessed	▲ risk of haemorrhage	Not assessed

IUGR = intrauterine growth restriction

1.3. Gastrointestinal tract

1.3.1. Overview

The gastrointestinal tract (GIT) comprises the oral cavity, oesophagus, stomach, small intestine (SI), large intestine as well as accessory organs and glands (salivary gland, gallbladder and pancreas, Fig. 1.4). Each of these organs plays a different role in nutrient ingestion, digestion, absorption, and excretion.

Carbohydrate digestion begins in the oral cavity where salivary α -amylases, produced by salivary glands present beneath the tongue, begin to digest polysaccharides into di- and monosaccharides [155, 156]. Carbohydrate digestion, however, is relatively minor in the oral cavity due to

the short time of exposure, pH sensitivity and subsequent acid inactivation of α -amylase in the stomach [156]. Digestion of dietary lipids also begins in the oral cavity where lingual lipase hydrolyses medium and long-chain triglycerides, producing partial glycerides and fatty acids [155, 156]. Next, the semi-liquefied food bolus travels down the oesophagus to the stomach.

Within the stomach, the nutrient bolus is bathed in gastric juice and continuously churned to permit access of digestive enzymes to nutrients present in the bolus. The digestive constituents of gastric juice comprise hydrochloric acid secreted by parietal cells, and the proenzyme pepsinogen and lipase secreted by chief cells [157]. Hydrochloric acid activates zymogen pepsinogen to the proteolytic enzyme pepsin, which cleaves peptide bonds of aromatic amino acids to release individual amino acids, di-, tri- and oligopeptides [155, 158]. Gastric lipase hydrolyses triglycerides rich in medium-chain fatty acids, producing partial glycerides and fatty acids [159]. Following partial digestion, the nutrient bolus leaves the stomach via the pyloric sphincter and enters the proximal duodenum.

The SI is divided into three segments: the duodenum, jejunum and ileum. The primary functions of the SI are to facilitate the final stages of enzymatic digestion of nutrients present in the bolus received from the stomach, and absorb the individual macro- and micronutrients

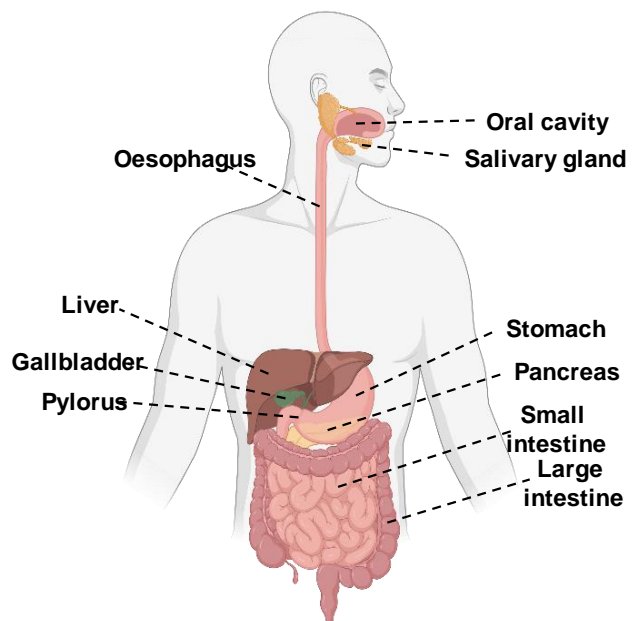


Figure 1.4 Overview of the gastrointestinal tract and its individual components including the stomach, pancreas, gallbladder, small and large intestines. Figure created using Biorender.com.

from the lumen and into the circulation. To facilitate the final stages of nutrient digestion, bile acids are produced and secreted into the duodenum by the gallbladder, where they emulsify lipids to facilitate actions of pancreatic lipases. Pancreatic and duodenal brush border carbohydrase and protease enzymes facilitate final catabolism of carbohydrates and amino acids respectively [158]. Pancreatic enzymes and bile acids are secreted directly into the duodenal lumen via the common bile duct. The rate at which pancreatic and gallbladder enzymes are secreted into the duodenal lumen is controlled by the Sphincter of Oddi [160]. The specific roles of the jejunum and ileum with regards to nutrient absorption are described in more detail below. Waste products and nutrients not absorbed by the SI are passed into the large intestine through the ileo-caecal valve.

The large intestine is divided into four segments: the caecum and ascending colon, transverse, descending and sigmoid colon [161]. In humans, the caecum is relatively small compared to the other segments of the large intestine and does not have any clear function [161]. In contrast, the murine caecum is proportionally large and plays an important role in the fermentation of plant material and production of vitamin K and B. The ascending colon is responsible for absorbing water, water-soluble vitamins, short chain fatty acids (SCFA), and electrolytes such as sodium, potassium and chloride present in the digesta received from the SI [161, 162]. Also present in the large intestine is an extensive microbiome, responsible for fermenting carbohydrates in the form of starches. This process yields short chain fatty acids as a by-product, which are the preferred metabolic substrate for colonocytes [162]. Electrolytes and water-soluble vitamins are readily absorbed by enterocytes in the colon via epithelial ion exchangers belonging to the solute carrier superfamily [158]. Absorption of water and remaining electrolytes solidifies the remaining waste products into stool, which is then stored in the transverse and descending colon prior to its excretion via the sigmoid colon and rectum [163]. In humans, the colon absorbs as much as 1.5 L of water and ~800 mm of sodium per day [158].

The sections below provide more detail on gastric and SI anatomy, functions of individual SI regions, gastric and SI neural innervation, macronutrient digestion and uptake. The effects of pregnancy on microbiome composition and function, i.e. substrate synthesis, are beyond the scope of this thesis and thus not covered to the same depth as the small intestine.

1.3.2. Gastric and SI anatomy

The stomach is responsible for the partial digestion of the nutrient bolus received from the oral cavity via the oesophagus. In humans, the stomach comprises two main segments; the fundus (upper 1/3rd) and the body (lower 2/3rd, [157]). The fundus connects to the oesophagus via the lower oesophageal sphincter, while the body connects to the duodenum via the pylorus. To

facilitate churning of gastric contents, the wall of the stomach comprises three layers of smooth muscle. The outermost layer is the longitudinal layer, the middle layer is the circular layer, while the innermost layer is the oblique layer [157]. The gastric mucosa comprises three layers of tissue; the columnar epithelium, lamina propria and muscularis mucosa [157]. The columnar epithelium which lines the stomach comprises different types of secretory cells, including parietal cells, chief cells, enterochromaffin-like cells which secrete histamine, and P/D1 cells [157, 164].

The duodenum constitutes the proximal and shortest SI region, which connects to the stomach via the pyloric sphincter [156, 160]. The duodenal wall is characterised by a thick smooth muscle layer which facilitates peristalsis, as well as mucosa and submucosa to accommodate secretory glands such as Brunner's glands. The Brunner's glands secrete an alkaline-rich mucus which protects the duodenal epithelium against the acidity of chyme by neutralising the gastric acid and provides a suitable digestive environment for pancreatic enzymes. The mucus also lubricates the gut wall, reducing the friction between chyme and the gut wall during movement through the intestinal lumen [160]. The duodenum is further characterised by the presence of slender 'finger-like' villi which protrude into the luminal space from submucosal folds called plicae circulares. The mucosa of these lumen-facing villi is lined with a single-cell thick epithelium. The anatomical structure of SI villi is described in more detail further below. Also found sparsely within the duodenum are Peyer's patches, situated between the serosa and muscularis propria. Peyer's patches constitute lymphoid follicles which act as reservoirs for immune cells such as B- and T-lymphocytes [156]. The abundance of Peyer's patches increases distally along the SI axis. Oxygenated blood is supplied to the duodenum via the superior mesenteric artery and branches of the gastroduodenal artery, while venous drainage is facilitated by the pancreaticoduodenal, right gastroepiploic and portal veins [155, 156]. In murine SI, the transition from duodenum to jejunum is demarked by the ligament of Treitz (Fig. 1.5).

The jejunum constitutes the middle SI region and is characterised by a thick smooth muscle layer to aid peristalsis. Here, villi are shorter than in duodenum and Peyer's patches are more abundant. The plicae circulares of the jejunum resemble those of the duodenum, but the villi become progressively shorter towards the distal end. Oxygenated blood is supplied to the jejunum via the superior mesenteric artery while venous drainage is facilitated by the superior mesenteric vein which joins with the splenic vein and drains into the portal vein [155, 156].

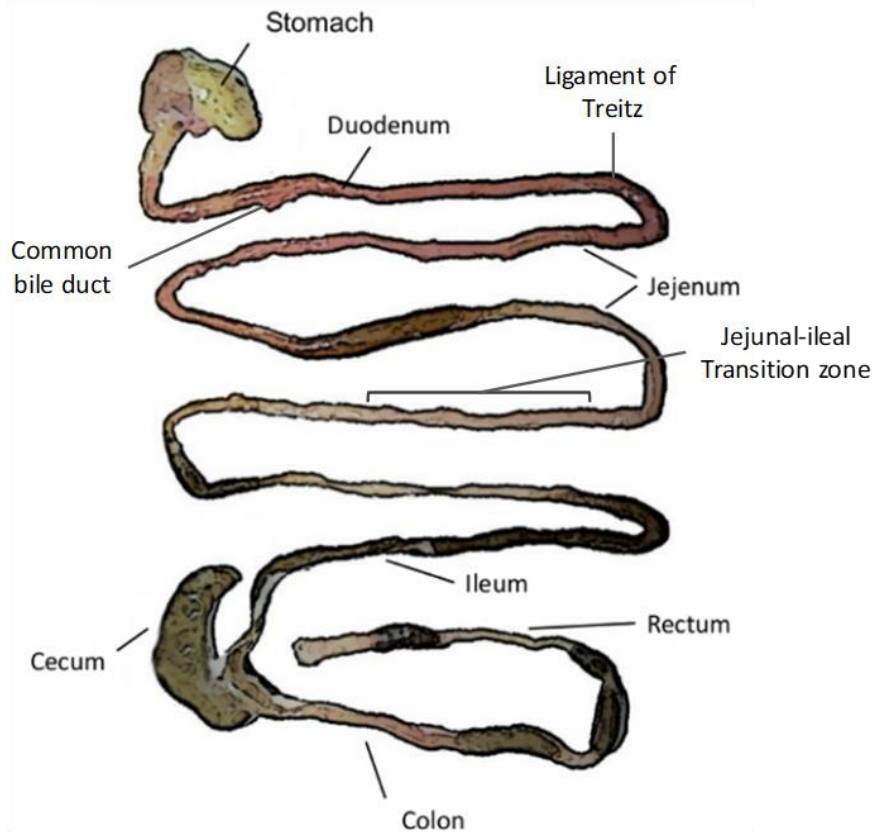


Figure 1.5 Schematic representation (not drawn to scale) of anatomical boundaries and transition zones along the SI axis in mice. Adapted from Mateer 2016 [165].

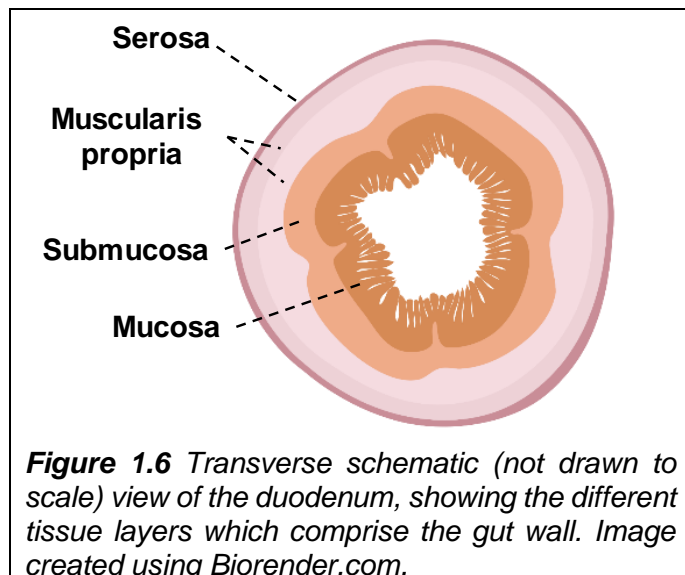
To identify the boundary between the jejunum and ileum, different techniques and definitions have been utilised. These include identifying macroscopic and microscopic changes such as an increase in the abundance of Peyer's patches, an increase in luminal diameter, a decrease in smooth muscle thickness, and changes in the spatial expression of local transcription factors [166-168]. This use of variable regional definitions has resulted in considerable variation in SI region-specific lengths reported previously in rodents [167, 169]. Unfortunately, a lack of whole SI functional data relating to uptake of specific micro- and macro-nutrients, which could be used to correlate function with region-specific anatomical structure, makes it impossible to accurately identify the exact point of transition from jejunum to ileum in rodents. While the smooth muscle layer of the duodenum and jejunum are comparable in thickness, ileum smooth muscle is considerably thinner, and effectively translucent. This high degree of translucency also enables identification of Peyer's patches, which are most abundant in the ileum [155].

At the microscopic level, the thickness of the jejunal muscularis mucosa is similar, but the luminal diameter wider, and the mucosal lining thinner, compared to the ileum [156]. Another distinct difference between the duodenum, jejunum and ileum is that plicae circulares found in the ileum are flat in appearance, in contrast to the folded appearance in the duodenum and jejunum [156]. Furthermore, ileal villi become progressively shorter, taking on a short and

stubby appearance. This contrasts the long and slender 'finger-like' villi found in the duodenum and jejunum. The ileocaecal valve marks the transition from the ileum to the large intestine. Oxygenated blood is supplied to the ileum via the superior mesenteric artery while venous drainage is facilitated by the superior mesenteric vein which joins with the splenic vein and drains into the portal vein [155].

The SI wall is comprised of the serosa, muscularis propria, submucosa and mucosa (Fig. 1.6, [156]). The outer serosal layer acts as a lubricated barrier between the abdominal wall and the muscularis propria, allowing for reduced friction during movement of the intestines within the abdominal cavity. The serosa consists of a thin lining of mesothelial cells sitting on top of a loose layer of connective tissue [155, 156]. Beneath the serosa sits the muscularis propria which comprises a circular and longitudinal layer of smooth muscle.

The muscularis propria is primarily responsible for facilitating peristalsis [155, 156]. Towards the lumen, the submucosa consists of a layer of connective tissue which sits between the muscularis propria and mucosa, composed of fibroblasts and mast cells [155]. The submucosa provides structural support for the muscularis mucosa. The inner-most mucosal layer comprises the muscularis mucosa, lamina propria and villi. The



muscularis mucosa is a thin layer of smooth muscle situated between the submucosa and lamina propria which plays a minor role in peristalsis [155]. Contained within the villous mucosa are extensive networks of capillaries and arterioles, responsible for providing oxygen and nutrients to the epithelium. Lymphatic capillaries called lacteals are responsible for immune surveillance and absorption of lipids and fat-soluble vitamins contained within chylomicrons, thereby facilitating circulatory uptake of nutrients [155]. Also found within the mucosa are nerve endings which facilitate neural innervation of the epithelium. A more in-depth overview of SI neural circuitry is provided below.

The different cell types which comprise the SI epithelium have a relatively short average lifespan of 3-6 days on average in humans [156], and 2 days on average in rats [170]. Thus, the different populations of cells are constantly turning over and being replaced with new populations which are derived from progenitor stem cells pools present within crypts located

between villi. These stem cells proliferate and differentiate into the epithelial cell types that comprise the epithelium and migrate vertically along the crypt-villous axis towards the apical portion of the villi [155, 156]. The decrease in SI villi length distally along the oral-aboral axis reflects changing anatomy and function, but also a concurrent decrease in the number of Wingless and Int-1 (Wnt) -activated stem cells residing in intestinal crypts (Fig. 1.7, [171]). The Wnt-signalling pathways are important regulators of cell proliferation, differentiation and migration [171]. Furthermore, Wnt-activated stem cells are most abundant in the proximal SI, and decrease distally, such that duodenal villi are the longest across multiple species (Fig. 1.7). This reflects, in part, the primary role of the duodenum in nutrient catabolism and uptake, and an optimised, large surface area to facilitate these processes, together with a greater population of Wnt-activated stem cells. In contrast, ileal villi are the shortest, in part due to the comparatively small amount of nutrients reaching the distal SI as a result of the ileal brake, but also because of a reduction in the number of Wnt-activated stem cells [171].

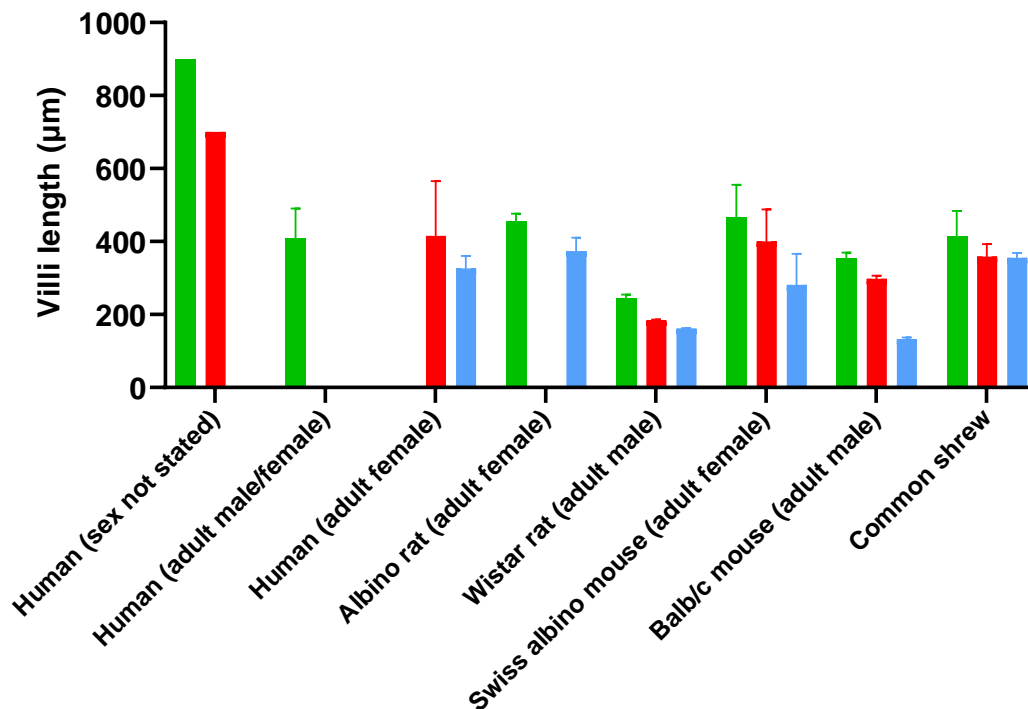


Figure 1.7 Region-specific villi length along the SI in humans [172-174], rats [175, 176], mice [177, 178] and shrews [179], determined via histomorphometric analysis. Green bar = duodenum, red bar = jejunum, blue bar = ileum.

The SI epithelium is comprised of five major cell types; absorptive cells (enterocytes), secretory cells (Goblet cells), immune cells (Paneth cells), enteroendocrine cells (enterochromaffin, K, L and I cells) and stem cells (Fig. 1.8) [155, 156]. Enterocytes are the most common, accounting for ~85-90% of the total cell population and are responsible for uptake of micro- and macronutrients from the SI lumen [155]. Microvilli are located on the apical surface of epithelial enterocytes and when combined with villi and plicae circulares, result in a ~600-fold

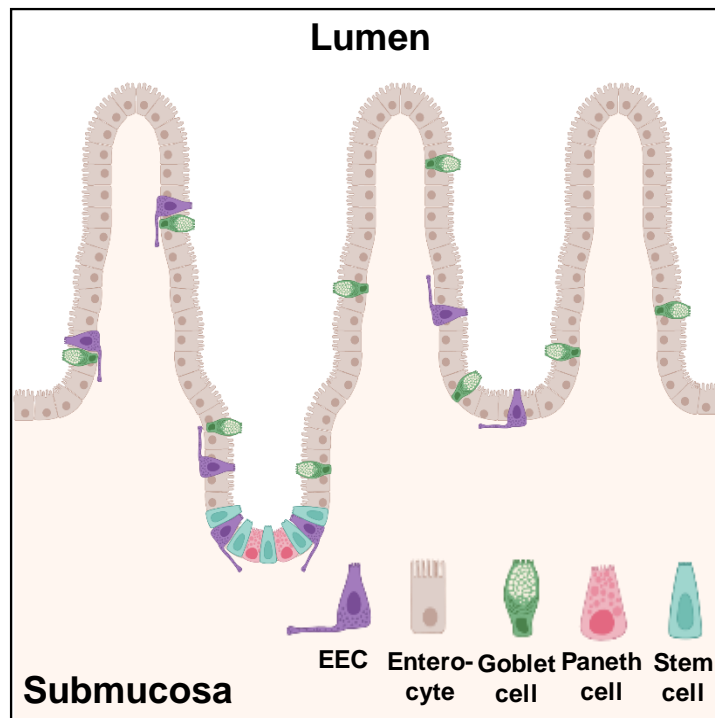


Figure 1.8 Schematic representation (not drawn to scale) showing the *abundance and distribution of different cell types in the SI epithelium*. EEC = enteroendocrine cell. Figure created using Biorender.com.

increase in available surface area for nutrient uptake [158]. Goblet cells secrete mucin which protects the gut wall against the acidity of chyme [155] and acts as a lubricant. Although present in all SI regions, the abundance of Goblet cells increases distally. Paneth cells provide immune surveillance and secrete antimicrobial agents such as lysozyme, α -defensins and phospholipase [156]. Like Goblet cells, Paneth cells are expressed throughout the SI, but increase in abundance distally. Enteroendocrine cells are present in all SI regions and are responsible for secreting gut hormones such as serotonin (5-HT), cholecystokinin (CCK), glucose-dependent insulintropic polypeptide (GIP), glucagon like peptide-1 (GLP-1) and peptide YY (PYY) in the presence of nutrients in the SI lumen [155, 156, 180]. 5-HT is released from enterochromaffin cells, the most abundant enteroendocrine cell type throughout the SI. CCK is secreted by I-cells located in the duodenum and jejunum. GIP is secreted by K-cells located in the duodenum. PYY and GLP-1 are secreted by L-cells. Within the SI, L-cells are mostly found in the ileum, but are also present in the duodenum and jejunum.

A major determinant of SI nutrient uptake is the rate at which the stomach releases its contents into the proximal SI, which is controlled by both gastric and intestinal mediators. Some of these mediators are also involved in regulating other processes such as food intake, which is reviewed in more detail elsewhere [181]. The gastric hormone ghrelin, referred as the “hunger”

hormone, is secreted from enteroendocrine P/D1-cells native to the fundus epithelium of the stomach. Ghrelin promotes gastric smooth muscle locomotor activity, gastric acid secretion, and to a lesser extent gastric emptying [182-184]. Ghrelin stimulates smooth muscle locomotor activity and gastric emptying via a dual positive feedback mechanism; peripherally by acting on the vagus nerve and centrally by binding to ghrelin receptors of Agouti-related peptide neurons in the arcuate nucleus of the hypothalamus [185]. Opposing effects are exerted through nutrient-evoked release of gut hormones such as GLP-1 and PYY in the ileum, which provide a negative feedback mechanism via vagal reflex circuits, and act as a powerful ‘ileal-brake’ [182] to slow gastric emptying, intestinal transit, the secretion of gastric acid and pancreatic digestive enzymes. An increase in the amount of nutrients reaching the terminal ileum could be due to malabsorption, high transit or following bariatric surgery (Fig. 1.9, [182]). Furthermore, GLP-1, and GIP which is secreted by duodenal K cells, exert insulinotropic effects by augmenting pancreatic insulin release to regulate postprandial glycaemia [182]. The gut hormones 5-HT, CCK, GLP-1 and PYY exert their effects via a negative feedback mechanism; in part by activating cognate receptors on vagal afferents within the vagus nerve, which ultimately results in slower rates of gastric emptying and pancreatic secretion [182, 186].

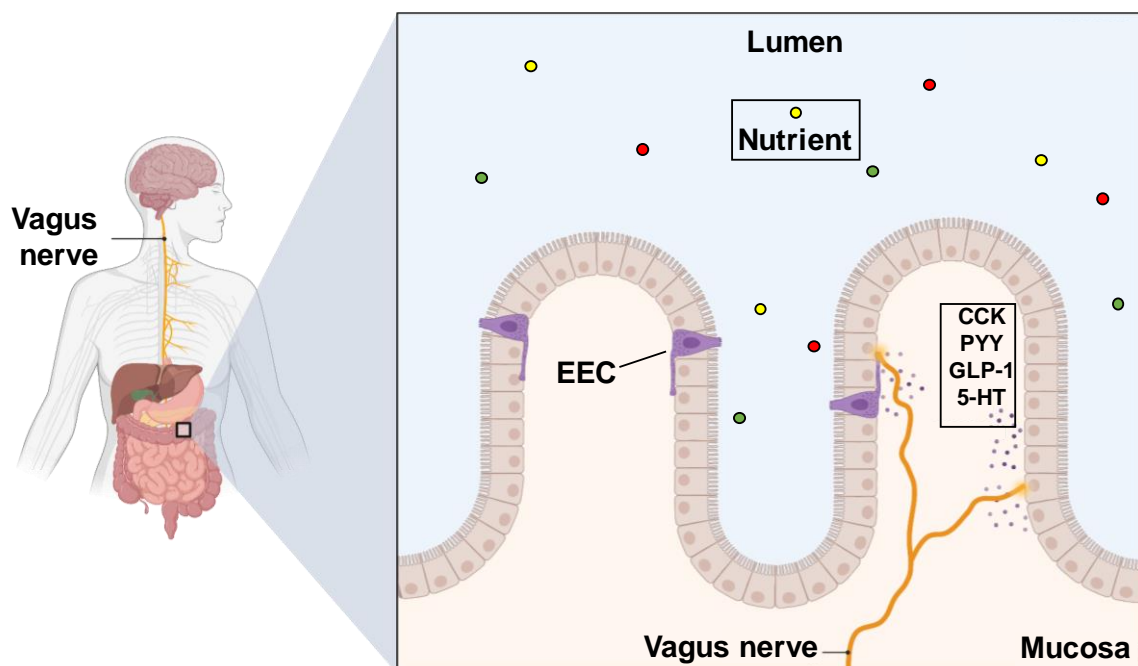


Figure 1.9 Enteroendocrine cells (EECs) in the SI epithelium secrete hormones such as CCK, PYY, GLP-1 and the pleiotropic bioamine 5-HT in the presence of luminal nutrients. These act on vagal afferent nerve endings to relay sensory cues to the brain via the vagus nerve. Image is a schematic representation (not drawn to scale), and created using Biorender.com based on information from Wang et al. 2020 [187].

1.3.3. Neural innervation of the upper GIT

Although the emphasis of this thesis is on SI nutrient absorption, the neural circuitry within the GIT is extensive and plays an important role in coordinating digestive and absorptive

processes. Thus, a basic overview of gastric and SI neural innervation is provided below, however in-depth reviews and sources of information are available elsewhere [187, 188].

Neural innervation of the GIT regulates functions and processes that directly and indirectly regulate gastric and SI nutrient catabolism and nutrient absorption. These include coordinating patterns of smooth muscle activity affecting gastric accommodation and emptying, peristalsis and intestinal transit, gut hormone and digestive enzyme secretion, nutrient sensing and absorption, regional blood flow and immune surveillance via interaction with the intrinsic immune system [156, 189]. To facilitate these functions, the GIT is innervated by both intrinsic and extrinsic neural circuitry. The enteric nervous system (ENS) functions largely independent of the CNS (central nervous system; brain and spinal cord) and primarily acts to coordinate the passage of food through the GIT, as well as digestive and absorptive processes [190]. The GIT is also densely innervated by extrinsic afferents which relay sensory information to the CNS to initiate reflexes through parasympathetic and sympathetic nerves, including those linked to nausea and vomiting, satiety and control of food intake, as well as visceral pain, particularly under pathophysiological conditions of hypersensitivity [190], such as irritable bowel syndrome and functional dyspepsia [191, 192].

1.3.3.1. *Intrinsic innervation: the enteric nervous system (ENS)*

The ENS consists of a network of ganglia that form two distinct plexuses, the myenteric plexus (also known as Auerbach's plexus) located between the external muscle layers, and the submucosal plexus (also known as Meissner's plexus) located in the submucosal layer [155, 157]. The myenteric plexus forms a continuous network of ganglia around the circumference of the GIT, extending from the oesophagus to the anal sphincter, which regulates peristaltic waves that move digesta along the gut through a reciprocal and coordinated action of smooth muscle contraction and relaxation directly behind and in front of the digesta respectively. The myenteric plexus is also involved in local muscular contractions responsible for stationary mixing and churning, including the churning of gastric content to aid mechanical and enzymatic nutrient digestion [156]. The submucosal plexus is present in the small and large intestine but the ganglia are sparse and smaller in the stomach and absent from the oesophagus. The submucosal plexus is involved in the regulation of peristaltic activity, blood flow, digestive secretions, secreto-motor innervation to the submucosal glands to lubricate and protect the mucosal lining, mixing and absorption of nutrients as well as immune and endocrine functions of the gut [190]. The ENS contains both sensory and motor neurons as well as interneurons that enable information from the GIT to be integrated.

1.3.3.2. *Extrinsic innervation*

Parasympathetic vagal and sympathetic spinal connections exist between the GIT and the CNS. Each of these pathways comprise sensory fibres (afferents, sending information from the GIT to the CNS) and motor fibres (efferents, sending information from the CNS to the GIT). Some of these efferents are pre-enteric neurons, with terminals on enteric ganglia to modulate the activity of enteric neurons, while others innervate distinct gastrointestinal effectors, including the oesophageal striated muscle (vagal innervation), sphincters (vagal and sympathetic innervation) and intrinsic blood vessels (sympathetic innervation, [190]).

1.3.3.3. *Vagal innervation*

The vagus nerve facilitates bi-directional afferent and efferent communication between the GIT and CNS; 70-80% of vagal nerve fibres are sensory in origin and their cell bodies are located in the nodose and jugular ganglia [190, 193].

The proximal GIT is highly innervated by vagal afferents, with density decreasing along the oral-aboral axis. Subtypes of these afferents are sensitive to one or more stimuli, including mechanical, chemical (e.g., hormones or nutrients), pH, temperature and osmolarity [187], providing the CNS precise information on the GIT environment. In addition, sensory information on luminal contents is detected by EEC cells which release hormones that activate cognate receptors on vagal afferent endings. The central endings of gastrointestinal vagal afferents terminate predominantly in the nucleus tractus solitarius (NTS) and regulate vago-vagal reflexes, which control gastrointestinal smooth muscle contractility in response to distention caused by the presence of food, gastrointestinal function, as well as behaviours such as food intake [194]. Three distinct morphological subtypes of vagal afferent ending sense GI cues, intraganglionic laminar endings (IGLEs), intramuscular arrays (IMAs) and mucosal afferents (Fig. 1.10, [190, 195]).

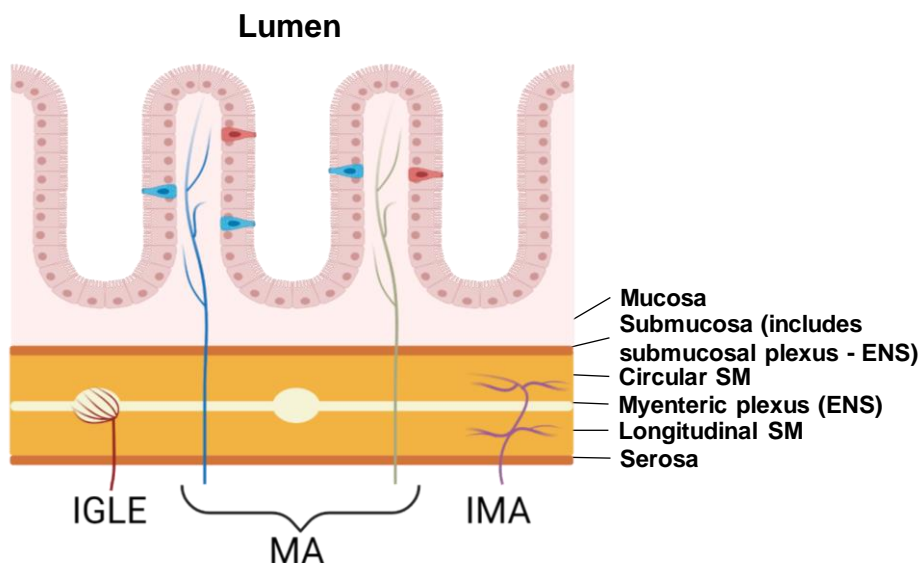


Figure 1.10 Gastric and SI vagal afferent innervation. Sensory information is received by vagal and tension- and chemo-sensitive mucosal afferent (MA) nerve endings, intra-muscular arrays (IMAs) and intra-ganglionic laminar endings (IGLEs). Figure created using Biorender.com.

IGLEs are branching nerve fibres that give rise to flat expansions within the myenteric ganglia and respond to stretch, and in the case of the stomach probably signal filling [196]. IMAs branch within the circular muscle layer forming arrays of varicose fibres that run parallel to muscle bundles and respond to tension [197, 198]. The third class, mucosal afferents are abundant in the stomach and intestine, and innervate the intestinal villi (villus afferents) and crypts (crypt afferents, [199]). Gastric mucosal afferents are sensitive to light stroking caused by the mechanical movement of ingesta across the mechanoreceptive field of the mucosal afferent nerve endings, and chemical stimuli (e.g., acid), but not stretch [199], and are thought to detect particle size and signal slowing of gastric emptying. Villus afferents project towards the intestinal villus tip and are ideally positioned to detect substances released from the epithelium, such as gut hormones (e.g., CCK and 5-HT, [190]). Crypt afferents form sub-epithelial rings of varicose processes below the crypt-villus junction [199].

Vagal afferent terminals in the NTS form direct and indirect connections with vagal efferents, which have cell bodies within the dorsal motor nucleus and which relay motor signals from the brain to the gut. Most of these efferents are pre-enteric, but some run directly to the oesophageal striated muscle [190]. The major roles of these vagal efferents are to i) control oesophageal propulsion, ii) relax the lower oesophageal sphincter to allow passage of food into the stomach, iii) increase gastric capacity to accommodate more food, iv) facilitate antral contractions, v) relax the pylorus, vi) increase gastric acid secretion, vii) contract the gallbladder and viii) promote pancreatic exocrine secretion.

1.3.3.4. *Spinal innervation*

The spinal connections with the GIT include spinal afferents, with cell bodies in the dorsal root ganglia, and sympathetic efferents [190]. Spinal afferents generally have high activation thresholds mostly cued to noxious levels of stimulation. Some spinal afferents, particularly those in the pelvic nerves, respond to lower levels of mechanical and chemical stimuli similar to vagal afferents, however, spinal afferents are primarily associated with nociception, particularly in pathophysiological conditions where afferents hypersensitivity leads to visceral pain [190]. A high proportion of spinal afferent endings are located around arterioles in the gut wall. The axons of some spinal afferent neurons also provide a sparse network of varicose axons in the myenteric ganglia, while a subset branch within the lamina propria of the mucosa throughout the GIT [190].

The sympathetic efferents have four major innervation targets, myenteric ganglia, submucosal ganglia, blood vessels and sphincter muscles, and coordinate locomotor activity and secretory

function [190]. During an acute stress response, activation of the sympathetic nervous system diverts blood flow away from the GIT in favour of a flight or fight response [190]. Furthermore, the sympathetic innervation of the myenteric ganglia inhibits the excitatory effects of enteric neurons on gastric and SI muscle to slow intestinal transit. Likewise, innervation of the submucosal ganglia inhibits secreto-motor neuron activity [189], while sympathetic post-ganglionic efferent neurons innervate the lower oesophageal and pyloric sphincters, the sphincter of Oddi, and regulate smooth muscle contractility to inhibit transit of digesta [189].

The sympathetic and enteric nervous systems act together in control of SI motility, hormone secretion and digestive processes. This is governed by enteroendocrine-released pro-motility hormones such as gastrin, substance P, vasoactive intestinal peptide, CCK and motilin as well as anti-motility hormones secretin and glucagon, which modify the electrical and/or contractility patterns of the smooth muscle layers of the gut wall, to regulate the rate at which chyme moves along the SI [156]. When sensory vagal and spinal motor efferents stimulate postganglionic intrinsic ENS neurons of the extrinsic nervous system, secretory and digestive processes are inhibited. Postganglionic ENS neurons can be cholinergic or peptidergic, the latter which release the motility hormones detailed above [156].

1.3.4. Small intestinal nutrient catabolism

The catabolism of ingesta begins in the oral cavity, stomach, and duodenum, while peri- and postprandial nutrient absorption occurs from the duodenum to proximal ileum, with indigestible starches passing into the large intestine for microbial-based catabolism and absorption.

Carbohydrate digestion begins in the oral cavity, however most carbohydrate digestion occurs in the duodenum and is completed by the proximal jejunum [155]. In the proximal duodenum, pancreatic γ -amylase cleaves α -(1.4) glycosidic-linkages of partially digested starches. This produces maltose, maltotriose, disaccharides and oligosaccharides which remain due to the inability of γ -amylase to cleave α -(1.6) glycosidic-linkages [155]. Oligosaccharides produced by γ -amylase are hydrolysed by isomaltase which cleaves α -(1.6) glycosidic-linkages, producing α -limited dextrans, which are in turn hydrolysed to glucose by α -dextrinase [155]. Duodenal brush border α -glucosidases such as maltase, lactase and sucrase hydrolyse maltose, lactose, and sucrose respectively by cleaving the remaining α -(1.4) glycosidic linkages. The final monosaccharide products are glucose, galactose and fructose which are readily absorbed by enterocytes via dedicated transporters (see below, 1.4.1).

Following initial digestion in the stomach by pepsin, polypeptides are progressively digested into smaller and simpler entities by proteolytic enzymes such as proteases (trypsin, chymotrypsin, and elastase) and peptidases (carboxypeptidase A and B), secreted by the pancreas into the proximal duodenum via the common bile duct. Pancreatic enzymes are

secreted in their inactive forms and activated by brush border enterokinases [155, 158]. Following activation, proteolytic enzymes digest polypeptides producing individual amino acids, di- and tripeptides. Carboxypeptidases located at the brush border and within the cytoplasm of enterocytes complete the digestion process by hydrolysing di- and tripeptides [155, 158]. The majority of protein present in the portal circulation are in the form of individual amino acids, which are readily absorbed by dedicated transporters (see below, 1.4.2)

Lipids are hydrophobic and are digested via a multi-step process prior to uptake in the jejunum. Following partial digestion by lingual and gastric lipases, duodenum bile salts secreted by the gallbladder emulsify triglycerides, permitting pancreatic lipases greater access [155]. Pancreatic lipase and colipase hydrolyse triglycerides, producing 2-monoacylglycerides and free fatty acids. Cholesterol is hydrolysed by carboxyl ester hydrolase, producing free cholesterol and fatty acids [159]. Bile salts also form micelles together with fatty acids, phospholipids, cholesterol and monoglycerides which enables these hydrophobic molecules to cross the unstirred water layer and contact the intestinal mucosa where uptake of specific fatty acids, phospholipids, cholesterol and monoglycerides occurs (see below, 1.4.3, [156, 158, 159]).

1.4. Nutrient absorption

1.4.1. Overview

Uptake of macro and micronutrients in the SI occurs via passive- and active- transport mechanisms [158, 200]. Passive transport includes simple and carrier-mediated diffusion across the brush border membrane. Neither simple nor facilitated diffusion require energy as nutrients are transported down a concentration gradient; i.e., the luminal concentration is greater than the intracellular or blood concentrations [200]. Active transport by specific transporter proteins, in contrast, requires an energy input in the form of adenosine triphosphate (ATP) which is utilised to generate ionic concentration gradients via the exchange of Na^+ , H^+ and K^+ ions by Na^+/H^+ -ATPase and Na^+/K^+ -ATPase complexes located at the brush border and basolateral membranes of enterocytes respectively [156, 158, 200]. This allows nutrients to be transported against nutrient-specific concentration gradients. In this manner, auxiliary ions such as Na^+ and Cl^- are directly and indirectly involved in carrier-mediated transport of macronutrients. For example, the transport of glucose across the apical brush border of enterocytes by the primary glucose transporter sodium-dependent glucose co-transporter 1 (SGLT1) involves co-transport of two Na^+ for each glucose molecule. Glucose is transported by SGLT1 against a glucose concentration gradient when the intracellular glucose concentration exceeds the luminal glucose concentration. When luminal Na^+ concentrations exceed the intracellular Na^+ concentration, Na^+ ions cross the brush border membrane down

a concentration gradient, thus allowing glucose to be transported against its concentration gradient. Numerous brush border and basolateral amino acid transporters also require co-transport or exchange of Na⁺, Cl⁻, H⁺ or K⁺ ions to transport individual amino acids across the brush border and basolateral membranes of enterocytes [158]. The digestion and uptake of each macronutrient and their associated transporters, as well as a brief overview of micronutrient transporters, are discussed below.

1.4.2. Carbohydrates

Dietary carbohydrates are consumed as simple hexose sugars and more complex polysaccharides. Simple hexose sugars consist of monosaccharides (e.g., glucose, galactose, and fructose), disaccharides (e.g., lactose [galactose-glucose dimer], sucrose [glucose-fructose dimer] and maltose [glucose-glucose dimer]) and polysaccharides. The main dietary polysaccharides are plant-derived and include digestible starches (glucose polymers), as well as polysaccharides that are not digested by non-ruminant species, such as the glucose polymer cellulose [158]. Glucose is the preferred fuel for cellular respiration and other physiological processes [201]. As described in section 1.3.4, carbohydrates undergo enzymatic digestion in the oral cavity and stomach, with final digestion taking place in the duodenum and proximal jejunum, prior to being absorbed from the duodenum, jejunum and ileum.

SI uptake of monosaccharides such as glucose, galactose and fructose involves active and passive transport mechanisms and a trio of specific carbohydrate transporters (Fig. 1.11, [158]); SGLT1, glucose transporter 2 (GLUT2) and glucose transporter 5 (GLUT5). Glucose and galactose are transported from the gut lumen into enterocytes via SGLT1 [158]. Fructose uptake occurs exclusively via the facilitated transporter GLUT5, a highly specific transmembrane uniporter located at the brush border membrane of enterocytes [158, 200]. Intracellular glucose, galactose and fructose then travel down their respective concentration gradients to the basolateral membrane, where the bi-directional transmembrane symporter GLUT2 provides egress for glucose and fructose across the basolateral membrane into the circulation [158, 200].

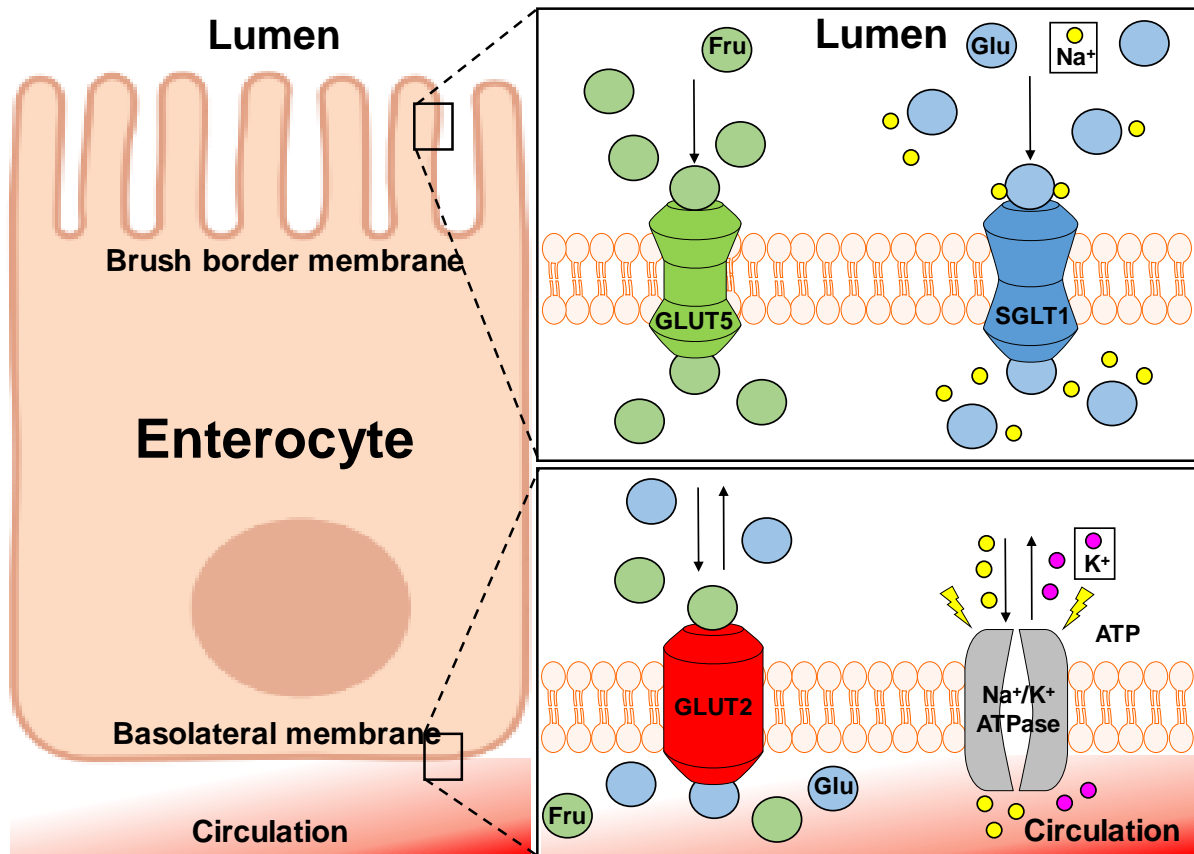


Figure 1.11 Uptake of glucose (Glu) and fructose (Fru) by SI enterocytes. Glucose and fructose are transported across the brush border membrane via SGLT1 and GLUT5. Exit across the basolateral into the circulation is facilitated by GLUT2.

Active glucose transport facilitated by SGLT1 accounts for 80-90% of total glucose transport across the brush border membrane [202, 203]. Transport of glucose via SGLT1 saturates at luminal glucose concentrations of 30-60 mM despite the fact that luminal glucose concentrations can exceed 100 mM in rats and reach as high as 300 mM at the brush border in humans following a meal [202, 204-206]. In contrast, the diffusive component of apical glucose transport remains unsaturated at luminal glucose concentrations exceeding 100 mM [202]. It has been proposed that the diffusive component of glucose transport involves solvent-drag through tight junctions [202, 207]. In addition, there is limited evidence that under specific circumstances, GLUT2 can translocate to the brush border membrane in humans and rats to provide an additional route for brush border glucose transport [208-210]. This evidence, however, is contrary to multiple lines of support that failed to replicate evidence of apical GLUT2 translocation under similar conditions, and is reviewed in more detail elsewhere [211].

1.4.3. Amino acids

Dietary proteins comprise individual amino acids and polypeptides. As described in section 1.3.4., proteins undergo enzymatic digestion in the oral cavity, stomach, and proximal duodenum, which yields individual amino acids and peptides that are then absorbed by the duodenum, jejunum, and ileum. Transport of di- and tripeptides across the brush border of enterocytes occurs via an indirect Na^+ -dependent process involving peptide-transporter 1 (PEPT1) and a H^+ -gradient established by the Na^+/H^+ Exchanger 3 (NHE3) complex situated at the brush border membrane [158]. Individual amino acids are transported across the brush border membrane of enterocytes in a transporter-mediated manner via specific amino acid transporters which belong to the solute carrier (SLC) superfamily (Fig. 1.12). At least nine individual brush border membrane amino acid transporters facilitate amino acid uptake into enterocytes via Na^+ , Cl^- , H^+ , K^+ and/or exchange-dependent mechanisms in the human and mouse SI (Table 1.14, [158, 212]). Egress of amino acids from enterocytes into the circulation across the basolateral membrane is facilitated by at least six different amino acid transporters, the majority of which involve the co-transport or exchange of H^+ , Na^+ , Cl^- and/or the exchange of amino acids from the circulation (Fig. 1.12, Table 1.14, [158]). Depending on luminal amino acid concentrations and cellular demand, some of these transporters can function in a bi-directional manner.

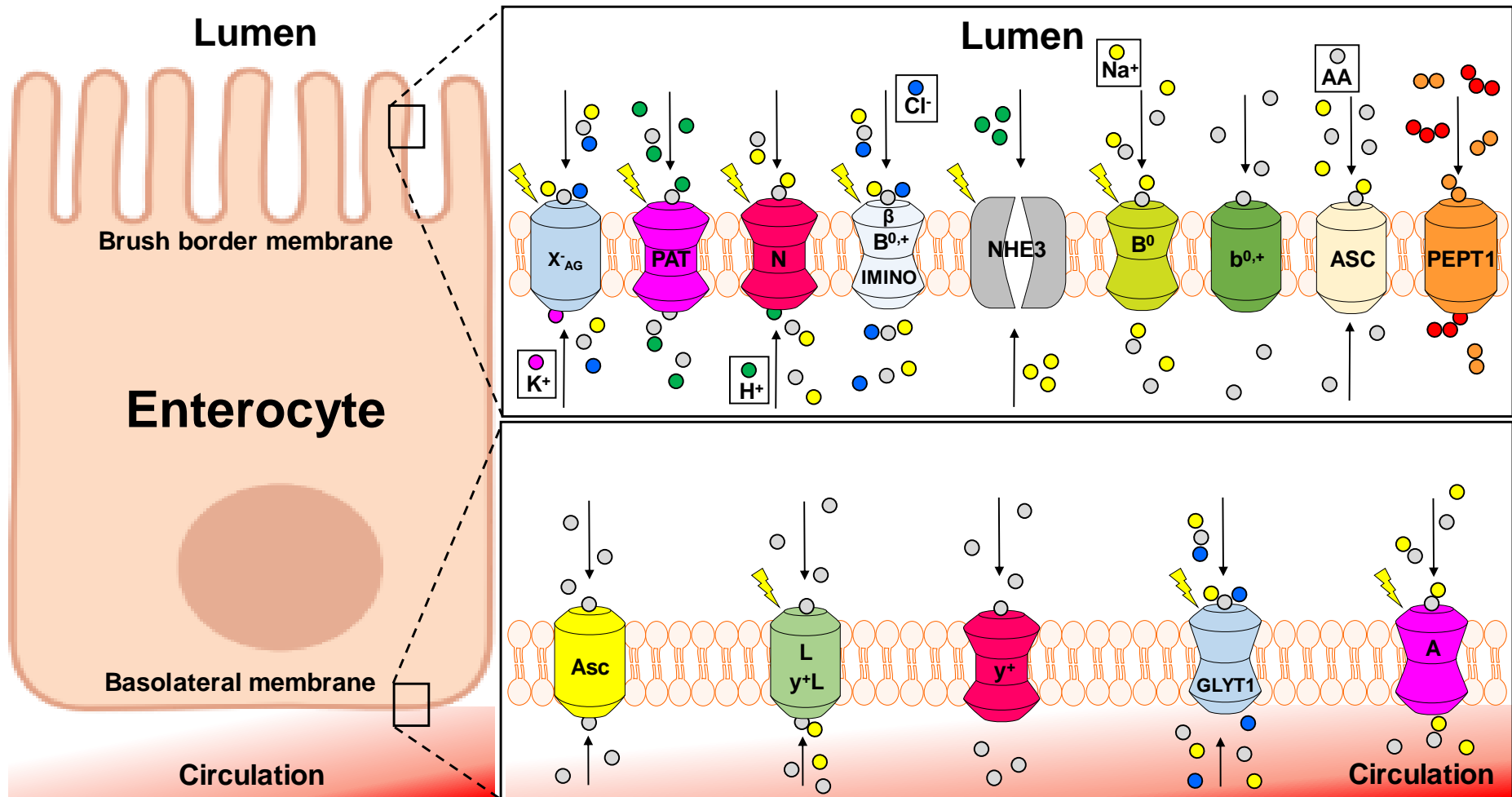


Figure 1.12 Brush border and basolateral membrane amino acid (AA) transport systems. Blue circles represent chloride, green circles represent hydrogen, purple circles represent potassium, yellow circles represent sodium, orange and red circles represent di- and tri-peptides, grey circles represent individual amino acids. Arrows represent direction of transport across membranes. Lightning symbol indicates active transport. Amino acid transporters are labelled with letters: A = System A, sodium-dependent neutral amino acid transporter 2 (SLC38A2), Asc = System Asc,

Asc-type amino acid transporter 1 (SLC7A10), ASC = System ASC, neutral amino acid transporter B(0) (SLC1A5), $b^{0,+}$ = System $b^{0,+}$, heterodimer of $b^{0,+}$ AT (SLC7A9) and rBAT (SLC3A1), B^0 = System B^0 , sodium-dependent neutral amino acid transporter 1 (SLC6A19), $B^{0,+}$ = System $B^{0,+}$, sodium/chloride-dependent neutral and basic amino acid transporter (SLC6A14), β = System β , sodium/chloride-dependent taurine transporter (SLC6A6), GLYT1 = System GLYT1, sodium/chloride-dependent glycine transporter 1 (SLC6A9), IMINO = System IMINO, sodium/chloride-dependent imino acid transporter 1 (SLC6A20), L = system L, large neutral amino acid transporter small subunit 2 (SLC7A8), N = System, sodium-dependent neutral amino acid transporter 3 (SLC38A3) and solute carrier family 38 member 5 (SLC38A5), PAT = System PAT, protein-coupled amino acid transporter 1 (SLC36A1), X_{AG} = System X_{AG} , excitatory amino acid transporter 3 (SLC1A1), y^+ = System y^+ , cationic amino acid transporter 1 (SLC7A1), y^+L = System y^+L , y^+L amino acid transporter 1&2 (SLC7A7 & SLC7A6), NHE3 = sodium-hydrogen exchange complex 3.

Table 1.15 Human SI brush border and basolateral membrane amino acid transporters, based on Kiela 2016 [158]

System	Gene	Protein(s)	Transports
Brush border membrane amino acid transporters			
B ⁰	SLC6A19	B ⁰ AT1 – sodium-dependent neutral amino acid transporter	Na ⁺ -dependent transport of neutral L-amino acids with amino group at α-position (glycine, alanine, valine, leucine, isoleucine, phenylalanine, tyrosine, tryptophan, serine)
B ^{0,+}	SLC6A14	ATB ⁰⁺ - sodium/chloride-dependent neutral and basic amino acid transporter	Na ⁺ /Cl ⁻ -dependent transport of neutral amino acids (alanine, glycine, leucine, isoleucine, methionine, tryptophan, phenylalanine, proline, valine), cationic L-amino acids (histidine, lysine, arginine) and certain neutral D-amino acids
b ^{0,+}	SLC7A9 SLC3A1	Heterodimer of b ⁰⁺ AT (b(0,+)-type amino acid transporter) and rBAT (neutral and basic amino acid transporter)	Na ⁺ -independent transport of neutral amino acids (alanine, glycine, leucine, isoleucine, methionine, tryptophan, phenylalanine, proline, valine), cationic L-amino acids (histidine, lysine, arginine) and cysteine
IMINO	SLC6A20	SIT1 – sodium/chloride-dependent imino acid transporter 1	Na ⁺ /Cl ⁻ -dependent transport of imino acids (hydroxyproline, pipecolic acid) and proline
β	SLC6A6	TAUT - sodium/chloride-dependent taurine transporter	Na ⁺ /Cl ⁻ -dependent transport of taurine and β-alanine
X ^{-AG}	SLC1A1	EAAT3 - excitatory amino acid transporter 3	K ⁺ -efflux driven Na ⁺ /Cl ⁻ -dependent transport of anionic amino acids (aspartate, glutamate)
ASC	SLC1A5	ASCT2 - neutral amino acid transporter B(0)	Na ⁺ -dependent obligatory neutral L-amino acid exchanger with specificity like system B ⁰ , and preference for alanine, serine, and cysteine
N	SLC38A3	SNAT3 - Sodium-dependent neutral amino acid transporter 3	Na ⁺ -coupled transport of glutamine, asparagine, and histidine in exchange for intracellular H ⁺ . Present predominantly in intestinal crypts

	SLC38A5	Solute carrier family 38-member 5	
PAT	SLC36A1	PAT1 – protein-coupled amino acid transporter 1	H ⁺ -coupled transport of short chain amino acids such as glycine, alanine, and proline
Basolateral membrane amino acid transporters			
A	SLC38A2	SNAT2 – Sodium-dependent neutral amino acid transporter 2	Na ⁺ -dependent transport of all neutral amino and imino acids
GLYT1	SLC6A9	GLYT1 – Sodium/chloride-dependent glycine transporter 1	Na ⁺ /Cl ⁻ -dependent transport of glycine
γ ⁺	SLC7A1	CAT1 – Cationic amino acid transporter 1	Na ⁺ -independent transport of cationic amino acids
L	SLC7A8	LAT2 – Large neutral amino acid transporter small subunit 2	Forms a heterodimer with CD98 (heavy chain associated with 4F2 antigen, 4F2hc). Na ⁺ -independent transport of neutral amino acids (excluding imino acids)
γ ^{+L}	SLC7A7	γ ⁺ LAT1 – γ ⁺ L amino acid transporter 1	Both γ ⁺ LAT1 and γ ⁺ LAT2 heterodimerise with CD98. Obligatory exchange system whereby an intracellular cationic amino acid is exchanged for Na ⁺ -coupled entry of a neutral amino acid from the circulation
	SLC7A6	γ ⁺ LAT2 – γ ⁺ L amino acid transporter 2	
Asc	SLC7A10	ASC1 – Asc-type amino acid transporter 1	Forms a heterodimer with CD98. Na ⁺ -independent transport of short chain amino acids. Also functions as a basolateral amino acid exchanger

1.4.4. Lipids

Dietary lipids comprise saturated and unsaturated fatty acids such as triglycerides, phospholipids, and cholesterol [156, 159]. As described in section 1.3.4., fatty acids undergo enzymatic digestion in the oral cavity, stomach and duodenum prior to being absorbed by passive and active mechanisms in the distal SI and large intestine. When the luminal fatty acid concentration exceeds the intracellular concentration, fatty acids freely diffuse across the brush border membrane. When intracellular concentration exceeds the luminal concentration, fatty acid uptake across the brush border membrane occurs through an active process facilitated by fatty acid translocase (FAT/CD36, Fig. 1.13) which transports monoglycerides and medium and long-chain fatty acids (MCFAs, LCFAs, [158, 159]). Cholesterol uptake across the brush border membrane occurs through an active process facilitated by Niemann-Pick C1 like-1 (NPC1L1), which accounts for ~70% of free cholesterol uptake in mice [156, 159]. Within the enterocyte, MCFAs and LCFAs are trafficked to mitochondria via fatty acid binding protein 1 (FABP1) to undergo lipid oxidation which yields ATP, or to the smooth endoplasmic reticulum via fatty acid binding protein 2 (FABP2) to be re-esterified with monoglycerol into triglycerides. The triglycerides are then processed by the Golgi apparatus where they are packaged into chylomicrons together with fat-soluble vitamins, phospholipids and fatty acids [158, 159]. Chylomicrons are then transported across the basolateral membrane via exocytosis and into the lacteal, before eventually entering peripheral circulation via the thoracic duct.

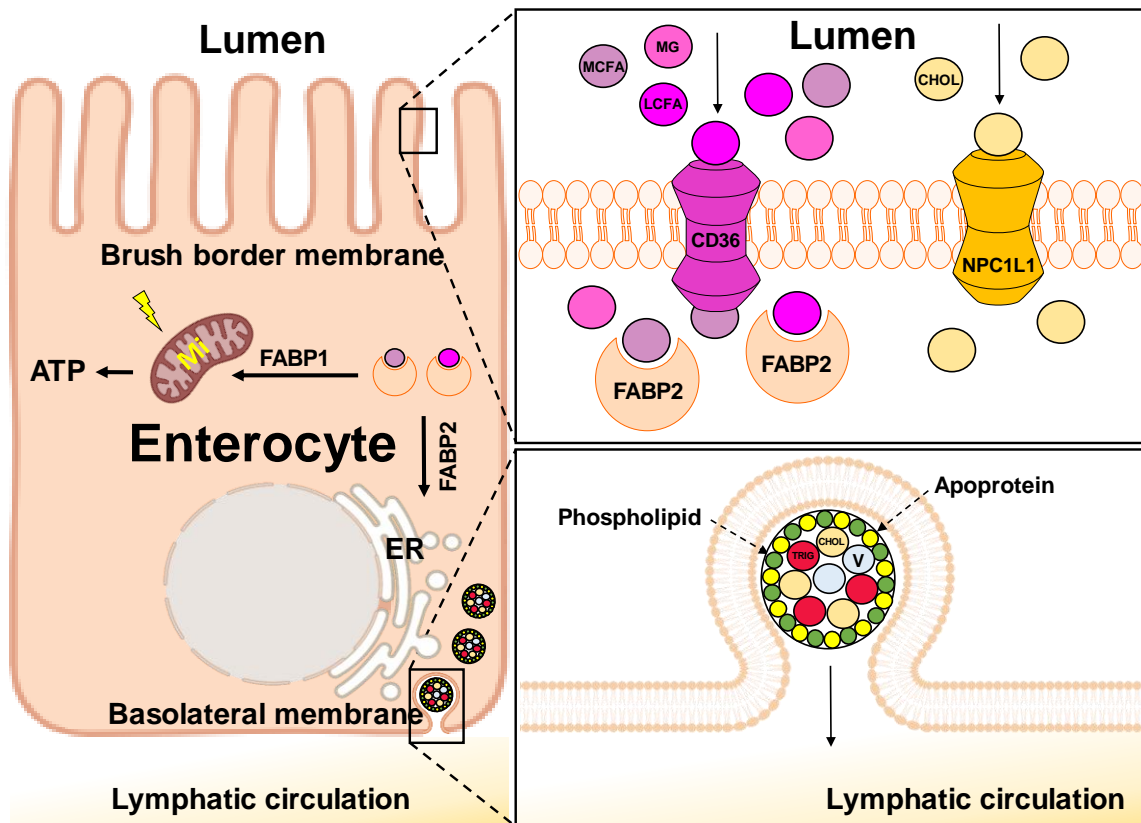


Figure 1.13 Uptake of medium and long-chain fatty acids (MCFA, LCFA), monoglycerides (MG) and cholesterol (CHOL) via CD36 and NPC1L1. Intracellular transporter FABP2 traffics fatty acids to the endoplasmic reticulum (ER) where they are re-esterified together with MG to triglycerides (TG) and packaged together with cholesterol into chylomicrons by the Golgi apparatus for export into the lymphatic system. V = fat-soluble vitamins (Vitamin A, E, D and K). Mi = mitochondria. Figure created in part by using Biorender.com.

1.4.5. Micronutrients

The uptake of micronutrient vitamins and minerals by the SI occurs via nutrient-specific transporters of the solute carrier superfamily [158]. Uptake of iron, calcium, zinc, copper and magnesium, and water-soluble vitamins, such as vitamin B₁₂ and vitamin C occur in a carrier-dependent manner via passive and active processes, while fat- and water-soluble vitamins, such as vitamin A, D, E and K, passively diffuse directly across the brush border membrane of enterocytes [158]. A summary of micronutrient transporters and their co-localisation throughout the SI is provided below (Table 1.15). Although the focus of this thesis is on SI adaptations of macronutrient absorption during pregnancy, adaptations in micronutrient uptake are equally important. To assess the current state of knowledge regarding adaptations of micronutrient absorption throughout pregnancy, a summary of literature describing changes in micronutrient absorption and expression of specific micronutrient transporters during pregnancy is included in the scoping review of maternal adaptations of gastrointestinal nutrient absorption and its determinants during pregnancy in monogastric mammals (Chapter 2 and 3).

Table 1.16 Micronutrient absorption, based on Kiela 2016 [158] and Uhlén et al. 2015 [213].

Micro-nutrient	Transporter			Site(s) of absorption
	Gene	Protein	Name (description)	
Iron	<i>SLC11A2</i>	DMT1	Divalent metal transporter 1 (brush border Fe ²⁺ transporter)	Duodenum
	<i>SLC46A1</i>	HCP1	H ⁺ -coupled folate transporter 1 – also transports heme iron	
	<i>SLC40A1</i>	FPN1	Ferroportin 1 – basolateral Fe ²⁺ transporter	
	<i>Hp</i>	HEPH	Ferroxidase (co-factor to FPN1, involved in basolateral iron transport)	
	<i>ECAC1</i>	TRPV5	Transient receptor potential cation channel subfamily V member 5 subunit – brush border Ca ²⁺ transporter	
Calcium	<i>ECAC2</i>	TRPV6	Transient receptor potential cation channel subfamily V member 6 subunit – brush border Ca ²⁺ transporter	Duodenum
	<i>CACNA1D</i>	Ca _v 1.3	Calcium channel, voltage-dependent, L-type, α-1D subunit – brush border Ca ²⁺ transporter	
	<i>CALB1</i>	Calbindin D28K	Intracellular Ca ²⁺ transporter	
	<i>ATP2B1</i>	PMCA1b	Ca ²⁺ -ATPase – basolateral membrane Ca ²⁺ transporter	
	<i>S100g</i>	Calbindin D9K	Intracellular Ca ²⁺ transporter	
	<i>SLC8A1</i>	NXC1	Na ⁺ /Ca ²⁺ exchanger - basolateral membrane Ca ²⁺ transporter	

Zinc	<i>SLC30A1</i>	ZnT1	Zinc transporter 1 – basolateral zinc transporter	
	<i>SLC30A2</i>	ZnT2	Zinc transporter 2 – vesicular zinc transporter	
	<i>SLC30A4</i>	ZnT4	Zinc transporter 4 – basolateral and vesicular zinc transporter	Duodenum, jejunum, colon
	<i>SLC39A4</i>	ZIP4	Zinc transporter protein 4 – brush border zinc transporter	
	<i>SLC39A5</i>	ZIP5	Zinc transporter protein 5 – basolateral zinc transporter	
Copper	<i>SLC31A1</i>	CRT1	Copper transporter 1 – brush border Cu ⁺ transporter	Duodenum
Magnesium	<i>TRPM6</i>	TRPM6	Transient receptor potential cation channel subfamily M member 6*	
	<i>TRPM7</i>	TRPM7	Transient receptor potential cation channel subfamily M member 7*	Jejunum, ileum
Phosphate	<i>SLC34A2</i>	NaPi-IIb	Na ⁺ -dependent phosphate transporter 2b – brush border PO ₄ ³⁻ transporter	Whole SI
Sulphate	<i>SLC13A1</i>	Solute carrier family 13 member 1/NAS1	Na ⁺ -dependent sulphate transporter 1 (sodium/sulphate symporter) – brush border SO ₄ ²⁻ transporter	
	<i>SLC26A1</i>	Solute carrier family 26 member 1/SAT1	Na ⁺ -independent sulphate transporter 1 (sulphate/oxalate, sulphate/bicarbonate or oxalate/bicarbonate anion exchange) – brush border SO ₄ ²⁻ transporter	Duodenum
	<i>SLC26A2</i>	DTDST	Diastrophic dysplasia sulphate transporter – brush border SO ₄ ²⁻ transporter	
Thiamine (vitamin B ₁)	<i>SLC19A2</i>	THTR1	Thiamine transporter 1 – brush border thiamine transporter	Duodenum, colon
	<i>SLC19A3</i>	THTR2	Thiamine transporter 2 – brush border thiamine transporter	

Riboflavin (vitamin B ₂)	<i>SLC52A1</i>	RFVT1	Riboflavin transporter 1 – brush border riboflavin transporter	Duodenum, colon	
	<i>SLC52A2</i>	RFVT2	Riboflavin transporter 2 – brush border riboflavin transporter		
Biotin (vitamin B ₇)	<i>SLC5A6</i>	SMVT	Na ⁺ -dependent multivitamin transporter – brush border vitamin transporter	Duodenum, colon	
Folic acid (vitamin B ₉)	<i>SLC19A1</i>	FOLT1	Folate transporter 1 – brush border folate transporter	Duodenum, colon	
	<i>SLC46A1</i>	HCP1	H ⁺ -coupled folate transporter 1 – basolateral folate transporter		
Cobalamin (vitamin B ₁₂)	<i>AMN/CUBN</i>	Amnionless/ Cubilin	Cubam – amnionless/cubilin heterodimeric receptor ligand – facilitates brush border transport of vitamin B ₁₂	Ileum, colon	
		<i>ABCC1</i>	MRP1		Multidrug-resistance protein 1 – basolateral vitamin B ₁₂ transporter
Ascorbic acid (vitamin C)	<i>SLC23A1</i>	SVCT1	Na ⁺ -dependent ascorbate cotransporter 1 – brush border vitamin C transporter	Duodenum, colon	
	<i>SLC23A2</i>	SVCT2	Na ⁺ -dependent ascorbate cotransporter 2 – brush border vitamin C transporter		

**TRPM6 and 7 heterodimerise to facilitate brush border transport of Mg²⁺*

1.5. Thesis Aims

Based on the knowledge gaps identified and described above, the aims of this thesis are:

Aim 1: To assess and summarise the current state of knowledge regarding adaptations in gastrointestinal nutrient absorption and its determinants during pregnancy in monogastric mammals.

The protocol and outcomes of the scoping review are described in Chapters 2 and 3.

Aim 2: To characterise changes in SI region-specific active glucose transport across the oestrous cycle in mice.

Outcomes of this aim, together with the establishment and validation of the experimental methodology utilised, are described in Chapter 4.

Aim 3: To characterise changes in whole SI anatomy, macronutrient transporter gene expression and active glucose transport throughout pregnancy in mice.

Outcomes of this aim are described in Chapter 5.

The thesis concludes with Chapter 6, which provides a summary of the data presented, and its significance in the broader context of the state of knowledge in this area of research. Strengths, weaknesses, and limitations of the work presented in the thesis are also discussed, as well as directions for future research.

2. CHAPTER 2: SCOPING REVIEW PROTOCOL

2.1. Overview

Sections 2.3-2.9 are taken directly from a scoping review protocol of which I am first author, and which has been published (Appendix 1, [214]). The content of these sections is unchanged as per University of Adelaide guidelines. The scoping review protocol established the initial search strategy to identify literature that describes adaptations of gastrointestinal nutrient absorption and its determinants in monogastric mammals during pregnancy. Once optimised for each database to be searched, the final search strings were used to search each database for the review itself, the results of which are described in Chapter 3. I compiled the initial search strings, ran the preliminary Pubmed database search, and contributed to drafting and editing of the final manuscript.

2.2. Statement of authorship - Adaptations in gastrointestinal nutrient absorption and its determinants during pregnancy in monogastric mammals: a scoping review protocol

Statement of Authorship

Title of Paper	Adaptations in gastrointestinal nutrient absorption and its determinants during pregnancy in monogastric mammals: a scoping review protocol
Publication Status	<input checked="" type="checkbox"/> Published <input type="checkbox"/> Accepted for Publication <input type="checkbox"/> Submitted for Publication <input type="checkbox"/> Unpublished and Unsubmitted work written in manuscript style
Publication Details	Overduin TS, Page AJ, Young RL, Gatford KL. Adaptations in gastrointestinal nutrient absorption and its determinants during pregnancy in monogastric mammals: a scoping review protocol. JBI Evid Synth. 2022 Feb;20(2):640-646. doi: 10.11124/JBIES-21-00025. PMID: 35165214.

Principal Author

Name of Principal Author (Candidate)	Sebastian Overduin			
Contribution to the Paper	Conception and design of research; drafted manuscript, edited and revised manuscript; approved final version of manuscript.			
Overall percentage (%)	50%			
Certification:	This paper reports on original research I conducted during the period of my Higher Degree by Research candidature and is not subject to any obligations or contractual agreements with a third party that would constrain its inclusion in this thesis. I am the primary author of this paper.			
Signature	<table border="1" style="width: 100%;"> <tr> <td style="width: 80%;"></td> <td style="width: 20%;">Date</td> <td>02/02/2023</td> </tr> </table>		Date	02/02/2023
	Date	02/02/2023		

Co-Author Contributions

By signing the Statement of Authorship, each author certifies that:

- i. the candidate's stated contribution to the publication is accurate (as detailed above);
- ii. permission is granted for the candidate to include the publication in the thesis; and
- iii. the sum of all co-author contributions is equal to 100% less the candidate's stated contribution.

Name of Co-Author	Amanda Page			
Contribution to the Paper	Conception and design of research, edited and revised manuscript, approved final version of manuscript.			
Signature	<table border="1" style="width: 100%;"> <tr> <td style="width: 80%;"></td> <td style="width: 20%;">Date</td> <td>21/2/2023</td> </tr> </table>		Date	21/2/2023
	Date	21/2/2023		

Name of Co-Author	Richard Young			
Contribution to the Paper	Conception and design of research; edited and revised manuscript; approved final version of manuscript.			
Signature	<table border="1" style="width: 100%;"> <tr> <td style="width: 80%;"></td> <td style="width: 20%;">Date</td> <td>Feb 13, 2023</td> </tr> </table>		Date	Feb 13, 2023
	Date	Feb 13, 2023		

Name of Co-Author	Kathryn Gafford		
Contribution to the Paper	Conception and design of research; drafted manuscript, edited and revised manuscript; approved final version of manuscript.		
Signature		Date	10/02/2023

Chapter 2 is reproduced exactly as published with the exception of formatting, which has been changed to maintain consistency throughout the thesis. It has been published as:

Overduin TS, Page AJ, Young RL, Gatford KL. Adaptations in gastrointestinal nutrient absorption and its determinants during pregnancy in monogastric mammals: a scoping review protocol. *JBIE Synthesis*. 2022 Feb;20(2):640-646. doi: 10.11124/JBIES-21-00025. PMID: 35165214. (Appendix 1)

2.3. Abstract

Objective: To characterize the current state of literature and knowledge regarding adaptations of gastrointestinal nutrient absorption, and its determinants, during pregnancy in monogastric mammals.

Introduction: Energy demands increase significantly during pregnancy, due to the metabolic demands associated with placental and fetal growth, and the deposition of fat stores, which support postnatal lactation. Previous studies have examined anatomical changes within the small intestine but have focused on specific pregnancy stages or specific regions of the small intestine. Importantly, little is known about changes in nutrient absorption during pregnancy, and the underlying mechanisms that lead to these changes. An understanding of these adaptations will inform research that aims to improve pregnancy outcomes for both mothers and newborns in the future.

Inclusion criteria: Primary literature that describes gastrointestinal nutrient absorption and/or its determinants during pregnancy in monogastric mammals, including humans and rodents. Only data for normal pregnancies will be included, and models of pathology and illness will be excluded. Studies must include comparisons between pregnant animals at known stages of pregnancy, and non-pregnant controls, or compare animals at different stages of pregnancy.

Methods: The following databases will be searched for literature on this topic: PubMed, Scopus, Web of Science, Embase, MEDLINE (Ovid), and ProQuest Dissertations and Theses. Evidence screening and selection will be carried out independently by two reviewers, and conflicts resolved by discussion with additional members of the review author team. Data will be extracted and presented in tables and/or figures together with a narrative summary.

Keywords: nutrient absorption; nutrient transport; plasticity; pregnancy; small intestine.

2.4. Introduction

Pregnancy represents a period of rapid physiological change in the mother, with multiple systems adapting quickly to meet the demands of the *conceptus*. Physiological adaptations

during pregnancy include increased blood volume and cardiac output (both \uparrow 40% in humans), increased consumption of oxygen (\uparrow 20% in humans), and an increased metabolic rate (\uparrow 15% in humans) [21, 215]. In humans, maternal weight will increase on average between 11.5 and 16 kg throughout gestation [11]. This includes a \sim 3.8 kg fetus [216], and \sim 800 g placenta [12], in addition to fat deposits that support lactation following parturition [49]. In litter-bearing species such as rats and mice, maternal weight gain increases significantly relative to the pre-pregnancy weight, and these species typically double their bodyweight between conception and parturition [13, 14, 16, 217].

During pregnancy, maternal food intake increases to meet increased nutrient demands [5, 218]. Food intake increases throughout pregnancy by \sim 10% to 15% in humans and \sim 25% to 50% in litter-bearing species, such as mice and rats, particularly during the last third of pregnancy [14, 49, 51, 217]. In mice, this is predominantly due to an increase in meal size during the light phase [53]. To support increased nutrient absorption during pregnancy, the gastrointestinal tract, and in particular the small intestine, must adapt. The small intestine is made up of three main segments: the duodenum, jejunum, and ileum. Following partial digestion in the stomach, nutrients are released into the duodenum where they undergo enzymatic digestion, with the breakdown of carbohydrates, fats, and proteins into smaller components to allow nutrient absorption [189]. While some nutrient absorption occurs in the duodenum, the majority of nutrient absorption occurs in the jejunum [189]. To maximize the surface area available for nutrient absorption, the small intestine is lined with villi protruding from the basement membrane into the luminal space [158, 189]. The villi are lined with a single cell epithelium, consisting of secretory cells and enterocytes that sense and absorb nutrients as they transit through the small intestine following digestion [158, 189]. In rats, small intestinal weight, length, and duodenal circumference increase during pregnancy [219]. In addition, duodenal and jejunal villi length increase by late pregnancy, further increasing the surface area available for nutrient absorption [175, 218]. Other determinants of nutrient absorption also change in pregnancy. *In vitro* experiments, using isolated segments of rat GIT, including the antrum, suggest that gut motility is decreased and transit time increased during pregnancy as a result of increased concentrations of progesterone [220-222]. An increased transit time would be expected to allow the small intestine to absorb more nutrients over a longer time span. Additional evidence that nutrient transport mechanisms upregulate in pregnancy comes from a study in rats, in which gene expression of nutrient and ion transporter proteins was upregulated in the duodenum by late pregnancy [223]. This included $>$ 1.5-fold higher SLC5A1 gene expression [223], encoding the sodium-linked glucose transporter 1 (SLGT1), the primary intestinal glucose transporter that accounts for the majority of glucose uptake [158, 224]. Similarly, SLC2A5 gene expression, encoding a highly specific fructose transporter

protein (GLUT5) [209], was ~1.5-fold higher in late pregnant than non-pregnant rats [223]. Additionally, duodenal absorption of the micronutrient calcium was significantly increased throughout pregnancy in mice due to upregulation of the transient receptor potential vanilloid sub-family member 6 (TRPV6) calcium channels [225]. Less has been reported regarding how and when nutrient absorption changes during pregnancy.

Given the significant gaps in current knowledge regarding adaptations of gastrointestinal nutrient absorption during pregnancy, it is important to assess current literature to summarize the current state of knowledge and to identify gaps in knowledge. This scoping review will provide a broad overview of published and unpublished evidence regarding changes in nutrient absorption during pregnancy and its determinants. In addition, this mapping will identify gaps in evidence in order to inform future research priorities to understand maternal adaptations to pregnancy and optimize maternal nutrition during pregnancy. A preliminary search of MEDLINE, the Cochrane Database of Systematic Reviews, *JBI Evidence Synthesis*, and PROSPERO was conducted; no current or in-progress systematic reviews or scoping reviews on the topic were identified.

2.5. Review question:

- What evidence is available regarding how gastrointestinal nutrient absorption and its determinants change during pregnancy in monogastric mammals?
- What are the key characteristics of the evidence in this field?
- What evidence gaps can be identified in the area?

2.6. Inclusion criteria

2.6.1. Participants

This review will include studies that investigated changes in nutrient absorption and its determinants during pregnancy in any monogastric mammal. Studies will be included if they contain data from normal pregnancies and compare known stages of pregnancy to each other and/or to non-pregnant subjects. Data from groups identified by authors or study reviewers as reflecting non-typical pregnancy or disease states (such as current obesity, pregnancies with growth-restricted fetus/es, *hyperemesis gravidum*), or altered physiology due to prior or current interventions (such as women who have undergone bariatric surgery before pregnancy, experimental diets, genetic modification) will be excluded.

2.6.2. Concept

The proposed scoping review will characterize current knowledge regarding adaptations in nutrient absorption and its determinants during pregnancy. Specifically, it will evaluate how, when, and where nutrient absorption changes occur within the small intestine during

pregnancy, and how determinants of nutrient absorption change during pregnancy (ie, gastric emptying/motility, small intestinal structure, nutrient transporter expression, and localization).

2.6.3. Context

Studies of any monogastric species will compare non-pregnant subjects with pregnant subjects at known pregnancy stages, and/or compare outcomes between different pregnancy stages. Only data collected in a non-pathological or non-disease setting is relevant for this review.

2.6.4. Types of studies

Quantitative research studies will be included in this review, whether published or unpublished (e.g., higher-degree theses). Eligible study designs include prospective and retrospective cohort studies, case-control studies, and analytical cross-sectional studies, where these studies include the populations and concepts of interest. Studies published in English will be included in this review. Resource limitations preclude inclusion of studies published in languages other than English. There will be no date or geographical limitations for inclusion in this review.

2.7. Methods

The proposed scoping review will be conducted in accordance with the JBI methodology for scoping reviews [226], utilizing the Preferred Reporting Items for Systematic Reviews and Meta-analysis extension for Scoping Reviews (PRISMA-ScR) reporting guideline and checklist [227].

2.7.1. Search strategy

The search strategy will include both published and unpublished literature. A limited search of PubMed was undertaken to obtain an initial overview of the current published literature including keywords and index terms of relevant articles. The search terms used appeared in the title and/or abstract of relevant articles. Together, these terms were used to develop a full search strategy for searching MEDLINE (PubMed; Appendix I), which will be adapted with assistance from a University of Adelaide research librarian for the different data bases to be searched. Final search strings for the remaining databases to be searched will be included as appendices in the final scoping review article. Reference lists of all included articles and key reviews will also be searched. All searches will be updated immediately prior to data synthesis.

The following databases will be searched as part of this review: MEDLINE (PubMed), Scopus (Elsevier), Web of Science, Embase (Elsevier) and ProQuest Theses and Dissertations.

2.7.2. Study selection

Following a search of selected databases, identified citations will be collated and uploaded into Covidence systematic review software (Veritas Health Innovation, Melbourne, Australia) via Endnote v.X9 (Clarivate Analytics, PA, USA) and duplicates removed. Titles and abstracts will be screened independently by at least two reviewers, and assessed against the inclusion criteria outlined for this review. Literature deemed relevant will be retrieved in full, and full text records will be assessed against the inclusion criteria by at least two independent reviewers. Reasons for exclusion will be recorded for any articles removed at full-text screening. The citation details of the relevant literature will be imported into the JBI System for the Unified Management, Assessment and Review of Information (JBI SUMARI; JBI, Adelaide, Australia) [228]. Any disagreement between reviewers at abstract or full-text screening stages will be resolved by discussion with additional members of the review author team.

2.7.3. Data extraction

Data will be extracted from included papers by two independent reviewers using the standardized data extraction tools in JBI SUMARI [227, 228]. The data extraction tool will be modified as required throughout the review, with any modifications documented in full in the final scoping review. Any disagreements between reviewers will be resolved through discussion or consultation with another reviewer on the team.

Data to be extracted includes, but is not limited to, information regarding the following parameters of interest: species and strain(s) examined (e.g. rat, mouse, human), nutrient/diet consumed throughout the study, pregnancy stage(s) assessed, analytical techniques used to measure outcomes or answer the research questions (e.g. polymerase chain reaction, histology), and comparison groups. Data regarding small intestinal parameters will also be extracted. This includes, but is not limited to: small intestinal weight (wet/dry), length (whole + individual regions, i.e., duodenum, jejunum, ileum) and data regarding nutrient absorption/transport.

2.7.4. Data analysis and presentation

Extracted data including what types of outcomes have been assessed and the stages of pregnancy included in relevant studies will be summarised in tables, with outcomes presented either as mean \pm SD or relative values where appropriate. Summaries of study characteristics will be presented visually where appropriate. Other aspects of the data (i.e., sample size and statistical methods used to analyze experimental data) will also be examined. A narrative synthesis will accompany these summaries and describe their relevance to the review question.

2.8. Appendix I: Search strategy

MEDLINE (PubMed)

The initial search was conducted on April 23, 2021, and returned 6938 results.

The search string is comprised of 3 substrings: search terms relating to pregnancy, gut or gut regions, and anatomical or functional outcomes: (Pregnan* [TW] OR "Pregnancy" [MeSH] OR Gestat* [TW]) AND (Gastrointest* [TW] OR "gastrointestinal tract" [MeSH] OR Gastric [TW] OR Alimentary [TW] OR Digestive tract [TW] OR Digestive system [TW] OR Small intestine [TW] OR Duoden* [TW] OR Jejun* [TW] OR Ileum [TW] OR Ileal [TW] OR Stomach [TW]) AND (Nutrient [TW] OR carbohydrate [TW] OR glucose [TW] OR fructose [TW] OR sucrose [TW] OR protein [TW] OR amino acid [TW] OR fatty acid [TW] OR lipid [TW] OR vitamin [TW] OR folic acid [TW] OR folate [TW] OR calcium [TW] OR iron [TW] OR zinc [TW]) AND ("biological transport" [Mesh] OR absorption [TW] OR uptake [TW] OR transport [TW] OR Motility [TW] OR "ileal brake" [TW] OR Transit [TW] OR Gastric emptying [TW] OR "anatomy" [MeSH] OR Weight [TW] OR Mass [TW] OR Length [TW] OR Surface area [TW] OR Enterocyte [TW] OR Vasculat* [TW] OR blood vessel [TW] OR capillary [TW] OR Innervation [TW] OR Nerve [TW] OR Vill* [TW] OR Crypt [TW] OR Muscle thickness [TW] OR Muscle depth [TW] OR SGLT1 [TW] OR SGLT-1 [TW] OR sodium linked glucose transporter 1 [TW] OR GLUT2 [TW] OR GLUT-2 [TW] OR glucose transporter 2 [TW] OR Slc2a2 [TW] OR GLUT5 [TW] OR GLUT-5 [TW] OR glucose transporter 5 [TW] OR Slc2a5 [TW] OR PEPT1 [TW] OR PEPT-1 [TW] OR peptide transporter [TW] OR SLC6A6 [TW] OR SLC6A19 [TW] OR "CD36" [TIAB] OR "cluster of differentiation 36" [TIAB] OR LFABP [TW] OR "Fatty acid binding protein 2" [TIAB]) AND eng[LA] NOT review[PT]

2.9. Appendix II: Data extraction instrument

Citation	
Reference location (PMID/DOI/URL)	
Study design	
Species and strain/breed	
Age during study	
Nutrition (diet, amount, timing) during study	
Housing during study	
Normal duration of pregnancy (days)	
Control group(s) characteristics (including sample size)	
Pregnant group(s) characteristics (including sample size, stage/s of pregnancy, litter size)	
Type of outcome of interests reported	Nutrient absorption or transport, food transit or tissue motility, gastrointestinal tissue weight or size, microstructure, transporter expression
Outcome of interest 1	
Assessment method for outcome of interest 1	
Outcome of interest 2	
Assessment method for outcome of interest 1	
Outcome of interest 3	
Assessment method for outcome of interest 1	
Statistical methods used to compare pregnancy stages	

3. CHAPTER 3: SCOPING REVIEW

3.1. Overview

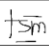
Sections 3.3-3.9 are taken directly from a scoping review protocol of which I am first author, and which has been submitted for publication in *Nutrition Reviews*. The content of these sections is unchanged as per University of Adelaide guidelines. Chapter 3 describes the results of a scoping review which was undertaken to identify and summarise literature which describes changes in small intestinal nutrient absorption and its determinants in monogastric mammals during pregnancy. The identified gaps in existing knowledge will help guide future research which will ultimately improve pregnancy outcomes for mother and child. For the scoping review, my contribution is as follows; I was involved in putting together the initial search strings and optimising them for each database to be searched, performed all database searches, screened titles and abstracts of identified citations, screened full texts of citations which met the inclusion criteria, and took part in conflict resolution. I also extracted, collated and summarised data from full texts which met the criteria for data extraction, co-wrote and edited the final manuscript. The data presented in Chapter 3 has been submitted for publication in the *Journal of Gastroenterology* (14th of December 2023, JOGA-D-23-01736), and I am first author of the final manuscript.

3.2. Statement of authorship - Adaptations in gastrointestinal nutrient absorption and its determinants during pregnancy in monogastric mammals: a scoping review

Statement of Authorship

Title of Paper	Adaptations in gastrointestinal nutrient absorption and its determinants during pregnancy in monogastric mammals: a scoping review
Publication Status	<input type="checkbox"/> Published <input type="checkbox"/> Accepted for Publication <input checked="" type="checkbox"/> Submitted for Publication <input type="checkbox"/> Unpublished and Unsubmitted work written in manuscript style
Publication Details	Teunis Sebastian Overduin, Amanda J. Page, Richard L. Young, Kathryn L. Gatford 2023 Adaptations in gastrointestinal nutrient absorption and its determinants during pregnancy in monogastric mammals: a scoping review. <i>Journal of Gastroenterology</i> , JOGA-S-23-02361, submitted 14 December 2023

Principal Author

Name of Principal Author (Candidate)	Teunis Sebastian Overduin		
Contribution to the Paper	Conception and design of research, performed all database searches, screened titles, abstracts and full texts, resolved conflicts, data extraction, collation and presentation, wrote, edited and approved final version of manuscript		
Overall percentage (%)	50%		
Certification:	This paper reports on original research I conducted during the period of my Higher Degree by Research candidature and is not subject to any obligations or contractual agreements with a third party that would constrain its inclusion in this thesis. I am the primary author of this paper.		
Signature		Date	4 th of December 2023

Co-Author Contributions

By signing the Statement of Authorship, each author certifies that:

- i. the candidate's stated contribution to the publication is accurate (as detailed above);
- ii. permission is granted for the candidate to include the publication in the thesis; and
- iii. the sum of all co-author contributions is equal to 100% less the candidate's stated contribution.

Name of Co-Author	Richard Young		
Contribution to the Paper	Conception and design of research, screened titles, abstracts and full texts, resolved conflicts, edited and approved final version of manuscript		
Signature		Date	Dec 12, 2023

Name of Co-Author	Amanda Page		
Contribution to the Paper	Conception and design of research, screened titles, abstracts and full texts, resolved conflicts, edited and approved final version of manuscript		
Signature		Date	15/12/23

Name of Co-Author	Kathryn Gatford		
Contribution to the Paper	Conception and design of research, performed all database searches, screened titles, abstracts and full texts, resolved conflicts, data extraction, collation and presentation, drafted, edited and approved final version of manuscript		
Signature		Date	14 December 2023

Chapter 3 is reproduced exactly as submitted, with the exception of formatting, which has been changed to maintain consistency throughout the thesis. It has been submitted for publication in the *Journal of Gastroenterology* (14th of December 2023, JOGA-D-23-01736).

3.3. Abstract

Pregnancy increases nutrient demand, but how nutrient uptake and its determinants adapt to facilitate nutrient delivery is unclear. We therefore aimed to identify and characterise evidence and evidence gaps regarding changes in gastrointestinal nutrient absorption and its determinants during pregnancy in monogastric mammals. We conducted a scoping review of peer-reviewed sources across PubMed, Scopus, Web of Science, Embase and ProQuest (theses and dissertations) databases. We extracted data including species, pregnancy stages and outcomes. Where sufficient data for a given outcome was available, relative values from multiple studies were summarised graphically or in tables to allow comparison across pregnancy stages and/or SI regions. We identified 26855 sources from database searches, of which only 159 were eligible. Mechanistic studies were largely restricted to rodents, and most compared non- and late-pregnant groups, with fewer reports including early- or mid-pregnant groups. During pregnancy, there is some evidence of greater capacity for glucose uptake but unchanged amino acid uptake, and good evidence for increased uptake of calcium, iron and zinc, and slower GI passage of nutrients. The available evidence indicates that acute glucose uptake, gastric emptying and activities of sucrase, maltase and lactase do not change during pregnancy. Gaps in knowledge include effects of pregnancy on uptake of specific amino acids, lipids, and most minerals and vitamins. We conclude that the gastrointestinal tract adapts during pregnancy to facilitate increased nutrient absorption. Additional data are required to assess the underlying mechanisms and impacts on absorption of many nutrients, as well as determining the timing of these adaptations.

3.4. Introduction

Maternal nutrient and energy demands increase during pregnancy to facilitate conceptus growth and development, support increased maternal organ function and deposit fat reserves in preparation for lactation [21, 215]. Gains in maternal body weight of ~15% occur across human pregnancy [11], while litter-bearing species such as rats and mice may double their body weight by the end of pregnancy [13, 14, 16, 217]. Maternal food intake increases by ~10-15% in humans and up to 50% in rodents, particularly towards the end of pregnancy, concurrent with rapid fetal growth [14, 49, 51, 217]. To support these greater nutrient demands, increases in absorption of several micronutrients have been well-characterised, particularly at late pregnancy. For example, serial stable-isotope studies conducted in women

recruited from early pregnancy show a 9-fold increase in absorption of orally administered non-haem iron between weeks 12 and 36 of gestation [229]. Intestinal transport of orally-administered non-haem iron was also 2-fold higher in late-pregnant compared to non-pregnant mice [230]. However, the effects of pregnancy on macronutrient absorption are less studied. There is some evidence for increased glucose absorption during mid-late pregnancy following glucose infusion into the whole small intestine (SI) in anaesthetised rats [231] and in ligated SI segments from anaesthetised hamsters at late pregnancy compared to non-pregnant [232]. Portal vein glucose concentrations following a standardised meal were also 20% higher in late-pregnant compared to non-pregnant dogs [233], consistent with increased SI absorption during pregnancy. Few studies have assessed effects of pregnancy on *in vivo* uptake of other macronutrients or have measured nutrient absorption at earlier stages of pregnancy, to identify when these changes occur.

Multiple mechanisms likely underlie increased nutrient absorption during pregnancy. The SI is a critical site of nutrient digestion, notably the duodenum, where pancreatic enzymes and bile enter the tract [155]. Most macronutrients are taken up from the duodenum and jejunum into the maternal circulation, while entry of nutrients to the ileum can slow motility of the gastrointestinal (GI) tract, acting as a brake to extend contact of nutrients with absorptive surfaces and hence minimise nutrient loss [182]. Absorption within the colon is also important for absorption of short-chain fatty acids generated by microbial digestion of complex carbohydrates, and for some minerals and vitamins [162]. Nutrient absorption can therefore be increased by adaptations in gross anatomy, microstructure such as greater surface area due to villi lengthening, slower transit of food through the tract, or increased activity of digestive enzymes or transporters required for facilitated or active nutrient uptake. Several of these adaptations occur in pregnancy: total SI weight and length increase in conjunction with food intake during rat pregnancy [234], while duodenal and jejunal villi are longer in late pregnant than non-pregnant rats [175, 218]. Duodenal transcript abundance of *Slc5a1*, encoding the primary intestinal carbohydrate transporter sodium-dependent glucose transporter 1 (SGLT1 [202, 203]) was also 1.5-fold higher in late-pregnant compared to non-pregnant rats [223]. However, it is unclear how these mechanisms change throughout pregnancy, and whether changes are consistent between species.

We therefore conducted a comprehensive scoping review of existing literature, to answer the following questions:

- What evidence is available regarding how gastrointestinal nutrient absorption and its determinants change during pregnancy in monogastric mammals?
- What are the key characteristics of the evidence in this field?

- What evidence gaps can be identified in the area?

3.5. Methods

3.5.1. Protocol and search strategy

This scoping review was conducted in accordance with the published protocol [235], with inclusion of peer-reviewed quantitative studies (including accepted Masters and PhD theses after examination), but with exclusion of pre-review sources. We followed the Joanna Briggs Institute (JBI) methodology for scoping reviews [226], utilising the PRISMA-ScR reporting guideline and checklist [227]. In brief, we searched PubMed, Scopus, Web of Science, Embase and ProQuest Dissertations and Theses Global databases for studies describing adaptations in nutrient absorption and/or its determinants during healthy pregnancy in monogastric mammals. There was no start date or geographical limitations for inclusion in this review; peer-reviewed studies were included if accepted and published on-line or in print by the end of June 2023. Search strings for all databases are provided in the supplementary files (Table S1). Reference lists of all included articles and key reviews were screened to identify additional sources, which were imported into Covidence at the full text stage.

3.5.2. Eligibility criteria

The literature search was limited to studies of monogastric mammals published in English. Studies without original data, such as reviews, were excluded, as were conference abstracts, case studies, and editorial letters. Primary sources were included if they contained quantitative data on nutrient absorption and/or its determinants from normal pregnancies and compared outcomes at one or more stages of pregnancy to each other and/or to non-pregnant subjects. Only data collected in a non-pathological/disease setting was accepted; we excluded data from groups with non-typical pregnancies or in disease states (such as current obesity, pregnancies with growth-restricted fetus/es, *hyperemesis gravidum*), or altered physiology due to prior or current interventions (such as women who have undergone bariatric surgery before pregnancy, experimental diets, genetic modification).

3.5.3. Study selection

Citations identified from each database were imported into Endnote X9 software (Clarivate Analytics, Philadelphia USA) and duplicates removed. Citations were then uploaded into Covidence systematic review software (Veritas Health Innovation, Melbourne, Australia). Titles and abstract text were screened independently by two reviewers (T.S.O., A.J.P, R.L.Y., K.L.G.) against the published inclusion and exclusion criteria [235]. Full text records were assessed independently by two reviewers (T.S.O and K.L.G.), and reasons for exclusion recorded. Any disagreements between reviewers at abstract or full-text screening stages were resolved by discussion with additional members of the review team.

3.5.4. Data extraction and synthesis

Two reviewers (T.S.O and K.L.G.) extracted data from included studies within Covidence using the standardised data extraction approach from JBI [227]. Information including species and strain, nutrition, pregnancy stage(s), and outcomes including measures of nutrient absorption and its determinants including SI anatomy, GI tract motility, nutrient transporter expression and digestive enzyme activity were extracted from each source [235]. Any disagreements between reviewers were resolved through discussion with at least one additional member of the review team (A.J.P and R.L.Y.). T.S.O and K.L.G. analysed the extracted data and synthesised the results. A summary of extracted data for each source is provided in Table S2. Extracted data were classified by outcome type, and the availability of evidence summarised graphically by species and stage of pregnancy. Where sufficient data was available to allow comparison of an outcome across pregnancy stages and/or SI regions, relative values from multiple studies were summarised graphically or in tables, while other data were summarised in text.

3.6. Results

3.6.1. Characteristics of published literature

Of the 26855 studies identified in literature searches, 8130 were excluded as duplicates, and 18725 papers screened at title and abstract stage (Fig. 3.1). Of these, 98% (18202 abstracts) were excluded as irrelevant, leaving 365 papers for full text review, in addition to 158 papers identified from screening reference lists. These 523 full texts were screened, and 364 excluded, primarily as they did not report outcomes of interest, did not include a comparator group, or did not include data from normal pregnancies. Data was extracted from 159 eligible studies (Fig. 3.1).

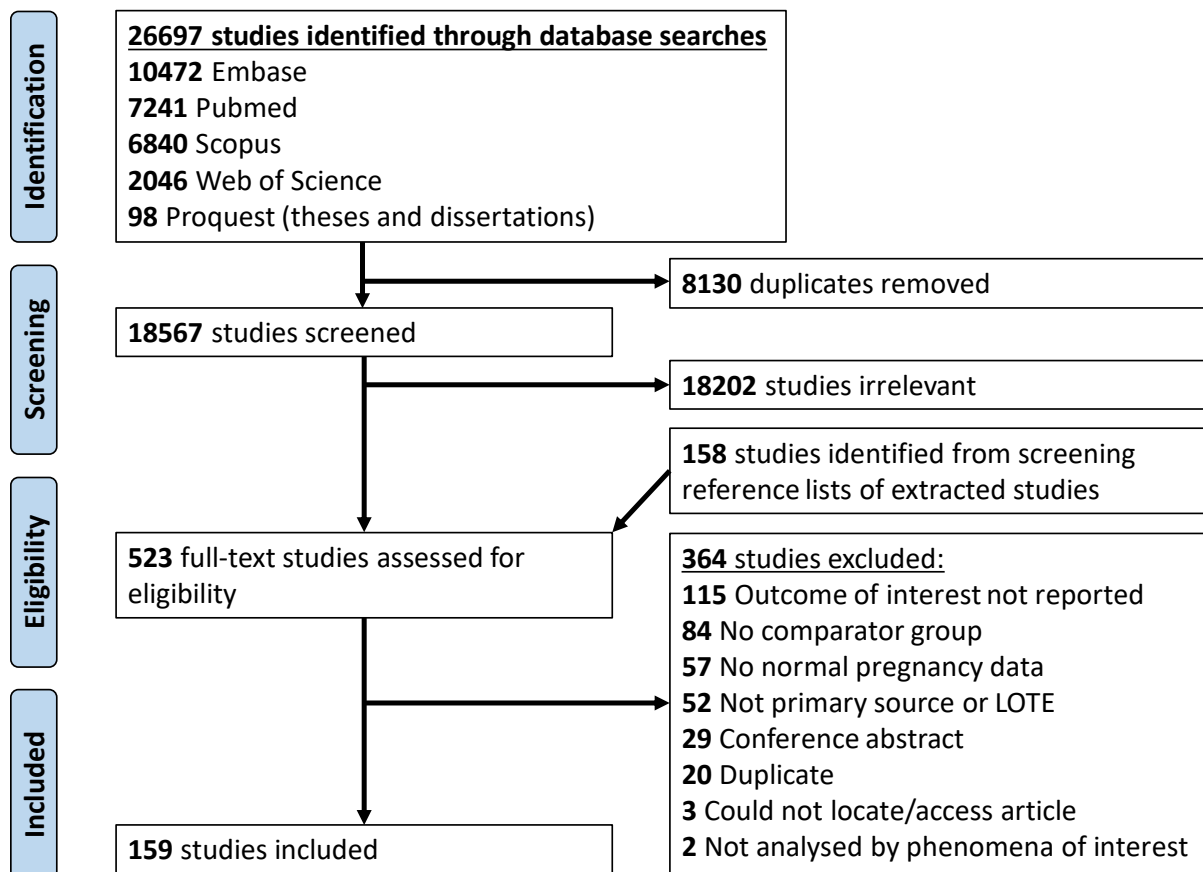


Figure 3.1 PRISMA flow diagram

The majority of extracted studies were performed in rats ($n=81$) or humans ($n=45$), with fewer studies in mice ($n=18$) and a range of other species of monogastric mammals ($n=15$), including dog, pig, common shrew (*Sorex araneus*), and common root vole (*Microtus oeconomus*). The species studied differed strikingly between outcome types (Fig. 3.2A): studies of gallbladder emptying during pregnancy were performed exclusively in humans, while studies of SI regional and overall anatomy, nutrient transporter expression and digestive enzyme activity were reported only in non-human species, mostly rodents (Fig. 3.2A). Both human and non-human studies of nutrient uptake during pregnancy were reported, with studies involving *ex vivo* measures less common and reported only in rats and mice (Fig. 3.2A). Similarly, coverage of outcomes across pregnancy stages was limited, with most outcomes characterised in late-pregnant and non-pregnant animals, with fewer outcomes characterised during early- and mid-pregnancy, particularly for regional and overall SI anatomy, nutrient transporter expression and digestive enzyme activity (Fig. 3.2B).

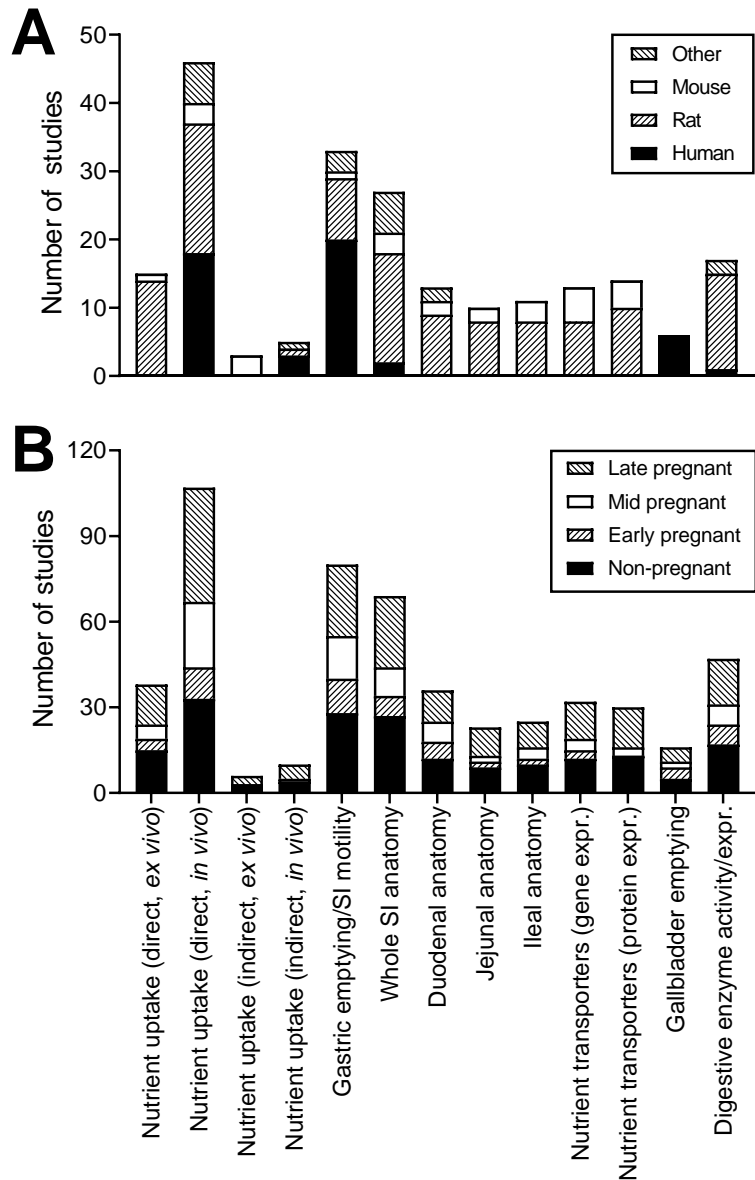
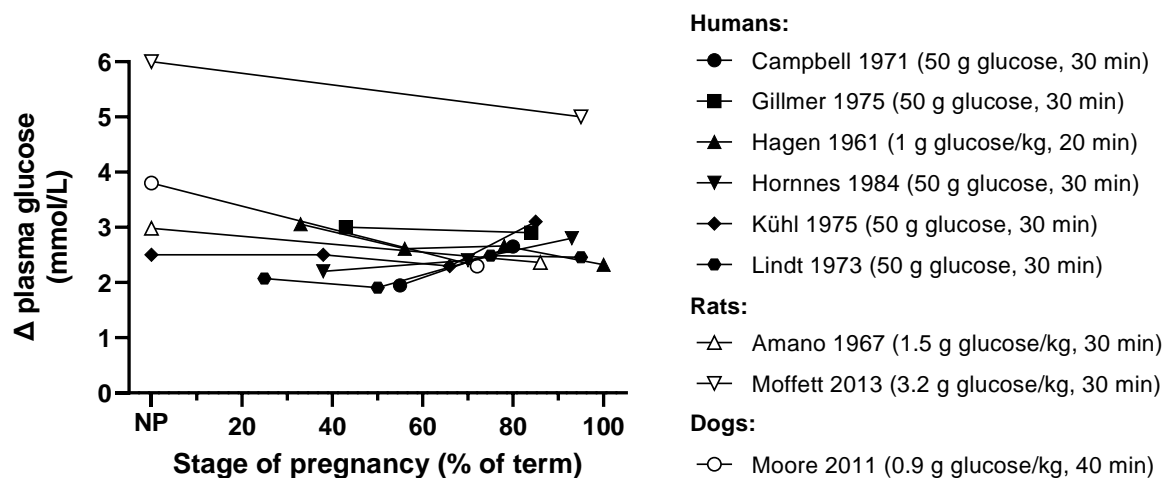


Figure 3.2 Characteristics of included studies. Numbers of studies reporting each outcome type in each species (A) and pregnancy stage (B). Studies were not included in counts for specific pregnancy stages where groups overlapped pregnancy stages or the stage of pregnancy was not stated

3.6.2. Macronutrient uptake – carbohydrates

Most eligible *in vivo* studies measured the rise in circulating glucose as a marker of SI carbohydrate uptake. Acute increases in systemic circulating glucose (Fig. 3.3A) after an oral glucose tolerance test (OGTT) were generally similar across pregnancy stages in humans (6 studies), rats (2 studies) and dogs (1 study). However, in these human studies, the rise in plasma glucose after oral glucose increased in amplitude and the peak was generally delayed with advancing pregnancy (Fig. 3.3B). A delayed rise in plasma glucose following OGTT could at least in part be due to dilution effects caused by an expansion of maternal blood volume, which peaks at 145% of non-pregnant blood volume in humans [21]. Patterns of glucose rise were not generally different between non-pregnant and late pregnant rats and dogs, possibly reflecting rapid placental nutrient uptake in these litter-bearing species (Fig. 3.3B). Similar to effects of human pregnancy on patterns after OGTT, circulating glucose concentrations in meal test studies were higher from 15 until 120 minutes after chow feeding in late pregnant compared to non-pregnant rabbits [236], and from 90 until 270 minutes following intra-gastric administration of a liquid meal including glucose in mid-late pregnant compared to non-pregnant dogs [233]. Effects of pregnancy stage on carbohydrate responses to mixed meal challenges were contradictory in two human studies. Plasma glucose responses following consumption of a mixed meal were similar at 16, 26 and 36 weeks of pregnancy in one study [237]. In contrast, Stanley *et al.* reported higher peak plasma glucose concentrations after a similar carbohydrate load in late (36-38 weeks) compared to early (14-16 weeks) or mid-pregnancy (26-28 weeks), although unlike OGTT findings, the timing of peak circulating glucose concentrations was similar between groups [238]. These human meal test studies did not include non-pregnant comparison groups.

A.



B.

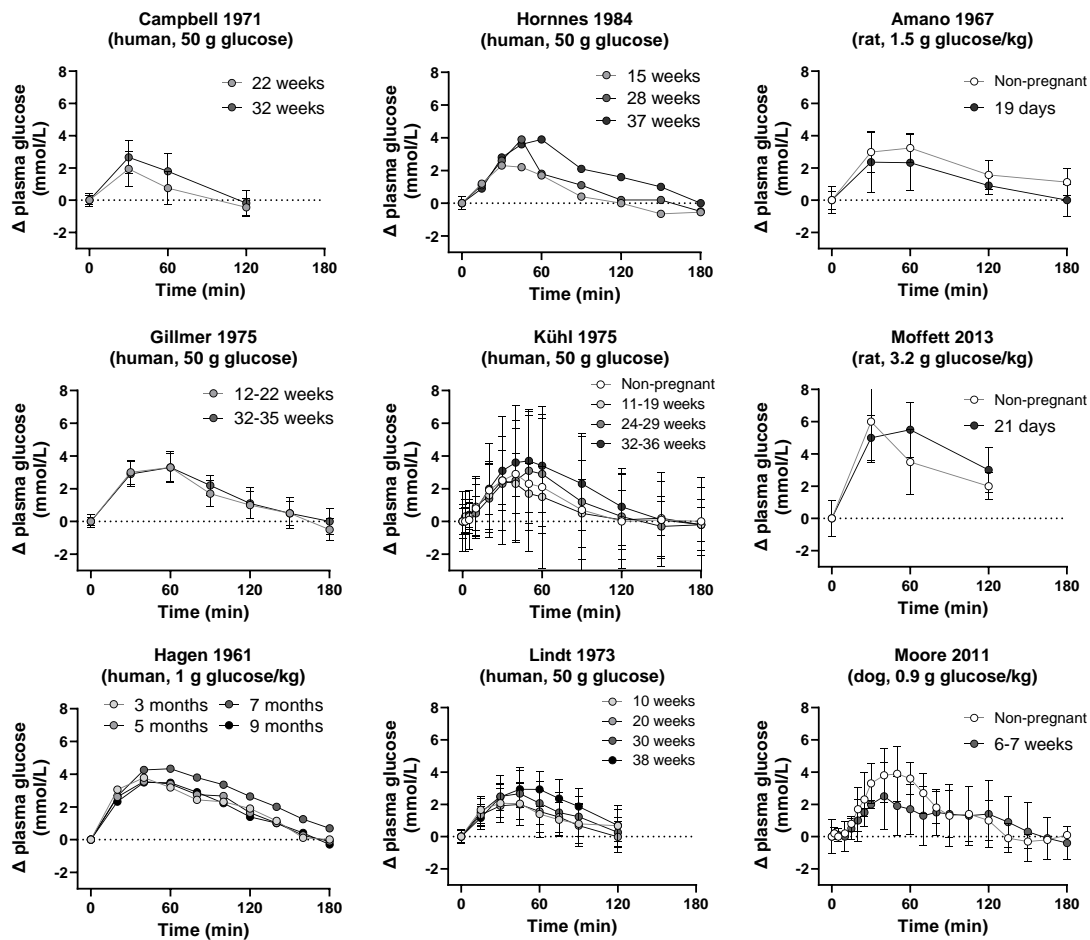


Figure 3.3 *In vivo* glucose uptake during pregnancy. A. Acute changes in systemic glucose concentrations after an oral glucose challenge. Symbols show the change in circulating glucose concentration from pre-test fasting values to 30 minutes after oral glucose challenge (or the closest available time-point). Each study is shown in different symbols and data from the same study are joined by lines. The legend indicates the dose of glucose given during the oral challenge and the time-point at which post-challenge glucose concentrations were measured. B. Changes in systemic glucose concentrations after oral glucose challenges. Symbols show the change in circulating glucose concentration from pre-test fasting values after oral glucose challenge. Each study is shown on a separate panel, with the species and dose of glucose given during the oral challenge indicated in the text above each figure. For ease of comparison, all data have been converted to plasma glucose equivalents, using the equation: Plasma glucose = blood glucose * 1.12. Data are means \pm standard deviations (where available) and are adapted from OGTT studies in humans [239-244], rats [245, 246], and dogs [247].

There is some, although limited, evidence that the greater rises in circulating glucose after oral glucose during pregnancy reflect greater capacity for glucose uptake. Consistent with the pattern in systemic circulation, the increase in portal blood glucose after a liquid meal including glucose was larger in late pregnant compared to non-pregnant dogs (Fig. 3.4 [233]). Curiously, postprandial net gut output of glucose, calculated using radiolabelled glucose tracers, was similar in pregnant and non-pregnant dogs [233], although postprandial gut glucose output was higher in late pregnant compared to non-pregnant rabbits [236]. Plasma glucose was also higher in pregnant than non-pregnant women from 60 minutes after an oral sucrose challenge, while the lack of difference in plasma fructose responses implies glucose-specific increases in transport rather than digestion [248]. Moreover, when the whole SI was infused continuously in anaesthetised rats, glucose uptake from infusate containing 20-300 mM glucose was 20-40% higher in mid-pregnant compared to non-pregnant rats in one study [231], although others reported no difference in glucose uptake from a 10 mM glucose infusate using a similar method [175]. It is important to consider that the use of anaesthesia during *in vivo* studies has the potential to attenuate SI nutrient absorption due to a reduction in gastric and SI smooth muscle motility due to suppression of peripheral and central neural circuits [249]. Furthermore, OGTT responses are likely to differ if performed during the light compared to dark phase [250], and regulation of SGLT1 by luminal nutrients can also impact OGTT responses depending on fasted or fed status [251]. Glucose absorption per g dry weight by ligated loops of jejunum and ileum in anaesthetised golden hamsters (*Mesocricetus auratus*) over a 30-minute static incubation with 5.6 mM glucose was 36% higher in mid-late pregnant compared to non-pregnant animals [232]. Conversely, glucose absorption by the proximal jejunum during a 5 minute static incubation with 10 or 20 mM glucose was similar in late pregnant and non-pregnant rats [252]. Surprisingly, only a single study has reported the impact of pregnancy on *ex vivo* glucose uptake, despite the importance of this approach to interrogate mechanisms. Uptake of alpha-methyl-D-glucoside, a non-metabolisable glucose analog transported by SGLT1 but not the GLUT family of hexose transporters, was 28% and 65% higher per length of jejunum and ileum, respectively, in everted sacs from late pregnant compared to non-pregnant rats [253]. The affinity of transporters was similar between groups, implying increased density rather than altered function of SGLT1 in pregnancy [253].

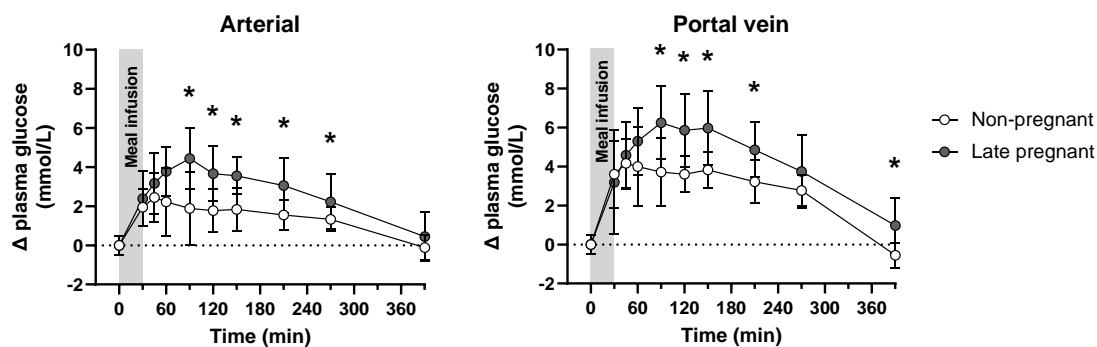


Figure 3.4 Changes in arterial and portal vein glucose following a meal test in dogs. Data are means \pm standard deviations and are adapted from the intragastric meal tolerance study reported by Moore et al. in dogs [233].

3.6.3. Macronutrient uptake – amino acids

Current evidence indicates that SI amino acid uptake is unchanged during pregnancy, although this evidence base is limited to one or two studies for most amino acids. Most of these studies have measured amino acid uptake during continuous or static perfusion of the SI in anaesthetised rats. A single non-rodent study showed that ileal digestibility (comprising both catabolism and uptake) of dietary crude protein and component amino acids was similar in late pregnant compared to non-pregnant conscious pigs [254]. During continuous infusion of the whole SI, removal of leucine from infusate containing 1.31 g/L leucine was similar in non-pregnant and mid-pregnant rats [175], while *in vivo* absorption of glycine from ligated loops of jejunum [252] and appearance of methionine in portal blood during static incubation of the whole SI [255] were unchanged during pregnancy. Lysine absorption from ligated loops of duodenum was also similar in non-, mid- and late-pregnant rats, but did increase during lactation [256]. Only a single *ex vivo* study has evidenced upregulation of amino uptake, albeit only for one amino acid, one SI region and at a single stage of pregnancy. Transfer of radiolabelled amino acids from the mucosal to serosal side of the distal ileum more than doubled in early pregnant compared to non-pregnant rats, then returned to non-pregnant concentrations at mid- and late-pregnancy; greater transfer was lysine-specific and did not change for alanine or proline [257].

3.6.4. Macronutrient uptake – lipids

A single study has directly assessed changes in lipid uptake during pregnancy, where plasma concentrations of ^{14}C -tripalmitate rose faster, and were higher from 1 until 24 h in late pregnant (GD20) compared to non-pregnant rats after oral administration of the lipids tripalmitine (4 mg), phosphatidylcholine (0.8 mg) and glycerol-tri-[^{14}C]-palmitate (10 μCi) [258]. Total uptake of ^{14}C -tripalmitate in the first 4 hours after administration was 37% higher at GD19 and

46% higher at GD20 compared to non-pregnant rats, consistent with enhanced SI absorption of triglycerides [258].

3.6.5. Micronutrient uptake – minerals

Studies of mineral uptake have focussed on calcium (16 studies), iron (9 studies) and zinc (8 studies), with two studies reporting uptakes of other metal ions by SI [259] and colon [260].

3.6.5.1. *Calcium*

Most evidence indicates that calcium absorption increases during pregnancy, due to increased duodenal absorption. In two human studies, fractional intestinal absorption of calcium in late pregnant women was 124-126% that of non-pregnant or early-pregnant women using double-label stable isotope approaches [261, 262]. Similarly, absorption of calcium from food or drinking water over 24-48 hours is increased from mid-pregnancy in rats; fractional calcium absorption was 19-56% higher in the last few days of pregnancy compared to non-pregnant rats [263, 264]. Indeed, plasma concentrations of ^{45}Ca were higher at 60 minutes after gavage with a labelled ^{45}Ca Cl solution in anaesthetised pregnant rats compared to non-pregnant rats [265]. Investigations of calcium uptake in rats are generally consistent with an upregulation of duodenal absorption during mid-late pregnancy. For example, duodenal uptake of ^{45}Ca during a 15-minute static incubation was similar in early- and non-pregnant rats, but increased at mid- (+36%) and late-pregnancy (+82%, [266]). In perfusion studies, duodenal ^{45}Ca absorption per cm was 92% higher in mid-pregnant compared to non-pregnant rats, but did not differ on a dry weight basis [267]. Duodenal active calcium transport is also upregulated in late pregnant compared to non-pregnant rats, with 33-250% greater active calcium transport in *ex vivo* everted sacs of proximal duodenum [268-272]. Results of studies using different *ex vivo* approaches concur; uptake of ^{45}Ca by proximal duodenal slices was similar at early pregnancy but greater at mid- (+21%) and late-pregnancy (+88%, [273]), while duodenal transcellular calcium flux in Ussing chambers was 33-39% higher in rats at mid-late pregnancy compared to non-pregnant rats [274]. In the only study to evaluate regional calcium uptake across pregnancy stages, Wróbel *et al.* reported that calcium transport by everted sacs increased with advancing pregnancy in rats, particularly in distal SI collected during the light phase, when calcium uptake was lower [272]. Evidence for altered calcium absorption in the jejunum is equivocal; *ex vivo* mucosal Ca^{2+} transport by proximal and mid-jejunum everted sacs was more than 2-fold higher in mid-pregnant compared to non-pregnant rats [259], while calcium uptake increased similarly with increasing luminal calcium concentration in mid-jejunal loops during static incubation *in situ* [273]. In contrast, there was no net uptake of calcium by perfused ileum in non-pregnant or late pregnant rats [267].

3.6.5.2. *Iron*

A single study in humans reported higher absorption of non-haem iron from food at 24 weeks (>5-fold) and 36 weeks (>9-fold) of pregnancy compared to non-pregnant women [229]. All other studies have been conducted in rodents and included only non- and late-pregnant groups. ^{59}Fe uptake from the GI lumen and ^{59}Fe transport (iron absorption) were substantially (5-10-fold) higher during late pregnant (GD55 of 65) compared to non-pregnant guinea pigs [275]. Iron uptake may increase particularly towards term, as ^{59}Fe uptake and transport were 78% and 117% higher, respectively, in mice at GD20-21, but similar at GD16-17 compared to non-pregnant controls [230]. Iron uptake and transport from ligated *in situ* duodenal loops were also consistently higher in late pregnant (GD20-21) than non-pregnant rats [276-278]. *In vitro* iron transfer across everted duodenal sacs was ~2-fold higher in rats during the last third of pregnancy compared to non-pregnant rats [278]. Similarly, the capacity for $^{59}\text{Fe}^{3+}$ uptake into mucosal fragments from mouse duodenum was 47% higher in late pregnant compared to non-pregnant mice, while the affinity constant for iron transport was similar in both groups [279]. Overall, the evidence for increased iron uptake and transport by the duodenum in late pregnancy is strong, however the onset of this increase is not well mapped.

3.6.5.3. *Zinc*

Variable changes in acute Zn uptake have been reported during pregnancy. Plasma concentrations were similar in non-pregnant women and women in the first, second or third trimester of pregnancy 2 and 3 hours after consuming 22.5 mg zinc [280], while intestinal absorption of fed ^{65}Zn over a 6 h period was similar in mid- and late-pregnant rats [281]. In contrast, ^{65}Zn absorption by ligated duodenal loops during a 15 minute static incubation was higher in rats at GD18 (per length) and GD21 (per length and per g dry weight), compared to non-pregnant controls [256]. Several studies have utilised double stable isotope approaches to calculate the fractional absorption of orally administered zinc in pregnant women. Two studies show increased relative fractional absorption of 145% [282] and 148% [283] in late pregnancy (34-36 week), compared to non-pregnant or early pregnant women, although the 133% relative fractional absorption in the third study [284] difference was not significantly different.

3.6.5.4. *Others*

Little has been reported on changes in uptake or transport of other minerals such as sodium, potassium, chloride and magnesium during pregnancy. In humans, colonic uptake of sodium but not potassium was higher during perfusion studies in mid-pregnant women (12-20 weeks) compared to non-pregnant women [260]. *Ex vivo* measures of jejunal sodium transport in everted sacs were 48-103% higher in early- (GD2-3) and mid-pregnant (GD12-13) compared to non-pregnant rats, while chloride transport was more than doubled in only early pregnancy

[259]. *Ex vivo* jejunal potassium and magnesium transport were over 3-fold and over 9-fold higher in mid-pregnant rats compared to non-pregnant rats, respectively [259].

3.6.6. Micronutrient uptake – vitamins

Few studies have examined vitamin uptake and transport during pregnancy. Results discussed below are limited to studies of vitamin B₁₂ and B₉

3.6.6.1. *Vitamin B₁₂*

Intestinal uptake of ⁵⁷Co-labelled vitamin B₁₂ (cobalamin) and transfer to the non-GI carcass (carcass excluding all GIT contents, i.e. stomach, pancreas, small and large intestines) 16 h after administration by gavage were increased by 138% and 189% at GD15-17 of mouse pregnancy, respectively, compared to non-pregnant controls [285]. Both intestinal vitamin B₁₂ uptake (229%) and extra-intestinal transfer (338%) increased further at GD18-21, near term [285]. Similarly, increases in circulating concentrations after 1 mg oral administration were more than 2-fold higher in pregnant than non-pregnant rats, but the increases did not differ after 0.25 or 0.5 mg B₁₂ doses [286]. Vitamin B₁₂ is absorbed in the distal ileum at cubulin receptors, which recognise B₁₂ complexed with the glycoprotein intrinsic factor (IF) [287]. *Ex vivo* binding of ⁵⁷Co-labelled B₁₂-IF to cubulin receptors in intestinal mucosa homogenate was 1.9- to 2.3-fold higher in late pregnant mice compared to non-pregnant mice, reflecting greater numbers of receptors (3.6- to 4.2-fold) and despite lower receptor affinity (~0.2-fold, [285, 288, 289]).

3.6.6.2. *Vitamin B₉*

The appearance of folic acid in circulation following oral administration has been reported in two older studies in human pregnancy, using microbiological assays to determine plasma folate activity. After a 3 mg oral folic acid dose, Girdwood *et al.* [290] reported lower plasma folate activity at 1 and 1.5 h, and lower peak plasma folic acid concentrations, in pregnant compared to non-pregnant women, however baseline activity was not reported; preventing assessment of uptake. In a more informative study, Langdon and colleagues [291] reported a slower rise in plasma folate activity after oral folate (15 µg/kg body weight) in mid-pregnant women (20 weeks), compared to women in early (10 weeks) or late pregnancy (30 or 38 weeks). In contrast, *ex vivo* uptake of radiolabelled folic acid from proximal jejunum everted sacs over 60 minutes was similar in non-pregnant and late-pregnant (GD18) rats [292].

3.6.7. Gastric emptying

The rate of gastric emptying during pregnancy has been investigated in multiple species using a range of methods, spanning phenol red disappearance assessed by repeat sampling of gastric contents, bioimpedance, and ultrasound, to passage of radioactive, barium or magnetic labels (Fig. 3.5). The available data is equivocal, likely due in part these different assessments

as well as the use of a variety of liquids or solids as stimuli for gastric emptying, however, most studies find no difference in rates of gastric emptying in pregnant compared to non-pregnant individuals (Fig. 3.5). For example, Hunt *et al.* [293] reported increased rate of gastric emptying of saline between week 20 and 30-40 of human pregnancy, but no difference in the emptying rate of water. Only a few studies have investigated changes in gastric motility in pregnancy, and these likewise report equivocal effects of pregnancy and variable changes across pregnancy stages. The frequency of gastric contractions, measured *in vivo* by EMG, was lower in mid-pregnant compared to non-pregnant rats, but not different from controls at early- or late-pregnancy [221]. Motor activity of the stomach measured through pressure changes of a saline-filled balloon in anaesthetised rats was lower at early-pregnancy (GD3, 4, 5 and 7), compared to non-pregnant rats [294]. Conversely, the frequency of spontaneous *ex vivo* antral muscle contractions was similar in late-pregnant and non-pregnant guinea pigs [295]. The *ex vivo* contractile force of gastric smooth muscle has been assessed in pregnant guinea pig and rat, with conflicting results. The force of spontaneous contractions by mid-antrum strips collected from late pregnant guinea pigs was ~71% that of non-pregnant controls [295]. However, acetylcholine-induced contraction of isolated stomach smooth muscle cells, measured as the proportional reduction in muscle cell length, was nearly doubled in late-pregnant compared to mid-pregnant rats [296]. Overall, available evidence indicates unaltered rate of gastric emptying in pregnancy.

A. Gastric emptying of liquids

Species	Strain/ population	Method	Liquid given	EP	MP	LP	Source
Human	N/A%	PR	Saline				[293]
	N/A%	PR	Water				[293]
	N/A	PR	Water				[297]
	N/A	IMP	Water/DOJ				[298]
	N/A	IMP	Water				[299]
	N/A	PC	Water				[300]
	N/A	PC	Water				[301]
	N/A	PC	Water				[302]
	N/A	PC	Water				[303]
	N/A	PC	Water				[304]
	N/A^	PC	Water^	N/A			[238]
	N/A	U/S	Formula®				[305]
	N/A#	U/S	10% LL				[306]
Rat	Sprague-	⁵¹ Cr	Saline				[307]
	Charles	BAR	Saline				[308]
	Wistar	PR	1.5% MC				[309]
Guinea	N/S	⁵¹ Cr	Saline				[310]

Outcome relative to non-pregnant (%)

200+
180-
160-
140-
120-
101-
Equal
80-
60-
40-
20-
0-

Slower ↑

↓ Faster

B. Gastric emptying of solids

Species	Strain/ population	Method	Liquid given	EP	MP	LP	Source
Human	N/A	FLUOR	Egg yolk	Grey	Dark Brown		[311]
	N/A	¹³ C	Bread+egg [§]	Grey	Diagonal	Grey	[312]
Rat	Wistar	Beads	Beads~	Diagonal	Grey	Blue	[309]
	Wistar	Mag	Fe+chow	Red	Diagonal	Blue	[221]

Figure 3.5 Gastric emptying of A. liquids and B. solids during pregnancy. Studies are grouped by species and method, with each row representing a single study. Numbers in square brackets indicate data source. Differences relative to non-pregnant controls are indicated by cell colour. Outcomes were available as times or have been converted from % emptied to % remaining, so that higher values consistently indicate slower emptying. Grey cells indicate that the outcome was not reported at that pregnancy stage, and diagonal lines indicate that outcomes at that pregnancy stage were not significantly different from non-pregnant controls from the same study.

¹³C, ¹³C-octanoic acid breath test; ⁵¹Cr, radiolabelled ⁵¹Cr; BAR, location/weight of barium label; DOJ, diluted orange juice; EP, early pregnant; FLUOR, fluoroscopy using a barium label; GA, gestational age; IMP, impedance tomography; LL, lactulose; LP, late pregnant; Mag, gastric emptying time calculated from magnetic intensity readings after feeding a meal containing 0.5 g ferrite powder plus 1.5 g chow; MC, methyl cellulose; MP, mid pregnant, N/A, not applicable; N/S, not stated; PC, time of maximal circulating paracetamol concentration from paracetamol test; PR, phenol red dilution; U/S, ultrasound. %Data from this study are expressed relative to mid-pregnant women (16-25 weeks GA). ^Data from this study are expressed relative to early-mid-pregnant women (14-16 weeks GA). Paracetamol was taken in 50 mL water, but after consumption of a breakfast meal consisting of two Crunch and Slim bars. #Data from this study are expressed relative to early pregnant women (1st trimester). ©Women were fed 300 mL (405 kcal) of a liquid formula containing 5 % protein, 5 % fat, and 17 % carbohydrates. §Women were fed a meal of 60 g white bread plus 1 egg, including a ¹³C-enriched egg yolk. ~Rats were gavaged with approx. 25 x 1 mm diameter polystyrene beads in 1.5 mL saline, and the proportion that passed from the stomach was assessed at 3 h.

3.6.8. Gastrointestinal and SI motility

Although the gastric emptying rate of liquids and solids is unchanged during pregnancy, there is good evidence that transit through the GI tract as a whole is slower, reflecting slower SI transit (Fig. 3.6). Slower transit from mouth to caecum, or through the SI, was reported in 11 of 13 studies comparing late-pregnant to non-pregnant women, rats and mice (Fig. 3.6). Different species may slow SI transit at different pregnancy stages, with slower transit consistently reported in mid-pregnant women in the three reports published to date [311, 313, 314], and no studies of transit in early pregnant women yet reported (Fig. 3.6). GI transit of a range of labels was similar in early- and mid-pregnant rats and mice as their non-pregnant controls (Fig. 3.6, [221, 307, 315, 316]). The mechanisms underlying slower SI transit are largely unknown, with only three studies of SI contractility. The frequency of *in vivo* contractions of jejunum-ileum was similar in mid-late pregnant rats (GD12-18) as in non-

pregnant controls, although contraction intervals were more variable in the pregnant group [317]. Slower SI motility could at least in part be due to a reduction in vagal afferent sensitivity in response to stretch and distention of the gut wall [59]. Although maximal contractile responses to electrical, acetylcholine and potassium stimuli were similar in ileum strips taken from mid-late pregnant mice (GD11-19) and non-pregnant mice, stimulus sensitivity was decreased in the pregnant groups [318]. Indeed, the maximal contractile force induced by carbachol in ileum strips isolated from mid-pregnant guinea pigs was less than 60% of that measured in non-pregnant tissue, whilst the sensitivity to carbachol was unchanged [319]. Given the consistent evidence for slower SI transit, particularly in late pregnancy, further research is needed to understand the underlying mechanisms.

Species	Strain/ population	Transit From → To	Method	Meal given	EP	MP	LP	Source
Human	N/A	Mouth → Duo Infl.	FLUOR	Egg yolk	Grey	Red	Red	[311]
	N/A	Mouth → Caecum	X-RAY	Normal diet	Grey	Light Red	Grey	[313]
	N/A	Mouth → Caecum	PILL	N/S	Grey	Grey	Blue	[320]
	N/A	Mouth → Caecum	LACT	10 g lactulose [#]	Grey	Red	Red	[314]
	N/A	Mouth → Caecum	LACT	Liquid meal [^]	Grey	Red	Red	[321]
	N/A	Mouth → Caecum	LACT	10 g lactulose [#]	Grey	Red	Red	[322]
	X-SECT	Mouth → Caecum	LACT	10 g lactulose [#]	Grey	Red	Red	[322]
	LONG	Mouth → Caecum	LACT	10 g lactulose [#]	Grey	Red	Red	[306]
	N/A	Mouth → Caecum	LACT	18 g lactulose [#]	Grey	Red	Red	[306]
	N/A	Mouth → Caecum	LACT	18 g lactulose [#]	Grey	Red	Red	[306]
Rat	Sprague- Dawley	Mouth → SI	CHAR	Char+gum~	Blue	Blue	Red	[315]
		Mouth → SI	CHAR	Char+saline [@]	Blue	Blue	Light Red	[316]
		Mouth → SI	⁵¹ Cr	Saline	Light Red	Light Red	Light Red	[307]
		Mouth → SI	BAR	Saline	Grey	Grey	Red	[308]
	Wistar	Mouth →	Mag	Fe+chow	Blue	Light Red	Light Red	[221]
Mouse	Alderley	Mouth → SI	CAR	Carbon meal	Grey	Red	Red	[318]

Figure 3.6 Changes in gastrointestinal motility during pregnancy. Studies are grouped by species and transit region, with each row representing a single study. Numbers in square brackets indicate data source. Differences relative to non-pregnant controls are indicated by cell colour, using the same scale as Fig. 3.5. Outcomes were available as times or have been converted from % travelled to % remaining, so that higher values consistently indicate slower transit. Grey cells indicate that the outcome was not reported at that pregnancy stage, and diagonal lines indicate that outcomes at that pregnancy stage were not significantly different from non-pregnant controls from the same study

⁵¹Cr, radiolabelled ⁵¹Cr; BAR, barium label; CAR, carbon meal; CHAR, charcoal label; Duo Infl., duodenal inflexion; EP, early pregnant; FLUOR, fluoroscopy using a barium label; LP, late pregnant; Mag, OCTT time calculated from magnetic intensity readings after feeding a meal containing 0.5 g ferrite powder plus 1.5 g chow; MP, mid-pregnant; N/A, not applicable; N/S, not stated; LONG, longitudinal arm of study with results in the same women compared during late pregnancy and after weaning; OCTT, oral-caecal transit time; PILL, transit time for pH radiotelemetry pill; X-SECT, cross-sectional arm of study with results of late pregnant women compared to non-pregnant women

[#] lactulose given as 10% solution in water, after overnight fast. [^]Subjects consumed a liquid standard test meal containing 420 kcal (15% protein, 35% fat, 50% carbohydrate), with 10 g lactulose, after overnight fast. ~Rats were fasted overnight then gavaged with 0.3 mL of 10% charcoal in 5% gum acacia. [@]Rats were fasted 18 h then gavaged with 1 mL of 10% charcoal in 154 mM NaCl.

3.6.9. Whole SI anatomy

Of the 25 studies that have reported measures of whole SI anatomy in pregnancy, 17 reported increased absolute wet weight and/or length of the SI relative to non-pregnant controls (Fig. 3.7). Absolute SI weight was greater in late pregnant than non-pregnant rats in most studies, but not different between late-pregnant and non-pregnant pigs in a single report (Fig. 3.7). Limited data was available in early- or mid-pregnant rats, with no evidence of greater wet SI weight compared to non-pregnant rats (Fig. 3.7); changes in wet SI weight during pregnancy have not been reported in mice. Increases in SI weight are likely proportional to increases in maternal body weight during pregnancy in rodents, with no significant difference in relative SI weight reported in rats at mid-pregnancy (106-108%) or late-pregnancy (72-116%) compared to non-pregnant controls [323, 324], or in early- (107%), mid- (108%) or late-pregnancy in mice (124%) relative to non-pregnant females [178]. Elongation of the SI during pregnancy was reported in some but not all studies in rats and in single studies of mice and of another small mammal, the shrew (Fig. 3.7).

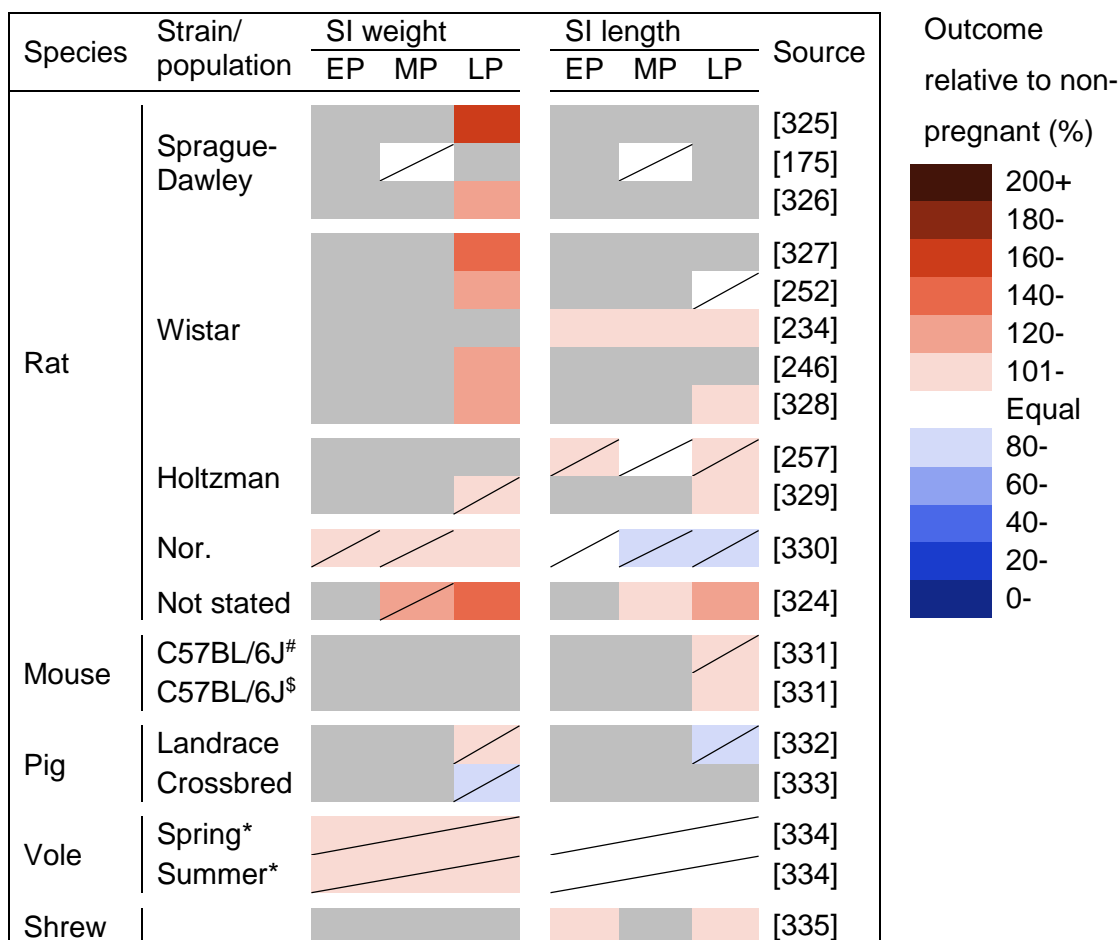


Figure 3.7 Changes in absolute small intestine wet weight and length during pregnancy. Studies are grouped by species, with each row representing a single study. Numbers in square brackets indicate data source. Differences relative to non-pregnant controls are indicated by cell colour. Grey cells indicate that the outcome was not reported at that pregnancy stage, and

diagonal lines indicate that outcomes at that pregnancy stage were not significantly different from non-pregnant controls from the same study

*EP, early pregnant; LP, late pregnant; MP, mid pregnant; Nor. Hood., Norwegian Hooded; Shrew, Common shrew (*Sorex araneus*); Vole, Common root vole (*Microtus oeconomus*). #Data for GD14.5 mice relative to non-pregnant. \$Data for GD18.5 mice relative to non-pregnant. *Data for voles are for all stages of pregnancy combined, within spring-caught and summer-caught animals.*

Few studies report other SI anatomical outcomes (Supplementary table S3.2). Intestinal permeability, assessed by appearance of fluorescein isothiocyanate (FITC)-dextran in blood following oral gavage, was 3-fold higher in late pregnant compared to non-pregnant mice in one study [336], while others reported ~1.4-fold higher permeability at GD14.5, but no differences at GD18.5 compared to non-pregnant mice [331]. Measures of blood supply to or from the small intestine have been reported in rabbit and guinea pig. Portal vein blood flow relative to body weight was similar in non-pregnant and late pregnant rabbits before and after feeding [236]. Absolute blood flow to the SI ($\text{ml}\cdot\text{min}^{-1}$) was also similar in non-pregnant and mid- or late- pregnant guinea pigs [337]. Blood flow relative to SI tissue weight was 1.6-fold higher in late-pregnant compared to non-pregnant guinea pigs, but not different at earlier pregnancy stages [337]. Numbers of specialist gastric cells have been assessed during rat pregnancy in a single study. The total number of hydrochloric acid-producing parietal cells, determined by multiplying parietal cell densities by the total surface area of the fundus, was 1.3-fold higher in late-pregnant than non-pregnant rats, but not different at earlier pregnancy stages [338]. Numbers of pepsin-producing peptic cells were 1.1 to 1.3-fold higher in mid- and late-pregnant rats than in non-pregnant controls [338].

3.6.10. Region-specific SI anatomy

Surprisingly few studies have reported effects of pregnancy on SI regional anatomy. Of five studies that reported absolute wet weights of SI regions, only one included data at stages earlier than late pregnancy, and only for duodenum (Fig. 3.8A). SI region weights were increased in most, but not all studies, with less consistent evidence for increased weight relative to region length (Fig. 3.8B). Consistent with these, the relative or absolute weights of mucosa were increased during rat pregnancy in duodenum [267, 328], jejunum [253, 339] and ileum [253, 267, 328]. Only two studies reported the length of SI regions, with no data on jejunum (Fig. 3.8C). Reported changes in villi length were inconsistent and varied between regions, with several studies reporting longer jejunal villi, but no consistent effects of pregnancy on duodenal or ileal villi length (Fig. 3.8D). Whether microvilli length changes during pregnancy, to further multiply surface area, has been reported only by a single research group. Penzes *et al.* found no differences in duodenal [340], jejunal [341] or ileal [342] microvilli size or density between non-pregnant and late pregnant rats. Only two studies in mice have reported crypt depth in pregnancy, with no consistent differences between pregnancy stages

across SI regions (Table S2, [178, 331]). In their assessments of ileal morphology, Ribeiro *et al.* also reported similar numbers of goblet cells per crypt at GD14.5 and GD18.5 as non-pregnant controls, and fewer goblet cells per villus only at GD14.5 [331]. Reports of SI muscle depth are also limited, without strong evidence for muscle hypertrophy in duodenum or ileum, however both studies reported ~1.5-2-fold thicker jejunal smooth muscle in mid and late-pregnant rats [218] and mice [178], compared to early-pregnant rats or non-pregnant mice.

A. Absolute weight

Species	Strain/ population	Duodenum			Jejunum			Ileum			Source
		EP	MP	LP	EP	MP	LP	EP	MP	LP	
Rat	Sprague-	[Grey]			[Grey]			[Grey]			[343]
	Sprague-	[Light Orange]			[Grey]			[Grey]			[344]
	Wistar [§]	[Grey]			[Grey]			[Light Orange]			[253]
Mouse	MF1	[Grey]			[Grey]			[Dark Brown]			[345]
Pig	Landrace [#]	[Grey]			[Grey]			[Grey]			[332]

B. Weight:length

Species	Strain/ population	Duodenum			Jejunum			Ileum			Source
		EP	MP	LP	EP	MP	LP	EP	MP	LP	
Rat	Sprague-	[Grey]			[Grey]			[Grey]			[346]
	Sprague-	[Light Orange]			[Grey]			[Grey]			[273]
	Sprague-	[Grey]			[Grey]			[Light Orange]			[347]
	Wistar ^{&}	[Grey]			[Light Orange]			[Light Orange]			[328]

C. Region length

Species	Strain/ population	Duodenum			Jejunum			Ileum			Source
		EP	MP	LP	EP	MP	LP	EP	MP	LP	
Rat	Sprague-	[Grey]			[Grey]			[Light Orange]			[343]
Shrew	<i>S. Araneus</i>	[Light Orange]			[Grey]			[Grey]			[335]

D. Villi length

Species	Strain/ population	Duodenum			Jejunum			Ileum			Source
		EP	MP	LP	EP	MP	LP	EP	MP	LP	
Rat	Sprague-Dawley	[Grey]			[Grey]			[Light Orange]			[175]
	Sprague-	N/A	[Blue]	[Light Blue]	N/A	[Dark Orange]	[Dark Brown]	N/A	[Blue]	[Light Blue]	[218]
	Not stated	[Grey]			[Grey]			[Light Orange]			[348]
Mouse	Swiss Albino	[Light Orange]			[Light Blue]			[Light Orange]			[178]
	C57BL/6J	[Grey]			[Grey]			[Light Orange]			[331]
	C57BL/6J	[Grey]			[Grey]			[Light Orange]			[331]
Shrew	<i>S. Araneus</i>	[Light Orange]			[Grey]			[Grey]			[335]

Figure 3.8 Changes in region-specific small intestine anatomy during pregnancy. Studies are grouped by species, with each row representing a single study. Numbers in square brackets indicate data source. Differences relative to non-pregnant controls are indicated by cell colour,

using the same scale as Fig. 7. Grey cells indicate that the outcome was not reported at that pregnancy stage, and diagonal lines indicate that outcomes at that pregnancy stage were not significantly different from non-pregnant controls from the same study

*EP, early pregnant; LP, late pregnant; MP, mid pregnant, N/A, not applicable; Shrew, Common shrew (Sorex araneus). *Data shown as ileum for these studies are for combined jejunum and ileum. [§]Methods for this study do not specify whether intestine was washed to remove contents before weighing; jejunum and ileum were split into similar lengths rather than divided based on anatomy. [#]Duodenal weight for this study is only for the region from the pylorus to the pancreatic duct. [^]Jejunal weight for this study is only for the most proximal 11 cm (approx. 1/3 of total jejunum length). [&]Jejunal weight for this study is for the proximal 1/3 of the combined jejunum-ileum, and ileum weight is for the distal 1/3 of the combined jejunum-ileum. [%]Data from this study are expressed relative to early-pregnant animals.*

3.6.11. Nutrient transporter expression – macronutrients

3.6.11.1. *Carbohydrates*

Only a single study has compared expression of carbohydrate transporters in pregnant and non-pregnant mono-gastric mammals. In duodenal mucosa, *Slc5a1* transcripts encoding sodium-dependent glucose co-transporter 1 (SGLT1), the primary apical transporter of glucose and galactose from the gut lumen into enterocytes, were 1.5-fold higher in late pregnant compared to non-pregnant rats [223]. Uptake of glucose by SGLT1 requires carriage of two sodium ions, and activity of the basolateral Na⁺/K⁺-ATPase pump to maintain the enterocyte sodium gradient [158]. The duodenum of late pregnant rats had higher abundance of *Atp1a4* and *Atp1b3* encoding sub-units of the Na⁺/K⁺-ATPase pump [223], consistent with increased glucose uptake capacity in pregnancy. In the same tissue, transcript abundance of *Slc2a5*, encoding the facilitated glucose transporter 5 (GLUT5), responsible for fructose uptake from the gut lumen into enterocytes, was 1.8-fold higher in late pregnant compared to non-pregnant rats [223]. Whether transcript abundance of *Slc2a2*, encoding the facilitated glucose transporter 2 (GLUT2), also increases during pregnancy to increase glucose and fructose transport out of enterocytes into the maternal circulation has not been reported. There are also no published reports that include data on protein expression of these transporters.

3.6.11.2. *Peptides and amino acids*

There are no published studies reporting effects of pregnancy or pregnancy stage on gene or protein expression of any SI amino acid or peptide transporters.

3.6.11.3. *Lipids*

There are no published studies reporting effects of pregnancy or pregnancy stage on transcript or protein expression of fatty acid translocase (FAT/CD36) or Niemann-Pick C1 like-1 (NPC1L1), required for fatty acid and cholesterol uptake from the lumen into enterocytes, respectively [159]. Likewise, changes at transcript or protein levels in fatty acid binding protein 2 (Fabp2), which traffics fatty acids to the endoplasmic reticulum (ER) for processing and

subsequent export to the lymphatic system [159], have not been reported through pregnancy. Interestingly, protein abundance of the apical sodium-dependent bile acid (ASBT) transporter, which mediates bile acid reuptake [349], was lower in the distal ileum of late pregnant compared to non-pregnant mice without changes in *Slc10a2* transcript expression [350]. In a second rodent study, ASBT protein expression was lower in brush border membrane vesicles from the most distal ileal segment of late pregnant compared to non-pregnant rats [351].

3.6.12. Nutrient transporter expression – micronutrients

Expression of transporters for iron and calcium have been investigated in multiple studies, although only in rodents (Table 3.1), while expression of transporters for zinc, magnesium, potassium and sulphate have each been reported in a single study and species (Table 3.1), as has gene expression of cellular retinal binding protein, CRBP(II), required for vitamin A uptake by enterocytes. Evidence on changes in other determinants of micronutrient transport during pregnancy, including tight junction proteins is also limited. Furthermore, it is unknown how expression of other vitamin transporters, such as the folate and heme iron transporter encoded by the *Slc46a1* gene, and transporters for other micronutrients including copper and phosphate, change during pregnancy.

3.6.12.1. *Calcium*

As with evidence for effects of pregnancy on SI iron transporters, changes reported in calcium transporters are equivocal. Only single studies have reported transcript abundance of two of the three key transporters responsible for uptake of Ca^{2+} into enterocytes at the brush border [352]: *Trpv5* (in mouse [353]) and *Cacna1d* (in rat [223]). Respective *Trpv5* and *Cacna1d* transcript abundance were similar in non-pregnant and late pregnant females (Table 3.1). Data on SI *Trpv6* transcript expression is extremely variable, ranging from more than 5-fold higher or lower in late pregnant compared to non-pregnant rodents, while no studies have reported protein expression of these apical Ca^{2+} transporters (Table 3.1). Binding of ^{45}Ca by duodenal mucosa, a measure of total calcium-binding capacity, was reported to be similar in non-pregnant and late-pregnant rats [354]. Gene and protein expression of the intracellular Ca^{2+} transporter calbindin D9K, was greater in late pregnant compared to non-pregnant rats and mice in most studies, although this difference was apparent in only the last few days of pregnancy (Table 3.1). Indeed, relative to expression at GD17.5, duodenal mucosal calbindin D9K protein abundance was higher at GD19.5, but not GD18.5, GD20.5 and GD21.5 [355]. A single study also reported greater duodenal mucosal transcript expression of *Calb1*, encoding Calbindin D28K, in late pregnant compared to non-pregnant rats [223]. There is no published evidence on protein abundance of the basolateral Ca^{2+} transporters, Ca^{2+} -ATPase PMCA1 and $\text{Na}^+/\text{Ca}^{2+}$ exchanger NCX1, required to transport calcium from the enterocytes to the circulation [352]. Expression of *Slc8a1* transcripts, encoding NCX1, has likewise not been

reported, while duodenal *Atp2b1* transcripts, encoding PMCA1, have been variably reported as unchanged or increased at late pregnancy in rodents (Table 1).

3.6.12.2. *Iron*

Despite evidence of enhanced iron uptake later in pregnancy, the available evidence for pregnancy changes in specific SI iron transporters is inconsistent (Table 3.1). A single study reported similar duodenal transcript abundance of *Slc11a2*, encoding the brush border Fe²⁺ transporter Dmt1, at early and mid-pregnancy in rats [356], and consistent with this report, protein expression of Dmt1 was similar in duodenal enterocytes from mid and non-pregnant rats [357]. At late pregnancy, variable increases, or no change in, gene and protein expression of Dmt1 are reported in rats and mice (Table 3.1). Higher transcript expression of duodenal cytochrome b (encoded by *CYBRD1*) has been reported at late pregnancy in rat duodenal enterocytes [357] and whole mouse duodenum [358], compared to non-pregnant controls, but whether protein expression also increases is unknown. This ferrireductase reduces dietary non-heme iron to allow its transport into enterocytes by Dmt1 [359]. Expression of the ferroxidase hephaestin and transporter ferroportin 1, which act together to transport of iron from enterocytes into the circulation at the basolateral surface [359], are reported inconsistently as increased or unchanged in late pregnant rats (Table 3.1). Duodenal abundance of *Slc40a1* transcript [358], encoding ferroportin 1, and membrane protein expression [360] are each over 5-fold higher in late pregnant compared to non-pregnant mice. Overall, the data suggests that components of the iron transport system are likely upregulated in late pregnancy, but additional studies, with larger sample sizes to provide greater power to evaluate small differences are needed to define which components change and the underlying signals driving changes in iron transporters.

3.6.12.3. *Others*

Consistent with evidence above of increased zinc uptake at late pregnancy, a single study [361] has evidenced increase transcript abundance of basolateral and intracellular zinc transporters *Slc30a1* and *Slc30a2*, but not *Slc30a4*, at late pregnancy in rats. Protein expression at GD15 and GD20 was reported only for pooled duodenal membrane samples generated from 2-3 rats at each stage. Effects of pregnancy on expression of the ZIP4 and ZIP5 zinc transporters (encoded by *Slc39a4* and *Slc39a5*) have not been reported. In a single study [223], transcript abundance of two subunits of the cation channel that transport magnesium at the brush border, *Trmp6* and *Trmp7*, were higher in duodenal mucosa from late pregnant compared to non-pregnant rats, although protein expression was not reported (Table 3.1). Likewise, only a single study in rats has reported effects of pregnancy on ileal gene expression of sulphate transporters and did not report protein expression [362]. Changes in transcript abundance amongst different members of the Slc26 transporter family were

inconsistent between gestational ages, with lower *Slc26a3* and *Slc26a6* transcript abundance only at some gestational ages relative to non-pregnant controls (Table 3.1). Both gene and protein expression of potassium resorbing H⁺/K⁺ ATPase Type 2 (encoded by *Atp12a*) were higher in the colon of late pregnant compared to non-pregnant rats [363]. Whole SI abundance of *Rbp2* transcript encoding cellular retinal binding protein, type II, required for vitamin A uptake by enterocytes, was ~1.8-fold higher in late pregnancy (GD19 and GD20), although not at earlier stages (GD15 and GD17), relative to non-pregnant rats [326]. When the SI was subdivided into thirds, the overall increase reflected upregulation of *Rbp2* transcripts in the proximal and (to a lesser extent) middle third of the SI, with unchanged *Rbp2* in the distal third [326]. These authors also reported ~1.6-fold higher *Rbp2* transcript abundance in enterocytes isolated from the proximal 2/3 of the SI at GD20 compared to non-pregnant rats [326]. Despite evidence of greater intestinal permeability during pregnancy [331, 336], only a single report has reported expression of tight junction proteins during pregnancy. Abundance of transcripts for three tight junction proteins, *Tjp1* (encoding ZO1), *Cldn9* and *Cldn2*, were higher in the duodenum from late pregnant rats than non-pregnant controls [223], but protein expression was not reported.

Table 3.1: Expression of mineral micronutrient transporters during pregnancy. Gene and protein names are given for rodent forms. Data are outcomes relative to non-pregnant controls, with sources cited after the relative expression data. Struck-through text indicates that outcomes at that pregnancy stage were not significantly different from non-pregnant controls from the same study.

Nutrient	Transporter Name (function); gene; protein	Species	Gene expression (tissue)			Protein expression (tissue)		
			EP	MP	LP	EP	MP	LP
Iron	Divalent metal transporter 1 (brush border Fe ²⁺ transporter); <i>Slc11a2</i> ; DMT1	Rat	81-94% (WD)[356]	75-88% (WD)[356] 123% ^N , 200% ^I (DE)[357]	344% (GD15), 300% (GD18), 538% (GD21) (WD)[356]	No data	132% (DE)[357]	320% (GD15), 800% (GD18), 960% (GD21), (DE)[357]
					215% ^N , 467% ^I (GD15) 246% ^N , 667% ^I (GD18) 238% ^N , 467% ^I (GD21) (DE)[357]			667% (WD)[358]
					286-528% (DE)[357]			882% (WD) [358]
					No data			No data
					No data			No data
	Duodenal cytochrome b (ferrireductase, works with DMT1 in brush border uptake of iron); <i>Cybrd1</i> ; DCYTB	Rat	No data	443% (DE)[357]	320% (GD15), 800% (GD18), 960% (GD21) (DE)[357]	No data	No data	No data
	H ⁺ -coupled folate transporter 1 (also transports heme iron); <i>Slc46a1</i> ; HCP1	-	No data	No data	No data	No data	No data	No data
	Hephaestin (ferroxidase, works with FPN1 in basolateral transport of iron to circulation); <i>Heph</i> ; HEPH	Rat	No data	104% (DE)[357]	320% (GD15), 800% (GD18), 960% (GD21) (DE)[357]	No data	No data	No data

	Ferroportin 1 (basolateral Fe ²⁺ transporter, also known as iron-regulated transporter 1); <i>Slc40a1</i> ; FPN1	Rat	No data	122% (DE)[357]	114-128% (DE)[357]	No data	80% (WD)[364] 108% (DE)[357]	140-250% (WD)[364] 184% (GD15), 164% (GD18), 169% (GD21), (DE)[357] 560% (DMe)[360]
		Mouse	No data	No data	542% (WD)[358]	No data	No data	
	Transient receptor potential cation channel subfamily V member 5 subunit (brush border Ca ²⁺ transporter); <i>Ecac1</i> ; TRPV5	Mouse	No data	No data	90% (WD)[353]	No data		
	Transient receptor potential cation channel subfamily V member 6 subunit (brush border Ca ²⁺ transporter); <i>Ecac2</i> ; TRPV6	Rat	No data	No data	157-260% (DMu)[223]	No data		
		Mouse	No data	No data	1177% (Dist. WD)[353] 20-33% (WD)[225]	No data		
Calcium	Calcium channel, voltage-dependent, L-type, alpha 1D subunit (brush border Ca ²⁺ transporter); <i>Cacna1d</i> ; Ca _v 1.3	Rat	No data	No data	107% (DMu)[223]	No data		
	Intracellular Ca ²⁺ transporter; <i>S100g</i> ; Calbindin D9K	Rat	90% (WD)[365]	140% (WD)[365]	210% (DMu)[365] 100-140% (Prox. WD)[366]	No data	85% (Prox. DMu)[367]	127-133% (GD15-16) 145-158% (GD18-20.5) (Prox. DMu)[367] 162% (WD)[368]
		Mouse	No data	No data	78% (WD)[225] 250% (Dist. WD)[353]	No data	No data	155% (Prox. WD)[353]

	Intracellular Ca ²⁺ transporter; <i>Calb1</i> ; Calbindin D28K	Rat	No data	No data	157% (DMu) [223]	No data		
		Rat	110% (DMu)[365]	170% (DMu)[365]	240% (DMu)[365]	No data		
	Ca ²⁺ -ATPase (basolateral membrane Ca ²⁺ transporter); <i>Atp2b1</i> ; PMCA1b	Mouse	No data	No data	96% (WD)[225] 190% (Dist. WD)[353]	No data		
	Na ⁺ /Ca ²⁺ exchanger (basolateral membrane Ca ²⁺ transporter); <i>Slc8a1</i> ; NXC1	-	No data			No data		
	Zinc transporter protein 4 (brush border zinc transporter); <i>Slc39a4</i> ; ZIP4	-	No data			No data		
Zinc	Zinc transporter 1 (basolateral and vesicular zinc transporter); <i>Slc30a1</i> ; ZnT1	Rat	No data	No data	160% (GD15), 240% (GD20) (DMu) [361] 200%	No data	No data	108%? (GD20 cf. GD15) (DMe) [361]
	Zinc transporter 2 (vesicular zinc transporter); <i>Slc30a2</i> ; ZnT2	Rat	No data	No data	291% (GD20) (DMu) [361]	No data	No data	126%? (GD20 cf. GD15) (DMe) [361]
	Zinc transporter 4 (vesicular zinc transporter); <i>Slc30a4</i> ; ZnT4	Rat	No data	No data	120% (GD15 & GD20) (DMu) [361]	No data	No data	52%? (GD20 cf. GD15) (DMe) [361]
	Zinc transporter protein 5 (basolateral zinc transporter); <i>Slc39a5</i> ; ZIP5	-	No data			No data		
Copper	Copper transporter 1 (brush border Cu ⁺ transporter); <i>Slc31a1</i> ; CRT1	-	No data			No data		

Mag- nesium	Transient receptor potential cation channel subfamily M member 6 (forms heterodimer with TRPM7 to transport Mg at brush border); <i>Trpm6</i> ; TRPM6	Rat	No data	No data	200-288% (DMu)[223]	No data
	Transient receptor potential cation channel subfamily M member 7 (forms heterodimer with TRPM6 to transport Mg at brush border); <i>Trpm7</i> ; TRPM7	Rat	No data	No data	150% (DMu)[223]	No data
Phos- phate	Na ⁺ -dependent phosphate transporter 2b (brush border PO ₄ ³⁻ transporter); <i>Slc34a2</i> ; NaPi-IIb	-	No data			No data
Sulph-ate	Na ⁺ -dependent sulphate transporter 1 (brush border SO ₄ ²⁻ transporter, NaS1); <i>Slc13a1</i> ; SLC13A1	Mouse	71-84% (WI)[362]	61-79% (WI)[362]	59-84% (WI)[362]	No data
	Diastrophic dysplasia sulphate transporter (brush border SO ₄ ²⁻ transporter, DTDST); <i>Slc26a2</i> ; SLC26A2	Mouse	90-97% (WI)[362]	83% (WI)[362]	69-97% (WI)[362]	No data
	Chloride anion exchanger (brush border SO ₄ ²⁻ transporter, DRA); <i>Slc26a3</i> ; SLC26A3	Mouse	84% (GD4.5) 75% (GD6.5) (WI)[362]	69% (GD8.5) 78% (GD10.5) (WI)[362]	63% (GD14.5) 94% (GD18.5) (WI)[362]	No data
	Sulphate anion transporter (brush border SO ₄ ²⁻ transporter, PAT1); <i>Slc26a6</i> ; SLC26A6	Mouse	64% (GD4.5) 82% (GD6.5) (WI)[362]	73-88% (WI)[362]	55% (GD14.5) 82% (GD18.5) (WI)[362]	No data
	Solute carrier family 26 member 11 (brush border SO ₄ ²⁻ transporter); <i>Slc26a11</i> ; SLC26A11	Mouse	75-100% (WI)[362]	25-75% (WI)[362]	50-75% (WI)[362]	No data
Na ⁺ -independent sulphate transporter 1 (sulphate/oxalate, sulphate/bicarbonate or oxalate/bicarbonate anion exchange, basolateral SO ₄ ²⁻ transporter, SAT1); <i>Slc26a1</i> ; SLC26A1	Mouse	0-100% (WI)[362]	100% (WI)[362]	0% (WI)[362]	No data	

Pot- assium	H ⁺ /K ⁺ ATPase Type 2 (apical membrane potassium resorption, <i>Atp12a</i> ; HKA2)	Rat	No data	No data	205% (WCo)	No data	No data	240% (WCo)
----------------	---	-----	---------	---------	------------	---------	---------	---------------

?, no significance tests provided; DE, duodenal enterocytes; DMu, duodenal mucosa; DMe, duodenal membrane fraction; EP, early pregnant; GD, gestational day; LP, late pregnant; MP, mid pregnant; Prox., proximal; WCo, whole colon; WD, whole duodenum; WI, whole ileum.

^N non-IRE splice variant of DMT1 Fe²⁺ transporter; ^I IRE splice variant of DMT1 Fe²⁺ transporter

3.6.13. Gallbladder emptying

Effects of pregnancy on the gall bladder have been reported only in humans, mostly using imaging to assess gallbladder volumes and emptying. Four of five studies reported slower fractional gallbladder emptying in pregnancy, with weaker evidence for lower proportional nutrient-induced emptying of the gallbladder (Fig. 3.9). These may be offset by greater gallbladder volumes, which were higher in women at mid-late pregnancy than in non-pregnant women (Fig. 3.9). Only one study reported lower gallbladder volume at mid-late pregnancy [369], but this was relative to early-pregnant women, when gallbladder expansion may already have occurred. Indeed, higher fasting and residual gallbladder volumes in early pregnant women, which increased further during the second and third trimesters, were reported by Everson *et al.* in a detailed ultrasound study [370]. Gallbladder volumes of pregnant women were consistently twice those of non-pregnant women throughout the 20-hour period of this study [370]. Consistent with evidence of unchanged bile volume released from the gallbladder during pregnancy, rates of ¹³C-labelled bile acid secretion into the duodenum, were similar in non-pregnant women and women in each trimester of pregnancy [371]

Gallbladder emptying stimulated by	Method	Time at final measure (min)	Fasting gallbladder volume (mL)			Gallbladder emptying at final time (%)			Rate of gallbladder emptying (min ⁻¹)			Source
			EP	M	LP	EP	M	LP	EP	MP	LP	
				P			P					
Modified Boyden test ^a	CC	40	N/			N/						[369]
Liquid standard test meal ^b	U/	90										[372]
Duodenal amino acid ^c	U/	90										[371]
Breakfast (early emptying)*	U/	90										[370]
Breakfast (late emptying)*	S	90										[370]
Liquid standard test meal ^d	U/	90										[321]
Liquid formula test meal ^e	U/	105										[305]

Figure 3.9 Changes in gallbladder volume and emptying during human pregnancy. Each row presents data from a single study; how gallbladder emptying was stimulated and the time at which final emptying was assessed are indicated. Numbers in square brackets indicate data source. Differences relative to non-pregnant controls are indicated by cell colour, using the same scale as Fig. 3.7. Grey cells indicate that the outcome was not reported at that pregnancy stage, and diagonal lines indicate that outcomes at that pregnancy stage were not significantly different from non-pregnant controls from the same study
CCG, cholecystogram (X-ray); EP, early pregnant; LP, late pregnant; MP, mid pregnant, N/A, not applicable; U/S, ultrasound. %Data from this study are expressed relative to early-pregnant animals. * Gallbladder emptying was fitted to a first-order exponential function, early emptying is the rate constant from meal intake to the point of inflexion (50% emptying, ~35 min after meal) and late emptying is the rate constant from the point on inflexion to the end of the study (35-90 min after meal)

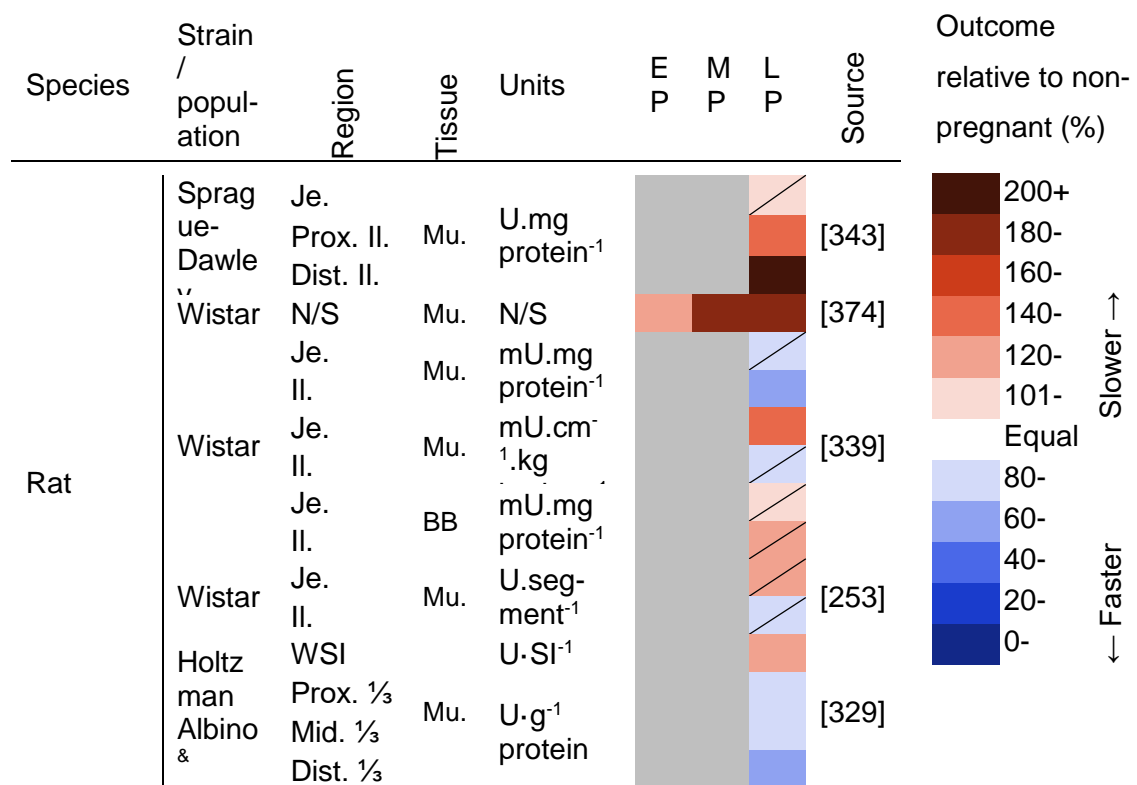
Stimuli: ^a Modified Boyden test meal consisted of 4 egg yolks mixed with an equal amount of milk; ^b Liquid standard test meal (420 kcal) comprised 15% protein, 35% fat, 50% carbohydrate; ^c continuous (6 mL/min) duodenal infusion of a solution containing a mixture of essential amino acids; [373] ^d Breakfast consisted of one egg, two slices of bacon, two pieces of buttered toast, 100 mL orange juice, 240 mL low fat milk and 200 mL of coffee or tea (610 cal, 12% protein, 44% fat); ^e Liquid formula test meal (300 mL) containing 135kcal, 5 g protein, 5 g fat, 17 g carbohydrate per 100 mL

3.6.14. Expression and activity of digestive enzymes

3.6.14.1. *Carbohydrate digestion*

Multiple studies have reported the activity of SI sucrase, lactase and maltase during pregnancy. Sucrase (Fig. 3.10A) and lactase (Fig. 3.10B) activities have been reported only in rat, and mostly in jejunal and ileal mucosa, with no consistent changes in activity evident during pregnancy. Maltase activity (Fig. 3.10C) was compared between pregnancy stages in one study in pigs [332] as well as multiple studies in rats, and showed no consistent changes. Only one report of enzyme abundance during pregnancy was identified – jejunal lactase abundance assessed as immunofluorescence intensity core was numerically 2.3-fold higher but not different in late pregnant (GD20) compared to non-pregnant rats [348].

A. Sucrase



B. Lactase

Species	Strain / population	Region	Tissue	Units	E P	M P	L P	Source
Rat	N/S	Je.	Mu	U·g ⁻¹ protein	Grey	Grey	Light Red	[348]
	Wistar	N/S	Mu	N/S	Dark Red	Dark Red	Light Red	[374]
	Wistar	Je.	Mu	mU·mg protein ⁻¹	Grey	Grey	Light Red	[339]
		Il.	Mu	mU·cm ⁻¹ ·kg ⁻¹	Grey	Grey	Dark Red	
	Wistar	Je.	BB	mU·mg protein ⁻¹	Grey	Grey	Light Blue	[253]
		Il.	Mu	U·segment ⁻¹	Grey	Grey	Light Red	
	Holtzman Albino &	WSI Prox. 1/3	Mu	U·SI ⁻¹	Grey	Grey	Light Red	[329]
		Mid. 1/3	Mu	U·g ⁻¹ protein	Grey	Grey	Light Red	
	Dist. 1/3	Mu	U·g ⁻¹ protein	Grey	Grey	Light Blue		

C. Maltase

Species	Strain / population	Region	Tissue	Units	E P	M P	L P	Source
Rat	Sprague-Dawley	Duo.	Whole	U	Light Red	Light Blue	Dark Blue	[344]
	Wistar	N/S	Mu	N/S	Light Blue	Light Blue	Light Blue	[374]
	Wistar	Je.	Mu	mU·mg protein ⁻¹	Grey	Grey	Light Blue	[339]
		Il.	Mu	mU·cm ⁻¹ ·kg ⁻¹	Grey	Grey	Light Red	
	Wistar	Je.	BB	mU·mg protein ⁻¹	Grey	Grey	Light Blue	[253]
		Il.	Mu	U·segment ⁻¹	Grey	Grey	Light Red	
	Holtzman Albino &	WSI Prox. 1/3	Mu	U·SI ⁻¹	Grey	Grey	Light Red	[329]
		Mid. 1/3	Mu	U·g ⁻¹ protein	Grey	Grey	Light Red	
	Dist. 1/3	Mu	U·g ⁻¹ protein	Grey	Grey	Light Red		
Pig	Landr	Duo.	Wh	U	Grey	Grey	Light Red	[332]

Figure 3.10 Changes in activity of carbohydrate-digesting enzymes during pregnancy in monogastric mammals. A. Sucrase, B. Lactase, C. Maltase. Studies are grouped by species, with each row representing a single study. Numbers in square brackets indicate data source. Differences relative to non-pregnant controls are indicated by cell colour. Grey cells indicate that the outcome was not reported at that pregnancy stage, and

diagonal lines indicate that outcomes at that pregnancy stage were not significantly different from non-pregnant controls from the same study.

BB, brush border; bodywt, body weight; Dist., distal; Duo., duodenum; EP, early pregnant; Il., ileum; Je., jejunum; LP, late pregnant; Mid., middle; MP, mid pregnant; Mu.; mucosa; N/A, not applicable; N/S, not stated; Prox., proximal; U, international units ($\mu\text{mol}/\text{min}$) is defined as the amount of enzyme that catalyses the conversion of 1 μmol of substrate per minute at 37°C; Whole, whole tissue; WSI, whole small intestine

&The excised SI was divided into equal thirds, so the data from this study does not correspond exactly to duodenum, jejunum and ileum.

3.6.14.2. Protein digestion

Key enzymes involved in protein digestion have been measured in stomach and pancreas, in only a few studies. Although stimulated pepsin output was unchanged throughout rat pregnancy, Takeuchi *et al.* [375] reported lower pepsin activity per ml of gastric secretion at GD10 and GD20 relative to non-pregnant rats, however mucosal pepsin activity at the gastric fundus was similar in late pregnant and non-pregnant pigs [332]. A low pH is required to activate pepsin, increased gastric acid output has been reported, particularly later in pregnancy. Basal gastric acid output was similar in non-pregnant, GD7 (2-fold) and GD14 (1.25-fold) anaesthetised rats, and 2.25-fold higher at GD21 [376]; however spontaneous gastric acid secretion did not change during pregnancy in a small longitudinal study in dogs [377]. Interestingly, pentagastrin-stimulated acid secretion was higher in rats at GD7 (2.2-fold), but not at GD14 (1.5-fold) or GD21 (1.6-fold), compared to non-pregnant rats [376]. In a third study, stimulated gastric acid secretion volume, acidity and acid output were each higher at GD20 than in non-pregnant rats [375]. In the rat, the total activities of trypsin and α -chymotrypsin per pancreas, as well as per gram of pancreas, were similar pregnant rats at GD7, GD14 and GD21 to non-pregnant rats [378]. In the SI, Rolls and colleagues reported that SI mucosal activity of two dipeptidases, glycyl-L-leucine dipeptidase and L-alanyl-L- glutamic acid dipeptidase, expressed relative to protein, increased during pregnancy and lactation, but their data suggests that activity of each increases only late in pregnancy, and even at late pregnancy remained <1.2-fold that of non-pregnant rats [378]. The activity of glutaminase, which converts glutamine to glutamate, and is essential for intestinal metabolism, was higher in homogenates of whole SI tissue and SI mucosa of late pregnant compared to non-pregnant rats [327]. Additional evidence is clearly required to draw conclusions about pregnancy-stage effects on protein digestion.

3.6.14.3. Others

As discussed above, available evidence indicates that secretion of bile acids essential for emulsification of fats in the intestine is unaltered during pregnancy. However, activities and secretion of the enzymes that subsequently digest lipids, such as pancreatic lipase, are

not yet reported. The duodenal-jejunal mucosa activity of carotene dioxygenase, which cleaves β -carotene to retinal, itself subsequently metabolised to retinoic acid or retinol, was similar in rats at GD7 and GD20 of pregnancy as in non-pregnant rats [379].

3.7. Discussion

This scoping review has identified 159 sources of evidence which describe several GI adaptations during pregnancy with unequivocal supporting evidence, often over several species, in addition to outcomes for which reported changes are equivocal and others for which there is insufficient evidence available to draw conclusions (Fig. 3.11).

Relative to non-pregnant groups, consistent differences in late pregnancy include greater rises in circulating glucose after oral consumption, increased SI uptake of iron, calcium and zinc, and slower GI passage of nutrients. The available evidence indicates that acute glucose uptake, gastric emptying and activities of sucrase, maltase and lactase do not change during pregnancy. Despite statements that villous hypertrophy occurs during pregnancy [5], reports of increased SI villous length are inconsistent between SI regions and available studies, all of which have been in small mammals. Evidence is insufficient to draw conclusions about whether other outcomes change during pregnancy, including uptake of specific amino acids and of lipids, most minerals and of vitamins, blood flow to and from the GI tract, region-specific anatomy, expression of macro- and micro-nutrient transporters and activity or expression of enzymes involved in protein and lipid digestion. A further gap in evidence is the timing of SI adaptations during pregnancy, as most studies have investigated outcomes in non- pregnant and late pregnant groups, without assessing groups at earlier pregnancy stages. Studies of early and mid-pregnancy stages have mostly been performed in laboratory rodents, where timed-mating protocols allow accurate identification of pregnancy stage.

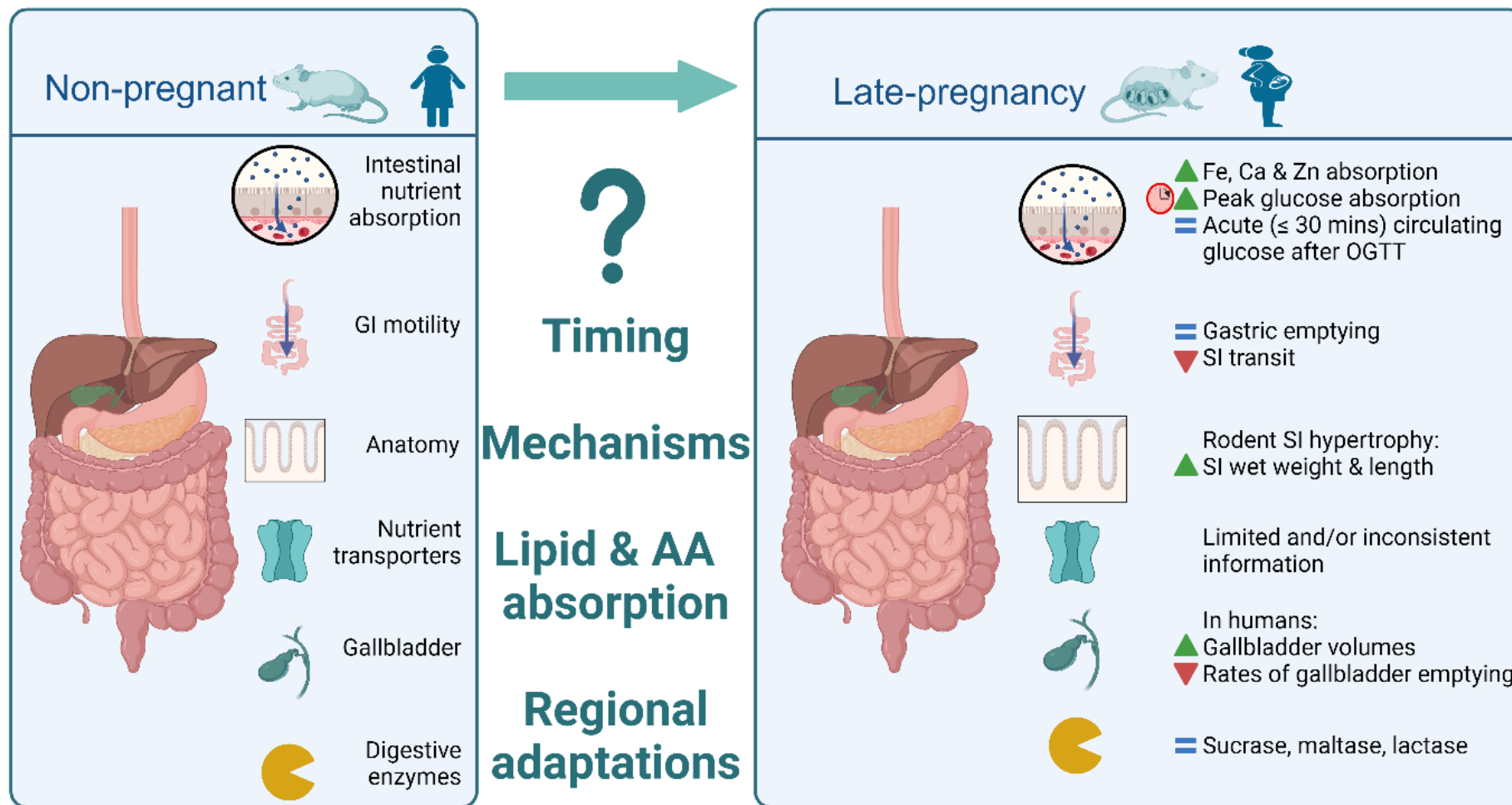


Figure 3.11 Changes in nutrient uptake and its determinants during pregnancy in monogastric mammals. Green triangles indicate an increase and red triangles indicate a decrease relative to non-pregnant controls, equal signs indicate no change during pregnancy relative to non-pregnant controls. Figure created with BioRender.com

Effects of pregnancy on some determinants of nutrient uptake capacity, such as SI hypertrophy, appear to differ between species. Evidence of regional or whole SI hypertrophy in late pregnancy, particularly in terms of SI weight, was consistent in studies of small rodents including rats, mice and common shrews (*Sorex araneus*), but not observed in a single study in pigs [332]. Although additional data from larger species of monogastric mammals, such as humans or dogs, is needed to confirm species differences in SI hypertrophy, these outcomes are consistent with the relative demands of pregnancy in small rodents and pigs. Maternal weight (including the uterus and concepti) increases 50-100% over the course of a few weeks during pregnancy in rats, mice [14, 53] and shrews [380], whereas relative maternal weight gains across a 115-day pregnancy are lower in pigs at 20-25% in mature sows [381, 382] and 25-37% in growing nulliparous females [332]. It is unknown whether SI hypertrophy occurs during human pregnancy, although based on the above relationships, it may not, given the lower relative pregnancy weight gain of 10-15% in healthy women carrying a singleton fetus [20, 380, 381], compared to litter bearing species. Despite a lack of data regarding changes in SI anatomy and nutrient transporter expression in humans, such adaptations may not be necessary to increase capacity for nutrient absorption. Slower SI motility would increase contact time between ingesta and the SI mucosa, allowing for increased absorption in the absence of greater surface area and nutrient transporter expression. To investigate the mechanisms responsible for slower SI motility, future studies in larger mammals such as pigs and dogs are needed to investigate changes in smooth muscle contractility. Studies in humans involving non-invasive techniques to measure changes in smooth muscle electrical impedance could also be considered. Unfortunately, the ability to compare adaptations of nutrient uptake and its determinants between species is limited because data for many outcomes is only available in rodents, particularly on mechanisms that may underlie changes in nutrient uptake such as region-specific anatomy and nutrient transporter expression. Conversely, although greater gallbladder volumes and slower relative rates of gallbladder emptying are consistently reported in late pregnant women, a lack of data in other species means such gallbladder changes cannot be generalised to pregnancy in monogastric mammals.

This review has highlighted gaps in evidence, where the impact of pregnancy on absorption of nutrients is not well understood. These include uptake and transport of amino acids, lipids and many minerals and vitamins. Although the majority of available evidence supports unaltered amino acid uptake during pregnancy, this is based on only one or two studies each for uptake of leucine [175], glycine [252], methionine [255], lysine [256, 257], alanine [257] and proline [257], mostly assessed *in vivo* by uptake from ligated SI sections

in anaesthetised rats. Uptake of other amino acids during pregnancy remains to be investigated, as does uptake in other monogastric species, such as mouse or pigs. Absorption of tripalmitate was higher in late pregnant than non-pregnant rats [258], but this was the only study to report effects of pregnancy on lipid uptake, and clearly requires validation. Whether SI absorption of other lipids changes during pregnancy also merits investigation, while the impacts of pregnancy on transcript and protein expression of peptide, amino acid and lipid transporters also remain to be reported. There is good evidence for increased uptake and absorption of iron, calcium and zinc from the gut lumen during pregnancy, although the mechanisms are less clear, with inconsistent changes in expression of iron and calcium transporters and only a single study reporting upregulation of zinc transporter transcript expression. An important gap in knowledge is whether SI uptake and transport of other micronutrients crucial for fetal development, such as iodine [383], change during pregnancy. Increased uptake and transport of vitamin B₁₂ during late pregnancy have been reported in several studies, likely due, in part, to increased numbers of intrinsic factor-B₁₂ receptors in the intestinal mucosa. Although uptake of folic acid (vitamin B₉) has been investigated in two *in vivo* human studies [290, 291] and one *ex vivo* rat study [292], it is not clear if, or how, its absorption changes during pregnancy. This gap in understanding is surprising given the importance of adequate periconceptional B₉ status for prevention of neural tube defects, and some evidence of poorer folic acid absorption in women with prior pregnancies affected by neural tube defects, compared to controls [384, 385]. Whether carrier-mediated intestinal uptake of other essential vitamins, such as vitamin B₁ (thiamine), vitamin B₇ (biotin), vitamin A or vitamin E [158] changes during pregnancy has also not been reported.

While many pregnancy outcomes have been assessed non-invasively in humans including gastric and gallbladder emptying (by ultrasound), the mechanistic basis of these changes is poorly understood. Even for outcomes where functional changes have been reported in multiple species, there are often gaps in understanding of underlying mechanisms. For example, although glucose responses to oral carbohydrates change in pregnancy, only a single report has examined the impact of pregnancy on *ex vivo* glucose uptake, despite the importance of these methods to interrogate and inform on mechanisms. Uptake of alpha-methyl-D-glucoside, a non-metabolisable glucose analogue transported by SGLT1 but not the GLUT family of hexose transporters, was 28% and 65% higher per length of jejunum and ileum, respectively, in everted sacs from late pregnant compared to non-pregnant rats [253]. Notwithstanding smaller relative jejunum changes, its functional impact on glucose uptake is likely to be greater than ileal changes, since glucose transport capacity in the jejunum is double that of ileum [253], despite the ileum being reported as

a third longer than jejunum in rats [168]. Furthermore, avid glucose absorption in the duodenum and proximal jejunum means that luminal glucose rarely reaches the ileum [386], although further investigation is needed to determine whether, in late pregnancy when food intake increases up to 50% in rodents [14, 51, 217], glucose escapes absorption in the upper SI and reaches the ileum.

Strengths of this review include use of a comprehensive search criteria and currency of the information achieved by including sources up to June 2023. We developed and published the review protocol [235] prior to commencing, and followed this throughout, with further refinement of inclusion and exclusion criteria to accept only peer-reviewed quantitative studies (including accepted Masters and PhD theses after examination), and excluded unreviewed sources. Our broad search criteria and inclusion of multiple databases, which returned nearly 27 thousand sources, and thorough screening to identify 159 sources that met the review criteria, means that few relevant sources are likely to have been missed. In accordance with JBI methodology [226] and PRISMA-ScR reporting guidelines [227], we applied strict eligibility criteria and performed independent double screening, with conflict adjudication by consensus in consultation with at least one other member of the review team. Limitations of the review include its restriction to articles written in English, although less than 15% of those papers excluded at full text were excluded based on not being primary sources or written in languages other than English. A lack of available evidence prevented development of overview summaries for several outcomes, while for other outcomes, the range of species and settings used made it difficult to draw conclusions about GI and SI adaptations during pregnancy across the range of monogastric mammalian species. We did not assess study quality within this scoping review, but note small sample sizes in some studies, which may have prevented detection of differences between groups. For example, the only studies of SI villi length in mice included 4 to 6 individuals in some groups [178, 331]. In human studies, pregnant and non-pregnant groups were not always matched, or drawn from the same population groups. An early study of gastric emptying by Boyden *et al.* compared outcomes in nursing students to those of pregnant women [311], however no demographic comparison was included in the paper. An additional limitation in too much of the literature was a lack of information on study settings including nutrition, or variables such as litter size; which are likely to impact the outcomes of interest.

To address these gaps in evidence, we suggest future studies adopt the following recommendations. Firstly, we recommend that all studies include a matched non-pregnant control group, and that individuals be randomised to groups where possible, such as preclinical, cross-sectional studies. In longitudinal studies, the control group may be the

same individuals before pregnancy or after weaning, although this may not be possible in mechanistic preclinical studies, and may create recruitment, retention and logistical challenges in human populations, where up to half of pregnancies are unintended [387]. Variation in time to conception could also be a challenge in human studies, given that only 30% of women conceive in the first month of trying, with ~90% conceiving within a year [388]. Lactating individuals should not be treated as a control group given the substantial upregulation of food intake and evidence of increased nutrient uptake and SI adaptations during lactation. For example, daily food intakes of outbred MF1 mice increased from 5.2 g/day before mating to a maximum of 7.7 g/day at GD16, and increased more than 3-fold further to peak at 23.1 g/day on days 13-16 of lactation [389]. Marked increases in determinants of nutrient absorption have also been reported during lactation, including a doubling of SI weight with hypertrophy, and increases in duodenal and ileal villi lengths of over 50% in rats [175]. Where differences in nutrient uptake and its determinants are identified between non-pregnant and late-pregnant individuals, we further recommend that subsequent studies should include groups at early- and mid-pregnancy, to identify the timing of adaptations. Finally, we recommend additional studies to identify the endocrine or other physiological signals that drive these adaptations in nutrient uptake and determinants during pregnancy.

3.8. Supplementary table S3.1 – search string for each database

Database (final search date)	Search string
Pubmed (20 November 2023)	(Pregnan* [TW] OR "Pregnancy" [MeSH] OR Gestat* [TW]) AND (Gastrointest* [TW] OR "gastrointestinal tract" [MeSH] OR Gastric [TW] OR Alimentary [TW] OR Digestive tract [TW] OR Digestive system [TW] OR Small intestine [TW] OR Duoden* [TW] OR Jejun* [TW] OR Ileum [TW] OR Ileal [TW] OR Stomach [TW]) AND (((Nutrient [TW] OR carbohydrate [TW] OR glucose [TW] OR fructose [TW] OR sucrose [TW] OR protein [TW] OR amino acid [TW] OR fatty acid [TW] OR lipid [TW] OR vitamin [TW] OR folic acid [TW] OR folate [TW] OR calcium [TW] OR iron [TW] OR zinc [TW]) AND ("biological transport" [MesH] OR absorption [TW] OR uptake [TW] OR transport [TW])) OR Motility [TW] OR Transit [TW] OR Gastric emptying [TW] OR "anatomy" [MeSH] OR Weight [TW] OR Length [TW] OR Surface area [TW] OR Enterocyte [TW] OR Vasculat* [TW] OR blood vessel [TW] OR capillary [TW] OR Innervation [TW] OR Nerve [TW] OR Vill* [TW] OR Crypt [TW] OR Muscle thickness [TW] OR Muscle depth [TW] OR SGLT1 [TW] OR SGLT-1 [TW] OR sodium linked glucose transporter 1 [TW] OR GLUT2 [TW] OR GLUT-2 [TW] OR glucose transporter 2 [TW] OR Slc2a2 [TW] OR GLUT5 [TW] OR GLUT-5 [TW] OR glucose transporter 5 [TW] OR Slc2a5 [TW] OR PEPT1 [TW] OR PEPT-1 [TW] OR peptide transporter [TW] OR SLC6A6 [TW] OR SLC6A19 [TW] OR "CD36" [TIAB] OR "cluster of differentiation 36" [TIAB] OR LFABP [TW] OR "Fatty acid binding protein 2" [TIAB]) AND eng[LA] NOT review[PT]
Scopus (20 November 2023)	(TITLE-ABS-KEY ((pregnan* OR gestat*))) AND (TITLE-ABS-KEY ((gastrointest* OR gastric OR alimentary OR "Digestive tract" OR "Digestive system" OR "gastrointestinal tract" OR intestine OR "Small intestine" OR duoden* OR jejun* OR ileum OR ileal OR stomach))) AND (TITLE-ABS-KEY ((nutrient OR carbohydrate OR glucose OR fructose OR sucrose OR protein OR "amino acid" OR "fatty acid" OR lipid OR vitamin OR "folic acid" OR folate OR calcium OR iron OR zinc))) AND (TITLE-

	<p>ABS-KEY ("transport at the cellular level" OR absorption OR uptake OR transport OR motility OR transit OR "Gastric emptying" OR anatomy OR weight OR length OR "Surface area" OR enterocyte OR vasculat* OR "blood vessel" OR capillary OR innervation OR nerve OR vill* OR crypt OR "Muscle thickness" OR "Muscle depth" OR sgl1 OR "SGLT-1" OR "sodium linked glucose transporter 1" OR glut2 OR "GLUT-2" OR "glucose transporter 2" OR slc2a2 OR glut5 OR "GLUT-5" OR "glucose transporter 5" OR slc2a5 OR pept1 OR "PEPT-1" OR "peptide transporter" OR slc6a6 OR slc6a19 OR "CD36" OR "cluster of differentiation 36" OR lfabp OR "Fatty acid binding protein 2"))</p>
<p>Web of Science (20 November 2023)</p>	<p>(Pregnan* OR Gestat*) AND (Gastrointest* OR Gastric OR Alimentary OR "Digestive tract" OR "Digestive system" OR "gastrointestinal tract" OR intestine OR "Small intestine" OR Duoden* OR Jejun* OR Ileum OR Ileal OR stomach) AND (((Nutrient OR carbohydrate OR glucose OR fructose OR sucrose OR protein OR "amino acid" OR "fatty acid" OR lipid OR vitamin OR "folic acid" OR folate OR calcium OR iron OR zinc) AND ("transport at the cellular level" OR absorption OR uptake OR transport)) OR Motility OR Transit OR "Gastric emptying" OR anatomy OR Weight OR Length OR "Surface area" OR Enterocyte OR Vasculat* OR "blood vessel" OR capillary OR Innervation OR Nerve OR Vill* OR Crypt OR "Muscle thickness" OR "Muscle depth" OR SGLT1 OR "SGLT-1" OR "sodium linked glucose transporter 1" OR GLUT2 OR "GLUT-2" OR "glucose transporter 2" OR Slc2a2 OR GLUT5 OR "GLUT-5" OR "glucose transporter 5" OR Slc2a5 OR PEPT1 OR "PEPT-1" OR "peptide transporter" OR SLC6A6 OR SLC6A19 OR "CD36" OR "cluster of differentiation 36" OR LFABP OR "Fatty acid binding protein 2")</p>
<p>ProQuest Dissertations and Theses Global (20</p>	<p>NOFT ((Pregnan* OR Gestat*) AND (Gastrointest* OR Gastric OR Alimentary OR "Digestive tract" OR "Digestive system" OR "gastrointestinal tract" OR intestine OR "Small intestine" OR Duoden* OR Jejun* OR Ileum OR Ileal OR stomach) AND (((Nutrient* OR carbohydrate* OR glucose OR fructose OR sucrose OR protein* OR ("amino acid" OR "amino acids") OR ("fatty acid" OR "fatty acids"))</p>

November 2023)	OR lipid* OR vitamin* OR "folic acid" OR folate OR calcium OR iron OR zinc) AND ("transport at the cellular level" OR absorption OR uptake OR transport)) OR Motility OR Transit OR "Gastric emptying" OR anatomy OR Weight OR Length OR "Surface area" OR Enterocyte OR Vasculat* OR "blood vessel" OR capillary OR Innervation OR Nerve OR Vill* OR Crypt OR "Muscle thickness" OR "Muscle depth" OR SGLT1 OR "sodium linked glucose transporter 1" OR GLUT2 OR "glucose transporter 2" OR Slc2a2 OR GLUT5 OR "glucose transporter 5" OR Slc2a5 OR PEPT1 OR "peptide transporter" OR SLC6A6 OR SLC6A19 OR "CD36" OR "cluster of differentiation 36" OR LFABP OR "Fatty acid binding protein 2")) AND la.exact("ENG")
Embase (20 November 2023)	((Pregnan*.af OR exp Pregnancy OR Gestat*.af) AND (Digestive system.sh OR exp gastrointestinal tract OR exp stomach OR exp intestine OR (Gastrointest* OR gastrointestinal tract OR Gastric OR Alimentary OR Digestive tract OR Small intestine OR Duoden* OR Jejun* OR Ileum OR Ileal OR stomach).af) AND (((Nutrient.af OR carbohydrate.af OR glucose.af OR fructose.af OR sucrose.af OR protein.af OR amino acid.af OR fatty acid.af OR lipid.af OR vitamin.af OR folic acid.af OR folate.af OR calcium.af OR iron.af OR zinc.af) AND (exp transport at the cellular level OR absorption.af OR uptake.af OR transport.af)) OR Motility.af OR Transit.af OR Gastric emptying.af OR exp anatomy OR Weight.af OR Length.af OR Surface area.af OR Enterocyte.af OR Vasculat*.af OR blood vessel.af OR capillary.af OR Innervation.af OR Nerve.af OR Vill*.af OR Crypt.af OR Muscle thickness.af OR Muscle depth.af OR SGLT1.af OR SGLT-1.af OR sodium linked glucose transporter 1.af OR GLUT2.af OR GLUT-2.af OR glucose transporter 2.af OR Slc2a2.af OR GLUT5.af OR GLUT-5.af OR glucose transporter 5.af OR Slc2a5.af OR PEPT1.af OR PEPT-1.af OR peptide transporter.af OR SLC6A6.af OR SLC6A19.af OR CD36.af OR cluster of differentiation 36.af OR LFABP.af OR Fatty acid binding protein 2.af) AND English.lg) NOT review.pt

3.9. Supplementary table S3.2 Main characteristics and key results for studies investigating changes in nutrient absorption and its determinants during pregnancy

First author year; species (strain); study design [source]	Nutrition		Pregnancy stage(s) (term gestation)	Outcome type(s)	Extracted outcome(s)	
	Diet	Availability			Outcome (units - where applicable)	Mean ± SD (n) unless stated, difference (comparisons are with non-pregnant group unless stated otherwise)
Ahokas 1984; rat (Sprague- Dawley); rand exp [390]	14% sprayed egg white, 67% dextrose (Teklad Mills, Madison, WI); 29.5 mg protein/kcal + drinking water with 13 mg zinc/L	Ad lib	NP, GD21 (22 d)	Whole SI anatomy	SI weight (g)	NP: 3.77 ± 0.73 (6) GD21: 6.09 ± 1.64 (10), P<0.05
					Organ blood flow (ml·min ⁻¹)	NP: 4.89 ± 0.7 (6) GD21: 9.25 ± 2.1 (10), P<0.05
					Organ blood flow (ml·min ⁻¹ ·g ⁻¹)	NP: 1.33 ± 0.34 (6) GD21: 1.53 ± 0.32 (10), N/S
Al-Shboul 2019; rat (Sprague- Dawley); non- rand exp [296]	N/S	N/S	GD10, GD20 (22 d)	Gastric emptying/SI motility	Stomach smooth muscle cell contraction - acetylcholine-induced (%)	GD10: 19 ± 6.3 (10) GD20: 36 ± 4.7 (10), P<0.05 vs GD10

Amano 1967; rat (Wistar); non-rand exp [391]	Commercial diet (OA-2, Japan CLEA Co.); 26.5% protein	Fasted 16 h before OGTT	NP, GD19 (22 d)	Direct measure of nutrient uptake – in vivo	Blood glucose, 0.5 h after 1.5 g·kg ⁻¹ oral glucose, mg (%)	NP: 138.5 ± 22.3 (8) GD19: 110.0 ± 21.1 (3), N/S
					Blood glucose, Δ fasting - 0.5 h after 1.5 g·kg ⁻¹ oral glucose, mg (%)	NP: 38 (8) GD19: 47 (3), lower
Ardawi 1987; rat (Wistar Albino); non-rand exp [392]	Standard laboratory diet	N/S	NP, GD19 (22 d)	Whole SI anatomy	SI weight (g)	NP: 4.81 ± 0.47 (12) GD21: 7.66 ± 1.65 (17), P<0.01
				Digestive enzyme activity/ expression	Glutaminase activity in SI mucosal scrapings (μmol·min ⁻¹ ·g ⁻¹ wet weight)	NP: 12.61 ± 2.95 (12) GD21: 20.92 ± 5.94 (17), P<0.01
					Glutaminase activity in SI mucosal scrapings (nmol·min ⁻¹ ·mg ⁻¹ protein)	NP: 117.73 ± 25.97 (12) GD21: 208.18 ± 35.94 (17), P<0.01
					Glutaminase activity in Whole SI anatomy (μmol·min ⁻¹ ·g ⁻¹ wet weight)	NP: 6.84 ± 1.63 (18) GD21: 9.22 ± 1.87 (19), P<0.01
					Glutaminase activity in Whole SI anatomy (nmol·min ⁻¹ ·mg ⁻¹ protein)	NP: 33.43 ± 7.45 (18) GD21: 42.87 ± 8.61 (19), P<0.01

Argiles 1989; rat (Wistar); non-rand exp [258]	Purina chow	Ad lib, except for fast after oral lipids	NP, GD19, GD20 (22 d)	Direct measure of nutrient uptake – in vivo	Plasma radioactivity after oral ¹⁴ C tripalmitate - lipid uptake (dpm·mL ⁻¹ plasma)	30 min	NP: 100 ± 245 (6-8) GD19: 830 ± 245 (6-8), nsd GD20: 780 ± 245 (6-8), nsd
						60 min	NP: 850 ± 367 (6-8) GD19: 1800 ± 612 (6-8), P<0.05 GD20: 3100 ± 980 (6-8), P<0.05
Bailey 1989; mouse (MF1); non-rand exp [345]	Mouse breeding diet (Heygate and Sons Ltd, Northampton, Northants, UK)	Ad lib	NP, GD19 (19 d)	Duodenal anatomy	Duodenum weight (mg)	NP: 233 ± 28 (8) GD19: 391 ± 88 (6), P<0.01	
				Jejunal anatomy	Jejunum weight (mg)	NP: 658 ± 127 (8) GD19: 1246 ± 186 (6), P<0.001	
				Ileal anatomy	Ileum weight (mg)	NP: 400 ± 85 (8) GD19: 891 ± 171 (6), P<0.001	
Balesaria 2012; mouse (129/Ola- C57BL/6 mixed strain); non-rand exp [358]	Dried egg albumin diet (RM1 diet, SDS, UK), 50 ppm iron (adequate iron diet)	N/S	NP, GD18 (N/S)	Nutrient transporter gene expression	Duodenal expression, relative to beta-actin expression (ΔCt)	<i>Dcytb</i>	NP: 0.85 ± 0.4 (4) GD18: 7.5 ± 2.4 (4), P<0.05
						<i>DMT1</i>	NP: 0.3 ± 0.2 (4) GD18: 2.0 ± 0.6 (4), P<0.05
						<i>FPN</i>	NP: 1.2 ± 0.6 (4) GD18: 6.5 ± 3.2 (4), P<0.05
Barboni 2016; human; case control [393]	Standardised meal (70 g pasta, 150 g meat, salad, 300 ml water) eaten over 10 minutes before study	Fasted 6 h before meal	NP, 3 rd Tri (280 d)	Gastric emptying/SI motility	Change in gastric antrum cross-sectional area, time periods after meal (cm ²)	10 - 90 min	NP: -4.98 ± 6.39 (10) 3 rd Tri: -2.74 ± 3.2 (10), P<0.05
						90 - 240 min	NP: -5.01 ± 6.89 (10) 3 rd Tri: -4.37 ± 3.05 (10), P<0.05
						10 - 240 min	NP: -9.99 ± 7.38 (10) 3 rd Tri: -1.62 ± 3.89 (10), P<0.05

Barrett 1994; human; prosp cohort study [229]	For 3 days before each iron study, daily dietary intake of 13 mg iron (avg. 4 mg from meat). Meal for iron intake study: 60 g of cooked lean bacon, 1 bread roll, and 50 ml fresh orange juice, total non-haem iron content of 3.2 mg	Fasted overnight before iron study	12 weeks, 24 weeks, 36 weeks (280 d)	Direct measure of nutrient uptake – in vivo	Absorption of non-haem iron from food (%)	12 weeks: 7.2, 95% CI 4.9-10.9 (12) 24 weeks: 36.3, 95% CI 27.6-47.3 (12), P<0.001 vs 12 weeks 36 weeks: 66.1, 95% CI 57.1-76.2 (12), P<0.001 vs 24 weeks
Batey 1977; mouse (Sydney White); non- rand exp [230]	Standard rat cubes	Fasted for 16 h prior to study	NP, GD16- 17, GD20-21 (21 d)	Direct measure of nutrient uptake – in vivo	Intestinal ⁵⁹ Fe uptake (% of dose)	NP: 16.4 ± 9.2 (16) GD16-17: 23.0 ± 4.9 (6), nsd GD20-21: 29.2 ± 13.5 (9), P<0.01
					Intestinal ⁵⁹ Fe transport (% of dose)	NP: 10.7 ± 4.8 (16) GD16-17: 17.0 ± 5.4 (6), nsd GD20-21: 24.3 ± 11.4 (9), P<0.01
Batey 1977; rat (Swiss Fulins-dorf); non-rand exp [276]	Rat cubes (iron content 280 ppm)	Fasted 18 h before study	NP, GD20- 21 (21 d)	Direct measure of nutrient uptake – in vivo	Duodenal ⁵⁹ Fe transport (% of dose)	NP: 18.9 ± 7.0 (15) GD20-21: 44.0 ± 15.9 (12), P<0.05
Batey 1977; rat (Swiss Fulins-dorf); non-rand exp [277]	Rat cubes (iron content 280 ppm)	Fasted 18 h before study	NP, GD15, GD20-21 (21 d)	Direct measure of nutrient uptake – in vivo	Duodenal ⁵⁹ Fe uptake (% of dose)	NP: 31.6 ± 11.6 (15) GD15: 41.9 ± 12.7 (7), P<0.05 GD20-21: 60.4 ± 12.9 (9), P<0.01
					Duodenal ⁵⁹ Fe transport (% of dose)	NP: 18.9 ± 7.0 (15) GD15: 18.1 ± 11.6 (7), nsd GD20-21: 44.0 ± 13.8 (9), P<0.01

Boass 1992; rat (Holtzman); non-rand exp [268]	Pellets: 75% whole wheat flour, 13% casein, 5% cellulose (Alphacel), 4.4% fat (mostly corn oil), 2% salt mixture, 1.3% vitamin D-free vitamin mixture (ICN Biochemicals, Cleveland, OH), 5 IU cholecalciferol/g diet, and 0.8% CaCO ₃ (ICN Biochemicals), containing 0.4 Ca, 0.4% P, 0.14% Mg	Unfasted	NP, GD18, GD20 (22 d)	Direct measure of nutrient uptake – ex vivo	Net calcium transport in everted sacs ($\mu\text{g}\cdot\text{g}^{-1}$ wet weight)	Proximal half of duodenum	NP: 69 ± 18 (5) GD18: 87 ± 12 (9), nsd GD20: 124 ± 22 (6), P<0.05 vs GD18
						Distal half of duodenum	NP: 23 ± 12 (4) GD18: 50 ± 24 (9), nsd GD20: 132 ± 23 (3), P<0.05
Boass 1997; rat (Holtzman); non-rand exp [266]	Pelleted 75% whole wheat flour, 13% casein, 5% cellulose (Alphacel), 4.4% fat (mostly from corn oil), 2% salt mixture, 1.3% vitamin D-free vitamin mixture (ICN Biochemicals, Cleveland, OH, U.S.A.), 5 IU of cholecalciferol/g of diet, and 0.8% CaCO ₃	N/S	NP, GD21 (22 d)	Direct measure of nutrient uptake – ex vivo	Slope jejunal calcium absorption vs. calcium concentration	NP: 0.22 ± 0.16 (10) GD21: 0.16 ± 0.14 (8), nsd	

Boyden 1944; human; cross sectional [311]	N/S	N/S	NP, combined 2 nd & 3 rd Tri (280 d)	Gastric emptying/SI motility	Time of appearance of food past stomach - pylorus opening (min)	NP: 5.06, range 0.25-20 (17) 2 nd & 3 rd Tri: 10.85, range 0.3-N/S (18), P<0.05
					Time of appearance of food at duodenal inflexion - pars inf (min)	NP: 11.39, range 1.68-35+ (17) 2 nd & 3 rd Tri: 20.16, range 0.6-33+ (18), P<0.05
Braverman 1980; human; cross sectional [372]	N/S	Overnight fast before study	NP, 9-11 weeks, 14- 37 weeks (280 d)	Gallbladder emptying	Gallbladder volume during fasting (ml)	NP: 15, range 4-24 (11) 9-11 weeks: 15 ± 14 (8), nsd 14-37 weeks: 25 ± 20 (25), P<0.005
					Rate of gallbladder emptying (slope of line)	NP: 0.0523 ± 0.0172 (11) 9-11 weeks: 0.0375 ± 0.0139 (8), P<0.05 14-37 weeks: 0.0332 ± 0.0135 (25), P<0.005
					Maximum gall bladder emptying (%)	NP: 70.4 ± 7.3 (11) 9-11 weeks: 63.1 ± 13.6 (8), nsd 14-37 weeks: 61.0 ± 11.5 (25), P<0.005
Braverman 1988; human; prospective cohort [321]	Standard liquid test meal w/ 420 kcal; 35% fat, 15% protein, 50% carbohydrates	Fasted on night before study	NP, 38-42 weeks (280 d)	Gastric emptying/SI motility, Gallbladder emptying	Intestinal transit time (min)	NP: 131 ± 23 (8) 38-42 weeks: 174 ± 47 (10), P<0.01
					Gallbladder rate of emptying, slope (min ⁻¹)	NP: 0.0498 ± 0.0023 (8) 38-42 weeks: 0.0173 ± 0.0007 (10), P<0.005
					Gallbladder emptying (%)	NP: 63.1 ± 1.3 (8) 38-42 weeks: 60.1 ± 1.2 (10), nsd

Brown 1977; mouse (Sydney White); non- rand exp [285]	N/S	N/S	NP, GD15- 17, GD18-21 (21 d)	Direct measure of nutrient uptake – in vivo, Indirect measure of nutrient uptake – ex vivo	Intestinal uptake (ng [⁵⁷ Co]B ₁₂)	NP: 12.7 ± 1.5 (9) GD15-17: 17.5 ± 6.5 (8), P<0.05 GD18-21: 29.1 ± 4.1 (10), P<0.001	
					Intestinal transport (ng [⁵⁷ Co]B ₁₂)	NP: 8.4 ± 2.7 (9) GD15-17: 15.9 ± 6.8 (8), P<0.001 GD18-21: 28.4 ± 4.4 (10), P<0.001	
					Intrinsic factor-[⁵⁷ Co]B ₁₂ binding to ileal homogenates (ng·mg ⁻¹ mucosal protein)	NP: 0.21 ± 0.05 (3) GD18-21: 0.40 ± 0.10 (3), P<0.05	
Burdett 1979; rat (Sprague- Dawley); non- rand exp [394]	Porton Mouse Diet (Oakes of Congleton, Cheshire, UK)	Ad lib	NP, GD18- 20 (22 d)	Whole SI anatomy, jejunal anatomy, ileal anatomy, digestive enzyme activity/ expression	Jejunum+ileum length (cm)	NP: 104 ± 4 (11) GD18-20: 118 ± 8 (11), P<0.001	
					Jejunum+ileum wet weight (g)	NP: 9.3 ± 0.9 (10) GD18-20: 13.1 ± 1.3 (11), P<0.001	
					Jejunum+ileum mucosal epithelium wet weight (g)	NP: 2.7 ± 0.6 (10) GD18-20: 3.6 ± 1.3 (10), P<0.05	
					Protein in mucosal epithelium (mg)	Overall (jejunum + ileum)	NP: 405 ± 7 (11) GD18-20: 561 ± 13 (11), P<0.03
						Jejunum	NP: 168 ± 8 (7) GD18-20: 263 ± 47 (6), P<0.01
						Proximal ileum	NP: 150 ± 22 (7) GD18-20: 226 ± 22 (6), P<0.0005
						Distal ileum	NP: 109 ± 23 (7) GD18-20: 148 ± 17 (6), P<0.003
					Lactate dehydrogenase specific activity (units·mg ⁻¹ protein)	Overall (jejunum + ileum)	NP: 2.46 ± 0.63 (10) GD18-20: 2.30 ± 0.63 (7), nsd
						Jejunum	NP: 3.10 ± 0.80 (4)

						GD18-20: 3.50 ± 0.70 (3), nsd
					Proximal ileum	NP: 2.70 ± 1.20 (4) GD18-20: 2.70 ± 0.20 (3), nsd
					Distal ileum	NP: 1.20 ± 0.20 (3) GD18-20: 1.20 ± 0.20 (3), nsd
				Succinate-tetrazolium reductase specific activity (units·mg ⁻¹ protein)	Overall (jejunum + ileum)	NP: 1.61 ± 0.56 (11) GD18-20: 1.25 ± 0.36 (9), nsd
					Jejunum	NP: 2.00 ± 0.80 (7) GD18-20: 1.70 ± 0.60 (15), nsd
					Proximal ileum	NP: 1.50 ± 0.50 (7) GD18-20: 1.40 ± 0.40 (5), nsd
					Distal ileum	NP: 1.60 ± 0.80 (7) GD18-20: 1.10 ± 0.70 (5), nsd
				Glucose-6-dehydrogenase specific activity (units·mg ⁻¹ protein)	Overall (jejunum + ileum)	NP: 10.4 ± 1.80 (9) GD18-20: 14.3 ± 3.20 (10), P<0.003
					Jejunum	NP: 11.5 ± 1.70 (6) GD18-20: 13.8 ± 2.60 (7), P<0.05
					Proximal ileum	NP: 9.50 ± 1.50 (6) GD18-20: 12.5±1.0 (6), P<0.002
					Distal ileum	NP: 10.8 ± 0.70 (6) GD18-20: 12.4 ± 2.60 (7), nsd
				Isocitrate dehydrogenase specific activity (units·mg ⁻¹ protein)	Overall (jejunum + ileum)	NP: 36.7 ± 4.0 (3) GD18-20: 54.8 ± 12.3 (5), P<0.02
					Jejunum	NP: 39.6 ± 7.0 (4) GD18-20: 54.9 ± 11.9 (5), P<0.02
					Proximal ileum	NP: 32.5 ± 4.0 (4) GD18-20: 52.3 ± 14.0 (4), P<0.02

						Distal ileum	NP: 40.6 ± 13.4 (4) GD18-20: 59.8 ± 17.2 (5), P<0.05
					Sucrase specific activity (units·mg ⁻¹ protein)	Overall (jejunum + ileum)	NP: 93 ± 32.2 (18) GD18-20: 106 ± 33.5 (13), P<0.05
						Jejunum	NP: 134 ± 56 (14) GD18-20: 146 ± 48 (7), nsd
						Proximal ileum	NP: 119 ± 45 (14) GD18-20: 167 ± 58 (7), P<0.05
						Distal ileum	NP: 21.3 ± 10.8 (13) GD18-20: 43 ± 27 (6), P<0.05
Campbell 1971; human; prosp cohort [239]	N/S	Fasted overnight before test	22 weeks, 32 weeks (280 d)	Direct measure of nutrient uptake – in vivo	Blood glucose before and after OGTT, 50 g glucose (mg/100 ml)	Fasting	22 weeks: 72.7 ± 5.3 (15) 32 weeks: 77.2 ± 7.2 (15), nsd vs 22 weeks
						30 min	22 weeks: 104 ± 20.0 (15) 32 weeks: 119.9 ± 18.3 (15), nsd vs 22 weeks
Campbell 1994; human; prosp cohort [237]	Test meal: 14.4 g protein, 17.5 g fat, 58.7 g carbohydrate, 453 kcal energy	Fasted pre-test	16 weeks, 26 weeks, 36 weeks (280 d)	Direct measure of nutrient uptake – in vivo	Plasma glucose before and after a test meal (mM·L ⁻¹)	Fasting	16 weeks: 4.35 ± 0.39 (27) 26 weeks: 4.20 ± 0.36 (29), nsd vs 16 weeks 36 weeks: 4.07 ± 0.46 (26), nsd vs 16 weeks
						30 min	16 weeks: 6.04 ± 0.76 (27) 26 weeks: 6.29 ± 0.68 (29), nsd vs 16 weeks 36 weeks: 6.12 ± 0.61 (26), nsd vs 16 weeks

Chang 1995; rat (Sprague- Dawley); non- rand exp [316]	Standard laboratory chow	Ad lib, then fasted 18 h before motility experiment	NP, GD7, GD14, GD21 (22 d)	Gastric emptying/SI motility	Gastrointestinal transit (% of SI traversed after 15 min)	NP: 42.6 ± 4.4 (10) GD7: 43.0 ± 11.3 (8), nsd GD14: 46.0 ± 17.0 (8), nsd GD21: 36.0 ± 8.5 (8), nsd
Chang 1998; rat (Sprague- Dawley); non- rand exp [395]	Standard laboratory chow	Ad lib, then overnight fast before study	NP, GD7, GD14, GD21 (22 d)	Gastric emptying/SI motility	Gastric emptying (% remaining after 15 min)	NP: 53.5 ± 7.0 (11) GD7: 50.1 ± 13.2 (7), nsd GD14: 58.2 ± 19.4 (6), nsd GD17: 57.7 ± 10.1 (7), nsd
					Intestinal transit (geometric centre of radioactivity/10 segments)	NP: 4.98 ± 0.43 (11) GD7: 4.54 ± 0.66 (7), nsd GD14: 4.47 ± 0.42 (6), nsd GD21: 3.61 ± 0.71 (7), P<0.01
Charoenphan- dhu 2009; rat (Sprague- Dawley), non- rand exp [274]	Standard pellets	Ad lib	NP, GD14, GD21 (22 d)	Direct measure of nutrient uptake – ex vivo	Duodenal transcellular calcium flux (nmol·h ⁻¹ ·cm ⁻²)	NP: 36 ± 6 (8) GD14: 48 ± 8 (8), P<0.05 GD21: 50 ± 8 (8), P<0.05
Chen 1995; rat (Sprague- Dawley); non- rand exp [376]	Rat chow	Ad lib	NP, GD7, GD14, GD21 (22 d)	Digestive enzyme activity/ expression	Basal acid output, stomach (µmol·35 minutes ⁻¹)	NP: 2.0 ± 0.6 (9) GD7: 4.0 ± 3.7 (6), nsd GD14: 2.5 ± 1.2 (6), nsd GD21: 4.5 ± 2.4 (6), P<0.01
					Pentagastrin-stimulated acid output, stomach (µmol·35 minutes ⁻¹)	NP: 10 ± 3.0 (9) GD7: 22 ± 12.2 (6), P<0.01 GD14: 15 ± 9.8 (6), nsd GD21: 16 ± 7.3 (6), nsd

Chiloiro 2001; human; prosp cohort [306]	N/S	Fasted overnight before study	1 st Tri, 3 rd Tri (280 d)	Gastric emptying/SI motility	Gastric emptying – half emptying time (min)	1 st Tri: median 38.2, IQR 25.2-87.3 (11) 3 rd Tri: median 39.8 (11), IQR 25.4-76.4, nsd vs 1 st Tri
					Gastric emptying – final time (min)	1 st Tri: median 95, IQR 70.0-170.0 (11) 3 rd Tri: median 70, IQR 50.0-167.0 (11), nsd vs 1 st Tri
					Orocecal transit time (min)	1 st Tri: median 80, IQR 50.0-235.5 (11) 3 rd Tri: median 100, IQR 50.5-240.0 (11), P<0.05 vs 1 st Tri
Clapp 2000; human; prosp cohort [396]	N/S	N/S	NP, 16 ± 2 weeks, 26 ± 2 weeks, 36 ± 2 weeks (280 d)	Whole SI anatomy	Portal vein diameter at recumbent rest (mm)	NP: 12.2 ± 1.5 (12) 16±2 weeks: 12.6 ± 1.5 (12), nsd 26±2 weeks: 12.8 ± 1.5 (12), nsd 36±2 weeks: 12.3 ± 1.2 (12), nsd
					Portal vein blood flow at recumbent rest (ml·min ⁻¹)	NP: 560 ± 196 (6) 16±2 weeks: 670 ± 245 (6), nsd 26±2 weeks: 1130 ± 588 (6), nsd 36±2 weeks: 1060 ± 416 (6), nsd
Clark 1957; dog; non-rand exp. [377]	Normal mixed kennel fare	N/S	NP, pregnant (59-63 d)	Digestive enzyme activity/ expression	Gastric acid secretion (m.Equiv)	NP: 1.12 ± 0.67 (3) Pregnant: 1.47 ± 0.49 (3), N/S

Clark 1983; human; rand double- blinded [300]	N/S	Fasted from 07.00, studied for 2 h prior to afternoon surgery	NP, 1 st Tri (280 d)	Gastric emptying/SI motility	Plasma paracetamol concentrations after oral 0.50 mg.kg ⁻¹ paracetamol ($\mu\text{g}\cdot\text{mL}^{-1}$)	15 min	NP: 7.5 ± 3.2 (10) 1 st Tri: 7.3 ± 3.2 (10), N/S
						30 min	NP: 15.4 ± 5.7 (10) 1 st Tri: 14.1 ± 5.9 (10), N/S
						45 min	NP: 19.3 ± 5.7 (10) 1 st Tri: 14.1 ± 7.0 (10), N/S
						60 min	NP: 19.6 ± 5.1 (10) 1 st Tri: 15.5 ± 4.5 (10), N/S
					AUC ₀₋₆₀ plasma paracetamol ($\mu\text{g}\cdot\text{min}^{-1}\cdot\text{mL}^{-1}$)	NP: 53.7 ± 16.5 (10) 1 st Tri: 44.7 ± 12.2 (10), P<0.05	
Coltart 1972; human; cross sectional [248]	N/S	Fasted overnight before sucrose tolerance test	NP, at term (280 d)	Indirect measure of nutrient uptake – in vivo	Plasma glucose ($\text{mg}\cdot 100 \text{ ml}^{-1}$), after oral 1 g.kg ⁻¹ sucrose	Fasting	NP: 81 ± 8.5 (10) Term: 69 ± 5.4 (10), P<0.01
						15 min	NP: 104 ± 17.7 (10) Term: 97 ± 16.1 (10), nsd
						30 min	NP: 115 ± 18.3 (10) Term: 116 ± 19.0 (10), nsd
					Δ plasma glucose ($\text{mg}\cdot 100 \text{ ml}^{-1}$) from fasting, time after 1 g.kg ⁻¹ sucrose	15 min	NP: 23 ± 25 (10) Term: 27 ± 32 (10), nsd
						30 min	NP: 34 ± 41 (10) Term: 47 ± 63 (10), nsd
					Plasma fructose ($\text{mg}\cdot 100 \text{ ml}^{-1}$), after oral 1 g.kg ⁻¹ sucrose	Fasting	NP: 0.5 ± 0.3 (10) Term: 0.7 ± 0.6 (10), nsd
						15 min	NP: 2.9 ± 1.3 (10) Term: 4.1 ± 2.8 (10), nsd
						30 min	NP: 5.3 ± 2.2 (10)

							Term: 5.5 ± 3.2 (10), nsd
					Δ plasma fructose (mg·100 ml ⁻¹) from fasting, time after oral 1 g·kg ⁻¹ sucrose	15 min	NP: 2.4 ± 3.2 (10) Term: 3.5 ± 3.8 (10), nsd
						30 min	NP: 4.7 ± 5.4 (10) Term: 4.9 ± 5.4 (10), nsd
Craft 1970; rat (Wistar); non- rand exp [397]	Cube diet (Oxoid No. 41B)	Ad lib, then fasted 18- 24 h before experiment s	NP, GD18- 20 (22 d)	Direct measure of nutrient uptake – ex vivo, Whole SI anatomy	SI length (cm)	NP: 107.1 ± 6.5 (25) GD18-20: 107.4 ± 7.5 (25), nsd	
					SI wet weight (g)	NP: 3.75 ± 0.50 (25) GD18-20: 4.49 ± 0.65 (25), P<0.001	
					SI wet weight (mg·cm ⁻¹)	NP: 35.15 ± 5.65 (25) GD18-20: 42.00 ± 6.60 (25), P<0.001	
					SI dry weight (g)	NP: 1.00 ± 0.15 (25) GD18-20: 1.20 ± 0.20 (25), P<0.001	
					SI dry weight (mg/cm)	NP: 9.34 ± 1.80 (25) GD18-20: 11.23 ± 1.95 (25), P<0.01	
					Glucose absorption by proximal jejunum (mg·g ⁻¹ dry intestine weight·5 min ⁻¹)	10 mM glucose	NP: 6.83 ± 0.9 (5) GD18-20: 14.1 (5), N/S
						20 mM glucose	NP: 14.1 ± 2.0 (12) GD18-20: 13.5 (7), N/S
					Ex vivo glycine absorption by proximal jejunum (mg·g ⁻¹ dry intestine weight·5 min ⁻¹)	10 mM glycine	NP: 2.95 ± 0.40 (5) GD18-20: 2.3 (4), nsd
						20 mM glycine	NP: 5.1 (5) GD18-20: 4.0 (5), nsd
						50 mM glycine	NP: 10.7 ± 2.7 (10) GD18-20: 10.5 (10), nsd

Crean 1971; rat (Wistar); non-rand. exp. [338]	N/S	N/S	NP, GD7, GD14, GD21 (22 d)	Whole SI anatomy	Total parietal cell population in stomach fundus (millions)	NP: 41.1 ± 2.4 (18) GD7: 38.7 ± 2.4 (6), nsd GD14: 42.7 ± 5.9 (6), nsd GD21: 49.2 ± 5.6 (6), P<0.01	
					Total peptic cell population in stomach fundus (millions)	NP: 61.3 ± 3.2 (18) GD7: 58.6 ± 6.8 (6), nsd GD14: 68.3 ± 10.0 (6), P<0.05 GD21: 81.3 ± 8.1 (6), P<0.01	
Cripps 1975; rat (Sprague- Dawley); non- rand exp [175]	Food cubes (Fielder's Pty Ltd, Tamworth, NSW, Australia); 20% crude protein, 7.5% fat	Ad lib	NP, GD12- 15 (22 d)	Direct measure of nutrient uptake – in vivo, Whole SI anatomy, duodenal anatomy, ileal anatomy	Small intestine wet weight (g)	NP: 7.450 ± 1.204 (13) GD12-15: 7.453 ± 0.688 (6), nsd	
					Small intestine dry weight (g)	NP: 1.528 ± 0.339 (13) GD12-15: 1.554 ± 0.213 (6), nsd	
					Small intestine length (mm)	NP: 1135 ± 83 (13) GD12-15: 1140 ± 27 (6), nsd	
					Duodenal villus height (µm)	NP: 456 ± 32 (13) GD12-15: 511 ± 42 (6), P<0.05	
					Duodenal smooth muscle thickness (µm)	Circular	NP: 41 ± 11 (13) GD12-15: 42 ± 7 (6), nsd
						Longitudinal	NP: 29 ± 7 (13) GD12-15: 30 ± 5 (6), nsd
					Ileal villus height (µm)	NP: 374 ± 58 (13) GD12-15: 428 ± 47 (6), nsd	
					Ileal smooth muscle thickness (µm)	Circular	NP: 33 ± 7 (13) GD12-15: 39 ± 12 (6), nsd
Longitudinal	NP: 27 ± 7 (13) GD12-15: 27 ± 12 (6), nsd						
Leucine absorption	(µmol·h ⁻¹)	NP: 328.4 ± 32 (9)					

						GD12-15: 352.4 ± 42.6 (6), nsd
					(mm)	NP: 0.294 ± 0.039 (9) GD12-15: 0.310 ± 0.042 (6), nsd
					(g-wet weight ⁻¹)	NP: 47.54 ± 6.7 (9) GD12-15: 47.30 ± 4.07 (6), nsd
					(g-dry weight ⁻¹)	NP: 235.1 ± 38.4 (9) GD12-15: 229.3 ± 35.3 (6), nsd
				Glucose absorption	(μmol·h ⁻¹)	NP: 377.1 ± 43.2 (9) GD12-15: 413.2 ± 62.2 (6), nsd
					(mm)	NP: 0.337 ± 0.051 (9) GD12-15: 0.364 ± 0.061 (6), nsd
					(g-wet weight ⁻¹)	NP: 54.89 ± 10.20 (9) GD12-15: 55.25 ± 4.58 (6), nsd
					(g-dry weight ⁻¹)	NP: 270.9 ± 51.0 (9) GD12-15 270.0 ± 33.8 (6), nsd

Datta 1974; mouse (Alderley Park); non- rand exp [318]	N/S	Fasted for 24 h before intestinal propulsion study. N/S for isolated ileum studies.	NP, GD11- 19 (21 d)	Gastric emptying/SI motility	Intestinal transit (% of tract traversed after 15 min)	NP: 46.0 ± 10.6 (28) GD11-19: 26.6 ± 7.6 (13), P<0.001
					Log EC ₅₀ for ileal response to acetylcholine stimulation (ng·ml ⁻¹)	NP: 1.399 ± 0.383 (10-30) GD11-19: 1.870 ± 0.263 (10-30), P<0.001
					Log EC ₅₀ for ileal response to potassium stimulation (ng·ml ⁻¹)	NP: 1.853 ± 0.241 (10-30) GD11-19: 0.183 ± 0.225 (10-30), P<0.001
					Log Hz ₅₀ for ileal response to electrical stimulation	NP: 0.642 ± 0.285 (10-30) GD11-19: 0.820 ± 0.268 (10-30), P<0.05
					Slope of log concentration-response relationship for acetylcholine (log ng·ml ⁻¹)	NP: 50.9 ± 11.5 (10-30) GD11-19: 79.2 ± 39.9 (10-30), P<0.01
					Slope of log concentration-response relationship for potassium (log ng·ml ⁻¹)	NP: 110.34 ± 67.59 (10-30) GD11-19: 117.32 ± 41.90 (10-30), nsd
					Slope of log concentration-response relationship for electrical stimulation (log Hz)	NP: 85.18 ± 35.82 (10-30) GD11-19: 80.86 ± 24.05 (10-30), nsd

Datta 1984; rat (Charles-Foster); non-rand exp [308]	N/S	Fasted 18-20 h before start of experiment, allowed free access to water	NP, GD20 (21 d)	Gastric emptying/SI motility	Gastric emptying (% release after 15 min)	NP: 76.99 ± 2.94 (7) GD20: 50.21 ± 2.74 (6), P<0.001	
					Intestinal transit (% travelled after 15 min)	NP: 65.52 ± 6.59 (7) GD20: 44.19 ± 5.13 (7), P<0.001	
Davies 1977; rat (Hooded Lister); non-rand exp [256]	Stock colony diet (Oxoid, H. C. Styles, Bewdley, Worcs); 100 mg/kg Zn, 20 mg/kg Cu	Ad lib	NP, GD12, GD15, GD18, GD21 (21 d)	Direct measure of nutrient uptake – in vivo	Duodenal Zn absorption	($\mu\text{g}\cdot 15\text{ min}^{-1}\cdot \text{loop}^{-1}$)	NP: 0.40 ± 0.11 (5) GD12: 0.37 ± 0.04 (5), nsd GD15: 0.47 ± 0.12 (4), nsd GD18: 0.55 ± 0.12 (6), P<0.01 GD21: 0.72 ± 0.11 (5), P<0.001
						($\mu\text{g}\cdot 15\text{ min}^{-1}\cdot \text{g}^{-1}$ dry wt tissue)	NP: 1.44 ± 0.47 (6) GD12: 1.16 ± 0.09 (5), nsd GD15: 1.60 ± 0.50 (4), nsd GD18: 1.55 ± 0.22 (6), nsd GD21: 2.43 ± 0.49 (5), P<0.001
					Duodenal lysine uptake	($\mu\text{g}\cdot 15\text{ min}^{-1}\cdot \text{loop}^{-1}$)	NP: 12.5 ± 0.51 (6) GD12: 12.6 ± 0.45 (5), nsd GD15: 12.5 ± 0.80 (4), nsd GD18: 13.1 ± 0.49 (6), nsd GD21: 11.6 ± 1.34 (5), nsd
						($\mu\text{g}\cdot 15\text{ min}^{-1}\cdot \text{g}^{-1}$ dry wt tissue)	NP: 44.3 ± 5.90 (6) GD12: 40.1 ± 2.95 (5), nsd GD15: 42.0 ± 5.60 (4), nsd GD18: 37.9 ± 4.41 (6), nsd

						GD21: 40.6 ± 6.73 (5), nsd
Davison 1970; human; cross sectional [297]	N/S	N/S	NP, ≥34 weeks (280 d)	Gastric emptying/SI motility	Gastric emptying half time (min)	NP: 11.2 ± 5.0 (11) ≥34 weeks: 17.75 ± 9.6 (11), nsd
					Gastric total emptying time (min)	NP: 74.8 ± 28.2 (11) ≥34 weeks: 119.5 ± 57.0 (11), P<0.05
Dawson 2012; mouse (CD1); rand exp [398]	Standard rodent chow (AIN93G; Glen Forrest Stockfeed); 46.6 mg/kg potassium sulfate, 0.275 mg/kg chromium potassium sulfate, L- cystine (3000 g/kg)	Ad lib	NP, GD4.5, GD6.5, GD8.5, GD10.5, GD14.5, GD18.5 (21 d)	Nutrient transporter gene expression	Ileal <i>Slc13a1</i> gene expression (relative to 18S rRNA)	NP: 38 ± 4 (3-5) GD4.5: 32 ± 5.5 (3-5), nsd GD6.5: 27 ± 1.625 (3-5), nsd GD8.5: 30 ± 3 (3-5), nsd GD10.5: 23 ± 6.25 (3-5), nsd GD14.5: 22.5 ± 1.75 (3-5), nsd GD18.5: 32 ± 1.75 (3-5), nsd
					Ileal <i>Slc26a1</i> gene expression (relative to 18S rRNA)	NP: 0.1 ± 0(3-5) GD4.5: 0.1 ± 0 (3-5), nsd GD6.5: 0 ± 0.025 (3-5), nsd GD8.5: 0.1 ± 0.025 (3-5), nsd GD10.5: 0.1 ± 0.025 (3-5), nsd GD14.5: 0 ± 0 (3-5), nsd GD18.5: 0 ± 0 (3-5), nsd
					Ileal <i>Slc26a2</i> gene expression (relative to 18S rRNA)	NP: 14.5 ± 2 (3-5) GD4.5: 13 ± 1.625 (3-5), nsd GD6.5: 14 ± 2 (3-5), nsd GD8.5: 12 ± 0.325 (3-5), nsd GD10.5: 12 ± 1.25 (3-5), nsd GD14.5: 10 ± 1.25 (3-5), nsd GD18.5: 14 ± 0.625 (3-5), nsd

					Ileal <i>Slc26a3</i> gene expression (relative to 18S rRNA)	<p>NP: 8 ± 1.25 (3-5)</p> <p>GD4.5: 6.5 ± 0.875 (3-5), nsd</p> <p>GD6.5: 6 ± 0.325 (3-5), P<0.05</p> <p>GD8.5: 5.5 ± 0.325 (3-5), P<0.05</p> <p>GD10.5: 6.25 ± 0.5 (3-5), nsd</p> <p>GD14.5: 5 ± 1.125 (3-5), P<0.01</p> <p>GD18.5: 7.5 ± 0.25 (3-5), nsd</p>
					Ileal <i>Slc26a6</i> gene expression (relative to 18S rRNA)	<p>NP: 8.25 ± 0.15 (3-5)</p> <p>GD4.5: 5.25 ± 0.1875 (3-5), P<0.05</p> <p>GD6.5: 6.75 ± 0.65 (3-5), nsd</p> <p>GD8.5: 6.0 ± 0.55 (3-5), nsd</p> <p>GD10.5: 7.25 ± 0.7 (3-5), nsd</p> <p>GD14.5: 4.5 ± 0.75 (3-5), P<0.05</p> <p>GD18.5: 6.75 ± 0.375 (3-5), nsd</p>
					Ileal <i>Slc26a11</i> gene expression (relative to 18S rRNA)	<p>NP: 0.4 ± 0.025 (3-5)</p> <p>GD4.5: 0.4 ± 0.1 (3-5), nsd</p> <p>GD6.5: 0.3 ± 0.05 (3-5), nsd</p> <p>GD8.5: 0.1 ± 0.075 (3-5), nsd</p> <p>GD10.5: 0.3 ± 0.05 (3-5), nsd</p> <p>GD14.5: 0.3 ± 0.075 (3-5), nsd</p> <p>GD18.5: 0.2 ± 0.1 (3-5), nsd</p>
Delorme 1979; rat (Wistar); non-rand exp [399]	UAR-103, 0.9% Ca, 0.9% P, 4000 IU vitamin D ₃ /kg	Ad lib	GD17.5, GD18.5, GD19.5, GD20.5, GD21.5 (22 d)	Nutrient transporter protein expression	Ca-binding protein in duodenal mucosa ($\mu\text{g}\cdot\text{mg}^{-1}$ protein)	<p>GD17.5: 4.0 ± 1.2 (4-6)</p> <p>GD18.5: 6.0 ± 2.5 (4-6), nsd vs GD17.5</p> <p>GD19.5: 9.0 ± 2.5 (4-6), P<0.05 vs GD17.5</p> <p>GD20.5: 7.0 ± 2.0 (4-6), nsd vs GD17.5</p> <p>GD21.5: 7.4 ± 2.9 (4-6), nsd vs GD17.5</p>

Doguer 2017; mouse (C57BL/6); non-rand exp [400]	N/S	Fasted 15- 16 h before iron absorption studies	NP, GD18-20 (21 d)	Direct measure of nutrient uptake – in vivo	Iron absorption (% of dose administered)	NP: 31.23 ± 13.37 (5) GD18-20: 47 ± 10 (5), N/S
Donangelo 2005; human; cross sectional [283]	EP: Energy 1910 +/- 660 (kcal/d), Protein (g/d) 69 +/- 30, Zinc (mg/d) 9 +/- 5, Iron (mg/d) 13 +/- 6, Dietary fibre (g/d) 20 +/- 9 LP: Energy 2130 +/- 400 (kcal/d), Protein (g/d) 79 +/- 26, Zinc (mg/d) 9 +/- 2, Iron (mg/d) 14 +/- 5, Dietary fibre (g/d) 22 +/- 8	N/S	10-12 weeks, 34-36 weeks (280 d)	Direct measure of nutrient uptake – in vivo	Fractional Zn absorption	10-12 weeks: 0.29 ± 0.06 (10) 34-36 weeks: 0.43 ± 0.10 (8), P<0.05 vs 10-12 weeks
Dudley 1992; rat (strain N/S); non- rand exp [401]	Purina Rodent Laboratory Chow (5001)	N/S	NP, GD20 (term N/S)	Jejunal anatomy, Digestive enzyme activity/ expression	Jejunal lactase specific activity ($\mu\text{mol}\cdot\text{min}^{-1}\cdot\text{g}^{-1}$ protein)	NP: 33 ± 8 (4) GD20: 34 ± 10 (4), nsd
					Jejunal villous length (μm)	NP: 244 ± 42 (4) GD20: 263 ± 12 (4), P<0.05
					Jejunal IF intensity (scale 0-4+), anti-lactase Mab	NP: 1.3 ± 0.8 (4) GD20: 2.9 ± 0.8 (4), nsd

Dugas 1970; rat (Holtzman); non-rand exp [402]	Purina Lab Chow	Ad lib	NP, GD7, GD14, GD21 (21 d)	Direct measure of nutrient uptake – ex vivo, Whole SI anatomy	SI length (cm)	NP: 113 ± 7.2 (36) GD7: 114 ± 6.0 (16), nsd GD14: 113 ± 9.3 (15), nsd GD21: 122 ± 6.7 (14), nsd
					SI length (cm·100 g ⁻¹ body weight)	NP: 49.7 ± 5.4 (36) GD7: 51.0 ± 3.2 (16), nsd GD14: 45.1 ± 3.5 (15), nsd GD21: 36.4 ± 3.0 (14), nsd
					Serosal accumulation of alanine (μmol·g ⁻¹ dry SI weight)	NP: 5.89 ± 2.08 (12) GD7: 6.83 ± 2.70 (9), nsd GD14: 5.89 ± 2.55 (8), nsd GD21: 6.52 ± 2.42 (12), nsd
					Serosal accumulation of lysine (μmol·g ⁻¹ dry SI weight)	NP: 2.63 ± 1.47 (24) GD7: 5.60 ± 2.40 (9), P<0.01 GD14: 2.39 ± 1.16 (15), nsd GD21: 1.90 ± 0.90 (9), nsd
					Serosal accumulation of proline (μmol·g ⁻¹ dry SI weight)	NP: 3.37 ± 2.42 (12) GD7: 1.95 ± 1.50 (9), nsd GD14: 3.03 ± 1.41 (8), nsd GD21: 1.62 ± 2.08 (12), nsd

Everson 1982; human; cross sectional [370]	Breakfast consisted of one egg, two slices of bacon, two pieces of buttered toast, 100 ml orange juice, 240 ml low fat milk, and 200 ml of coffee or tea (610 kcal, 12% protein, 44% fat).	Evening before study: ½ turkey sandwich, 250 ml whole milk, then overnight fast. Diet on study day: 2228 cal, 15% protein, 46% fat; ate at 0830h, 1200 h, 1700 h, 2000 PM.	NP, 1 st Tri, 2 nd Tri, 3 rd Tri (280 d)	Gallbladder emptying	Gallbladder fasting volume (ml)	NP: 17.2 ± 5.2 (22) 1 st Tri: 23.7 ± 6.3 (7), P<0.04 2 nd Tri: 33.7 ± 9.0 (10), P<0.001 3 rd Tri: 32.4 ± 9.0 (8), P<0.001
					Early rate constant of emptying (min ⁻¹)	NP: 0.022 ± 0.003 (22) 1 st Tri: 0.025 ± 0.006 (7), nsd 2 nd Tri: 0.026 ± 0.005 (10), nsd 3 rd Tri: 0.018 ± 0.003 (8), nsd
					Late rate constant of emptying (min ⁻¹)	NP: 0.009 ± 0.002 (22) 1 st Tri: 0.007 ± 0.002 (7), nsd 2 nd Tri: 0.005 ± 0.002 (10), nsd 3 rd Tri: 0.004 ± 0.002 (8), P<0.005
					Gallbladder emptying (%)	NP: 74.1 ± 12.2 (22) 1 st Tri: 71.8 ± 7.2 (7), nsd 2 nd Tri: 70.8 ± 12.3 (10), nsd 3 rd Tri: 67.0 ± 6.6 (8), nsd
Fairweather-Tait 1984; rat (Wistar); non-rand exp [403]	Synthetic diet (g/kg): 326 starch, 326 sucrose, 168 casein, 80 maize oil, 40 solka floc, 40 mineral mix, 20 vitamin mix	Ad lib, overnight fast prior to each Zn absorption study	NP, GD3, GD10, GD17 (22 d)	Direct measure of nutrient uptake – in vivo	⁶⁵ Zn retention (% of administered dose)	NP: 0.188 ± 0.042 (17) GD3: 0.224 ± 0.045 (19), nsd GD10: 0.182 ± 0.045 (19), nsd GD17: 0.208 ± 0.045 (19), P<0.01

Fudge 2010; mouse (Black Swiss); non-rand exp [225]	2% calcium, 1.25% phosphorus, 20% lactose (TekLad TD96348; Harlan Tek-lad, Madison, WI)	N/S	NP, GD16.5 (19 d)	Nutrient transporter gene expression	Duodenal <i>Trpv6</i> , microarray (fold-expression relative to NP)	NP: 1 (2) GD16.5: 0.33 (2), P<0.01
					Duodenal <i>Pmca1</i> , microarray (fold-expression relative to NP)	NP: 1 (2) GD16.5: 0.96 (2), nsd
					Duodenal <i>S100g</i> , microarray (fold-expression relative to NP)	NP: 1 (2) GD16.5: 0.78 (2), nsd
					Duodenal <i>Trpv6</i> , RT-PCR (fold-expression relative to GAPDH and NP)	NP: 1.0 ± 0.4 (3) GD16.5: 0.2 ± 0.4 (3), P<0.05
Fung 1997; human; prosp. cohort [284]	Non-vegetarian	Overnight fast before Zn absorption studies	NP, 24-26 weeks, 34-36 weeks (280 d)	Direct measure of nutrient uptake – in vivo	Fractional Zn absorption (%)	NP: 14.6 ± 4.7 (13) 24-26 weeks: 18.9 ± 8.3 (13), nsd 34-36 weeks: 19.4 ± 9.4 (13), nsd
Gallagher 1982; rat (Wistar); non-rand exp [404]	N/S	Fasted for 16 h before tissue collection	NP, GD18-19 (22 d)	Nutrient transporter protein expression	IF- ⁵⁷ CoCbl binding to ileal brush borders (pg·mg ⁻¹ protein)	NP: 126.3 ± 58.4 (10) GD18-19: 270.8 ± 69.2 (12), P<0.01
					Number of ileal brush border IF-Cbl receptors	NP: 7.2 x 10 ¹⁰ (10) GD18-19: 16 x 10 ¹⁰ (12), different (text)
					Affinity constant of ileal brush border IF-Cbl receptors	NP: 11.7 x 10 ¹¹ mol ⁻¹ (10) GD18-19: 6.9 x 10 ¹¹ mol ⁻¹ (12), different (text)

Gao 2015; rat (Sprague-Dawley); non-rand exp [364]	Standard rodent pellet diet (370 mg iron/kg)	N/S	NP, GD9, GD15, GD18, GD21 (22 d)	Nutrient transporter protein expression	Duodenal FPN1 protein (relative to beta-actin)	NP: 1.0 ± 0.05 (12) GD9: 0.8 ± 0.15 (12), nsd GD15: 1.4 ± 0.20 (12), $P < 0.05$ GD18: 2.5 ± 0.02 (12), $P < 0.01$ GD21: 2.1 ± 0.15 (12), $P < 0.01$	
Gębczyńska 1971; Root vole (<i>Microtus oeconomus</i>); cross sectional [334]	N/S	N/S	NP, Pregnant (20-22 d)	Whole SI anatomy	SI length (mm)	Spring-caught	NP: 215 ± 28 Pregnant: 216 ± 13 , N/S
						Summer-caught	NP: 248 ± 17 Pregnant: 248 ± 25 , N/S
					Empty SI weight (g)	Spring-caught	NP: 73 ± 16 Pregnant: 83 ± 15 , N/S
						Summer-caught	NP: 96 ± 10 Pregnant: 98 ± 16 , N/S

Gerdes 1938; human; cross sectional [369]	Evening before study: tea & toast.	Test meal: 4 egg yolks mixed w/ equal amt milk	1 st Tri, combined 2 nd & 3 rd Tri (280 d)	Gallbladder emptying	Basal gallbladder volume, 2 min after test meal (cm ³)	1 st Tri: 56.1 ± 36.2 (5) 2 nd -3 rd Tri: 41.2 ± 16.0 (13), N/S	
					Gallbladder emptying after test meal (%)	8 min	1 st trimester: 16.3 ± 11.4 (5) 2 nd -3 rd trimester: 8.2 ± 10.4 (13), P<0.05 vs 1 st trimester
						12 min	1 st trimester: 32.5 ± 19.4 (5) 2 nd -3 rd trimester: 14.0 ± 15.1 (13), P<0.05 vs 1 st trimester
						20 min	1 st trimester: 52.3 ± 13.1 (5) 2 nd -3 rd trimester: 28.0 ± 21.2 (13), P<0.05 vs 1 st trimester
						30 min	1 st trimester: 62.9 ± 6.3 (5) 2 nd -3 rd trimester: 42.1 ± 21.1 (13), P<0.05 vs 1 st trimester
						40 min	1 st trimester: 69.7 ± 10.2 (5) 2 nd -3 rd trimester: 49.3 ± 18.2 (13), P<0.05 vs 1 st trimester
Gillmer 1975; human; prosp. cohort [240]	Day before study: fed 180 g/d carbohydrate	Fasted overnight before OGTT	12-22 weeks, 32- 35 weeks (280 d)	Direct measure of nutrient uptake – in vivo	Plasma glucose before and after 50 g glucose OGTT (mmol·L ⁻¹)	Fasting	12-22 weeks: 4.4 ± 0.4 (9) 32-35 weeks: 4.2 ± 0.2 (9), N/S
						30 min	12-22 weeks: 7.0 ± 0.7 (9) 32-35 weeks: 6.6 ± 0.7 (9), N/S
						60 min	12-22 weeks: 7.3 ± 0.8 (9) 32-35 weeks: 7.0 ± 0.8 (9), N/S

Girdwood 1961; human; cross sectional [290]	N/S	N/S	NP, Pregnant (280 d)	Direct measure of nutrient uptake – in vivo	Serum folic acid after 3 mg oral folic acid ($\mu\text{g}\cdot\text{mL}^{-1}$)	60 min	NP: 87.5 (23) Pregnant: 55.1 (21), N/S
						90 min	NP: 100 (23) Pregnant: 60 (21), N/S
					Time to peak serum [folic acid] after 3 mg oral folic acid (min)	NP: 107.9 \pm 41.5 (23) Pregnant: 63.19 \pm 45.6 (21), N/S	
Gohir 2019; mouse (C57BL/6); non-rand exp [405]	17% fat, 29% protein, 54% carbohydrate, 3.40 kcal (HT8640 Teklad 22/5 Rodent Diet; Harlan, Indianapolis, IN, USA)	Ad lib	NP, GD18.5 (21 d)	Whole SI anatomy	Plasma FITC-dextran (Maternal intestinal barrier functional integrity), RFU $\times 10^4$	NP: 0.15 \pm 0.15 (6) GD18.5: 0.45 \pm 1.0 (14), P<0.05	

Hagen 1961; human; prosp cohort [241]	N/S	N/S	3 months, 5 months, 7 months, 9 months (280 d)	Direct measure of nutrient uptake – in vivo	Blood sugar after 1 g glucose.kg ⁻¹ OGTT (mg·100 ml ⁻¹)	Fasting	3 rd month: 88.4 (28) 5 th month: 89.5 (28), N/S 7 th month: 83.1 (28), P<0.05 vs other pregnancy stages 9 th month: 89.6 (28), N/S
						20 min	3 rd month: 137.6 (28) 5 th month: 131.5 (28), N/S 7 th month: 125.9 (28), N/S 9 th month: 127.0 (28), N/S
						40 min	3 rd month: 149.3 (28) 5 th month: 146.7 (28), N/S 7 th month: 151.9 (28), N/S 9 th month: 145.9 (28), N/S
						60 min	3 rd month: 139.7 (28) 5 th month: 144.3 (28), N/S 7 th month: 152.9 (28), N/S 9 th month: 145.6 (28), N/S
Halloran 1980; rat (Holtzman); non-rand exp [269]	Purified diet: 0.44% Ca, 0.30% P, plus 25 IU vitamin D/day in 0.1 ml cottonseed-soybean oil (Wesson).	N/S	NP, GD20 (21 d)	Direct measure of nutrient uptake – ex vivo	Duodenal calcium transport ratio (serosal:mucosal [Ca] ratio)	NP: 3.1 ± 1.1 (5) GD20: 5.9 ± 1.3 (5), P<0.001	
Hambidge 2017; human; prosp cohort [282]	Major food staple maize	N/S	8 weeks, 34 weeks (280 d)	Direct measure of nutrient uptake – in vivo	Fractional Zn absorption	8 weeks: 0.22 ± 0.10 (8) 34 weeks: 0.32 ± 0.15 (8), P=0.0008 vs 8 weeks	
					Total absorbed zinc (mg·d ⁻¹)	8 weeks: 1.87 ± 0.70 (8) 34 weeks: 3.12 ± 1.37 (8), P<0.05 vs 8 weeks	

Hellegers 1957; rat (Sprague- Dawley); non- rand exp [286]	Basic casein diet	N/S	NP, GD12- 20 (22 d)	Direct measure of nutrient uptake – in vivo	Vitamin B ₁₂ absorption (μg of 50 μg dose)	NP: 20 (14) GD12-20: 40.2 (14), $P < 0.05$	
Hirst Bruns 1978; rat (Sprague- Dawley); non- rand exp [367]	Normal rat chow (Ralston Purina, St Louis)	Ad lib	NP, GD13, GD15, GD16, GD18, GD19, GD20.5 (22 d)	Nutrient transporter protein expression	Calcium binding protein in proximal duodenal mucosa ($\mu\text{g CaBP}\cdot\text{mg}^{-1}$ protein)	NP: 3.3 ± 1.3 (20) GD13: 2.8 ± 0.5 (3-7), nsd GD15: 4.2 ± 1.3 (3-7), nsd GD16: 4.4 ± 2.1 (3-7), nsd GD18: 5.2 ± 2.1 (3-7), $P < 0.05$ GD19: 4.8 ± 2.1 (3-7), $P < 0.05$ GD20.5: 4.9 ± 1.3 (11), $P < 0.05$	
Hornes 1984; human; prosp cohort [242]	Normal diet	N/S	15 \pm 1 weeks, 28 \pm 1 weeks, 37 \pm 0 weeks (280 d)	Direct measure of nutrient uptake – in vivo	Change in plasma glucose after 50 g glucose OGTT ($\text{mmol}\cdot\text{L}^{-1}$)	15 min	15 \pm 1 weeks: 1.2 (17) 28 \pm 1 weeks: 1.1 (17), N/S 37 weeks: 0.9 (17), N/S
						30 min	15 \pm 1 weeks: 2.3 (17) 28 \pm 1 weeks: 2.6 (17), N/S 37 weeks: 2.8 (17), N/S
						45 min	15 \pm 1 weeks: 2.2 (17) 28 \pm 1 weeks: 3.9 (17), N/S 37 weeks: 3.6 (17), N/S
						60 min	15 \pm 1 weeks: 1.7 (17) 28 \pm 1 weeks: 1.8 (17), N/S 37 weeks: 3.9 (17), N/S

Hunt 1958; human; prosp cohort [293]	Test meal containing phenol red marker	Fasted overnight before each study	16-25 weeks, 26- 30 weeks, 31-35 weeks, 35- 40 weeks (280 d)	Gastric emptying/SI motility	Gastric volume 10 minutes after a 750 ml saline test meal (mL)	16-25 weeks: 407 ± 107 (6) 26-30 weeks: 345 ± 130 (6), N/S 31-35 weeks: 345 ± 175 (6), N/S 35-40 weeks: 330 ± 85 (7), lower than 16-25 weeks (text)	
					Gastric volume 20 minutes after a 750 ml water test meal (mL)	16-25 weeks: 325 ± 122 (6) 26-30 weeks: 393 ± 73 (6), N/S 31-35 weeks: 378 ± 98 (6), N/S 35-40 weeks: 363 ± 68 (7), N/S	
Ibrahim 1984; rat (strain N/S); non- rand exp [270]	Purina Rodent Laboratory Chow (Ralston Purina Co., St. Louis, Mo.) w. 1.2% Ca, 0.2% Mg, 0.8% P	Ad lib	NP, GD21 (22 d)	Direct measure of nutrient uptake – ex vivo	SI calcium transport ratio (serosal/mucosal ⁴⁵ Ca ratio), proximal duodenum	NP: 1.5 ± 0.5 (5-7) GD21: 3.0 ± 0.8 (5-7), P<0.001	
Jaroszewska 2006; common shrew (<i>Sorex araneus</i>); cross sectional [335]	N/S	N/S	NP, first 2 weeks, 3 rd week (20 d)	Whole SI anatomy, Duodenal anatomy	Duodenum length (mm)	NP: 5.9 ± 0.5 (5) First 2 weeks: 7.0 ± 0.6 (7), nsd 3 rd week: 8.2 ± 2.1 (7), P=0.05	
					Mesenteric SI (jejunum+ileum) length (mm)	NP: 94.5 ± 11.1 (5) First 2 weeks: 98.0 ± 15.6 (7), nsd 3 rd week: 103.1 ± 33.1 (7), nsd	
					Height of villi (µm)	Duodenum	NP: 415.6 ± 68.5 (5) First 2 weeks: 428.7 ± 90.5 (7), nsd 3 rd week: 410.6 ± 58.6 (7), nsd
Proximal mesenteric intestine	NP: 442.5 ± 62.7 (5) First 2 weeks: 415.8 ± 26.7 (7), nsd 3 rd week: 499.8 ± 42.9 (7), P<0.05						

					Middle mesenteric intestine	NP: 358.5 ± 34.3 (5) First 2 weeks: 380.8 ± 44.5 (7), nsd 3 rd week: 398.3 ± 64.6 (7), nsd
					Distal mesenteric intestine	NP: 355.8 ± 12.6 (5) First 2 weeks: 308.7 ± 38.7 (7), nsd 3 rd week: 297.8 ± 36.2 (7), nsd
				External area (mm ²)	Duodenum	NP: 53.3 ± 15.8 (5) First 2 weeks: 63.1 ± 8.0 (7), nsd 3 rd week: 87.1 ± 28.2 (7), nsd
					Proximal mesenteric intestine	NP: 279.9 ± 54.4 (5) First 2 weeks: 271.0 ± 60.7 (7), nsd 3 rd week: 348.8 ± 95.3 (7), nsd
					Middle mesenteric intestine	NP: 258.9 ± 72.9 (5) First 2 weeks: 260.9 ± 35.6 (7), nsd 3 rd week: 285.8 ± 79.2 (7), nsd
					Distal mesenteric intestine	NP: 253.1 ± 45.8 (5) First 2 weeks: 240.6 ± 60.7 (7), nsd 3 rd week: 263.2 ± 88.4 (7), nsd
				Total internal area (mm ²)	Duodenum	NP: 554.7 ± 154.9 (5) First 2 weeks: 394.7 ± 61.8 (7), nsd 3 rd week: 786.4 ± 127.9 (7), nsd
					Proximal mesenteric intestine	NP: 2213.2 ± 823.2 (5) First 2 weeks: 2221.4 ± 726.6 (7), nsd 3 rd week: 3293.5 ± 1235.4 (7), nsd
					Middle mesenteric intestine	NP: 2216.4 ± 705.1 (5) First 2 weeks: 2092.9 ± 232.9 (7), nsd 3 rd week: 2368.8 ± 728.4 (7), nsd

						Distal mesenteric intestine	NP: 1842.6 ± 541.4 (5) First 2 weeks: 1895.9 ± 625.3 (7), nsd 3 rd week: 1853.6 ± 514.1 (7), nsd
				Total internal area/length of segment (mm ² ·mm ⁻¹)		Duodenum	NP: 94.5 ± 23.5 (5) First 2 weeks: 57.1 ± 8.0 (7), nsd 3 rd week: 85.8 ± 21.3 (7), nsd
						Proximal mesenteric intestine	NP: 73.5 ± 28.4 (5) First 2 weeks: 68.9 ± 15.1 (7), nsd 3 rd week: 91.9 ± 21.6 (7), nsd
						Middle mesenteric intestine	NP: 73.9 ± 24.1 (5) First 2 weeks: 67.1 ± 9.6 (7), nsd 3 rd week: 71.9 ± 18.1 (7), nsd
						Distal mesenteric intestine	NP: 60.2 ± 19.4 (5) First 2 weeks: 61.3 ± 12.3 (7), nsd 3 rd week: 59.6 ± 8.2 (7), nsd
						Duodenum	NP: 66.5 ± 21.4 (5) First 2 weeks: 41.8 ± 4.4 (7), nsd 3 rd week: 78.2 ± 21.1 (7), nsd
				Total internal area/body mass (mm ² ·g ⁻¹)		Proximal mesenteric intestine	NP: 267.8 ± 101.9 (5) First 2 weeks: 245.4 ± 91.2 (7), nsd 3 rd week: 332.7 ± 148.3 (7), nsd
						Middle mesenteric intestine	NP: 254.5 ± 90.9 (5) First 2 weeks: 228.8 ± 29.4 (7), nsd 3 rd week: 242.7 ± 67.2 (7), nsd
						Distal mesenteric intestine	NP: 221.2 ± 60.9 (5) First 2 weeks: 215.4 ± 80.1 (7), nsd 3 rd week: 188.1 ± 40.7 (7), nsd

					Internal surface area of whole small intestine (mm ²)	NP: 6826.6 ± 1007.7 (5) First 2 weeks: 6598.9 ± 1284.3 (7), nsd 3 rd week: 8302.2 ± 1690.4 (7), nsd
Johnson 2019; rat (Wistar); non-rand exp [234]	Standard rodent breeding diet (801730, Special Diets Service Essex, UK)	Ad lib	NP, GD4, GD12, GD18 (22 d)	Whole SI anatomy, Duodenal anatomy	SI wet mass (g)	GD4: 5.4 ± 1.3 (7) GD12: 6.0 ± 2.1 (7), P<0.05 vs GD4 GD18: 6.3 ± 1.3 (7), P<0.05 vs GD4
					SI length (cm)	NP: 70 (6) GD4: 73 ± 2.6 (7), P<0.05 GD12: 76 ± 2.6 (7), P<0.05 GD18: 82 ± 2 (7), P<0.05
					Duodenal circumference (mm)	NP: 8.4 (6) GD4: 11.3 ± 2.1 (7), P<0.001 GD12: 10.7 ± 4.0 (7), nsd GD18: 10.8 ± 1.3 (7), nsd
Jolicoeur 1981; rat (Sprague-Dawley); rand exp [344]	N/S	Fasted overnight before tissue collection	NP, GD7, GD14, GD21 (22 d)	Duodenal anatomy, Digestive enzyme activity/ expression	Duodenum weight (mg)	NP: 319.7 ± 94.3 (41) GD7: 375.9 ± 47.1 (11), P<0.05 GD14: 421.3 ± 44 (12), P<0.001 GD21: 439.5 ± 63.9 (10), P<0.001
					Duodenal total protein content (mg)	NP: 40.5 ± 7.9 (41) GD7: 44.1 ± 6.0 (11), P<0.01 GD14: 51.9 ± 8.7 (12), P<0.001 GD21: 52.9 ± 7.6 (10), P<0.001
					Duodenal total maltase activity (U)	NP: 1.5 ± 0.7 (41) GD7: 2.0 ± 1.0 (11), nsd GD14: 1.4 ± 0.7 (12), nsd GD21: 1.0 ± 0.3 (10), P<0.05

Kent 1991; human; cross sectional [261]	N/S	Fasted overnight before study	NP, 36 weeks (280 d)	Direct measure of nutrient uptake – in vivo	Fractional calcium absorption (%)	NP: 58.7 ± 11.7 (26) 36 weeks: 72.5 ± 11.9 (49), P<0.001
Kern 1981; human; cross sectional [371]	Asked to follow a standard diet containing 500 mg/d of cholesterol without other restrictions 1 week before being studied	N/S	NP, 1 st Tri, 2 nd Tri, 3 rd Tri (280 d)	Gallbladder emptying	Bile acid secretion ($\mu\text{mol}\cdot\text{kg}^{-1}\cdot\text{h}^{-1}$)	NP: 19.1 ± 5.2 (16) All pregnant combined: 18.4 ± 6.4 (18), nsd 1 st Tri: 19.3 ± 6.5 (8), nsd 2 nd Tri: 16.7 ± 4.5 (9), nsd 3 rd Tri: 19.1 ± 9.0 (9), nsd
					Indices of gallbladder function, b (rate constant of emptying)	NP: 0.041 ± 0.017 (8) All pregnant combined: 0.022 ± 0.008 (8), P<0.02
					Gallbladder fasting volume (ml)	NP: 18.5 ± 5 (8) All pregnant combined: 21.3 ± 6 (8), nsd
					Gallbladder residual volume (ml)	NP: 6.1 ± 3 (8) All pregnant combined: 7.6 ± 4 (8), nsd
					Gallbladder emptying (%)	NP: 68.1 ± 12.7 (8) All pregnant combined: 61.3 ± 11.3 (8), nsd

Kirksey 1967; rat (Sprague-Dawley); non-rand exp [346]	26% casein, 18.85% sucrose-vitamin mix, 34% cornstarch, 10% fat, 5% corn oil, 4% Jones-Foster salt mix, 2% agar, 0.15% L-cystine, 0.8 % pyridoxine	Ad lib	NP, GD21 (22 d)	Duodenal anatomy	Duodenum weight (g·20 cm ⁻¹)	NP: 1.12 (10) GD21: 1.25 (10), nsd
Kostial 1972; rat (Albino); non-rand exp [406]	1.2% Ca, 1.86 µg Sr, 0.8% P per 100 g dry food	N/S	NP, GD7-10, GD16-19 (21 d)	Direct measure of nutrient uptake – in vivo	⁴⁵ Ca or ⁴⁷ Ca absorption from oral dose (%)	NP: 13.8 ± 2.6 (18) GD7-10: 16.9 ± 2.3 (11), text states higher in pregnancy GD16-19: 16.4 ± 1.3 (10), text states higher in pregnancy
					Calcium absorption (mg·d ⁻¹)	NP: 26.8 ± 4.5 (18) GD7-10: 34.7 ± 4.6 (11), N/S GD16-19: 40.5 ± 3.2 (10), N/S
					⁸⁵ Sr absorption from oral dose (%)	NP: 7.3 ± 2.5 (18) GD7-10: 8.1 ± 1.0 (11), N/S GD16-19: 7.0 ± 0.6 (10), N/S
					Daily Sr absorption (µg·d ⁻¹)	NP: 21.9 ± 3.4 (18) GD7-10: 25.6 ± 3.0 (11), text states increased in pregnancy GD16-19: 26.8 ± 2.5 (10), text states increased in pregnancy

Krishnamra 1990; rat (Wistar); non- rand exp [265]	Laboratory rat pellets (F.F. Zuellig Ltd., Thailand)	Ad lib, fasted overnight prior to experiment s	NP, GD20 (22 d)	Direct measure of nutrient uptake – in vivo	Calcium absorption under anaesthesia: plasma ⁴⁵ Ca after gavage with 5 mM CaCl labelled with ⁴⁵ Ca (% administered dose)	5 min	NP: 2.2 ± 0.4 (5) GD20: 4.0 ± 2.9 (5), nsd
						10 min	NP: 2.5 ± 0.3 (5) GD20: 5.0 ± 3.8 (5), nsd
						15 min	NP: 3.1 ± 0.2 (5) GD20: 5.4 ± 1.5 (5), nsd
						30 min	NP: 3.5 ± 0.3 (5) GD20: 5.2 ± 0.9 (5), nsd
						60 min	NP: 3.1 ± 0.3 (5) GD20: 4.8 ± 0.7 (5), P<0.05
Krisinger 1992; rat (Sprague- Dawley); non- rand exp [407]	Standard diet (1% Ca, 0.61% P, 4.5 IU/g vitamin D)	Ad lib	NP, GD16, GD18, GD20 (22 d)	Nutrient transporter gene expression	<i>Calbindin</i> mRNA (AU – absolute), proximal duodenum	NP: 100 ± 29 (6) GD16: 55 ± 54 (6), nsd GD18: 52.3 ± 34 (6), P<0.05 GD20: 90 ± 50 (6), nsd	
						<i>Calbindin</i> mRNA (AU – relative to beta-actin), proximal duodenum	NP: 1 ± 0.3 (6) GD16: 1.18 ± 0.5 (6), N/S GD18: 1 ± 0.5 (6), N/S GD20: 1.4 ± 0.5 (6), N/S
Krisinger 1993; rat (Sprague- Dawley); non- rand exp [366]	Standard diet (1% Ca, 0.61% P, 4.5 IU/g vitamin D)	Ad lib	GD20, GD21, GD22 (22 d)	Nutrient transporter transcript expression	<i>Calbindin-D9K</i> mRNA (densitometric units), proximal duodenum	GD20: 95 ± 20 (6-11) GD21: 135 ± 40 (6-11), nsd vs GD20 GD22: 175 ± 15 (6-11), nsd vs GD21	

Kühl 1975; human; pregnant cohort longitudinal, non-pregnant cohort cross sectional [243]	Normal full diet	Fasted 10- 12h before test	NP, 11-19 weeks, 24-29 weeks, 32-36 weeks (280 d)	Direct measure of nutrient uptake – in vivo	Serum glucose (mmol·L ⁻¹) – after 50 g glucose OGTT	Basal	NP: 4.5 ± 1.4 (46) 11-19 weeks: 4.7 ± 0.3 (9), nsd 24-29 weeks: 4.7 ± 0.3 (9), nsd 32-36 weeks: 4.7 ± 0.3 (9), nsd
						2 min	NP: 4.5 ± 1.4 (46) 11-19 weeks: 5.0 ± 0.3 (9), nsd 24-29 weeks: 4.7 ± 0.3 (9), nsd 32-36 weeks: 4.8 ± 0.3 (9), nsd
						5 min	NP: 4.6 ± 1.4 (46) 11-19 weeks: 5.0 ± 0.3 (9), nsd 24-29 weeks: 5.0 ± 0.3 (9), nsd 32-36 weeks: 5.1 ± 0.3 (9), nsd
						10 min	NP: 5.3 ± 1.4 (46) 11-19 weeks: 5.6 ± 0.6 (9), nsd 24-29 weeks: 5.2 ± 0.3 (9), nsd 32-36 weeks: 5.4 ± 0.6 (9), nsd
						20 min	NP: 6.4 ± 2.1 (46) 11-19 weeks: 6.3 ± 0.6 (9), nsd 24-29 weeks: 6.1 ± 0.9 (9), nsd 32-36 weeks: 6.7 ± 0.9 (9), nsd
						30 min	NP: 7.0 ± 3.5 (46) 11-19 weeks: 7.2 ± 0.6 (9), nsd 24-29 weeks: 7.0 ± 1.2 (9), nsd 32-36 weeks: 7.8 ± 1.2 (9), P<0.05
						40 min	NP: 7.4 ± 3.5 (46) 11-19 weeks: 7.0 ± 0.6 (9), nsd 24-29 weeks: 7.2 ± 1.5 (9), nsd

							32-36 weeks: 8.3 ± 1.2 (9), P<0.05
						50 min	NP: 6.8 ± 3.5 (46) 11-19 weeks: 6.4 ± 0.6 (9), nsd 24-29 weeks: 7.6 ± 1.5 (9), nsd 32-36 weeks: 8.4 ± 1.2 (9), P<0.05
Landon 1972; human; prosp cohort [291]	N/S	Fasted on morning of test	10 weeks, 20 weeks, 30 weeks, 38 weeks (280 d)	Direct measure of nutrient uptake – in vivo	Plasma folate activity after 15 µg oral folic acid (ng·mL ⁻¹)	Basal	10 weeks: 8.3 ± 8.4 (12) 20 weeks: 6.1 ± 3.3 (10), N/S 30 weeks: 6.8 ± 2.7 (10), N/S 38 weeks: 5.3 ± 2.0 (9), N/S
						15 minutes	10 weeks: 9.9 ± 9.6 (12) 20 weeks: 6.5 ± 3.1 (10), N/S 30 weeks: 6.9 ± 2.9 (10), N/S 38 weeks: 6.0 ± 1.8 (9), N/S
						30 minutes	10 weeks: 15.5 ± 13.0 (12) 20 weeks: 10.4 ± 7.4 (10), N/S 30 weeks: 14.8 ± 16.5 (10), N/S 38 weeks: 11.1 ± 6.3 (9), N/S
					Change in plasma folate activity activity after 15 µg oral folic acid (ng·mL ⁻¹)	15 minutes	10 weeks: 1.5 ± 4.6 (12) 20 weeks: 0.5 ± 1.3 (10), N/S 30 weeks: 0.1 ± 1.4 (10), N/S 38 weeks: 0.7 ± 1.5 (9), N/S
						30 minutes	10 weeks: 7.1 ± 7.6 (12) 20 weeks: 4.3 ± 6.1 (10), N/S 30 weeks: 8.0 ± 15.3 (10), N/S 38 weeks: 5.7 ± 6.6 (9), N/S

Larralde 1966; rat (Wistar); non-rand exp [231]	N/S	N/S	NP, GD12-15 (22 d)	Direct measure of nutrient uptake – in vivo	Whole SI anatomy absorption of glucose from perfusate ($\mu\text{mol}\cdot\text{cm}^{-1}$)	20 mM glucose	NP: 5.0 ± 0.09 (7) GD12-15: 7.0 ± 0.4 (7), $P < 0.01$
						75 mM glucose	NP: 13.0 ± 0.02 (12) GD12-15: 16.8 ± 0.2 (10), $P < 0.01$
						150 mM glucose	NP: 20.0 ± 0.05 (9) GD12-15: 26.1 ± 0.7 (10), $P < 0.01$
						300 mM glucose	NP: 43.3 ± 0.8 (8) GD12-15: 52.1 ± 0.5 (9), $P < 0.01$
Lawson 1985; human; prosp cohort [314]	N/S	Fasted overnight before test	1 st Tri, 2 nd Tri, 3 rd Tri (280 d)	Gastric emptying/SI motility	Gastrointestinal transit time (min)	1 st Tri: 99 ± 39 (8) 2 nd Tri: 125 ± 48 (12), $P < 0.005$ vs 1 st Tri 3 rd Tri: 137 ± 58 (22), $P < 0.005$ vs 1 st Tri	
Leazer 2002; rat (Sprague- Dawley); non- rand exp [356]	Rodent chow (Teklad, Harland Sprague- Dawley, Indianapolis, IN)	Ad lib	NP, GD3, GD6, GD9, GD12, GD15, GD18, GD21 (22 d)	Nutrient transporter gene expression	Duodenal <i>Dmt1</i> mRNA (relative to total RNA)	NP: 80 ± 30 (4) GD3: 75 ± 20 (4), nsd GD6: 65 ± 30 (4), nsd GD9: 70 ± 30 (4), nsd GD12: 60 ± 15 (4), nsd GD15: 275 ± 200 (4), $P < 0.05$ GD18: 240 ± 60 (4), nsd GD21: 430 ± 300 (4), $P < 0.05$	

Lefebvre 1998; rat (Wistar); non-rand exp [309]	N/S	Fasted 24 h prior to gastric emptying studies	NP, GD6-7, GD18-20 (22 d)	Gastric emptying/SI motility	Gastric emptying of a liquid meal, 100 ml of 1.5% methylcellulose (% emptied @ 20 min)	NP: 54 ± 19 (10) GD6-7: 58 ± 20 (8), nsd GD18-20: 78 ± 21 (9), P<0.05		
					Gastric emptying of beads, 25 x 1 mm diameter polystyrene bead sin 1.5 mL saline (% emptied @ 3 h)	NP: 53 ± 40 (11) GD6-7: 36 ± 23 (8), nsd GD18-20: 70 ± 23 (8), nsd		
Levy 1994; human; cross sectional [304]	N/S	Fasted at least 4 h before test	NP, 8-12 weeks (280 d)	Gastric emptying/SI motility	Maximum [paracetamol] (µg·mL ⁻¹)	NP: 29.9 ± 11.5 (20) 8-12 weeks: 23.3 ± 7.5 (20), P<0.05		
					Time at maximum [paracetamol] (min)	NP: 48.0 ± 28.2 (20) 8-12 weeks: 69.0 ± 29.0 (20), P<0.05		
					Paracetamol appearance after 1.5 g oral paracetamol (µg·ml ⁻¹ ·min)	AUC 0-60 min	NP: 1075 ± 534 (20) 8-12 weeks: 636 ± 330 (20), P<0.01	
						AUC 0-120 min	NP: 2275 ± 743 (20) 8-12 weeks: 1172 ± 514 (20), P<0.05	

Lind 1973; human; prosp cohort [244]	N/S	Fasted at least 10 h before test	10 weeks, 20 weeks, 30 weeks, 38 weeks (280 d)	Direct measure of nutrient uptake – in vivo	Plasma glucose after 50 g glucose OGTT (mg·100 mL ⁻¹)	Fasting	10 weeks: 75.0 ± 8.3 (19) 20 weeks: 71.1 ± 7.2 (19), N/S 30 weeks: 74.3 ± 7.2 (19), N/S 38 weeks: 68.8 ± 7.7 (19), N/S
						15 min	10 weeks: 104.9 ± 14.9 (19) 20 weeks: 95.4 ± 11.4 (19), N/S 30 weeks: 101.3 ± 16.0 (19), N/S 38 weeks: 89.7 ± 12.8 (19), N/S
						30 min	10 weeks: 112.3 ± 21.5 (19) 20 weeks: 105.5 ± 18.9 (19), N/S 30 weeks: 119.1 ± 23.4 (19), N/S 38 weeks: 113.1 ± 15.5 (19), N/S
						45 min	10 weeks: 111.9 ± 24.0 (19) 20 weeks: 107.1 ± 23.8 (19), N/S 30 weeks: 122.3 ± 28.8 (19), N/S 38 weeks: 121.7 ± 20.7 (19), N/S
					Time to maximum glucose after 50 g glucose OGTT (min)	10 weeks: 33.9 ± 15.2 (19) 20 weeks: 36.9 ± 15.2 (19), N/S 30 weeks: 44.1 ± 16.3 (19), N/S 38 weeks: 54.9 ± 15.3 (19), N/S	

Liuzzi 2003; rat (Sprague- Dawley); non- rand exp [408]	Commercial diet (Teklad 8604; Harlan; 60 mg Zn/kg)	Ad lib	NP, GD15, GD20 (22 d)	Nutrient transporter gene expression, nutrient transporter protein expression	Duodenal <i>Zinc transporter</i> <i>1 (ZnT1)</i> , relative mRNA abundance	NP: 1 ± 0.5 (3) GD15: 1.6 ± 0.4 (3), nsd GD20: 2.4 ± 1.2 (3), P<0.05
					Duodenal <i>Zinc transporter</i> <i>2 (ZnT2)</i> , relative mRNA abundance	NP: 1.1 ± 0.4 (3) GD15: 2.3 ± 1 (3), nsd GD20: 3.2 ± 0.4 (3), P<0.05
					Duodenal <i>Zinc transporter</i> <i>4 (ZnT4)</i> , relative mRNA abundance	NP: 1 ± 0.4 (3) GD15: 1.2 ± 0.8 (3), nsd GD20: 1.2 ± 0.6 (3), nsd
					Duodenal ZnT1 protein (relative densitometric units)	GD15: 1.2 ± 1 (2-3) GD20: 1.3 ± 1 (2-3), N/S
					Duodenal ZnT2 protein (relative densitometric units)	GD15: 3.4 ± 1 (2-3) GD20: 4.3 ± 1 (2-3), N/S
					Duodenal ZnT4 protein (relative densitometric units)	GD15: 3.3 ± 1 (2-3) GD20: 1.7 ± 1 (2-3), N/S

Macfie 1991; human; cross sectional [302]	N/S	Fasted for > 6 h prior to gastric emptying study	NP, 10-12 weeks, 15-18 weeks, 37-40 weeks (280 d)	Gastric emptying/SI motility	Time to peak paracetamol concentration, after 1.5 g oral paracetamol (min)	NP: 61 ± 27 (15) 10-12 weeks: 74 ± 33 (15), nsd 15-18 weeks: 59 ± 36 (15), nsd 37-40 weeks: 45 ± 19 (15), nsd
					Maximum concentration of paracetamol (µg·ml ⁻¹)	NP: 28 ± 6 (15) 10-12 weeks: 23 ± 8 (15), nsd 15-18 weeks: 27 ± 10 (15), nsd 37-40 weeks: 28 ± 8 (15), nsd
					Paracetamol AUC 0-60 min (µg·min·ml ⁻¹)	NP: 750 ± 387 (15) 10-12 weeks: 550 ± 484 (15), P<0.05 15-18 weeks: 700 ± 484 (15), nsd 37-40 weeks: 950 ± 581 (15), nsd
					Paracetamol AUC 0-120 min (µg·min·ml ⁻¹)	NP: 2200 ± 387 (15) 10-12 weeks: 1500 ± 387 (15), P<0.05 15-18 weeks: 1800 ± 581 (15), nsd 37-40 weeks: 2100 ± 310 (15), nsd

Maes 1999; human; cross sectional [312]	N/S	Test meal – 60 g white bread & 1 egg yolk (250 kcal) w/ 91 mg of [1- ¹³ C]- octanoic acid (99% enrichment)	NP, 17 ± 3.7 weeks (280 d)	Gastric emptying/SI motility	Gastric emptying coefficient	NP: 3.39, IQR 3.10-3.56 (36) 17 ± 3.7 weeks: 2.29, IQR 2.90-3.23 (10), nsd	
					Gastric half-emptying time (min)	NP: 72, IQR 59-85 (36) 17 ± 3.7 weeks: 94, IQR 76-102 (10), nsd	
					Duration of lag phase (min)	NP: 37, IQR 28-50 (36) 17 ± 3.7 weeks: 38, IQR 22-68 (10), nsd	
Mainoya 1975; rat (Sprague- Dawley); non- rand exp [259]	Purina rat breeder “white diet” (Simonsen Labs)	N/S	NP, GD2-3, GD12-13 (22 d)	Direct measure of nutrient uptake – ex vivo	Mucosal fluid transport (ml·g ⁻¹ wet wt·h ⁻¹)	Segment III (jejunum)	NP: 1.11 ± 0.26 (7) GD2-3: 1.77 ± 0.34 (4), P<0.01 GD12-13: 1.50 ± 0.39 (9), P<0.05
						Segment IV (jejunum)	NP: 1.32 ± 0.13 (7) GD2-3: 1.77 ± 0.38 (4), P<0.05 GD12-13: 1.95 ± 0.45 (9), P<0.01
					Mucosal Na ⁺ transport (uequiv·g ⁻¹ wet wt·h ⁻¹)	Segment III (jejunum)	NP: 123.9 ± 27.5 (7) GD2-3: 252.3 ± 60.6 (4), P<0.001 GD12-13: 183.4 ± 43.2 (9), P<0.01
						Segment IV (jejunum)	NP: 138.1 ± 33.3 (7) GD2-3: 252.9 ± 59.4 (4), P<0.01 GD12-13: 253.1 ± 62.7 (9), P<0.001
					Mucosal Cl ⁻ transport (uequiv·g ⁻¹ wet wt·h ⁻¹)	Segment III (jejunum)	NP: 23.3 ± 11.6 (7) GD2-3: 60.4 ± 26.8 (4), P<0.01

						GD12-13: 32.1 ± 27.9 (9), nsd
					Segment IV (jejunum)	NP: 15.8 ± 16.9 (7) GD2-3: 48.0 ± 4.6 (4), P<0.01 GD12-13: 49.2 ± 42.6 (9), nsd
				Mucosal K ⁺ transport (uequiv.·g ⁻¹ wet wt·h ⁻¹)	Segment III (jejunum)	NP: 1.5 ± 0.2 (6) GD12-13: 4.8 ± 1.1 (8), P<0.001
					Segment IV (jejunum)	NP: 1.6 ± 0.5 (6) GD12-13: 5.4 ± 1.1 (8), P<0.001
				Mucosal Ca ²⁺ transport (uequiv.·g ⁻¹ wet wt·h ⁻¹)	Segment III (jejunum)	NP: 1.1 ± 1.0 (6) GD12-13: 2.7 ± 1.4 (8), P<0.05
					Segment IV (jejunum)	NP: 1.7 ± 0.5 (6) GD12-13: 3.9 ± 1.1 (8), P<0.001
				Mucosal Mg ²⁺ transport (uequiv.·g ⁻¹ wet wt·h ⁻¹)	Segment III (jejunum)	NP: 0.1 ± 0.5 (6) GD12-13: 0.9 ± 0.6 (8), P<0.05
					Segment IV (jejunum)	NP: 0.1± 0.2 (6) GD12-13: 1.2 ± 0.8 (8), P<0.01

Manis 1962; rat (Sherman); non-rand exp [278]	N/S	N/S	NP, 3 rd week (N/S)	Direct measure of nutrient uptake – ex vivo, Direct measure of nutrient uptake – in vivo	Fe transferred to serosal side, duodenum ($\mu\text{mol}\cdot\text{gut sac}$)	NP: 23 (7) 3 rd week: 49 (7), N/S	
					Fe concentration ratio, serosal/mucosal, duodenum	NP: 2.0 (7) 3 rd week: 4.7 (7), P<0.001	
					Absorption of ⁵⁹ Fe from lumen, duodenum (counts min(10 ⁻³)·loop ⁻¹)	Exp. 1	NP: 2.3 (5) 3 rd week: 3.1 (6), P<0.01
						Exp. 2	NP: 2.8 (6) 3 rd week: 3.1 (6), nsd
					⁵⁹ Fe transferred to blood from lumen, duodenum (counts min(10 ⁻³)·loop ⁻¹)	Exp. 1	NP: 0.8 (5) 3 rd week: 1.9 (6), P<0.001
Exp. 2	NP: 1.3 (6) 3 rd week: 1.9 (6), nsd						
Matos 2016; rat (Wistar); rand exp [409]	Presence Nutrição Animal, Paulínia, SP, Brazil	Ad lib	NP, GD7, GD14, GD20 (22 d)	Gastric emptying/SI motility	Gastric emptying (min)	NP: 113 ± 15 (6) GD7: 168 ± 17 (6), P<0.001 GD14: 165 ± 15 (6), P<0.001 GD20: 95 ± 7 (6), nsd	
					Gastric contraction frequency (cpm)	NP: 70 ± 7.0 (6) GD7: 66 ± 6.0 (6), P<0.03 GD14: 59 ± 7.0 (6), P<0.03 GD20: 65 ± 9.0 (6), nsd	
					Oro-caecum transit time (min)	NP: 254 ± 10.8 (6) GD7: 244 ± 16.0 (6), nsd GD14: 255 ± 14.8 (6), nsd GD20: 259 ± 19.9 (6), nsd	

Mazgaj 2021; mouse (B6; 129S7); non- rand exp [360]	Control diet containing 48 ppm Fe (Harlan Laboratories, Madison, WI, USA)	N/S	NP, GD18.5 (20 d)	Nutrient transporter protein expression	FPN protein in duodenum membrane fractions (AU, density relative to beta-actin)	NP: 0.25 ± 0.25 (N/S) GD18.5: 1.40 ± 0.50 (N/S), P<0.001
Millard 2004; rat (Sprague- Dawley); non- rand exp [357]	Standard rodent pellet diet (370 mg Fe·kg ⁻¹)	N/S	NP, GD9, GD15, GD18, GD21 (22 d)	Nutrient transporter gene expression, nutrient transporter protein expression	<i>Dmt</i> (non-IRE form) gene expression, isolated duodenal enterocytes (AU relative to GAPDH)	NP: 0.13 ± 0.14 (4) GD9: 0.16 ± 0.16 (4), nsd GD15: 0.28 ± 0.14 (4), P<0.05 GD18: 0.32 ± 0.14 (4), P<0.01 GD21: 0.31 ± 0.30 (4), nsd
					<i>Dcytb</i> gene expression, isolated duodenal enterocytes (AU relative to GAPDH)	NP: 0.28 ± 0.28 (4) GD9: 0.40 ± 0.10 (4), nsd GD15: 0.80 ± 0.32 (4), P<0.05 GD18: 0.95 ± 0.20 (4), P<0.05 GD21: 0.90 ± 0.30 (4), P<0.05
					<i>DMT</i> (IRE form) gene expression, isolated duodenal enterocytes (AU relative to GAPDH)	NP: 0.15 ± 0.10 (4) GD9: 0.30 ± 0.25 (4), nsd GD15: 0.70 ± 0.50 (4), nsd GD18: 1.00 ± 0.40 (4), P<0.05 GD21: 0.70 ± 0.50 (4), nsd
					<i>Hephaestin (Hp)</i> gene expression, isolated duodenal enterocytes (AU relative to GAPDH)	NP: 0.54 ± 0.14 (4) GD9: 0.56 ± 0.16 (4), nsd GD15: 0.58 ± 0.08 (4), nsd GD18: 0.59 ± 0.10 (4), nsd GD21: 0.64 ± 0.04 (4), nsd
					<i>Ireg1 (Slc40a1)</i> gene expression, isolated	NP: 0.87 ± 0.28 (4) GD9: 1.06 ± 0.47 (4), nsd GD15: 0.99 ± 0.05 (4), nsd

					duodenal enterocytes (AU relative to GAPDH)	GD18: 1.08 ± 0.09 (4), nsd GD21: 1.11 ± 0.09 (4), nsd
					Ireg1 (FPN) relative protein expression, isolated duodenal enterocytes (AU)	NP: 1.86 ± 0.86 (4) GD9: 2.00 ± 1.00 (4), nsd GD15: 3.42 ± 0.71 (4), P<0.05 GD18: 3.00 ± 0.71 (4), nsd GD21: 3.14 ± 1.00 (4), nsd
					DMT relative protein expression, isolated duodenal enterocytes (AU)	NP: 0.25 ± 0.20 (4) GD9: 0.33 ± 0.34 (4), nsd GD15: 0.80 ± 0.60 (4), nsd GD18: 2.00 ± 0.60 (4), P<0.05 GD21: 2.40 ± 2.20 (4), nsd

Moffett 2013; rat (Wistar); non-rand exp [246]	Standard rodent maintenance diet (10% fat, 30% protein and 60% carbohydrate, Trouw Nutrition, Cheshire, UK)	Ad lib, 18 h fast before tests	NP, GD21 (22 d)	Direct measure of nutrient uptake – in vivo, Indirect measure of nutrient uptake – in vivo, Whole SI anatomy	Plasma glucose after OGTT, 3.2 g glucose/kg (mM)	Basal	NP: 6 ± 1 (6) GD21: 4 ± 1 (6), P<0.01
						30 min	NP: 12 ± 5 (6) GD21: 9 ± 3 (6), nsd
					Plasma GIP after OGTT, 3.2 g glucose/kg (mM)	Basal	NP: 160 ± 25 (6) GD21: 140 ± 25 (6), nsd
						30 min	NP: 340 ± 50 (6) GD21: 260 ± 75 (6), nsd
					Plasma GIP after oral fat challenge, 1.38 g corn oil/kg (mM)	Basal	NP: 180 ± 25 (6) GD21: 210 ± 25 (6), nsd
						30 min	NP: 310 ± 50 (6) GD21: 310 ± 50 (6), nsd
						60 min	NP: 400 ± 50 (6) GD21: 430 ± 50 (6), nsd
					Intestinal wet weight (g)	NP: 5.5 ± 2.5 (6) GD21: 7.0 ± 2.0 (6), P<0.01	
Intestinal GIP content (pmol·g ⁻¹ wet weight)	NP: 180 ± 50 (6) GD21: 380 ± 100 (6), P<0.01						
Moore 2011; dog (mongrel); non-rand exp [247]	PMI Nutrition canine diet (5006, St. Louis, MO, and Kal Kan, Vernon, CA); 31% protein, 26% fat, 42% carbohydrate, 1,650 –1,850 kcal/day	Overnight fast before OGTT	NP, 6-7 weeks (63 d)	Direct measure of nutrient uptake – in vivo	Plasma glucose after OGTT 0.9 g glucose/kg (mmol·L ⁻¹)	Basal	NP: 5.9 ± 0.4 (3) 6-7 weeks: 5.7 ± 0.4 (4), nsd
						40 min	NP: 9.5 ± 0.8 (3) 6-7 weeks: 8.0 ± 0.8 (4), nsd

Moore 2012; dog (mongrel); non-rand exp [410]	Once daily a diet of meat (Pedigree; Mars PetCare, Franklin, TN, USA) and chow (Purina Lab Canine Diet no. 5006; PMI Nutrition, Henderson, CO, USA) combined: 34% protein, 14.5% fat, 46% carbohydrate, 5.5% fibre dry weight. Diet nutritionally adequate for P dogs, animals in both groups consumed approximately 6908–7745 kJ/d (1650–1850 kcal/d).	Fed once per day. Fasted for 18 h prior to experiment	NP, 7-8 weeks (63 d)	Direct measure of nutrient uptake – in vivo	Arterial plasma glucose (mg·L ⁻¹), time from start of 30 min infusion of liquid diet (2.8 g/kg whey protein, 0.6 g/kg lipid, 3.6 g/kg D-glucose, labelled with 250 µCi [U- ¹⁴ C])	Fasted	NP: 1100 ±75 (8) 6-7 weeks: 1100 ± 75 (8), nsd
						30 min	NP: 1450 ± 150 (8) 6-7 weeks: 1530 ± 200 (8), nsd
						45 min	NP: 1500 ± 200 (8) 6-7 weeks: 1670 ± 200 (8), nsd
						60 min	NP: 1480 ± 300 (8) 6-7 weeks: 1780 ± 150 (8), nsd
						90 min	NP: 1400 ± 300 (8) 6-7 weeks: 1900 ± 200 (8), P<0.05
					Portal vein plasma glucose, time from start of liquid meal as above (mg·L ⁻¹)	Fasted	NP: 1100 ± 75 (6) 6-7 weeks: 1100 ± 75 (6), nsd
						30 min	NP: 1750 ± 75 (8) 6-7 weeks: 1700 ± 1000 (8), nsd
						45 min	NP: 1850 ± 200 (8) 6-7 weeks: 1950 ± 500 (8), nsd
						60 min	NP: 1820 ± 500 (8) 6-7 weeks: 2080 ± 300 (8), nsd
						90 min	NP: 1770 ± 300 (8) 6-7 weeks: 2250 ± 400 (8), P<0.05
					Net gut glucose balance, time from start of liquid meal as above (mg·kg ⁻¹ ·min ⁻¹)	Fasted	NP: -0.8 ± 0.3 (8) 6-7 weeks: -0.2 ± 0.3 (8), nsd
						30 min	NP: 5.0 ± 1.4 (8) 6-7 weeks: 2.8 ± 1.4 (8), nsd
						45 min	NP: 5.8 ± 1.4 (8) 6-7 weeks: 4.8 ± 0.8 (8), nsd
						60 min	NP: 5.2 ± 2.0 (8)

							6-7 weeks: 4.9 ± 1.4 (8), nsd
						90 min	NP: 5.3 ± 2.8 (8) 6-7 weeks: 6.0 ± 1.0 (8), nsd
Mottino 2001; rat (Sprague- Dawley); non- rand exp [411]	N/S	Ad lib	NP, GD19- 20 (22 d)	Jejunal anatomy	Intestine mass, proximal jejunum (g·cm ⁻¹)		NP: 0.071 ± 0.015 (3) GD19-20: 0.077 ± 0.012 (3), nsd
					Mucosal mass, proximal jejunum (g·cm ⁻¹)		NP: 0.046 ± 0.012 (3) GD19-20: 0.051 ± 0.008 (3), nsd
Mottino 2002; rat (Sprague- Dawley); non- rand exp [412]	N/S	Ad lib	NP, GD20 (22 d)	Nutrient transporter protein expression	Asbt protein expression in ileal brush border membrane vesicles (AU)	Segment VI (ileum)	NP: 0.4 ± 0.1 (3)- v GD20: 0.7 ± 0.3 (3), nsd
						Segment VII (ileum)	NP: 1.6 ± 0.6 (3) GD20: 2.3 ± 0.4 (3), nsd
						Segment VIII (ileum)	NP: 1.8 ± 0.3 (3) GD20: 1.6 ± 0.4 (3), nsd
						Segment IX (ileum)	NP: 4.0 ± 0.8 (3) GD20: 2.6 ± 0.6 (3), P<0.05
Musacchai 1970; Golden Hamster (<i>Mesocricetus auratus</i>); non- rand. exp. [413]	Wayne Lab Blox	Ad lib, fasted 24 h prior to experiment ation	NP (virgin and breeder), GD8-GD15 (15-18 d)	Direct measure of nutrient uptake – in vivo	D-glucose absorbed in 30 minutes, jejunum and ileum (µmol. g ⁻¹ dry weight)		Virgin: 77 ± 13 (10) Breeder: 64 ± 20 (13) GD15-18: 87 ± 11 (9), P<0.001 vs breeder, P<0.025 vs virgin

Nakai 2002; human; cross sectional [414]	N/S	N/S	NP, 1 st Tri, 2 nd Tri, 3 rd Tri (280 d)	Whole SI anatomy	Portal vein cross-sectional area (cm ²)	NP: 1.23 ± 0.42 (22) 1 st Tri: 1.28 ± 0.28 (13), nsd 2 nd Tri: 1.01 ± 0.63 (25), nsd 3 rd Tri: 1.82 ± 0.72 (29), P<0.05
					Portal vein blood flow (L·min ⁻¹)	NP: 1.25 ± 0.46 (22) 1 st Tri: 0.93 ± 0.38 (13), nsd 2 nd Tri: 1.04 ± 0.79 (25), nsd 3 rd Tri: 1.92 ± 0.83 (29), nsd
Omi 2001; rat (Sprague-Dawley); non-rand exp [264]	F-2 diet (Funabashi Co., Japan); 1.2% Ca, 0.96% P	Ad lib	NP, GD1-3, GD4-6, GD7-9, GD10-12, GD13-15, GD16-18 (22 d)	Direct measure of nutrient uptake – in vivo	Intestinal calcium absorption, from diet (mg/d)	NP: 100 ± 32 (10) GD1-3: 160 ± 30 (10), P<0.001 GD4-6: 145 ± 25 (10), P<0.01 GD7-9: 170 ± 35 (10), P<0.01 GD10-12: 165 ± 32 (10), P<0.01 GD13-15: 210 ± 25 (10), P<0.001 GD16-18: 180 ± 15 (10), P<0.001
					Rate of calcium absorption, from diet (%)	NP: 60 ± 20 (10) GD1-3: 75 ± 5 (10), P<0.05 GD4-6: 70 ± 5 (10), nsd GD7-9: 65 ± 8 (10), P<0.05 GD10-12: 67 ± 5 (10), P<0.05 GD13-15: 80 ± 5 (10), P<0.001 GD16-18: 78 ± 5 (10), P<0.001
O'Sullivan 1984; human; cross sectional [320]	N/S	Overnight fast prior to study	NP, 3 rd Tri (280 d)	Gastric emptying/SI motility	Gut transit time, mouth to excretion (h)	NP: 55.0 ± 29.2 (11) 3 rd Tri: 53.6 ± 35.2 (14), nsd

O'Sullivan 1987; human; cross sectional [298]	N/S	Fasted for at least 4 h prior to study	NP, 3 rd Tri (280 d)	Gastric emptying/SI motility	Time at 30% gastric emptying, after drinking 500 ml of water or diluted orange concentrate (min)	NP: 5.2 ± 2.2 (13) 3 rd Tri: 4.4 ± 2.1 (18), nsd
					Time at 50% gastric emptying, as above (min)	NP: 8.3 ± 3.2 (13) 3 rd Tri: 7.2 ± 2.5 (18), nsd
					Time at 70% gastric emptying, as above (min)	NP: 11.1 ± 4.7 (13) 3 rd Tri: 9.8 ± 3.4 (18), nsd
Ovadia 2019; mouse (C57BL/6); non-rand exp [350]	Normal chow diet (RM3 control diet, Special Diets Services, Essex, UK)	Ad lib	NP, GD18 (19.5 d)	Nutrient transporter gene expression,	Asbt gene expression, distal ileum (relative mRNA normalised to cyclophilin)	NP: median 1.1, IQR 0.8-1.35 (6-8) GD18: median 0.9, IQR 0.7-1.3 (6-8), nsd
				Nutrient transporter protein expression	Asbt protein expression, distal ileum (relative mRNA normalised to beta-actin)	NP: median 0.7, IQR 0.4-1.9 (6-8) GD18: median 0.25, IQR 0.2-0.3 (6-8), P=0.036
Oyesola 2009; rat (Wistar); non-rand exp [374]	N/S	N/S	NP, GD1-7, GD8-14, GD15-21 (22 d)	Digestive enzyme activity/ expression	Sucrase activity, SI mucosa (N/S)	NP: 0.852 ± 0.329 (N/S) GD1-7: 1.190 ± 0.066 (N/S), P<0.01 GD8-14: 1.538 ± 0.253 (N/S), P<0.01 GD15-21: 1.640 ± 0.454 (N/S), P<0.01
					Lactase activity, SI mucosa (N/S)	NP: 0.117 ± 0.038 (N/S) GD1-7: 0.224 ± 0.339 (N/S), nsd GD8-14: 0.280 ± 0.100 (N/S), P<0.01 GD15-21: 0.164 ± 0.097 (N/S), nsd
					Maltase activity, SI mucosa (N/S)	NP: 2.020 ± 0.239 (N/S) GD1-7: 1.728 ± 0.152 (N/S), nsd

						GD8-14: 1.940 ± 0.246 (N/S), nsd GD15-21: 1.910 ± 0.606 (N/S), nsd
Palmer 1980; rat (Norwegian Hooded); non- rand exp [415]	Commercial laboratory diet (Spratts Laboratory Diet 1)	Ad lib	NP, 1 st week, 2 nd week, 3 rd week (22 d)	Whole SI anatomy	Gut weight, Whole SI anatomy (g)	NP: 8.36 ± 1.53 (9) 1 st week: 9.46 ± 1.08 (9), nsd 2 nd week: 9.70 ± 1.19 (8), nsd 3 rd week: 9.86 ± 0.85 (8), P<0.05
					Gut length, Whole SI anatomy (cm)	NP: 110.0 ± 12.9 (9) 1 st week: 110.2 ± 3.3 (9), nsd 2 nd week: 107.9 ± 6.5 (8), nsd 3 rd week: 108.5 ± 6.5 (8), nsd
					Protein in mucosa, Whole SI anatomy (mg)	NP: 341 ± 126 (9) 1 st week: 432 ± 84 (9), nsd 2 nd week: 389 ± 42 (8), nsd 3 rd week: 424 ± 54 (8), nsd
Parkman 1993; guinea pig (N/S); non-rand exp [295]	N/S	Fasted overnight before study	NP, GD50- 55 (70 d)	Gastric emptying/SI motility	Force of spontaneous antral contractions, in vitro circular muscle strips (kg·cm ²)	NP: 1.10 ± 0.29 (7) GD50-55: 0.78 ± 0.32 (7), P<0.05
					Slow wave frequency, in vitro as above (n·min ⁻¹)	NP: 5.9 ± 0.5 (7) GD50-55: 6.3 ± 0.8 (7), nsd
					Frequency of spontaneous antral contractions (n·min ⁻¹)	NP: 6.0 ± 0.5 (7) GD50-55: 6.1 ± 0.5 (7), nsd
Parry 1970; human; cross sectional [313]	N/S	N/S	NP, 12-20 weeks (280 d)	Gastric emptying/SI motility	Mean transit time – time to reach caecum (h)	NP: 51.7 ± 9.6 (8) 12-20 weeks: 57.9 ± 12.1 (22), P<0.05

Parry 1970; human; cross sectional [260]	N/S	Given fluids but not solid foods in 8 hrs before each test	NP, 12-20 weeks (280 d)	Direct measure of nutrient uptake – in vivo	Net transport (uptake) of Na ⁺ across colon ($\mu\text{Eq}\cdot\text{min}^{-1}$)	NP: 323 ± 79 (5) 12-20 weeks: 470 ± 99 (15), $P < 0.001$
					Net transport (efflux) of K ⁺ across colon ($\mu\text{Eq}\cdot\text{min}^{-1}$)	NP: -15.9 ± 7.4 (5) 12-20 weeks: -19.9 ± 9.1 (15), nsd
Peeters 1980; guinea pig (Albino); non- rand exp [337]	N/S	Ad lib	NP, 39-56 days, 57-66 days (68 d)	Whole SI anatomy	Regional blood flow, small intestine ($\text{ml}\cdot\text{min}^{-1}$)	NP: 15.6 ± 2.0 (5) GD39-56: 16.1 ± 5.1 (8), nsd GD57-66: 18.0 ± 2.7 (6), nsd
					Regional blood flow, small intestine ($\text{ml}\cdot\text{min}^{-1}\cdot 100\text{ g}^{-1}$)	NP: 107 ± 27 (5) GD39-56: 127 ± 45 (8), nsd GD57-66: 168 ± 34 (6), $P < 0.05$

Pelletier 1987; pig (Landrace); non-rand. exp. [416]	Pelleted commercial nonpurified concentrated diet	2.35 kg/day, once daily	NP, GD110 (114 d)	Whole SI anatomy, Duodenal anatomy, Digestive enzyme activity/ Expression	SI weight (g)	NP: 1471 ± 248 (10) GD110: -2 ± 242 (12), nsd
					SI length (cm)	NP: 1817 ± 191 (10) GD110: 1630 ± 186 (12), nsd
					Duodenum weight (g)	NP: 20.3 ± 13.9 (10) GD110: 24.1 ± 15.3 (12), nsd
					Duodenum DNA content (mg)	NP: 109.5 ± 88.9 (10) GD110: 108.4 ± 97.4 (12), nsd
					Duodenum protein content (mg)	NP: 2.22 ± 1.93 (10) GD110: 2.44 ± 2.12 (12), nsd
					Duodenum RNA content	NP: 72.5 ± 59.0 (10) GD110: 66.7 ± 64.7 (12), nsd
					Log (maltase) activity, duodenum (k units)	NP: 3.82 ± 1.25 (10) GD110: 3.94 ± 1.37 (12), nsd
					Log (pepsin) activity, fundic mucosa of stomach (k units)	NP: 17.30 ± 1.72 (10) GD110: 17.25 ± 1.89 (12), nsd
Penzes 1968; rat (Wistar); non-rand exp [323]	Standard laboratory chow (Phylaxia, Budapest; 3.1% fibre, 20% protein)	Ad lib	NP, GD10, GD16, GD21 (22 d)	Whole SI anatomy	SI weight (% of body weight)	NP: 3.2 (12-15) GD10: 3.4 (4-5), nsd GD16: 3.1 (4-5), nsd GD21: 2.3 (4-5), nsd
Penzes 1968; rat (Wistar); non-rand exp [417]	N/S	Fasted 18 h before study	NP, GD10, GD16, GD21 (22 d)	Direct measure of nutrient uptake – in vivo	Absorption of dL- methionine from SI perfusion (%)	NP: 81.1 ± 7.1 (69) GD10: 83.1 ± 4.7 (5), nsd GD16: 78.2 ± 5.0 (10), nsd GD21: 83.1 ± 3.3 (20), nsd

Penzes 1985; rat (RLEF1/LAT1) ; non-rand exp [341]	Standard laboratory diet (LAT1), Godollo, Hungary	Ad lib	NP, GD18 (22 d)	Jejunal anatomy	Jejunal microvilli height (μm)	NP: 1.143 ± 0.266 (10) GD18: 1.298 ± 0.208 (9), nsd
					Jejunal microvilli width (μm)	NP: 0.106 ± 0.006 (10) GD18: 0.103 ± 0.009 (9), nsd
					Jejunal microvilli density ($\text{n} \cdot \mu\text{m cell surface}^{-1}$)	NP: 6.8 ± 0.398 (10) GD18: 6.2 ± 0.501 (9), nsd
					Jejunal microvilli surface area per μm^2	NP: 17.66 ± 3.92 (10) GD18: 16.06 ± 2.48 (9), nsd
Penzes 1988; rat (RLEF1/LAT1) ; non-rand exp [342]	Standard laboratory diet (LAT1), Godollo, Hungary	Ad lib	NP, GD18 (22 d)	Ileal anatomy	Ileal microvilli height (μm)	NP: 0.769 ± 0.144 (9) GD18: 0.910 (2), nsd
					Ileal microvilli width (μm)	NP: 0.114 ± 0.012 (9) GD18: 0.109 (2), nsd
					Ileal microvilli density ($\text{n} \cdot \mu\text{m cell surface}^{-1}$)	NP: 7.032 ± 0.828 (9) GD18: 6.763 (2), nsd
					Ileal microvilli surface area per μm^2	NP: 14.386 ± 4.653 (9) GD18: 15.402 (2), nsd
Penzes 1988; rat (RLEF1/LAT1) ; non-rand exp [340]	Standard laboratory diet (LAT1), Godollo, Hungary	Ad lib	NP, GD18 (22 d)	Duodenal anatomy	Duodenal microvilli height (μm)	NP: 1.518 ± 0.285 (9) GD18: 1.662 ± 0.141 (9), nsd
					Duodenal microvilli width (μm)	NP: 0.140 ± 0.015 (9) GD18: 0.133 ± 0.009 (9), nsd
					Duodenal microvilli density ($\text{n} \cdot \mu\text{m cell surface}^{-1}$)	NP: 5.2 ± 0.6 (9) GD18: 5.1 ± 0.4 (9), nsd
					Duodenal microvilli surface area per μm^2	NP: 18.28 ± 2.49 (9) GD18: 18.75 ± 2.88 (9), nsd

Pere 1992; rabbit (New- Zealand); non-rand exp [236]	Laboratory chow (16% protein, 15% carbohydrate, 3% fat, 14% fibre)	Ad lib	NP, GD27 (31-32 d)	Direct measure of nutrient uptake – in vivo, Whole SI anatomy	Portal vein blood flow, time after 15 g meal (ml·min ⁻¹ ·kg ⁻¹)	Basal	NP: 40.4 ± 5.7 (10) GD27: 44.5 ± 4.2 (12), nsd
						15 min	NP: 38.9 ± 13.9 (10) GD27: 47.8 ± 8.3 (12), nsd
						30 min	NP: 42.8 ± 10.1 (10) GD27: 50.2 ± 12.8 (12), nsd
						45 min	NP: 41.3 ± 7.6 (10) GD27: 41.9 ± 17.0 (12), nsd
						60 min	NP: 44.0 ± 9.2 (10) GD27: 50.2 ± 11.4 (12)
						Basal	NP: 5.3 ± 0.9 (10) GD27: 4.5 ± 0.7 (12), P<0.001
					Arterial blood glucose, time after 15 g meal (mM)	15 min	NP: 5.75 ± 0.9 (10) GD27: 6.2 ± 1.0 (12), P<0.001
						30 min	NP: 5.7 ± 1.3 (10) GD27: 6.3 ± 1.0 (12), P<0.001
						Basal	NP: -3 ± 3 (10) GD27: -2 ± 3 (12), nsd
					Net gut glucose balance, time after 15 g meal (μM·min ⁻¹ ·kg ⁻¹)	15 min	NP: 13 ± 11 (10) GD27: 14 ± 7 (12), nsd
						30 min	NP: 8.5 ± 11 (10) GD27: 17.5 ± 10 (12), nsd
						NP: 13 ± 0.4 (5) GD20: 14 ± 0.5 (6), nsd	
Peshin 1976; rat (Charles River); non- rand exp [354]	N/S	N/S	NP, GD22 (22 d)	Nutrient transporter protein expression	CaBP, specific activity of [⁴⁵ Ca]BP (count·min ⁻¹ ·μg protein ⁻¹)	NP: 13 ± 0.4 (5) GD20: 14 ± 0.5 (6), nsd	

Peters 1967; rat (Wistar); non-rand exp [418]	Purina laboratory chow	Ad lib	NP, 3 rd week (22 d)	Whole SI anatomy	SI dry weight (g)	NP: 0.555 (26) 3 rd week: 0.620 ± 0.156 (16), P<0.01
Pond 1986; pig (Chester White x Landrace x Large White x Yorkshire); non-rand exp [333]	Standard corn-soybean meal-type gestation diet containing 14% protein, 1.0% Ca and 0.8% P	6000 kcal, once daily	NP, GD84, GD108 (115 d)	Whole SI anatomy	SI wet weight (g)	NP: 978 ± 49 (17) GD84: 975 ± 49 (8), nsd GD108: 925 ± 49 (9), nsd
					SI wet weight (% of bodyweight)	NP: 0.736 ± 0.155 (17) GD84: 0.698 ± 0.155 (8), nsd GD108: 0.630 ± 0.155 (9), nsd

Prieto 1994; rat (Wistar); non-rand exp [419]	Standard animal chow (UAR A03, Panlab, Barcelona)	Ad lib	NP, GD19±2 (22 d)	Whole SI anatomy, duodenal anatomy, jejunal anatomy, ileal anatomy	SI length (cm)	NP: 112.09 ± 3.01 (6) GD19±2: 128.02 ± 2.87 (6), P<0.05		
					SI weight (g)	NP: 5.83 ± 0.56 (6) GD19±2: 7.51 ± 0.51 (6), P<0.05		
					Intestinal weight (mg·cm ⁻¹)	Duodenum	NP: 52 ± 8 (6) GD19±2: 73 ± 3 (6), P<0.05	
						Proximal jejunum- ileum	NP: 51 ± 2 (6) GD19±2: 66 ± 7 (6), P<0.05	
						Medial jejunum-ileum	NP: 50 ± 5 (6) GD19±2: 64 ± 8 (6), P<0.05	
						Distal jejunum-ileum	NP: 45 ± 2 (6) GD19±2: 47 ± 6 (6), nsd	
					Mucosal weight (mg·cm ⁻¹)	Duodenum	NP: 26 ± 5 (6) GD19±2: 38 ± 5 (6), P<0.05	
						Proximal jejunum- ileum	NP: 23 ± 3 (6) GD19±2: 35 ± 15 (6), P<0.05	
						Medial jejunum-ileum	NP: 22 ± 5 (6) GD19±2: 30 ± 4 (6), P<0.05	
						Distal jejunum-ileum	NP: 15 ± 3 (6) GD19±2: 18 ± 4 (6), P<0.05	
					Mucosal DNA (µg·cm ⁻¹)	Duodenum	NP: 130 ± 37 (6) GD19±2: 150 ± 17 (6), nsd	
						Proximal jejunum- ileum	NP: 110 ± 24 (6) GD19±2: 125 ± 12 (6), nsd	
						Medial jejunum-ileum	NP: 100 ± 17 (6) GD19±2: 95 ± 24 (6), nsd	
						Distal jejunum-ileum	NP: 70 ± 17 (6)	

						GD19±2: 75 ± 6 (6), nsd
				Mucosal protein (µg·cm ⁻¹)	Duodenum	NP: 3.4 ± 0.6 (6) GD19±2: 4.8 ± 1.5 (6), P<0.05
			Proximal jejunum- ileum		NP: 2.8 ± 0.4 (6) GD19±2: 4.0 ± 0.5 (6), P<0.05	
			Medial jejunum-ileum		NP: 2.5 ± 0.8 (6) GD19±2: 2.2 ± 0.5 (6), nsd	
			Distal jejunum-ileum		NP: 1.2 ± 0.2 (6) GD19±2: 1.4 ± 0.4 (6), nsd	
			Mucosal protein:DNA ratio	Duodenum	NP: 22 ± 5 (6) GD19±2: 33 ± 5 (6), P<0.05	
				Proximal jejunum- ileum	NP: 24 ± 1 (6) GD19±2: 30 ± 4 (6), P<0.05	
				Medial jejunum-ileum	NP: 23 ± 2 (6) GD19±2: 23.5 ± 6 (6), nsd	
				Distal jejunum-ileum	NP: 18 ± 4 (6) GD19±2: 21 ± 4 (6), nsd	

Prieto 1994; rat (Wistar); non-rand exp [339]	Standard animal chow (UAR A03, Panlab, Barcelona)	Ad lib	NP, GD19 (22 d)	Jejunal anatomy, Ileal anatomy, Digestive enzyme activity/ expression	Jejunal mucosal weight (mg·cm ⁻¹)	NP: 22 ± 4 (8) GD19: 35 ± 6 (8), P<0.05	
					Ileal mucosal weight (mg·cm ⁻¹)	NP: 15 ± 6 (8) GD19: 18 ± 6 (8), P<0.05	
					Jejunal mucosal disaccharidase enzyme activity (mU·mg ⁻¹ protein)	Lactase	NP: 17 ± 6 (8) GD19: 19 ± 2 (4), nsd
						Sucrase	NP: 88 ± 11 (80) GD19: 86 ± 78 (4), nsd
						Maltase	NP: 286 ± 79 (8) GD19: 209 ± 2 (4), nsd
						Trehalase	NP: 110 ± 6 (8) GD19: 107 ± 2 (4), nsd
					Ileal mucosal disaccharidase enzyme activity (mU·mg ⁻¹ protein)	Lactase	NP: 6 ± 3 (8) GD29: 6 ± 2 (4), nsd
						Sucrase	NP: 47 ± 8 (8) GD19: 30 ± 8 (4), P<0.05
						Maltase	NP: 176 ± 8 (8) GD19: 155 ± 34 (4), nsd
						Trehalase	NP: 20 ± 3 (8) GD19: 20 ± 8 (4), nsd
					Jejunal brush border membrane disaccharidase enzyme activity (mU·mg ⁻¹ protein)	Lactase	NP: 169 ± 65 (8) GD19: 154 ± 20 (8), nsd
						Sucrase	NP: 396 ± 141 (8) GD19: 402 ± 28 (8), nsd
						Maltase	NP: 1387 ± 458 (8) GD19: 1374 ± 153 (8), nsd
						Trehalase	NP: 468 ± 119 (8)

						GD19: 363 ± 23 (8), P<0.05
				Ileal brush border membrane disaccharidase enzyme activity (mU·mg ⁻¹ protein)	Lactase	NP: 30 ± 11 (8) GD19: 33 ± 11 (8), nsd
			Sucrase		NP: 158 ± 48 (8) GD19: 190 ± 88 (8), nsd	
			Maltase		NP: 808 ± 320 (8) GD19: 895 ± 303 (8), nsd	
			Trehalase		NP: 140 ± 59 (8) GD19: 110 ± 8 (8), nsd	
			Jejunal mucosal disaccharidase enzyme activity (mU·cm ⁻¹ ·kg ⁻¹ bodyweight)	Lactase	NP: 200 ± 141 (8) GD19: 300 ± 100 (4), P<0.05	
				Sucrase	NP: 900 ± 141 (8) GD19: 1300 ± 200 (4), P<0.05	
				Maltase	NP: 2800 ± 707 (8) GD19: 2700 ± 100 (4), nsd	
				Trehalase	NP: 1100 ± 141 (8) GD19: 1600 ± 100 (4), P<0.05	
			Ileal mucosal disaccharidase enzyme activity (mU·cm ⁻¹ ·kg ⁻¹ bodyweight)	Lactase	NP: 50 ± 50 (8) GD19: 100 ± 25 (4), nsd	
				Sucrase	NP: 250 ± 50 (8) GD19: 200 ± 50 (4), nsd	
				Maltase	NP: 750 ± 50 (8) GD19: 800 ± 200 (4), nsd	
				Trehalase	NP: 150 ± 50 (8) GD19: 150 ± 50 (4), nsd	

Prieto 1996; rat (Wistar); non-rand exp [253]	Standard animal chow (UAR A-03. Panlab, Barcelona, Spain); dry wt: 26.7% protein, 56.6% carbohydrate, 5.7% lipids, 4.5% cellulose, 6.5% ashes (13.4 MJ/kg)	Ad lib	NP, GD19 ± 1 (22 d)	Direct measure of nutrient uptake – ex vivo, Jejunal anatomy, Ileal anatomy, Digestive enzyme activity/ expression	Jejunal anatomy	Tissue mass (g)	NP: 2.84 ± 0.34 (6+) GD19±1: 4.13 ± 0.69 (6+), P<0.05
						Mucosal mass (g)	NP: 1.12 ± 0.24 (6+) GD19±1: 2.03 ± 0.42 (6+), P<0.05
						Nominal surface area (cm ²)	NP: 48.7 ± 3.43 (6+) GD19±1: 69.8 ± 4.2 (6+), P<0.05
					Jejunal mucosa enzyme activities (U)	Sucrase	NP: 11.3 ± 2.4 (6+) GD19±1: 13.6 ± 2.2 (6+), nsd
						Maltase	NP: 37.5 ± 4.2 (6+) GD19±1: 35.4 ± 3.7 (6+), nsd
						Lactase	NP: 2.2 ± 0.5 (6+) GD19±1: 2.8 ± 0.2 (6+), nsd
					Ileum anatomy	Tissue mass (g)	NP: 2.55 ± 0.27 (6+) GD19±1: 2.77 ± 0.42 (6+), nsd
						Mucosal mass (g)	NP: 0.77 ± 0.32 (6+) GD19±1: 1.05 ± 0.66 (6+), P<0.05
						Nominal surface area (cm ²)	NP: 49.2 ± 3.7 (6+) GD19±1: 70.9 ± 3.2 (6+), P<0.05
					Ileal mucosa enzyme activities (U)	Sucrase	NP: 6.4 ± 1.2 (6+) GD19±1: 5.4 ± 1.2 (6+), nsd
						Maltase	NP: 23.5 ± 4.2 (6+) GD19±1: 19.8 ± 5.9 (6+), nsd
						Lactase	NP: 1.1 ± 0.7 (6+) GD19±1: 1.2 ± 0.5 (6+), nsd
						K _m (mM)	NP: 8.83 ± 2.86 (8+) GD19±1: 9.74 ± 3.17 (8+), nsd

					Kinetic parameters for active uptake of α -methyl-D-glucose (jejunum)	V_{max} (nmol·100 mg ⁻¹ ·min ⁻¹)	NP: 252 ± 56 (8+) GD19±1: 251 ± 58 (8+), nsd
						V_{max} (μ mol·cm ⁻¹ ·min ⁻¹)	NP: 12.7 ± 2.83 (8+) GD19±1: 16.3 ± 3.7 (8+), P<0.05
						K_d (nmol·cm ⁻¹ ·min ⁻¹ ·mM ⁻¹)	NP: 646 ± 178 (8+) GD19±1: 724 ± 153 (8+), P<0.05
					Kinetic parameters for active uptake of α -methyl-D-glucose (ileum)	K_m (mM)	NP: 6.1 ± 3.7 (8+) GD19±1: 5.5 ± 2.6 (8+), nsd
						V_{max} (nmol·100 mg ⁻¹ ·min ⁻¹)	NP: 108 ± 44 (8+) GD19±1: 169 ± 49 (8+), P<0.05
						V_{max} (μ mol·cm ⁻¹ ·min ⁻¹)	NP: 4.75 ± 1.92 (8+) GD19±1: 7.83 ± 2.29 (8+), P<0.05
						K_d (nmol·cm ⁻¹ ·min ⁻¹ ·mM ⁻¹)	NP: 746 ± 144 (8+) GD19±1: 728 ± 116 (8+), nsd
Quan-Sheng 1989; rat (Sprague-Dawley); non-rand exp [273]	Purified diet similar to the AIN-76A diet, containing 0.7% Ca and 0.55% P	N/S	NP, GD7, GD14, GD20 (22 d)	Direct measure of nutrient uptake – ex vivo, Duodenal anatomy	In vitro uptake of ⁴⁵ Ca, proximal duodenum (% in 10 min)	NP: 33 ± 9 (5) GD7: 37 ± 18 (5), nsd GD14: 40 ± 9 (5), P<0.05 GD20: 62 ± 18 (5), P<0.05	
					In situ duodenal absorption of ⁴⁵ Ca (% in 15 min)	NP: 44 ± 12 (5) GD7: 48 ± 10 (5), nsd GD14: 60 ± 10 (5), P<0.05 GD20: 80 ± 22 (5), P<0.05	
					Duodenum weight (g·mm ⁻¹)	NP: 7.5 ± 0.9 (5) GD7: 7.7 ± 1.3 (5), nsd GD14: 8.8 ± 0.4 (5), P<0.05 GD20: 9.7 ± 0.9 (5), P<0.05	

Quick 1989; rat (Sprague- Dawley); non- rand exp [326]	Standard rat chow (Wayne #8604-00, Continental Grain Co.)	Ad lib	NP, GD15, GD17, GD19, GD20 (22 d)	Whole SI anatomy, Nutrient transporter protein expression	SI weight (% of pre-trial controls)	NP: 100 (3) GD15: 100 ± 35 (3), N/S GD17: 85 ± 14 (3), N/S GD19: 120 ± 14 (3), N/S GD20: 117 ± 25 (3), N/S	
					CRBP protein, whole SI (% of pre-trial controls)	NP: 100 (3) GD15: 105 ± 35 (3), N/S GD17: 80 ± 12 (3), N/S GD19: 120 ± 12 (3), N/S GD20: 110 ± 22 (3), N/S	
					CRBP(II) protein, whole SI (% of pre-trial controls)	NP: 100 (3) GD15: 95 ± 35 (3), N/S GD17: 105 ± 20 (3), N/S GD19: 182 ± 12 (3), N/S GD20: 180 ± 30 (3), N/S	
					CRBP(II) nmol·segment ⁻¹	Proximal	NP: 25 ± 4.3 (3) GD15: 29 ± 11.3 (3), N/S GD17: 25 ± 6.9 (3), N/S GD19: 54 ± 4.3 (3), N/S GD20: 47 ± 8.7 (3), N/S
						Middle	NP: 23 ± 1.7 (3) GD15: 16 ± 4.3 (3), N/S GD17: 21 ± 4.3 (3), N/S GD19: 29 ± 5.2 (3), N/S GD20: 35 ± 8.7 (3), N/S
						Distal	NP: 4 ± 1.7 (3) GD15: 3 ± 0.5 (3), N/S

							GD17: 5 ± 0.5 (3), N/S GD19: 5 ± 1.7 (3), N/S GD20: 5 ± 1.7 (3), N/S
					CRBP(II) nmol·g ⁻¹ wet tissue	Proximal	NP: 9.5 ± 1.7 (3) GD15: 11.0 ± 3.5 (3), N/S GD17: 10.0 ± 1.7 (3), N/S GD19: 17.5 ± 1.5 (3), N/S GD20: 16.8 ± 2.4 (3), N/S
				Middle		NP: 8.8 ± 0.5 (3) GD15: 6.0 ± 0.5 (3), N/S GD17: 8.2 ± 0.5 (3), N/S GD19: 9.6 ± 1.2 (3), N/S GD20: 13.0 ± 4.3 (3), N/S	
				Distal		NP: 1.7 ± 0.5 (3) GD15: 1.5 ± 0.2 (3), N/S GD17: 2.6 ± 0.2 (3), N/S GD19: 2.3 ± 0.5 (3), N/S GD20: 2.5 ± 1.7 (3), N/S	
					CRBP nmol·g ⁻¹ wet tissue	Proximal	NP: 0.160 ± 0.021 (3) GD15: 0.178 ± 0.017 (3), N/S GD17: 0.150 ± 0.017 (3), N/S GD19: 0.173 ± 0.012 (3), N/S GD20: 0.170 ± 0.010 (3), N/S
				Middle		NP: 0.155 ± 0.021 (3) GD15: 0.162 ± 0.008 (3), N/S GD17: 0.148 ± 0.025 (3), N/S GD19: 0.173 ± 0.017 (3), N/S	

							GD20: 0.163 ± 0.017 (3), N/S
						Distal	NP: 0.188 ± 0.010 (3) GD15: 0.190 ± 0.030 (3), N/S GD17: 0.148 ± 0.017 (3), N/S GD19: 0.154 ± 0.012 (3), N/S GD20: 0.175 ± 0.038 (3), N/S

Rådberg 1989; human; cross sectional [305]	N/S	Fasted overnight before study	NP, 33-39 weeks (280 d)	Indirect measure of nutrient uptake – in vivo, Gastric emptying/SI motility, Gallbladder emptying	Gastric volume change (%) following ingestion of 300 ml liquid test meal	15 min	NP: 90 ± 5 (16) 33-39 weeks: 112 ± 10 (14), nsd
						30 min	NP: 85 ± 7 (16) 33-39 weeks: 110 ± 8 (14), nsd
						45 min	NP: 85 ± 5 (16) 33-39 weeks: 102 ± 7 (14), nsd
						60 min	NP: 87 ± 5 (16) 33-39 weeks: 92 ± 7 (14), nsd
						75 min	NP: 80 ± 5 (16) 33-39 weeks: 86 ± 6 (14), nsd
						90 min	NP: 72 ± 5 (16) 33-39 weeks: 100 ± 8 (14), nsd
						105 min	NP: 73 ± 6 (16) 33-39 weeks: 87 ± 8 (14), nsd
				Plasma CCK before and after following ingestion of 300 ml liquid test meal (pmol·L ⁻¹)	Basal	NP: 4 ± 1 (8) 33-39 weeks: 2.5 ± 1 (9), nsd	
					15 min	NP: 23 ± 6 (8) 33-39 weeks: 16.5 ± 5 (9), nsd	
					30 min	NP: 18.5 ± 4 (8) 33-39 weeks: 16.5 ± 2 (9), nsd	
					45 min	NP: 17 ± 30 (8) 33-39 weeks: 20 ± 4 (9), nsd	
				Gallbladder volume - residual volume 75-105 min after 300 ml liquid test meal (%)	NP: 40 ± 5 (19) 33-39 weeks: 38 ± 6 (16), nsd		

					Gallbladder volume - basal volume (ml)	NP: 10.7 ± 1.3 (19) 33-39 weeks: 15.5 ± 1.9 (16), $P < 0.01$
Raja 1987; mouse (To); non-rand exp [279]	Standard rodent diet (K and K. Greef Chemicals Ltd, Croydon, England)	N/S	NP, GD18 (21 d)	Direct measure of nutrient uptake – ex vivo	Apparent affinity constant for $[^{59}\text{Fe}^{3+}]$ uptake by duodenal fragments, $K^{\text{app}}_{\text{t}}$ ($\mu\text{mol}\cdot\text{L}^{-1}$)	NP: 61.0 ± 24.5 (6) GD18: 78.0 ± 25.5 (8), nsd
					Apparent maximal capacity for $[^{59}\text{Fe}^{3+}]$ uptake by duodenal fragments, $V^{\text{app}}_{\text{max}}$ ($\text{pmol}\cdot\text{min}^{-1}\cdot\text{mg}^{-1}$ tissue)	NP: 9.7 ± 2.0 (6) GD18: 14.3 ± 4.0 (8), $P < 0.05$

Remesar 1981; rat (<i>Rattus norvegicus</i>); non-rand exp [420]	Breeding-type rat pellets (Saunders, Barcelona, Spain)	Ad lib	NP, GD12, GD19, GD21 (22 d)	Whole SI anatomy	SI weight (g)	NP: 4.48 ± 0.72 (6-9) GD12: 5.51 ± 2.01 (6-9), nsd GD19: 5.68 ± 0.84 (6-9), P<0.05 GD21: 6.49 ± 1.47 (6-9), P<0.05
					SI weight (% of bodyweight)	NP: 2.35 ± 0.52 (6-9) GD12: 2.53 ± 0.75 (6-9), nsd GD19: 2.47 ± 0.57 (6-9), nsd GD21: 2.72 ± 0.48 (6-9), nsd
					SI DNA (mg·g ⁻¹)	NP: 2.43 ± 1.23 (6-9) GD12: 2.03 ± 1.23 (6-9), nsd GD19: 2.03 ± 1.16 (6-9), nsd GD21: 2.05 ± 3.21 (6-9), nsd
					SI protein (mg·g ⁻¹)	NP: 111 ± 12 (6-9) GD12: 105 ± 15 (6-9), nsd GD19: 107 ± 18 (6-9), nsd GD21: 103 ± 24 (6-9), nsd
					SI length (cm)	NP: 94 ± 12 (6-9) GD12: 106 ± 9 (6-9), P<0.05 GD19: 109 ± 12 (6-9), P<0.05 GD21: 115 ± 12 (6-9), P<0.05

Ribeiro 2023; mouse (C57BL/6J); non-rand exp [331]	Standard chow: 17% kcal fat, 54% kcal carbohydrates, 29% kcal protein, 3 kcal/g; Harlan 8640 Teklad 22/5 Rodent Diet	Ad lib	NP, GD14.5, GD18.5 (18.5 d)	Whole SI anatomy, Ileal anatomy	Intestinal permeability, FITC fluorescence (AUC, RFU x 10 ⁴ ·min ⁻¹)	NP: median 6.5, IQR 5-8 (12) GD14.5: median 9, IQR 7.5-12.5 (12), P<0.05 GD18.5: median 8.5, IQR 7-10 (7), nsd
					Small intestine length (cm)	NP: median 36, IQR 35.25-38 (4) GD14.5: median 38.5, IQR 38-42 (5), nsd GD18.5: median 42, IQR 41.5-42.5 (6), P<0.05
					Ileal crypt depth (µm)	NP: median 120, IQR 105-125 (4) GD14.5: median 130, IQR 120-140 (9), nsd GD18.5: median 125, IQR 110-145 (6), nsd
					Ileal villus length (µm)	NP: median 225, IQR 200-230 (4) GD14.5: median 235, IQR 220-240 (8), nsd GD18.5: median 225, IQR 215-235 (6), nsd
					Ileal goblet cells/crypt (n)	NP: median 12, IQR 11-14 (4) GD14.5: median 11.5, IQR 11-13 (9), nsd GD18.5: median 13, IQR 10.5-14.5 (5), nsd
					Ileal goblet cells/villus (n)	NP: median 22, IQR 20-26 (4) GD14.5: median 16, IQR 14.5-19 (8), P<0.05 GD18.5: median 19, IQR 18-21 (6), nsd

Robertson 1979; mouse (QS); non- rand exp [288]	N/S	N/S	NP, GD19- 20 (21 d)	Indirect measure of nutrient uptake – ex vivo	IF-Cbl bound to homogenate, ileal mucosa (ng [⁵⁷ Co]cobalamin· mg ⁻¹ protein)	NP: 0.21 ± 0.03 (3) GD19-20: 0.40 ± 0.05 (3), P<0.001
					K _a , binding affinity of IF receptors for CoCbl, ileal mucosa (M ⁻¹)	NP: 2.8 × 10 ¹² (3) GD19-20: 0.7 × 10 ¹² (3), text states lower
					Number of IF receptors, ileal mucosa (n·mg ⁻¹ protein)	NP: 0.8 × 10 ¹² (3) GD19-20: 3.4 × 10 ¹² (3), text states higher
Robertson 1983; mouse (QS); non- rand exp [289]	N/S	N/S	NP, GD18- 20 (21 d)	Indirect measure of nutrient uptake – ex vivo	IF-Cbl binding to receptors, ileal mucosa (ng [⁵⁷ Co]cobalamin· mg ⁻¹ protein)	NP: 0.18 ± 0.04 (3) GD18-20: 0.42 ± 0.09 (3), P<0.001
					IF-receptors, ileal mucosa (n·mg ⁻¹ protein)	NP: 0.8 × 10 ¹¹ (3) GD18-20: 2.9 × 10 ¹¹ (3), text states increased
					Association constant (B ₁₂ affinity) of IF-receptors, ileal mucosa (M ⁻¹)	NP: 2.8 × 10 ¹² (3) GD18-20: 0.6 × 10 ¹² (3), text states decreased

Rolls 1975; rat (Norwegian Hooded); rand exp [421]	Autoclaved Spillers' Small Animal Diet	Ad lib	NP, GD7, GD14, GD21 (22 d)	Digestive enzyme activity/ expression	Total activity of glycyL-leucine dipeptidase, SI mucosa ($\mu\text{mol}\cdot\text{mol}^{-1}$)	NP: 1200 ± 190 (14) GD7: 1300 ± 120 (6), N/S GD14: 1400 ± 240 (6), N/S GD21: 1500 ± 240 (6), N/S Text states increased during pregnancy
					Total activity of L-alanyl-L-glutamic acid dipeptidase, SI mucosa ($\mu\text{mol}\cdot\text{mol}^{-1}$)	NP: 650 ± 200 (14) GD7: 700 ± 240 (6), N/S GD14: 800 ± 240 (6), N/S GD21: 850 ± 480 (6), N/S Text states increased during pregnancy
					Specific activity of glycyL-L-leucine dipeptidase, SI mucosa ($\mu\text{mol}\cdot\text{mol}^{-1}$)	NP: 21 ± 2 (14) GD7: 21 ± 2 (6), N/S GD14: 23 ± 1 (6), N/S GD21: 25 ± 2 (6), N/S Text states increased during pregnancy
					Specific activity of L-alanyl-L-glutamic acid dipeptidase, SI mucosa ($\mu\text{mol}\cdot\text{mol}^{-1}$)	NP: 12 ± 4 (14) GD7: 11.5 ± 2 (6), N/S GD14: 13 ± 1 (6), N/S GD21: 14 ± 5 (6), N/S Text states increased during pregnancy

Rolls 1979; rat (Norwegian Hooded); non-rand exp [378]	Spratts laboratory diet 1	Ad lib	NP, GD7, GD14, GD21 (22 d)	Digestive enzyme activity/ expression	Total trypsin activity, pancreas ($\mu\text{mol substrate hydrolysed}\cdot\text{min}^{-1}\cdot\text{pancreas}^{-1}$)	NP: 8.92 ± 3.95 (12) GD7: 8.65 ± 3.79 (8), nsd GD14: 6.52 ± 1.43 (7), nsd GD21: 6.97 ± 3.51 (7), nsd
					Relative trypsin activity, pancreas ($\mu\text{mol substrate hydrolysed}\cdot\text{min}^{-1}\cdot\text{g}^{-1}$)	NP: 7.77 ± 2.74 (12) GD7: 7.66 ± 2.94 (8), nsd GD14: 5.58 ± 1.88 (7), nsd GD21: 5.78 ± 1.43 (7), nsd
					Total α -chymotrypsin activity, pancreas ($\mu\text{mol substrate hydrolysed}\cdot\text{min}^{-1}\cdot\text{pancreas}^{-1}$)	NP: 20.45 ± 9.35 (12) GD7: 18.02 ± 7.81 (8), nsd GD14: 13.41 ± 4.95 (7), nsd GD21: 14.44 ± 6.40 (7), nsd
					Relative α -chymotrypsin activity, pancreas ($\mu\text{mol substrate hydrolysed}\cdot\text{min}^{-1}\cdot\text{g}^{-1}$)	NP: 17.99 ± 7.24 (12) GD7: 16.02 ± 6.25 (8), nsd GD14: 11.44 ± 3.86 (7), P<0.05 GD21: 11.94 ± 4.31 (7), nsd
Rummens 2003; mouse (Leuven); non-rand exp [422]	Standard murine diet, containing 1.04% Ca, 0.76% P and 2000 IU D/kg (Carfil, Oud-Turnhout, Belgium)	N/S	NP, GD18.5 (19 d)	Nutrient transporter protein expression	Duodenal calbindin-D9K protein content ($\mu\text{g}\cdot\text{mg protein}^{-1}$)	NP: 21 ± 15 (14) GD18.5: 34 ± 19 (14), N/S

Ryan 1982; rat (Sprague- Dawley); non- rand exp [315]	N/S	Ad lib thenfasted 18 h before intestinal transit studies	NP, GD12, GD18 (22 d)	Gastric emptying/SI motility	SI transit (% of intestine traversed 15 min after intra gastric charcoal meal)	NP: 60 ± 20.6 (10) GD12: 63 ± 33.2 (10), nsd GD18: 40 ± 23.7 (10), P<0.01	
					Slope, distance vs cumulative radioactivity 25 min after intraduodenal ⁵¹ Cr	NP: -13.5 ± 4.7 (10) GD12: -13.4 ± 3.2 (10), nsd GD18: -12.8 ± 4.1 (10), nsd	
					SI transit 25 min after intraduodenal ⁵¹ Cr, geometric center (segment # of 10)	NP: 5.9 ± 2.5 (10) GD12: 5.7 ± 2.8 (10), nsd GD18: 3.7 ± 2.5 (10), P<0.01	
Ryan et al. 1987; guinea pig; non-rand exp [310]	N/S	Ad lib	NP, GD50- 55 (69-71 d)	Gastric emptying/SI motility	Gastric emptying, time after 1 mL intra gastric ⁵¹ Cr-labelled saline (% remaining)	5 min	NP: 68.9 ± 16.3 (5-7) GD50-55: 92.2 ± 4.7 (5-7), P<0.05
						15 min	NP: 31.1 ± 14.5 (5-7) GD50-55: 74.2 ± 13.6 (5-7), P<0.05
						30 min	NP: 21.7 ± 10.3 (5-7) GD50-55: 48.2 ± 11.9 (5-7), P<0.05
						60 min	NP: 13.8 ± 4.7 (5-7) GD50-55: 32.7 ± 9.4 (5-7), P<0.05

Sabet Sarvestani 2015; rat (Sprague-Dawley); rand exp [423]	Standard laboratory chow	Ad lib	GD7, GD14, GD21 (22 d)	Duodenal anatomy, Jejunal anatomy, Ileal anatomy	Villi length (µm)	Duodenum	GD7: 475 ± 90 (6) GD14: 350 ± 15 (6), P<0.05 vs GD7 GD21: 425 ± 15 (6), nsd vs GD7
						Jejunum	GD7: 280 ± 30 (6) GD14: 400 ± 30 (6), P<0.05 vs GD7 GD21: 530 ± 25 (6), P<0.05 vs GD7
						Ileum	GD7: 310 ± 90 (6) GD14: 220 ± 15 (6), P<0.05 vs GD7 GD21: 250 ± 15 (6), P<0.05 vs GD7
					Villi width (µm)	Duodenum	GD7: 100 ± 15 (6) GD14: 170 ± 30 (6), P<0.05 vs GD7 GD21: 225 ± 30 (6), P<0.05 vs GD7
						Jejunum	GD7: 70 ± 30 (6) GD14: 130 ± 90 (6), P<0.05 vs GD7 GD21: 215 ± 50 (6), P<0.05 vs GD7
						Ileum	GD7: 110 ± 50 (6) GD14: 75 ± 25 (6), nsd vs GD7 GD21: 130 ± 50 (6), nsd vs GD7
					Lamina propria thickness (µm)	Duodenum	GD7: 270 ± 30 (6) GD14: 260 ± 40 (6), nsd vs GD7 GD21: 270 ± 90 (6), nsd vs GD7
						Jejunum	GD7: 100 ± 15 (6) GD14: 220 ± 40 (6), P<0.05 vs GD7 GD21: 230 ± 70 (6), P<0.05 vs GD7
						Ileum	GD7: 190 ± 70 (6) GD14: 220 ± 40 (6), nsd vs GD7 GD21: 170 ± 30 (6), nsd vs GD7

					Tunica muscularis thickness (μm)	Duodenum	GD7: 135 ± 25 (6) GD14: 140 ± 15 (6), nsd vs GD7 GD21: 155 ± 50 (6), nsd vs GD7
						Jejunum	GD7: 60 ± 10 (6) GD14: 120 ± 15 (6), $P < 0.05$ vs GD7 GD21: 125 ± 15 (5), $P < 0.05$ vs GD7
						Ileum	GD7: 110 ± 25 (6) GD14: 150 ± 25 (6), nsd vs GD7 GD21: 100 ± 25 (6), nsd vs GD7
					1 st layer of tunica muscularis thickness (μm)	Duodenum	GD7: 90 ± 25 (6) GD14: 85 ± 35 (6), nsd vs GD7 GD21: 105 ± 25 (6), nsd vs GD7
						Jejunum	GD7: 35 ± 25 (6) GD14: 75 ± 30 (6), $P < 0.05$ vs GD7 GD21: 80 ± 15 (6), $P < 0.05$ vs GD7
						Ileum	GD7: 65 ± 50 (6) GD14: 90 ± 35 (6), nsd vs GD7 GD21: 60 ± 30 (6), nsd vs GD7
					2 nd layer of tunica muscularis thickness (μm)	Duodenum	GD7: 45 ± 12 (6) GD14: 54 ± 12 (6), nsd vs GD7 GD21: 57 ± 30 (6), nsd vs GD7
						Jejunum	GD7: 22 ± 10 (6) GD14: 50 ± 8 (6), $P < 0.05$ vs GD7 GD21: 38 ± 5 (6), $P < 0.05$ vs GD7
						Ileum	GD7: 41 ± 15 (6) GD14: 53 ± 12 (6), nsd vs GD7 GD21: 36 ± 8 (6), nsd vs GD7

Sandhar 1992; human; prosp cohort [299]	N/S	Fasted 4 h prior to study	NP, 37-40 weeks (280 d)	Gastric emptying/SI motility	Time to 50% emptying after 400 mL distilled water (min)	NP: 15 ± 19 (10) 37-40 weeks: 15 ± 17 (10), nsd
Schachter 1960; rat (N/S); non- rand exp [271]	N/S	N/S	NP, 3 rd week (22 d)	Direct measure of nutrient uptake – ex vivo	Proximal duodenal active transport of ⁴⁵ Ca (⁴⁵ Ca concentration ratio inside/outside)	NP: 2.0 ± 2.6 (7) 3 rd week: 4.6 ± 2.6 (7), P<0.001
Schachter 1970; rat (N/S); non- rand exp [424]	N/S	N/S	NP, 3 rd week (22 d)	Direct measure of nutrient uptake – ex vivo	Net transfer of total Ca to serosal surface, duodenum (μmol·sac per hr ⁻¹)	NP: 0.18 (20) 3 rd week: 0.24 (20), text states increased
					Net transfer of Ca ions to serosal surface, duodenum (μmol·sac per hr ⁻¹)	NP: 0.035 (20) 3 rd week: 0.08 (20), text states increased
Scott 1983; rat (Sprague- Dawley); non- rand exp [317]	Standard pelleted rat diet	Ad lib, fasted overnight before recordings	NP, GD12-18 (22 d)	Gastric emptying/SI motility	Mean interval between contractions, jejunum- ileum (min)	NP: 12.61 ± 1.79 (10) GD12-18: 14.08 ± 2.21 (15), nsd
					Coefficient of variation of contraction interval times, jejunum-ileum	NP: 0.248 (10) GD12-18: 0.401 (15), P<0.05

Scott 1989; guinea pig; non-rand exp [319]	N/S	N/S	NP, GD30-40 (65 d)	Gastric emptying/SI motility	Ileal maximal tension (g·mg ⁻¹ dry weight)	NP: 10.0 ± 4.5 (20) GD30-40: 5.8 ± 1.4 (8), P<0.05		
					Ileal EC ₅₀ values for carbachol stimulated muscle-strips (M)	NP: 13.9 x 10 ⁻⁷ ± 4.6 x 10 ⁻⁷ (20) GD30-40: 11.6 x 10 ⁻⁷ ± 1.4 x 10 ⁻⁷ (8), nsd		
Şensoy 2019; mouse (Swiss Albino); non-rand exp [425]	N/S	Ad lib	NP, GD3, GD10, GD17 (19-21 d)	Whole SI anatomy, Duodenal anatomy, Jejunal anatomy, Ileal anatomy	Relative intestine weight (%)	NP: 11.77 ± 1.49 (6) GD3: 12.64 ± 1.37 (6), nsd GD10: 12.66 ± 3.01 (6), nsd GD17: 14.65 ± 1.45 (6), nsd		
					Villus length (µm)	Proximal duodenum	NP: 468 ± 87 (6) GD3: 502 ± 22 (6), nsd GD10: 414 ± 64 (6), nsd GD17: 400 ± 82 (6), nsd	
						Mid-jejunum	NP: 400 ± 89 (6) GD3: 366 ± 48 (6), nsd GD10: 475 ± 49 (6), P<0.05 GD17: 310 ± 67 (6), nsd	
						Mid-ileum	NP: 281 ± 85 (6) GD3: 302 ± 21 (6), nsd GD10: 256 ± 19 (6), nsd GD17: 181 ± 10 (6), P<0.05	
					Villus width (µm)	Proximal duodenum	NP: 93 ± 5 (6) GD3: 90 ± 21 (6), nsd GD10: 100 ± 12 (6), nsd GD17: 98 ± 20 (6), nsd	
						Mid-jejunum	NP: 84 ± 12 (6) GD3: 82 ± 18 (6), nsd	

						GD10: 89 ± 11 (6), nsd GD17: 70 ± 13 (6), nsd
					Mid-ileum	NP: 81 ± 10 (6) GD3: 90 ± 17 (6), nsd GD10: 80 ± 10 (6), nsd GD17: 64 ± 15 (6), nsd
				Crypt depth (µm)	Proximal duodenum	NP: 112 ± 14 (6) GD3: 127 ± 12 (6), nsd GD10: 148 ± 11 (6), P<0.05 GD17: 134 ± 23 (6), P<0.05
					Mid-jejunum	NP: 132 ± 26 (6) GD3: 145 ± 35 (6), nsd GD10: 142 ± 20 (6), nsd GD17: 134 ± 22 (6), nsd
					Mid-ileum	NP: 140 ± 14 (6) GD3: 142 ± 19 (6), nsd GD10: 166 ± 10 (6), P<0.05 GD17: 109 ± 19 (6), P<0.05
				Muscle width (µm)	Proximal duodenum	NP: 23.8 ± 3.9 (6) GD3: 27.5 ± 4.3 (6), nsd GD10: 38.2 ± 4.4 (6), P<0.05 GD17: 32.8 ± 6.8 (6), P<0.05
					Mid-jejunum	NP: 27.4 ± 4.5 (6) GD3: 49.4 ± 4.2 (6), P<0.05 GD10: 41.6 ± 7.1 (6), P<0.05 GD17: 40.0 ± 7.4 (6), P<0.05
					Mid-ileum	NP: 30.6 ± 7.4 (6)

							GD3: 39.4 ± 5.2 (6), P<0.05 GD10: 55.6 ± 5.7 (6), P<0.05 GD17: 33.2 ± 8.8 (6), nsd
					Villus height: crypt depth	Proximal duodenum	NP: 4.22 ± 0.78 (6) GD3: 3.84 ± 0.61 (6), nsd GD10: 2.51 ± 0.49 (6), P<0.05 GD17: 3.22 ± 0.98 (6), P<0.05
				Mid-jejunum		NP: 3.07 ± 0.44 (6) GD3: 2.66 ± 0.83 (6), nsd GD10: 3.20 ± 0.32 (6), nsd GD17: 2.38 ± 0.71 (6), nsd	
				Mid-ileum		NP: 2.32 ± 0.66 (6) GD3: 2.15 ± 0.32 (6), nsd GD10: 1.83 ± 0.34 (6), nsd GD17: 1.70 ± 0.27 (6), nsd	
Simpson 1988; human; cross sectional [301]	N/S	Fasted 4 h before study	NP, 8-11 weeks, 12-14 weeks (280 d)	Gastric emptying/SI motility	Paracetamol AUC after 1.5 g oral paracetamol (µg·ml ⁻¹ ·h)	0-1 h	NP: 19 ± 11 (14) 8-11 weeks: 15 ± 8 (16), nsd 12-14 weeks: 11 ± 10 (12), P<0.05
						0-2 h	NP: 37 ± 11 (14) 8-11 weeks: 32 ± 12 (16), nsd 12-14 weeks: 25 ± 10 (12), P<0.05
					Paracetamol peak concentration (µg·ml ⁻¹)	NP: 34.4 ± 16.1 (14) 8-11 weeks: 26.8 ± 10.8 (16), nsd 12-14 weeks: 21.4 ± 7.6 (12), P<0.05	
					Time to peak paracetamol concentration (min)	NP: 45.0 ± 22.1 (14) 8-11 weeks: 46.4 ± 32.4 (16), nsd 12-14 weeks: 71.9 ± 31.9 (12), P<0.05	

Stanley 1995; human; prosp cohort [238]	N/S	N/S, Fasted 8 h before study. Test meal: 2 Crunch & Slim bars + 60g Vitafood (Boots, Nottingham) made up with 200 ml water eaten over 10 min (59 g carbohydrate, 17.9 g protein, 21.2 g fat)	14-16 weeks, 26-28 weeks, 36-38 weeks (280 d)	Indirect measure of nutrient uptake – in vivo, gastric emptying/SI motility	Time at maximal concentration of paracetamol after 1.5 g oral paracetamol (min)	14-16 weeks: 114 ± 30 (10) 26-28 weeks: 113 ± 22 (9), N/S vs 14-16 weeks 36-38 weeks: 118 ± 22 (10), N/S vs 14-16 weeks
					Maximal concentration of paracetamol (µg·ml ⁻¹)	14-16 weeks: 22 ± 5.1 (10) 26-28 weeks: 20 ± 6.3 (9), N/S vs 14-16 weeks 36-38 weeks: 21 ± 5.0 (10), N/S vs 14-16 weeks
					Time at maximal concentration of glucose after test meal (min)	14-16 weeks: 88 ± 49 (10) 26-28 weeks: 66 ± 51 (9), N/S vs 14-16 weeks 36-38 weeks: 66 ± 48 (10), N/S vs 14-16 weeks
					Maximal concentration of glucose after test meal (min)	14-16 weeks: 5.6 ± 0.52 (10) 26-28 weeks: 5.4 ± 0.50 (9), N/S vs 14-16 weeks 36-38 weeks: 6.1 ± 0.72 (10), N/S vs 14-16 weeks
					AUC _{0-60 min} of glucose after test meal (mmol·min·L ⁻¹)	14-16 weeks: 281 ± 56 (10) 26-28 weeks: 284 ± 78 (9), N/S vs 14-16 weeks 36-38 weeks: 316 ± 84 (10), P<0.05 vs 14-16 weeks

Swanson 1983; human; cross sectional [292]	Diets each ~16 mg Zn/day. Diet A, 70% of total Zn from animal products (meat & milk), 30% from plant sources (cereals, nuts and vegetables. Diet B, Zn % from each source reversed.	N/S	NP, 28 ± 5 weeks, 30 ± 4 weeks (280 d)	Direct measure of nutrient uptake – in vivo	⁷⁰ Zinc absorption, stable isotope method (%)	Diet A	NP: 23.8 ± 4.5 (5) 28 ± 5 weeks: 24.2 ± 4.9 (5), nsd
						Diet B	NP: 25.4 ± 3.8 (5) 30 ± 4 weeks: 26.6 ± 7.2 (4), nsd
Swanston-Flatt 1980; rat (N/S); non-rand exp [426]	N/S	Ad lib	NP, GD18 (22 d)	Direct measure of nutrient uptake – ex vivo	Folic acid transfer, proximal jejunum (pmol·h ⁻¹ ·mg dry weight ⁻¹)	NP: 18.49 ± 9.10 (5) GD18: 15.49 ± 3.87 (5), nsd	
					Corrected folic acid transfer, proximal jejunum (pmol·h ⁻¹ ·mg dry weight ⁻¹)	NP: 12.92 ± 6.60 (5) GD18: 10.51 ± 2.39 (5), nsd	
Szilagyi 1996; human; non-rand exp [322]	N/S	Fasted 12-14 h before test	NP, 22-36 weeks (280 d)	Gastric emptying/SI motility	Oro-caecal transit time (min)	NP: 63.5 ± 35.9 (17) 22-36 weeks: 99.2 ± 42.7 (30), P=0.0042	

Takeuchi 1984; rat (Donryu); non- rand exp [375]	N/S	Fasted 18 h prior to gastric secretion studies	NP, GD5, GD10, GD20 (N/S)	Digestive enzyme activity/ expression	Volume of gastric secretion (mL)	NP: 3.9 ± 1.6 (10) GD5: 3.8 ± 0.9 (10), nsd GD10: 6.0 ± 1.9 (10), P<0.05 GD20: 9.0 ± 2.5 (10), P<0.05
					Acidity of gastric secretion (mEq·L ⁻¹)	NP: 120 ± 22 (10) GD5: 114 ± 9 (10), nsd GD10: 124 ± 16 (10), nsd GD20: 138 ± 13 (10), P<0.05
					Pepsin activity in gastric secretion (mg·ml ⁻¹)	NP: 26 ± 3 (10) GD5: 25 ± 3 (10), nsd GD10: 22 ± 3 (3), P<0.05 GD20: 13 ± 3 (3), P<0.05
					Acid output in gastric secretion (μEq·h ⁻¹)	NP: 120 ± 47 (10) GD5: 110 ± 32 (10), nsd GD10: 180 ± 63 (10), P<0.05 GD20: 300 ± 63 (10) P<0.05
					Pepsin output in gastric secretion (mg·h ⁻¹)	NP: 140 ± 47 (10) GD5: 130 ± 63 (10), nsd GD10: 180 ± 63 (10), P<0.05 GD20: 160 ± 47 (10), nsd
					Antral gastrin (μg·g ⁻¹)	NP: 4.6 ± 1.6 (8) GD5: 3.8 ± 1.6 (8), nsd GD10: 3.9 ± 2.0 (8), nsd GD20: 4.8 ± 2.0 (8), nsd

Teerapornpun takit 2014; rat (Sprague-Dawley); non-rand exp [427]	Standard chow containing 1.0% Ca, 0.64% P, 3,000 IU/kg vitamin D (CP Co., Ltd., Bangkok, Thailand)	Ad lib	NP, GD21 (22 d)	Nutrient transporter gene expression	Duodenal mucosal gene expression, fold change from control (microarray)	<i>Atp1a3</i>	NP: 1 (3) GD21: 1.52 (3), P<0.05
						<i>Atp1b4</i>	NP: 1 (3) GD21: 1.86 (3), P<0.05
						<i>Slc5a1</i>	NP: 1 (3) GD21: 1.50 (3), P<0.05
						<i>Slc2a5</i>	NP: 1 (3) GD21: 1.80 (3), P<0.05
						<i>Trmp6</i>	NP: 1 (3) GD21: 2 (3), P<0.05
						<i>Trmp7</i>	NP: 1 (3) GD21: 1.50 (3), P<0.05
						<i>ZO-1</i>	NP: 1 (3) GD21: 1.62 (3), P<0.05
						<i>Cldn2 no.3</i>	NP: 1 (3) GD21: 1.52 (3), P<0.05
						<i>Cldn9</i>	NP: 1 (3) GD21: 1.56 (3), P<0.05
						<i>Calbindin-D28k</i>	NP: 1 (3) GD21: 1.57 (3), P<0.05
					<i>Trpv6 no.3</i>	NP: 1 (3) GD21: 1.57 (3), P<0.05	
					Duodenal mucosal gene expression, fold change from control (RT-PCR)	<i>Trpv6</i>	NP: 1 (7-10) GD21: 2.60 (7-10), P<0.05
						<i>ZO-1</i>	NP: 1 (7-10) GD21: 3.77 (7-10), P<0.05
<i>Trpm6</i>	NP: 1 (7-10)						

							GD21: 2.88 (7-10), P<0.05
						Ca _v 1.3	NP: 1 (7-10) GD21: 1.07 (7-10), nsd
Toraason 1983; rat (Sprague- Dawley); non- rand exp [267]	Purina rat chow (1.2% Ca; 0.8% P; 3.3 IU/g vitamin D)	Ad lib	NP, GD13±2 (22 d)	Direct measure of nutrient uptake – in vivo, Duodenal anatomy, Ileal anatomy	Duodenal mucosal dry weight (mg·cm ⁻¹)	NP: 5.4 ± 1.2 (9) GD13±2: 8.7 ± 1.7 (8), P<0.05	
					Ileal mucosal dry weight (mg·cm ⁻¹)	NP: 4.3 ± 1.5 (9) GD13±2: 6.6 ± 1.4 (8), P<0.05	
					Duodenal net calcium absorption (µg·cm ⁻¹ ·20 min ⁻¹)	NP: 1.46 ± 0.78 (9) GD13±2: 2.80 ± 1.47 (8), P<0.05	
					Distal ileal net calcium absorption (µg·cm ⁻¹ ·20 min ⁻¹)	NP: 0.02 ± 0.84 (9) GD13±2: 0.24 ± 1.24 (8), nsd	
					Duodenal net calcium absorption (µg·mg dry mucosa ⁻¹ ·20 min ⁻¹)	NP: 0.26 ± 0.12 (9) GD13±2: 0.35 ± 0.23 (8), nsd	
					Distal ileal net calcium absorption (µg·mg dry mucosa ⁻¹ ·20 min ⁻¹)	NP: 0.01 ± 0.84 (9) GD13±2: 0.05 ± 0.20 (8), nsd	

Uçkan 2001; human; cross sectional [280]	N/S	Overnight fast before study	NP, 1 st Tri, 2 nd Tri, 3 rd Tri (280 d)	Direct measure of nutrient uptake – in vivo	Plasma zinc – basal, 2 and 3 h after 120 mg ZnSO ₄ orally, containing 22.5 mg Zn (µg·dL ⁻¹)	Fasting	NP: 73.3 ± 7.5 (7) 1 st Tri: 67.5 ± 8.8 (6), nsd 2 nd Tri: 62.8 ± 11.1 (10), nsd 3 rd Tri: 65.7 ± 14.9 (9), nsd Combined pregnant: 65 ± 10, P<0.05
						2 h	NP: 129.8 ± 17.0 (7) 1 st Tri: 127.0 ± 24.3 (6), nsd 2 nd Tri: 114.1 ± 27.9 (10), nsd 3 rd Tri: 109.9 ± 10.7 (9), nsd
						3 h	NP: 127.3 ± 15.0 (7) 1 st Tri: 126.2 ± 30.1 (6), nsd 2 nd Tri: 115.6 ± 20.0 (10), nsd 3 rd Tri: 112.4 ± 19.8 (9), nsd
Uriu-Hare 1988; rat (Sprague- Dawley); non- rand exp [281]	Semi-purified control diet containing 25 µg Zn/g, 21% protein	Fasted 4 h prior to experiment	GD12, GD18 (22 d)	Direct measure of nutrient uptake – in vivo	Apparent absorption of ⁶⁵ Zn after gavage with 0.5 mL containing 0.125 g of low Zn diet labelled with ⁶⁵ Zn (%)	GD12: 40.7 ± 10.6 (7) GD18: 46.6 ± 23.5 (6), N/S vs GD12	
Van Cromphaut 2003; mouse (VDR WT); non-rand exp [428]	Normal diet (1.1% Ca, 0.8% P, 0% lactose (Standard; Carfil, Oud- Turnhout, Belgium)	N/S	NP, GD18.5 (21 d)	Nutrient transporter gene expression, Nutrient transporter protein expression	Proximal duodenal protein expression, Calbindin-D9k (% of total protein)	NP: 2.9 ± 0.8 (8) GD18.5: 4.5 ± 1.4 (8), P<0.05	
						<i>Trpv6</i>	NP: 368 ± 339 (8) GD18.5: 4333 ± 12256 (8), P<0.05
						<i>Trpv5</i>	NP: 1.0 ± 0.6 (8) GD18.5: 0.9 ± 0.3 (8), nsd
					<i>Calbindin-D9k</i> (% of NP)	NP: 100 ± 57 (8) GD18.5: 250 ± 141 (8), P<0.05	

						<i>PMCA1b</i> (% of NP)	NP: 100 ± 28 (8) GD18.5: 190 ± 99 (8), P<0.05
Van Dijk 1983; guinea pig (Albino); non-rand exp [275]	Pellets and green vegetables	Fasted for 24 h prior to iron absorption studies	NP, GD55 (65 d)	Direct measure of nutrient uptake – in vivo	Intestinal uptake of ⁵⁹ Fe(II) at time after oral iron, amount N/S (%)	4 h	NP: 3.8 ± 3.4 (5-10) GD55: 36.0 ± 23.5 (5-7), text states increase
						24 h	NP: 7.2 ± 4.2 (5-10) GD55: 47.5 ± 32.4 (5-7), text states increase
					Intestinal absorption of ⁵⁹ Fe(II) at time after oral iron, amount N/S (%)	4 h	NP: 1.4 ± 1.8 (5-10) GD55: 11.8 ± 10.1 (5-7), text states increase
						24 h	NP: 3.5 ± 4.7 (5-10) GD55: 33.8 ± 23.5 (5-7), text states increase
Vargas Zapata 2004; human; prosp cohort [429]	N/S	Standard breakfast; 50 g French bread, 10 g butter, 50 ml whole milk + 50 ml coffee, total Ca intake 74 mg. Fasted overnight	10-12 weeks, 34-36 weeks (280 d)	Direct measure – in vivo	Intestinal calcium absorption, double isotope method with standard breakfast (%)	10-12 weeks: 69.7 ± 16.2 (9) 34-36 weeks: 87.6 ± 13.5 (9), P<0.05 vs 10-12 weeks	

		before Ca absorption study					
Velayudhan 2019; pig (Yorkshire-Landrace female x Duroc male); rand exp [254]	Cornstarch-based diet containing 31.3% canola meal as the only source of amino acids	3 kg/day, offered as 2 equal meals of dry mash at 0700 and 1300 h	MP [GD or weeks N/S], LP [GD or weeks N/S] (115 d)	Direct measure of nutrient uptake – in vivo	Standardised ileal digestibility, crude protein (%)	MP: 79.9 ± 2.3 (8) LP: 79.7 ± 2.7 (8), N/S	
					Standardised ileal digestibility, indispensable amino acids (%)	Arginine	MP: 88.7 ± 2.5 (8) LP: 89.8 ± 2.1 (8), N/S
						Histidine	MP: 93.5 ± 1.6 (8) LP: 92.6 ± 2.1 (8), N/S
						Isoleucine	MP: 85.9 ± 3.1 (8) LP: 86.0 ± 3.1 (8), N/S
						Leucine	MP: 88.8 ± 2.0 (8) LP: 89.5 ± 1.8 (8), N/S
						Lysine	MP: 86.9 ± 1.7 (8) LP: 87.0 ± 2.3 (8), N/S
						Methionine	MP: 91.6 ± 2.1 (8) LP: 92.9 ± 1.5 (8), N/S
						Phenylalanine	MP: 88.7 ± 3.8 (8) LP: 89.6 ± 1.8 (8), N/S
						Threonine	MP: 84.7 ± 3.6 (8) LP: 83.9 ± 7.4 (8), N/S
						Tryptophan	MP: 87.5 ± 5.4 (8) LP: 88.8 ± 1.8 (8), N/S
Valine	MP: 85.8 ± 2.8 (8) LP: 86.1 ± 2.2 (8), N/S						
					Alanine	MP: 85.8 ± 2.6 (8)	

						LP: 87.5 ± 4.1 (8), N/S	
					Standardised ileal digestibility, dispensable amino acids (%)	MP: 84.8 ± 3.3 (8) LP: 82.5 ± 6.7 (8), N/S	
						Cysteine	MP: 87.0 ± 4.3 (8) LP: 87.5 ± 3.7 (8), N/S
						Glycine	MP: 90.2 ± 1.4 (8) LP: 91.0 ± 1.9 (8), N/S
						Glutamic acid	MP: 90.6 ± 1.4 (8) LP: 93.6 ± 1.2 (8), N/S
						Proline	MP: 101.8 ± 13 (8) LP: 103.0 ± 22.4 (8), N/S
						Serine	MP: 88.8 ± 2.1 (8) LP: 90.6 ± 1.6 (8), N/S
						Tyrosine	MP: 86.5 ± 3.3 (8) LP: 86.1 ± 4.0 (8), N/S

Villard 1986; rat (Norwegian Hooded – experiment 1 & Sprague- Dawley – experiment 2); non-rand exp [379]	Purified diet: (g/kg): sucrose 706, casein 'low in vitamins' (British Drug Houses, Poole, Dorset) 210, Briggs salt mixture 50, arachis oil 30, choline chloride 2, cystine 1.5, calcium pantothenate 0.02, thiamin hydrochloride 0.004, riboflavin 0.015, pyridoxine hydrochloride 0.009, nicotinamide 0.025, biotin 0.001, folic acid 0.001, cyanocobalamin 5×10^{-5} , alpha-tocopherol 0.16, menadione 0.009, vitamin D2 7.5×10^{-6} with addition of retinyl acetate to yield 1.55 mg retinol/kg diet.	N/S	NP, GD7, GD20 (22 d)	Digestive enzyme activity/ expression	Carotene dioxygenase activity, SI mucosa (μmol retinal + retinol formed·mg ⁻¹ protein·min ⁻¹ $\times 10^{-7}$) – experiment 1	NP: 5.4 ± 0.8 (7) GD7: 4.3 ± 0.4 (4), N/S GD20: 4.9 ± 1.0 (11), N/S
					Carotene dioxygenase activity, SI mucosa (μmol retinal + retinol formed·mg ⁻¹ protein·min ⁻¹ $\times 10^{-7}$) – experiment 2	NP: 2.4 ± 0.3 (7) GD7: 2.4 ± 0.6 (4), N/S GD20: 2.8 ± 0.6 (10), N/S

West 2018; rat (Sprague- Dawley); non- rand exp [363]	Harlan Teklad LM-485 Mouse/Rat Diet (0.3% Na, 0.8% K)	Ad lib.	NP, GD19-21 (22 d)	Nutrient transporter gene expression, Nutrient transporter protein expression	Colon <i>BK-α</i> mRNA expression (% of virgin control)	NP: 100 ± 24 (6) GD19-22: 85 ± 12 (6), nsd
					Distal colon BK-α protein abundance (% of virgin control)	NP: 100 ± 24 (6) GD19-22: 85 ± 12 (6), P<0.05
Whitehead 1993; human; cross sectional [303]	N/S	Fasted >4 h before study	NP, 8-10 weeks, 16-24 weeks, ≥34 weeks (280 d)	Gastric emptying/SI motility	Maximum concentration of paracetamol after 1.5 g oral paracetamol (mg·L ⁻¹)	NP: median 20.8, range 8.8-64.5 (32) 8-10 weeks: median 21., range 3.4-39.6 (18), nsd 16-24 weeks: median 25.7, range 16.5-33.1 (10), nsd >34 weeks: median 21.0, range 4.1-37.2 (36), nsd
					Time of maximum concentration of paracetamol (min)	NP: median 40, range 10-120 (32) 8-10 weeks: median 45, range 10-120 (18), nsd 16-24 weeks: median 30, range 10-60 (10), nsd >34 weeks: median 40, range 10-120 (36), nsd
					Paracetamol absorption, AUC _{0-120 min} (mg·L ⁻¹ ·h ⁻¹)	NP: median 13.5, range 5.5-28.8 (32) 8-10 weeks: median 14.2, range 1.4-27.2 (18), nsd 16-24 weeks: median 13.6, range 11.3-14.8 (10), nsd >34 weeks: median 12.6, range 2.4-20.3 (36), nsd

Wróbel 1980; rat (Wistar); non-rand exp [272]	Standard LSM diet, 0.3% Ca	N/S	NP, GD7, GD14, GD21 (22 d)	Direct measure of nutrient uptake – ex vivo	Duodenal active calcium transport at 0900h (nmol·90 min ⁻¹)	NP: 100 ± 86 (4-6) GD7: 115 ± 86 (4-6), N/S GD14: 260 ± 70 (4-6), N/S GD21: 350 ± 122 (4-6), N/S	
					Proximal jejunum active calcium transport at 0900h (segments 2-4, nmol·90 min ⁻¹)	Segment 2 (most proximal):	NP: 10 ± 25 (4-6) GD7: 80 ± 70 (4-6), N/S GD14: 250 ± 200 (4-6), N/S GD21: 300 ± 86 (4-6), N/S
						Segment 3:	NP: 2 ± 25 (4-6) GD7: 35 ± 25 (4-6), N/S GD14: 100 ± 60 (4-6), N/S GD21: 200 ± 122 (4-6), N/S
						Segment 4:	NP: 0 ± 0 (4-6) GD7: 2 ± 5 (4-6), N/S GD14: 25 ± 25 (4-6), N/S GD21: 75 ± 86 (4-6), N/S
					Duodenal active calcium transport at 2100h (segment 1, nmol·90 min ⁻¹)	NP: 345 ± 86 (4-6) GD7: 300 ± 61 (4-6), N/S GD14: 290 ± 122 (4-6), N/S GD21: 320 ± 145 (4-6), N/S	
					Proximal jejunum active calcium transport at 2100h (segments 2-4, nmol·90 min ⁻¹)	Segment 2 (most proximal):	NP: 220 ± 86 (4-6) GD7: 190 ± 86 (4-6), N/S GD14: 280 ± 200 (4-6), N/S GD21: 340 ± 200 (4-6), N/S
Segment 3:	NP: 75 ± 25 (4-6), N/S GD7: 60 ± 40 (4-6), N/S GD14: 120 ± 70 (4-6), N/S						

						GD21: 200 ± 86 (4-6), N/S
					Segment 4:	NP: 50 ± 40 (4-6) GD7: 30 ± 25 (4-6), N/S GD14: 35 ± 25 (4-6), N/S GD21: 100 ± 70 (4-6), N/S
Younoszai 1976; rat (Holtzman Albino); non- rand exp [329]	Commercial stock diet; Wayne Lab Blox (Allied Mills, Libertyville, Illinois)	N/S	NP, GD22 (22 d)	Whole SI anatomy, Digestive enzyme activity/ expression	SI weight (g)	NP: 6.3 ± 1.4 (8) GD22: 7.1 ± 0.6 (9), nsd
					SI length (cm)	NP: 114 ± 14 (8) GD22: 123 ± 3 (9), P<0.005
					Lactase specific activity, SI mucosa (µmol disaccharide hydrolysed·min ⁻¹ ·g protein ⁻¹)	NP: 4.1 ± 0.8 (8) GD22: 6.1 ± 1.2 (9), P<0.05
					Sucrase specific activity, SI mucosa (µmol disaccharide hydrolysed·min ⁻¹ ·g protein ⁻¹)	NP: 23 ± 4 (8) GD22: 29 ± 9 (9), nsd
					Maltase specific activity, SI mucosa (µmol disaccharide hydrolysed·min ⁻¹ ·g protein ⁻¹)	NP: 109 ± 50 (8) GD22: 131 ± 30 (9), nsd

Zherebak 2018; rat (White nonlinear); non-rand exp [294]	Laboratory chow	Ad lib then test 12h after last meal	NP, GD3, GD4, GD5, GD7 (22 d)	Gastric emptying/Sl motility	Spontaneous gastric motility (index of gastric motility)	NP: 146.9 ± 25.9 (10) GD3: 110.4 ± 11.7 (10), P<0.01 GD4: 108.1 ± 14.9 (10), P<0.01 GD5: 102.2 ± 10.4 (10), P<0.01 GD7: 103.8 ± 10.8 (10), P<0.01
Zhu 1998; rat (Holtzman Sprague-Dawley); non-rand exp [365]	Rat lab diet: 1% Ca, 0.74% P, no. 5012 (PMI Feeds, Inc., St. Louis, MO)	N/S	NP, GD7, GD14, GD21 (22 d)	Nutrient transporter gene expression	Duodenal <i>Calbindin-D9K</i> mRNA (AU, relative to beta-actin, ratio to NP)	NP: 1.0 (4) GD7: 1.1 ± 0.4 (4), nsd GD14: 1.7 ± 0.5 (4), nsd GD21: 2.3 ± 0.7 (4), P<0.01
					Duodenal <i>PMCA1</i> mRNA (AU, relative to beta-actin, ratio to NP)	NP: 1.0 (4) GD7: 1.1 ± 0.8 (4), nsd GD14: 1.7 ± 1.0 (4), nsd GD21: 2.4 ± 1.2 (4), P<0.05

Ad lib, ad libitum; *Asbt*, sodium/bile cotransporter (encoded by *Slc10a2*); *Atp1a3*, ATPase Na⁺/K⁺ Transporting Family Member alpha 3 (Na,K-ATPase subunit); *Atp1b4*, ATPase Na⁺/K⁺ Transporting Family Member Beta 4 (Na,K-ATPase subunit); AU, arbitrary units; AUC, area under the curve; *BK-α*, big potassium channel; *CaBP*, calcium binding protein; *CCK*, cholecystokinin; *Cldn2*, claudin 2; *Cldn9*, claudin 9; *CRBP*, cellular retinol binding protein; *Dcytb*, duodenal cytochrome b (ferrireductase); *DMT1*, divalent metal transporter 1 (brush border iron transporter); *EP*, early pregnant; *FITC*, Fluorescein isothiocyanate; *FPN*, Ferroportin, encoded by *Ireg1/Slc401*; *GAPDH*, glyceraldehyde-3-phosphate dehydrogenase; *GD*, gestational day; *GIP*, glucose-dependent insulinotropic polypeptide; *Hp*, hephaestin (iron oxidase); *HPRT*, hypoxanthine phosphoribosyltransferase 1; *IF*, intrinsic factor; *IF-Cbl*, intrinsic factor-cobalamin; *IQR*, inter-quartile range; *IRE*, iron responsive element; *Ireg*, iron regulated transporter 1 (encodes *FPN*), now known as *Slc40a1*; *IU*, international units; *LP*, late pregnant; *MP*, mid pregnant; *non-rand exp*, non-randomised experimental; *NP*, non-pregnant; *N/S*, not stated; *nsd*, no significant difference; *OGTT*, oral glucose tolerance test; *PMCA1b*, plasma membrane calcium ATPase; *ppm*, parts per million; *prosp cohort*, prospective cohort; *rand double-blinded*, randomised double-blinded; *rand exp*, randomised experimental; *RFU*, relative fluorescence units; *RT-PCR*, real time polymerase chain reaction; *S100g*, gene encoding calbindin-9k; *Sl*, small intestine; *Slc2a5*, solute carrier family 2 member 5 (encodes *GLUT5*); *Slc5a1*, solute carrier family 5 member 1 (encodes *SGLT1*); *Slc13a1*, solute carrier family 13 member 1 (apical Na⁺-sulphate cotransporter); *Slc26a1*, solute family 26 member 1 (sulphate/anion transporter); *Slc26a2*, solute carrier family 26 member 2 (diastrophic dysplasia sulphate transporter); *Slc26a3*, solute carrier family 26 member 3 (chloride-bicarbonate exchange transporter); *Slc26a6*, solute carrier family 26 member 6 (anion transporter); *Slc26a11*, solute carrier family 26 member 11 (Na-independent sulphate transporter); *Tri*, trimester; *Trmp6*, transient receptor potential cation channel, subfamily M, member 6

(magnesium channel subunit); Trmp7, transient receptor potential cation channel, subfamily M, member 7 (magnesium channel subunit); Trpv6, transient receptor potential cation channel subfamily V member 6 (calcium channel); ZnT1, zinc transporter 1; ZnT2, zinc transporter 2; ZnT4, zinc transporter 4; ZO1, also known as Tjp1, tight junction protein 1

4. CHAPTER 4: ACTIVE GLUCOSE TRANSPORT VARIES BY SMALL INTESTINAL REGION AND OESTROUS CYCLE STAGE IN C57BL/6 MICE

4.1. Overview

Sections 4.3-4.7 are taken directly from a scoping review protocol of which I am first author, and which has been published (Appendix 2, [430]). The content of these sections is unchanged as per University of Adelaide guidelines. Chapter 4 describes a series of experiments I performed to optimise and validate existing Ussing chamber methodology to characterise the region-specific contribution of SGLT1 to facilitated glucose transport by the small intestine. Once optimised, I then applied this methodology to characterise SGLT1-dependent glucose transport across the jejunum at each stage of the oestrous cycle in mice. As part of the optimisation and validation experiments described in this chapter, I performed all Ussing chamber experiments. This included tissue collection and data acquisition, validating the efficacy of the SGLT1-antagonist phlorizin and the use of dimethyl sulfoxide (DMSO) as a solvent for phlorizin. I also performed all Ussing chamber experiments in the oestrous cycle study. I was also involved in the analysis of the data generated, preparation of all figures and drafting of the manuscript. The data described in Chapter 4 has been published as a manuscript, of which I am first author (Appendix 2. [430]).

4.2. Statement of authorship - Active glucose transport varies by small intestinal region and oestrous cycle stage in C57BL/6 mice

Statement of Authorship

Title of Paper	Active glucose transport varies by small intestinal region and oestrous cycle stage in C57/BL6 mice
Publication Status	<input type="checkbox"/> Published <input checked="" type="checkbox"/> Accepted for Publication <input type="checkbox"/> Submitted for Publication <input type="checkbox"/> Unpublished and Unsubmitted work written in manuscript style
Publication Details	Overduin, T.S., Wardill, H.R., Young, R.L., Page, A.J., Gatford, K.L. 2023 Active glucose transport varies by small intestinal region and oestrous cycle stage in C57BL/6 mice. <i>Experimental Physiology in press</i>

Principal Author

Name of Principal Author (Candidate)	Sebastian Overduin		
Contribution to the Paper	Conception and design of research, performed experiments described within the manuscript, analysed experimental data presented within the manuscript, interpreted results presented within the manuscript, drafted, edited and approved final version of manuscript.		
Overall percentage (%)	50%		
Certification:	This paper reports on original research I conducted during the period of my Higher Degree by Research candidature and is not subject to any obligations or contractual agreements with a third party that would constrain its inclusion in this thesis. I am the primary author of this paper.		
Signature		Date	07/02/2023

Co-Author Contributions

By signing the Statement of Authorship, each author certifies that:

- i. the candidate's stated contribution to the publication is accurate (as detailed above);
- ii. permission is granted for the candidate to include the publication in the thesis; and
- iii. the sum of all co-author contributions is equal to 100% less the candidate's stated contribution.

Name of Co-Author	Hannah Wardill		
Contribution to the Paper	Contributed to project methodology/provided technical assistance, interpreted results presented within the manuscript, edited and approved final version of manuscript		
Signature		Date	08/03/23

Name of Co-Author	Richard Young		
Contribution to the Paper	Conception and design of research, interpreted results presented within the manuscript, edited and approved final version of manuscript.		

Signature		Date	07/03/2023
-----------	--	------	------------

Name of Co-Author	Amanda Page		
Contribution to the Paper	Conception and design of research, interpreted results presented within the manuscript, edited and approved final version of manuscript.		
Signature		Date	8/3/23

Name of Co-Author	Kathryn Gatford		
Contribution to the Paper	Conception and design of research, performed experiments described within the manuscript, analysed experimental data presented within the manuscript, interpreted results presented within the manuscript, drafted, edited and approved final version of manuscript.		
Signature		Date	8 March 2023

Chapter 4 is reproduced exactly as published with the exception of formatting, which has been changed to maintain consistency throughout the thesis. It has been published as:

Overduin TS, Wardill HR, Young RL, Page AJ, Gatford KL. Active glucose transport varies by small intestinal region and oestrous cycle stage in mice. *Exp Physiol*. 2023 Jun;108(6):865-873. doi: 10.1113/EP091040. Epub 2023 Apr 6. PMID: 37022128.
(Appendix 2)

4.3. Abstract

Food intake changes across the ovarian cycle in rodents and humans, with a nadir during the pre-ovulatory phase and a peak during the luteal phase. However, it is unknown whether the rate of intestinal glucose absorption also changes. We therefore mounted small intestinal sections from C57BL/6 female mice (8–9-week-old) in Ussing chambers and measured active *ex vivo* glucose transport via the change in short-circuit current (ΔI_{sc}) induced by glucose. Tissue viability was confirmed by a positive ΔI_{sc} response to 100 μ M carbachol following each experiment. Active glucose transport, assessed after addition of 5, 10, 25 or 45 mM D-glucose to the mucosal chamber, was highest at 45 mM glucose in the distal jejunum compared to duodenum and ileum ($P < 0.01$). Incubation with the sodium glucose-cotransporter 1 (SGLT1)-inhibitor phlorizin reduced active glucose transport in a dose-dependent manner in all regions ($P < 0.01$). Active glucose uptake induced by addition of 45 mM glucose to the mucosal chamber in the absence or presence of phlorizin were assessed in jejunum at each oestrous cycle stage (N = 9-10 mice per stage). Overall, active glucose uptake was lower at estrus compared to proestrus ($P = 0.025$). This study establishes an *ex vivo* method to measure region-specific glucose transport in the mouse small intestine. Our results provide the first direct evidence that SGLT1-mediated glucose transport in the jejunum changes across the ovarian cycle. The mechanisms underlying these adaptations in nutrient absorption remain to be elucidated.

4.4. Introduction

Digestion and absorption of nutrients occurs within the gastrointestinal tract, where complex organic molecules are progressively digested into smaller and simpler entities as they pass through the tract. Nutrient absorption begins in the duodenum and peaks in the jejunum [155]. The terminal ileum acts to brake intestinal motility in the presence of high nutrient concentrations to maximize nutrient uptake in the small intestine [158, 200]. The small intestine absorbs nutrients by passive and active transport, the latter via specific nutrient transporters [155, 158]. For example, active absorption of glucose is facilitated by sodium-dependent co-transporter-1 (SGLT1), a high affinity, low-capacity transmembrane protein located at the brush border membrane of absorptive enterocytes along the upper third of small intestinal villi [158]. SGLT1 accounts for ~90% of small intestinal glucose absorption under normal circumstances [431].

Food intake, appetite and the rate of gastric emptying change across the ovarian cycle in humans [432-434], rhesus monkeys [435] and rodents [436-438]. Indeed, energy intake is decreased by 10-20% in humans [432-434] and food intake is halved in rhesus monkeys in the follicular compared to the luteal phase of the menstrual cycle [435]. Feeding behaviors also change during the oestrous cycle in mice, with a nadir in the number of feeding bouts (10% lower) and amount of time spent eating per bout (30% lower) at proestrus compared to metestrus and diestrus [436]. These food intake behaviors are likely to be mediated, at least in part, by cyclic changes in circulating estrogen and progesterone concentrations. Whether nutrient absorption also changes during the ovarian cycle is less clear. Post-prandial blood glucose concentrations following a standardized meal are 15% lower during the follicular compared to the luteal phase in women [432], reflecting the combined effect of intestinal glucose uptake, hepatic first-pass extraction, insulin, and glucagon [439]. As glucose absorption is a major contributor to the increase in post-prandial glucose [439], higher post-prandial glucose concentrations during the luteal phase supports the hypothesis that intestinal glucose absorption is more rapid during this period than the follicular phase. Nevertheless, there is no direct evidence for this, reflecting the difficulties in interrogating this mechanism. We therefore optimized Ussing chamber methodology to directly measure active glucose transport across the mouse small intestine. We then used this method to characterize oestrous cycle differences in total and SGLT1-mediated active glucose uptake in the mouse jejunum, the region of highest active glucose uptake.

4.5. Materials and Methods

4.5.1. Ethics approval

All experiments conformed to the principles of Grundy [440], the ARRIVE 2.0 guidelines [441] and were conducted in accordance with the Australian Code of Practice for the Care and Use of Animals for Scientific Purposes [442]. All experiments were approved by the South Australian Health and Medical Research Institute Animal Ethics Committee (SAHMRI AEC approval: SAM-21-049). The initial number of mice (N=14) per condition provided 80% power at $\alpha=0.05$ to detect a 20% difference in short-circuit current responses to glucose, based on variation in pilot experiments. As outcome variation decreased with protocol optimization, fewer mice were required in latter experiments, as indicated below.

4.5.2. Mice

Adult C57BL/6JSAH female mice (8-10 weeks old) were sourced from SAHMRI Bioresources and housed in home cages in groups of 2-5 under a 12-hour light cycle (07:00-19:00) and constant temperature of 23°C with *ad libitum* access to water and a standard laboratory chow (Teklad standard diet, Envigo, Cambridgeshire, UK). For dose response and inhibitor (method optimization) studies, mice remained group-housed under breeding colony conditions until use. For oestrous cycle studies, mice were pair-housed in individually-ventilated cages with crinkle-nest and cotton nestlet bedding material and cardboard tubes as enrichment. After at least a week acclimatization, vaginal smears were collected and assessed daily for at least a further week to determine oestrous cycle stage.

4.5.3. Tissue preparation and Ussing chamber conditions

Mice were humanely killed via cervical dislocation, a laparotomy performed and viscera exposed to ice-cold Krebs-Ringers Bicarbonate (KRB) buffer (115 mM NaCl, 2.4 mM K₂HPO₄, 0.4 mM KH₂PO₄, 25 μ M NaHCO₃, 1.2 mM MgCl₂·6H₂O, 1.2 mM CaCl₂·2H₂O) containing 5 mM D-glucose and gassed with carbogen (95% O₂/5% CO₂), as described previously [443]. Peak food consumption occurs early in the dark period in mice, with a secondary peak shortly before lights on [444]. To minimize potential circadian and food-induced variation in nutrient absorption, all mice had *ad libitum* access to food throughout the studies and were humanely killed for tissue collection ~1-4 h after lights on. This timing avoided the period of rapid upregulation of SGLT1 expression at the onset of the dark period or before feeding [445]. The small intestine was then excised, laid flat and measured unstretched, then divided into duodenum, jejunum, and ileum. The duodenal/jejunal transition zone was defined by the Ligament of Treitz, while the jejunal/ileal transition zone was identified by narrowing of the intestinal lumen, a reduction in smooth muscle thickness, a change in tissue translucency reflective of thinner smooth muscle and the presence of Peyer's patches [155].

The duodenum, jejunum or ileum from each mouse was gently flushed with ice-cold KRB buffer to remove ingesta. Eight evenly spaced sections, ~1 cm in length, were opened longitudinally and collected across the duodenum, jejunum, or ileum; four sections from the proximal and four sections from the distal half of the segment were mounted for each mouse. Each section was placed between two sliders with an exposed aperture of 0.1 cm² (P2303A, Physiologic Instruments, Reno, AZ, USA) and mounted into Ussing chambers. In all experiments, intestinal tissues were mounted in the first chamber between 8 and 19 minutes after the mouse was humanely killed (usually by 15 minutes) and tissue mounting was completed between 17 and 29 minutes. All water-jacketed chambers were maintained at 37°C, and tissues bathed in 5 ml KRB continuously gassed with carbogen. Tissues were voltage-clamped to zero potential difference which was maintained throughout each experiment. Short circuit current (I_{sc}) was monitored and recorded continuously (Acquire and Analyse 2.3, v2.3.4, Physiologic Instruments, Reno, NV, USA). All tissues were equilibrated for 20 minutes prior to D-glucose challenge. D-mannitol (25 mM) was added to the serosal chamber concurrent with D-glucose addition to the mucosal chamber to provide an osmotic balance. The absolute difference in short circuit current, expressed as ΔI_{sc} ($\mu\text{A}/\text{cm}^2$), was calculated as the difference between the maximum I_{sc} reached during the four minutes following D-glucose challenge and the average I_{sc} during the 2 minutes prior to the D-glucose challenge. Carbachol (100 μM), a chloride secretagogue, was added to both chambers 10 minutes after the D-glucose challenge to evoke a positive I_{sc} flux as a marker of tissue viability [443].

Data from individual samples were excluded if any of the following occurred: 1) a negative I_{sc} reading immediately prior to D-glucose challenge, 2) high baseline drift, defined as change in I_{sc} of $\pm 20 \mu\text{A}/\text{cm}^2$ in the 2 minutes preceding the D-glucose challenge, 3) high baseline noise, defined as an average I_{sc} point-to-point variation of $\geq 3 \mu\text{A}/\text{cm}^2$ in the 2 minute interval preceding the D-glucose challenge, and 4) poor tissue viability, defined as ΔI_{sc} of $\leq 20 \mu\text{A}/\text{cm}^2$ in response to 100 μM carbachol.

4.5.4. Study 1 - Region-specific glucose dose response

Following equilibration, tissue segments from the proximal (four segments) and distal (four segments) half of each SI region were randomized and challenged with D-glucose in the mucosal chamber. A stimulus of 5, 10, 25 or 45 mM D-glucose was added to the basal glucose concentration of 5 mM, resulting in final D-glucose concentrations of 10, 15, 30 or 50 mM (N = 5-10 observations per concentration in each region, samples from a total of 50 mice). These D-glucose concentrations were selected based on SGLT1 saturation at ~50 mM D-glucose in rat jejunum [202], and our findings of short-circuit current reversal at higher D-glucose concentrations (100 mM and 250 mM; data not shown).

4.5.5. Study 2 - SGLT1 inhibition

Dimethyl sulfoxide (DMSO) was utilized as a vehicle for the SGLT1 antagonist phlorizin and, therefore, we first assessed whether DMSO affected short-circuit current responses to D-glucose and carbachol. Small intestinal regions (duodenum, jejunum, ileum) from a total of 25 mice were prepared as described previously and incubated for 20 minutes in 0, 0.5 or 1% vol/vol DMSO in KRB in the mucosal chamber, followed by a 45 mM D-glucose challenge.

We next tested a range of phlorizin concentrations (0.1-1 mM) in jejunum to determine an appropriate concentration to attenuate SGLT1-mediated intestinal D-glucose transport in mice. The highest concentration tested (1 mM) was based on inhibition of glucose-evoked release of glucagon-like peptide-1 ($\geq 90\%$) in human ileum [180]. Jejunal segments from a total of 13 mice were incubated for 20 minutes with DMSO (1% vol/vol) containing 0, 0.1, 0.3, 0.5 or 1 mM phlorizin in the mucosal chamber, followed by a 45 mM D-glucose challenge.

4.5.6. Study 3 - Oestrous cycle

To determine any effect(s) of oestrous cycle stage on SGLT1-mediated jejunal glucose transport, the oestrous cycle was tracked in mice via daily vaginal smears [446] for at least a week. Mice were humanely killed by cervical dislocation at proestrus, diestrus, metestrus, and estrus stages (N = 9-10 per stage) and jejunum segments incubated for 20 minutes with 0, 0.1, 0.3 or 1 mM phlorizin in DMSO vehicle (1% vol/vol) followed by a 45 mM D-glucose challenge.

4.5.7. Statistical analysis

Data were analyzed using the mixed models procedure of SPSS version 28 (IBM Corporation, Armonk, New York, USA), treating data from multiple sections from individual mice as repeated measures. Glucose dose-response data (Study 1) were analyzed for effects of region (proximal duodenum, distal duodenum, proximal jejunum, distal jejunum, proximal ileum, distal ileum), glucose concentration and interaction. DMSO response data (Study 2) were analyzed for effects of region (proximal duodenum, distal duodenum, proximal jejunum, distal jejunum, proximal ileum, distal ileum), DMSO concentration and interaction. Phlorizin response data (Study 2) were analyzed for effects of region (proximal or distal jejunum), phlorizin concentration and interaction. Oestrous cycle data (Study 3) were analyzed for effects of cycle stage, region (proximal or distal jejunum), phlorizin concentration and interactions. Negative short-circuit current responses in some experiments with inhibitors were corrected to a minimum response of 0.001. Data were log-transformed before analysis to reduce inequality of variance between groups. All data are presented as mean \pm standard deviation and individual responses, and $P < 0.05$ is accepted as statistically significant.

4.6. Results

4.6.1. Study 1 – Region-specific glucose dose response

The length of the small intestine in glucose dose-response experiments averaged 31.9 ± 1.5 cm. Short-circuit current responses to glucose differed between regions ($P < 0.001$) and glucose concentrations ($P = 0.002$), with the greatest responses seen in distal jejunum (Fig. 4.1A and 4.1B). Responses to addition of 25 mM ($P = 0.004$) or 45 mM ($P = 0.010$) were greater than those generated by addition of 5 mM glucose (Fig. 4.1A and 4.1B). Short-circuit current responses to carbachol (Figures 4.1C and 4.1D) did not differ between regions ($P = 0.159$), but were affected by preceding glucose dose ($P = 0.034$). Responses to carbachol were lower following a glucose challenge with 25 mM glucose than at 5 mM glucose ($P = 0.026$) but did not differ between any other dose pairs (Fig. 4.1C and 4.1D).

4.6.2. Study 2 – SGLT1 inhibition

The length of the small intestine in experiments to evaluate effects of DMSO averaged 32.3 ± 1.9 cm. Our initial experiments confirmed that short-circuit current responses to glucose ($P = 0.788$) and carbachol ($P = 0.966$) were not altered by addition of DMSO to the incubation media (Fig. 4.2). Responses to glucose varied between regions ($P < 0.001$), and were again greater in the distal jejunum (Fig. 4.2A and 4.2B). Short-circuit current responses to carbachol (Fig. 4.2C and 4.2D) did not differ between regions ($P = 0.056$). Given the markedly greater glucose transport in jejunum, subsequent experiments were conducted in this region.

The length of the small intestine in experiments to confirm inhibition of active glucose transport by phlorizin averaged 33.0 ± 1.0 cm. Addition of phlorizin to the incubation media attenuated short-circuit current responses to glucose ($P < 0.001$, Fig. 4.3A and 4.3B). Short-circuit current responses to glucose ($P = 0.086$), and effects of phlorizin ($P = 0.055$), were similar in proximal and distal jejunum. Short-circuit current responses to carbachol (Fig. 4.3C and 4.3D) were unaffected by phlorizin ($P = 0.970$) or region ($P = 0.096$).

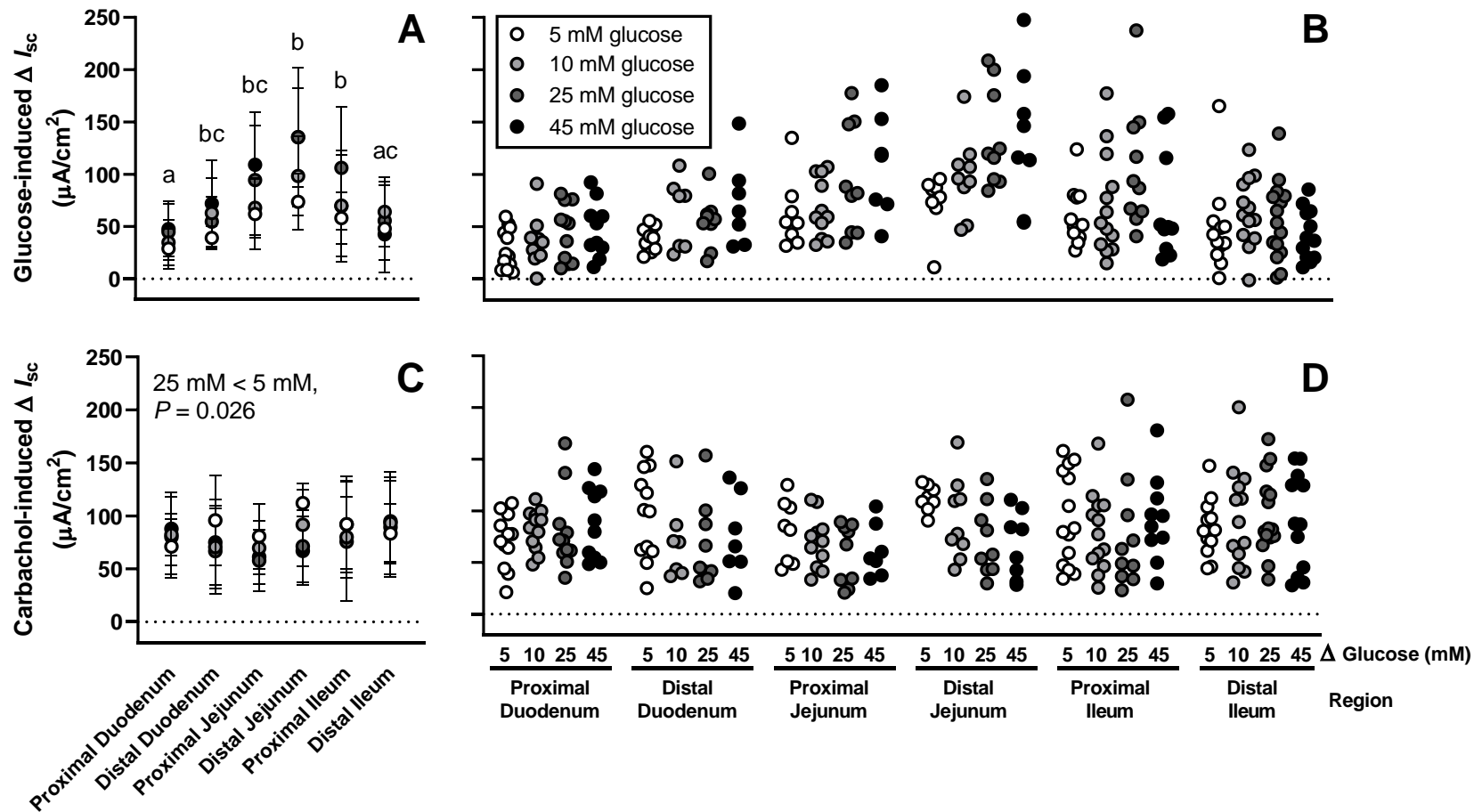


Figure 4.1 Glucose dose-response. Average (4.1A) and individual (4.1B) changes in short-circuit current (ΔI_{sc}) induced by a 5, 10, 25 or 45 mM D-glucose challenge were assessed in each small intestine region of 9-10 week old C57BL/6 female mice. Peak active glucose transport occurred in the presence of 50 mM D-glucose in the distal jejunum (A and B). Tissue viability assessed by short-circuit current responses to 100 μ M carbachol did not differ by region, but were lower following challenge with 25 mM than 5 mM glucose (4.1C and 4.1D). Responses to glucose or carbachol were assessed by repeated measures mixed model for effects of region and glucose concentration ($N = 7-15$ mice/group). The change in short-circuit current differed between regions that do not share a common superscript ($P < 0.05$).

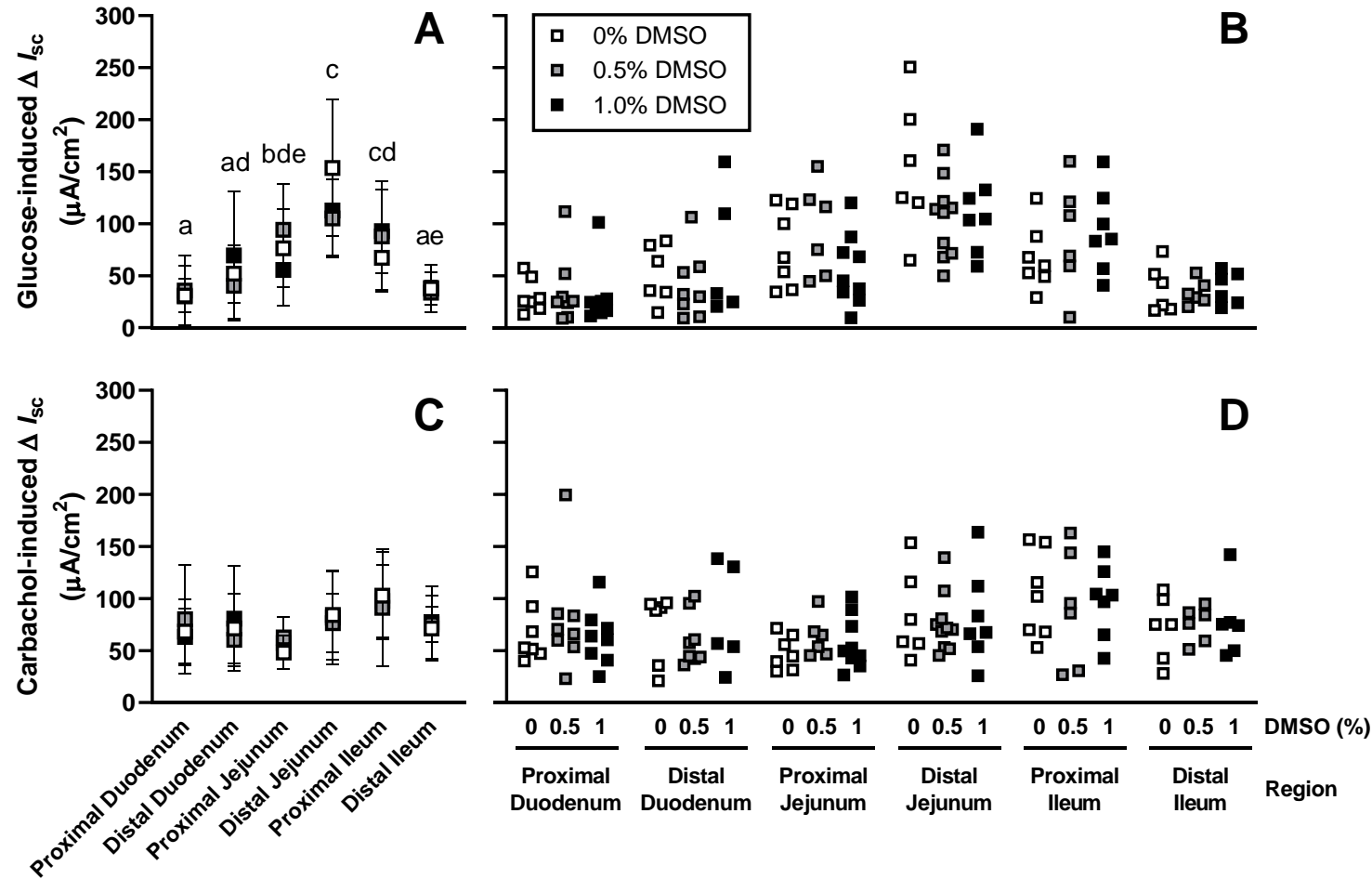


Figure 4.2 DMSO does not inhibit glucose or carbachol responses. Average (4.2A) and individual (4.2B) changes in short-circuit current (ΔI_{sc}) induced by 45 mM D-glucose in the presence of 0%, 0.5% or 1% DMSO were assessed in each small intestine region of 9-10 week old C57BL/6 female mice. DMSO did not affect short-circuit current responses to glucose (4.2A and 4.2B) or carbachol (4.2C and 4.2D) challenge. Responses to glucose or carbachol were assessed by repeated measures mixed model for effects of region and DMSO concentration ($N = 5-10$ mice/group). The change in short-circuit current differed between regions that do not share a common superscript ($P < 0.05$).

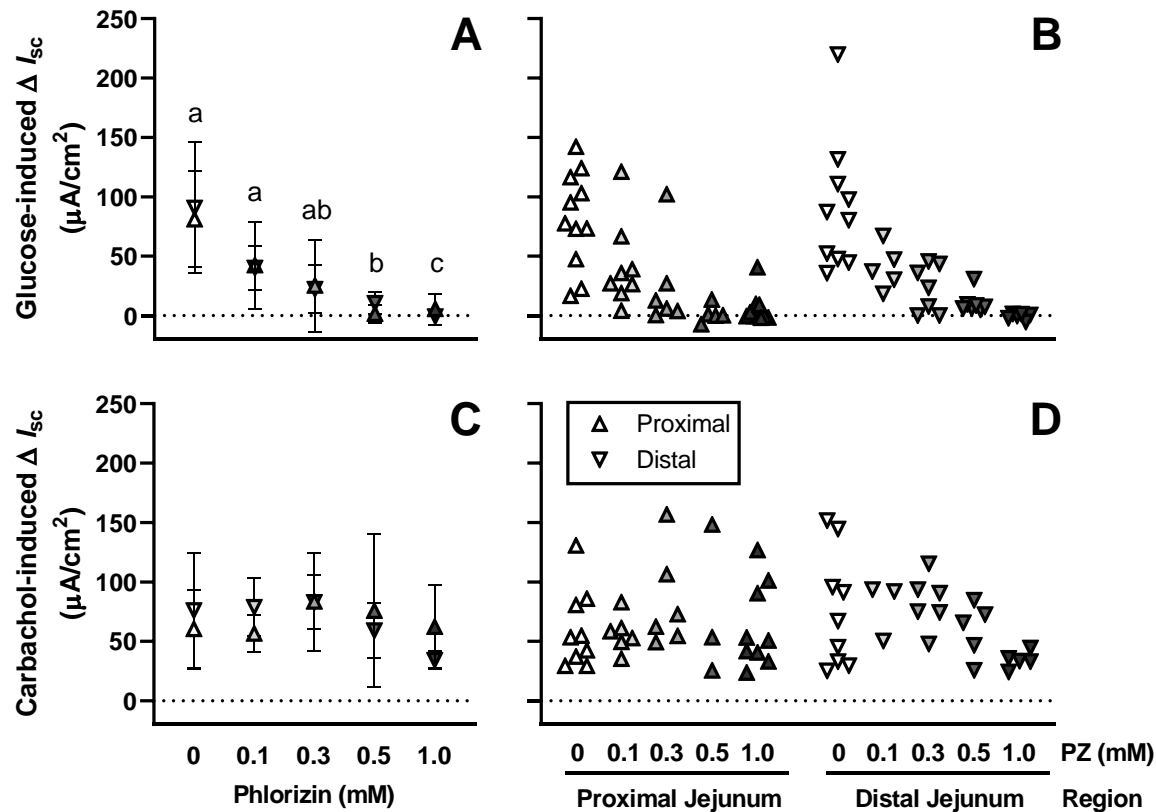


Figure 4.3: Phlorizin inhibits active glucose uptake. Average (4.3A) and individual (4.3B) changes in short-circuit current (ΔI_{sc}) induced by 45 mM D-glucose in the presence of 0, 0.1, 0.3, 0.5 or 1 mM phlorizin were assessed in proximal and distal jejunum of 9-10 week old C57BL/6 female mice. Phlorizin inhibited short-circuit current responses to glucose in a dose-dependent manner (4.3A and 4.3B), but did not affect responses to carbachol (4.3C and 4.3D). Responses to glucose or carbachol were assessed by repeated measures mixed model for effects of region and phlorizin concentration ($N = 5-11$ mice/group). The change in short-circuit current differed between phlorizin concentrations that do not share a common superscript ($P < 0.05$).

4.6.3. Study 3 – Oestrous cycle

The length of the small intestine did not differ between oestrous cycle stages (diestrus: 31.1 ± 1.4 cm; proestrus: 31.7 ± 1.8 cm; estrus: 31.1 ± 1.8 cm; metestrus: 31.9 ± 1.6 cm; $P = 0.579$). Short-circuit current responses to glucose changed across the oestrous cycle ($P = 0.030$) and were higher at proestrus compared to estrus ($P = 0.025$) but did not differ between other stages (Fig. 4.4A and 4.4B). Responses to glucose were similar in the proximal and distal jejunum ($P = 0.989$) and were attenuated by phlorizin ($P < 0.001$) with the highest phlorizin concentration tested (1 mM) reducing short-circuit current responses to glucose by ~90% (Figures 4.4A and 4.4B). All concentrations of phlorizin reduced responses to glucose relative to control (each $P < 0.001$).

Short-circuit current responses to carbachol did not change across the oestrous cycle ($P = 0.326$), while the effect of phlorizin on response to carbachol differed between regions (interaction $P = 0.006$, Fig. 4.4C and 4.4D). Phlorizin affected the response to carbachol in proximal and distal jejunum (each $P < 0.001$), with carbachol responses attenuated at 1 mM phlorizin in both regions (Fig. 4.4C).

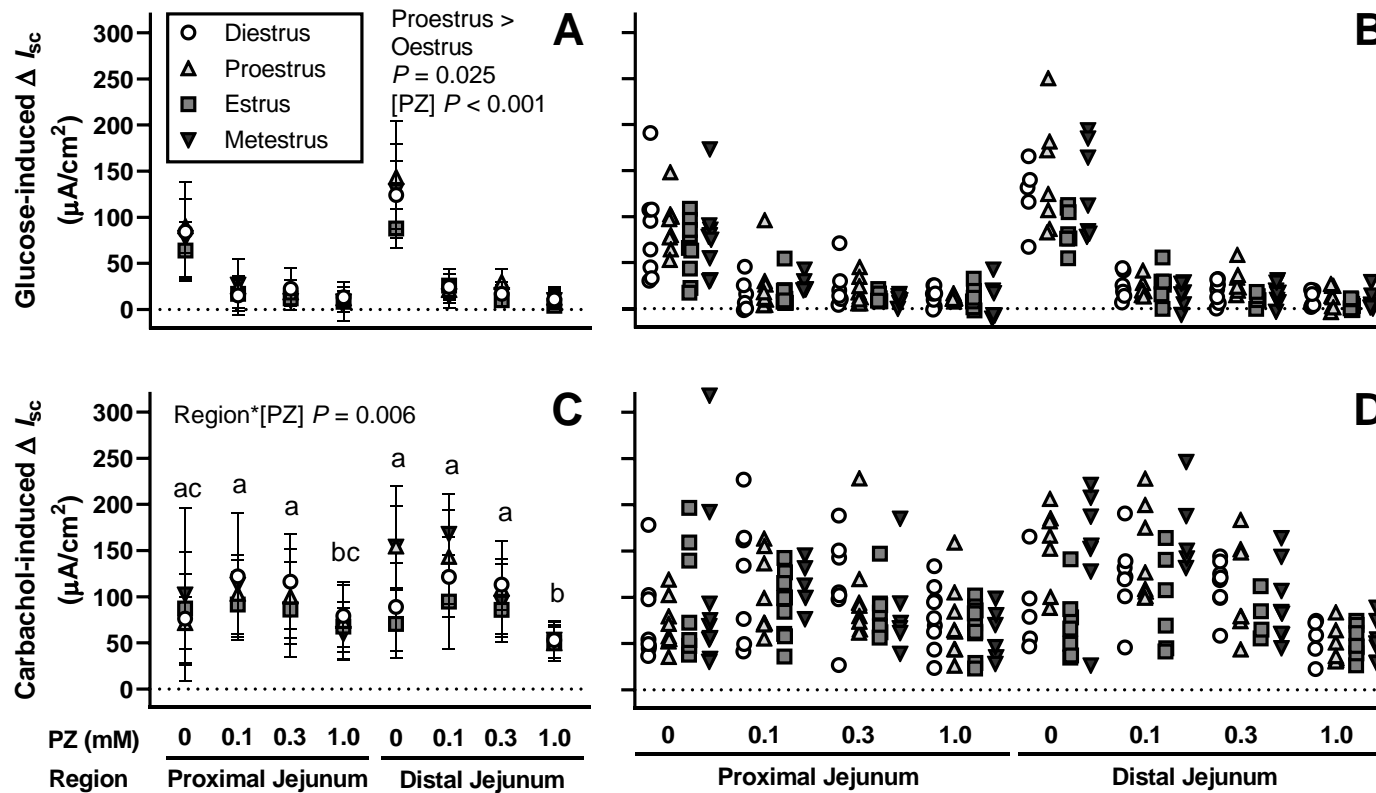


Figure 4.4: Active glucose uptake varies across the oestrous cycle in mice. Average (4.4A) and individual (4.4B) changes in short-circuit current (ΔI_{sc}) induced by 45 mM D-glucose in the presence of 0, 0.1, 0.3 or 1 mM phlorizin (PZ) were assessed in proximal and distal jejunum of 9-10 week old C57BL/6 female mice at each oestrous cycle stage. Active glucose transport was lower at estrus than proestrus ($P = 0.025$, 4.4A and 4.4B). Phlorizin inhibited short-circuit current responses to glucose ($P < 0.001$, A and B). Incubation with 1 mM phlorizin reduced short-circuit current responses to carbachol in the distal jejunum (4.4C and 4.4D). Responses to glucose or carbachol were assessed by repeated measures mixed model for effects of oestrous cycle stage, region and phlorizin concentration ($N = 5-9$ mice/group). Within each region, the change in short-circuit current differed between phlorizin concentrations that do not share a common superscript ($P < 0.05$).

4.7. Discussion

This study provides the first direct evidence that active glucose transport by the jejunum varies during the ovarian cycle. This adds support that to the hypothesis that differences in post-prandial blood glucose during the human menstrual cycle [432] reflect changes in glucose uptake, at least in part. This validated *ex vivo* method enables future assessment of region-specific changes in active glucose transport by mouse small intestine induced by physiological states, environmental challenges, and pharmacological agents.

We observed peak short-circuit current responses to a stimulus of 45 mM glucose in mice, consistent with saturation of SGLT1-dependent glucose transport at 30-50 mM glucose in rat jejunum [202]. In Ussing chamber studies using human small intestine, active glucose transport was maximal at 35-65 mM luminal glucose [205, 206, 447, 448]. Regional luminal glucose concentrations measured *in vivo* via indwelling catheters ranged from 2-48 mM glucose, in rodents, rabbits and dogs fed standard laboratory diets [449], confirming that glucose concentrations used in Ussing experiments were physiological. Regional differences in active glucose transport across the small intestine were consistent between the present study and that of Smith and colleagues [450], using similar methodology in the same strain of mice. We observed peak active glucose transport in the distal jejunum, consistent with previous reports in mice [450] and rats [451]. Corresponding to this regional pattern of active glucose transport, SGLT1 gene and protein expression are higher in jejunum than ileum or duodenum in rat [452-454] and pig [455]. In contrast, SGLT1 gene expression was ~2.5 and ~4-fold higher in the duodenum than jejunum and ileum, respectively in a single study in male BALB/c mice [456]. A limitation of our study is that we did not collect tissues to assess gene and tissue expression of SGLT1 after Ussing experiments. Nevertheless, our data on region-specific active glucose transport, together with gene expression patterns in rats and humans, are consistent with the jejunum as the primary site of glucose uptake across mammalian species. Interestingly, we observed proximal-distal differences in active glucose transport within each SI region, suggesting gradients in function, rather than sharp changes at the boundaries between regions.

Adding DMSO up to 1% to KRB buffers did not alter short-circuit current responses or tissue viability, reaffirming DMSO as a suitable vehicle for testing pharmacological compounds, such as phlorizin, in epithelial tissues such as the small intestine. In our subsequent experiments, 1 mM phlorizin attenuated active glucose transport by 90-97% in mouse jejunum, consistent with the proportion of SGLT1-mediated active glucose transport reported in human ileum [180]. There is some evidence that the facilitative glucose transporter 2 (GLUT2) may translocate from a basolateral location to the brush border membrane to facilitate glucose and fructose absorption [208, 209]. However, this has been reported in limited settings – severely

insulin resistant non-diabetic mice fed a high-fat, low-carbohydrate diet for 12 months starting from weaning, and in morbidly obese human subjects [208-210]. Indeed, individuals with inactivating mutations in GLUT2 (Fanconi-Bickel syndrome) do not have defective intestinal glucose uptake [457]. Our data thus supports evidence that GLUT2 does not play a major role in glucose transport under normal circumstances. We did observe that short-circuit current responses to carbachol were lower in the presence of 1 mM phlorizin than at lower phlorizin concentrations in oestrous cycle experiments, suggesting that 1 mM phlorizin may compromise tissue viability. Addition of 0.3-0.5 mM phlorizin inhibited 73-83% of active glucose transport without loss of carbachol response. We therefore suggest using a maximum concentration of 0.5 mM phlorizin in mouse intestine.

Active glucose transport across the jejunum in our study was lower at estrus compared to proestrus, while short-circuit current responses to carbachol did not differ with cycle stage. This finding supports the hypothesis that the rate of small intestinal glucose transport is higher during the luteal than follicular phase of the mammalian ovarian cycle. Interestingly, we only saw differences in glucose transport between the late follicular (proestrus) and early luteal (estrus) stages of the murine oestrous cycle. In cycling women, blood glucose concentrations after ingestion of a liquid test meal were lower during the mid-follicular phase compared to the luteal phase, around a week after ovulation [432]. The mechanisms underlying changes in active glucose transport during the ovarian cycle are unclear, but may include changes in food intake, gastric emptying and circulating hormones, or a combination of factors. The small intestine did not differ in length between cycle stages, concurrent with altered glucose transport. Although individual food intake, body mass and hormone concentrations were not assessed in the present study, future investigation of these across the oestrous cycle may assist in identifying the underlying mechanisms. Further studies are also required to determine whether active glucose transport varies across the ovarian cycle during the dark period, when food intake and SGLT1 expression peak in mice [444, 445]. The lower active glucose transport observed at estrus in the current study corresponds to the timing of nadirs in meal size and duration reported previously in mice [436], rats [438] and humans [433]. Indeed, lower blood glucose concentrations after a test meal were shown to correspond to higher circulating estrogen during the follicular phase than luteal phase in cycling women [432]. In rats, small intestinal glucose uptake was increased following ovariectomy but normalized to that of sham-operated controls following 2 weeks of 17β -estradiol and/or progesterone treatment at physiological or pharmacological doses [458]. Together, these data suggest a high plasticity of glucose transport, potentially driven by cyclic changes in circulating sex steroids, and corresponding to changes in food intake across the oestrous cycle in rats and mice. Whether glucose transport is perturbed in conditions of dysregulated ovarian cycles, such as polycystic

ovarian syndrome, or by endocrine-disrupting chemicals with estrogenic activity, is yet to be determined.

In conclusion, our study provides the first direct evidence of changes in SGLT1-mediated glucose transport in the jejunum across the ovarian cycle. We next plan to use this validated method to investigate whether region-specific active glucose transport changes during sustained physiological states in which food intake and circulating hormones change, such as during pregnancy and lactation.

5. CHAPTER 5: DIFFERENTIAL CHANGES IN ANATOMICAL, MOLECULAR AND FUNCTIONAL DETERMINANTS OF INTESTINAL GLUCOSE ABSORPTION DURING MURINE PREGNANCY

5.1. Overview

Chapter 5 describes a series of experiments undertaken to characterise concurrent anatomical, molecular and functional adaptations of intestinal glucose absorption during pregnancy in mice. Within this chapter, data from two separate cohorts of mice are described. The first cohort was used to obtain tissue samples for histological analysis and qRT-PCR to characterise concurrent SI anatomical and molecular adaptations throughout pregnancy compared to age-matched non-pregnant controls. The second cohort was used to obtain tissue samples for Ussing chamber experiments to characterise the contribution of SGLT1 to active glucose transport across each SI region between age-matched non- and late-pregnant mice. For the studies described in this chapter, my contributions were as follows: I cut, stained, imaged, and took measurements from sections of jejunum and ileum tissues collected from the first cohort of mice. I was also involved in analysis of the histology and qRT-PCR data. As part of the Ussing chamber pregnancy study which utilised mice from the second cohort, I was involved in managing timed matings and tissue collection, performed all Ussing chamber experiments and data collection, was involved in data analysis and preparation of all figures, co-wrote and edited the final manuscript. The data described in Chapter 5 is unpublished.

5.2. Statement of authorship - Differential changes in anatomical, molecular and functional determinants of intestinal glucose absorption during murine pregnancy

Statement of Authorship

Title of Paper	Differential changes in anatomical, molecular and functional determinants of intestinal glucose absorption during murine pregnancy
Publication Status	<input type="checkbox"/> Published <input type="checkbox"/> Accepted for Publication <input type="checkbox"/> Submitted for Publication <input checked="" type="checkbox"/> Unpublished and Unsubmitted work written in manuscript style
Publication Details	

Principal Author

Name of Principal Author (Candidate)	Teunis Sebastian Overduin		
Contribution to the Paper	Conception and design of research, performed experiments described within the manuscript, analysed experimental data presented within the manuscript, interpreted results presented within the manuscript, drafted, edited and approved final version of manuscript.		
Overall percentage (%)	30%		
Certification:	This paper reports on original research I conducted during the period of my Higher Degree by Research candidature and is not subject to any obligations or contractual agreements with a third party that would constrain its inclusion in this thesis.		
Signature		Date	10-07-2023

Co-Author Contributions

By signing the Statement of Authorship, each author certifies that:

- i. the candidate's stated contribution to the publication is accurate (as detailed above);
- ii. permission is granted for the candidate to include the publication in the thesis; and
- iii. the sum of all co-author contributions is equal to 100% less the candidate's stated contribution.

Name of Co-Author	Georgia Clarke		
Contribution to the Paper	Conception and design of research, performed experiments described within the manuscript, analysed experimental data presented within the manuscript, interpreted results presented within the manuscript, drafted, edited and approved final version of manuscript.		
Signature		Date	10/7/2023

Name of Co-Author	Hui Li		
Contribution to the Paper	Conception and design of research, performed experiments described within the manuscript, analysed experimental data presented within the manuscript, interpreted results presented within the manuscript, drafted, edited and approved final version of manuscript.		
Signature		Date	11/07/2023

Name of Co-Author	Richard Young		
Contribution to the Paper	Conception and design of research, interpreted results presented within the manuscript, drafted, edited and approved final version of manuscript.		
Signature		Date	10/7/2023

Name of Co-Author	Kathryn Gafford		
Contribution to the Paper	Conception and design of research, performed experiments described within the manuscript, analysed experimental data presented within the manuscript, interpreted results presented within the manuscript, drafted, edited and approved final version of manuscript.		
Signature		Date	14/7/2023

Name of Co-Author	Amanda Page		
Contribution to the Paper	18% - Conception and design of research, performed experiments described within the manuscript, analysed experimental data presented within the manuscript, interpreted results presented within the manuscript, drafted, edited and approved final version of manuscript.		
Signature		Date	10/7/2023

5.3. Abstract

Aim: Pregnancy demands increased food intake and nutrient delivery to support fetal growth and development. The timing of region-specific adaptations in small intestinal (SI) anatomy, nutrient transporter expression and their functional consequences on nutrient absorption, remain unclear. We therefore assessed differential changes in anatomical, molecular and functional determinants of SI glucose absorption during mouse pregnancy.

Methods: Time-mated pregnant and age-matched non-pregnant diestrus female C57BL/6 mice were humanely killed at gestational day (GD) 6.5, 12.5 or 17.5. Concurrent changes in duodenal, jejunal and ileal anatomy and macronutrient transporters expression were determined. Region-specific *ex vivo* active glucose transport was measured in a separate cohort of late- and non-pregnant mice.

Results: The SI was 20% heavier and SI villi were 18% longer in late- than non-pregnant mice (all $p < 0.001$). Differences in carbohydrate (*SLC5A1*, *SLC2A2*, *SLC2A5*) and amino acid (*SLC6A19*) transporter expression between pregnancy stages were region-specific. Expression of fatty acid transporter *FABP2* was 11-46% higher in non-pregnant mice than mice at any stage of pregnancy ($p < 0.001$). Active glucose transport was ~6-fold higher in distal jejunum and proximal ileum than in duodenum or distal ileum, but did not differ between non- and late-pregnant mice.

Conclusion: Despite anatomical and molecular changes that would support an increase in SI capacity for nutrient absorption, active glucose transport per unit area was similar in non-pregnant and late-pregnant mice. Increased nutrient demand during pregnancy may therefore be met largely through SI hypertrophy and surface area expansion, although contributions of other nutrient transport mechanisms require evaluation.

5.4. Introduction

The small intestine (SI) is the primary site of nutrient uptake in rodents, as in humans, and is highly plastic, able to respond to changes in food intake and nutrient demand. The SI is comprised of 3 distinct regions; the duodenum, jejunum and ileum, each of which has unique anatomy, nutrient transporter expression and function [155, 158]. Nutrient uptake from the SI lumen occurs by passive and facilitated transport, and the contribution of each varies between nutrients. In facilitated transport, nutrient-specific transporters located at the apical and basolateral membranes of the absorptive cells (enterocytes) transport nutrients across the SI epithelium and into the maternal circulation [158]. Increased nutrient uptake capacity can thus be generated by overall expansion of the SI, increased villi length to increase the epithelial surface area and/or upregulation of nutrient transporters.

Pregnancy demands adaptations in food intake and nutrient uptake to support growth of the fetus and placenta and maternal tissue gain, including increased adiposity, which acts as an energy store to support lactation [25]. To meet these demands, food intake increases during pregnancy by 10-15% in humans and 25-50% in rodents [59]. In concert, the SI undergoes anatomical, molecular and functional adaptations which increase its capacity for nutrient uptake and delivery [5]. In rats, increases of up to 20% have been reported in SI weight and length by late pregnancy [175, 234], although these increases are generally smaller than those seen during lactation, and not always significant [175, 178]. In rodents, there is some, although variable, evidence for microstructural changes including a ~1.5-fold increase in villi length and width, crypt depth and smooth muscle thickness at mid- and late-pregnancy [178, 218]. Transcript and protein expression of many micronutrient transporters, and intestinal uptake of calcium and iron each increase during pregnancy [5]. Pregnancy effects on macronutrient transporters, however, are less well described. Indeed, the reported changes in SI amino acid absorption during rodent pregnancy are variable, with unchanged [252, 255], increased [459] and decreased [257] absorption all described. Transcript expression of glucose-galactose transporter sodium-glucose co-transporter 1 (*Sglt1*) and fructose transport, *Glut5*, increase 50% and 80% respectively at late pregnancy in the duodenum of rats relative to non-pregnant controls [223]. It is, however, unknown whether this occurs in other SI regions, or at earlier pregnancy stages. Consistent with upregulation of carbohydrate transporters, glucose absorption per unit length of SI following intraluminal glucose perfusion (20-300 mM) of anaesthetised animals was 20-40% higher in pregnant rats at gestational day (GD) 12-15 than in non-pregnant rats [231]. Similarly, glucose absorption from ligated jejunal and ileal segments was 25% higher in anaesthetised hamsters at late-pregnancy compared to non-pregnant controls [232]. Few studies have directly measured glucose absorption in conscious pregnant animals, but portal vein glucose concentrations following a standardized meal were

20% higher in late-pregnant than non-pregnant dogs [233], consistent with enhanced glucose absorption during pregnancy. Whether abundance or function of fatty acid transporters *CD36* and fatty acid binding protein 2 (*FABP2*), or the amino acid transporters *SLC6A6* and *SLC6A19*, change during pregnancy have not been reported.

Although the studies above provide evidence of anatomical and molecular adaptations in the SI at late pregnancy, the timing and regional changes, as well as the functional consequences, remain unclear. The current study, therefore, determined regional SI anatomy and expression of macronutrient transporters in non-, early-, mid- and late-pregnant mice. Changes in carbohydrate transporter expression represented the largest pregnancy change and, therefore, optimised Ussing chamber methods were used to compare active glucose transport in mice at late-pregnancy to that in non-pregnant mice in the functional experiments.

5.5. Methods

5.5.1. Ethics

Experiments were approved by the Animal Ethics Committee of the South Australian Health and Medical Research Institute (SAHMRI, SAM395.12 & SAM-21-049). All studies were conducted in accordance with the Australian Code of Practice for the Care and Use of Animals for Scientific Purposes [442] and the ARRIVE guidelines [441].

5.5.2. Study 1 – Animals

Animal management was as previously described [53]. Briefly, eight-week-old C57BL/6JSah female mice sourced from SAHMRI Bioresources were individually housed in metabolic monitoring cages (Promethion Sable System, Las Vegas, NV) to acclimatise for 7 days under a 12-hour light cycle (0700-1900 h). Throughout the entire study, mice had access to standard laboratory chow (Teklad standard diet, Envigo, Cambridgeshire, UK) and water *ad libitum*. Mice were randomised to mating for pregnancy groups or not mated for age-matched non-pregnant controls. Females for mating were housed in pairs with a C57BL/6JSah stud male for mating at 1700 h. All females were checked every morning at 0700 h for a copulatory plug which was indicative of successful mating and recorded as gestational day (GD) 0.5 of pregnancy. Following mating, plugged females were returned to metabolic cages and randomized to pregnancy-stage groups; early (GD6.5), mid (GD12.5) or late-stage pregnancy (GD17.5). Non-pregnant controls were transferred to metabolic cages on age-matched days. Pregnant (GD 6.5, 12.5 or 17.5) and age-matched non-pregnant females were anaesthetised with isoflurane (5% in oxygen) and humanely killed via exsanguination with terminal cardiac blood collection.

5.5.3. Study 1 - Small intestine histology

A laparotomy was performed, the SI excised and total weight was recorded. Next, a single segment ~1 cm in length was resected from the middle of the duodenum (pyloric sphincter to ligament of Treitz), the jejunum (ligament of Treitz to the middle of SI mesenteric fan), and the ileum (aboral end of the mesenteric fan to the caecum). Tissue segments were flushed with PBS then fixed in 4% paraformaldehyde for 2 hours, prior to overnight cryo-protection in 30% sucrose in 0.1 M phosphate buffer; tissues were then mounted in optimal cutting temperature (OCT) compound (ProSciTech, Thuringowa, Qld, Australia) and snap frozen in liquid nitrogen. OCT-embedded intestinal segments were sectioned at 10 µm (Cryocut 1800; Leica Biosystems, Nussloch, Germany) and mounted on Superfrost Plus slides (Thermo Fisher, Waltham, MA, USA). Slides were stained with haematoxylin and eosin (adapted from [460]) then imaged at high resolution (Nanozoomer; Hamamatsu, Hamamatsu City, Shizuoka Prefecture, Japan). Villous height, crypt depth and smooth muscle thickness were measured using NDP Viewer 2.0 software (Hamamatsu); all tissue measures were blinded to group. From each animal, up to 40 measurements of villous height, crypt depth and smooth muscle thickness were averaged for each small intestinal region.

5.5.4. Study 1 – Gene expression

Fresh SI mucosa was collected into an Eppendorf tube from a separate ~1 cm middle segment of the duodenum, jejunum and ileum from the same mice (Section 5.5.3) by gently scraping from the serosa with a sterile scalpel blade, snap-frozen in liquid nitrogen then stored at -80°C until use. Mucosal mRNA from each SI region was extracted using a PuraLink RNA Mini Kit (Invitrogen, 12183018A) according to manufacturer's instructions and mRNA yield and quality were determined using a NanoDrop (NanoDrop Technologies, Wilmington, DE, USA). Quantitative real-time PCR (qRT-PCR) was conducted using TaqMan™ or SYBR® green methods, depending on the pre-designed primers (Table 5.1), to determine the relative expression of carbohydrate (*SLC5A1*, *SLC2A2*, *SLC2A5*), amino acid (*SLC15A1*, *SLC6A6*, *SLC6A19*) and fatty acid (*CD36*, *FABP2*) transporter transcripts for each SI region and pregnancy stage according to the manufacturer's instructions.

Table 5.1 Information for gene targets assessed by qRT-PCR study

Gene target	Common name/Function	NCBI accession no.	Protocol
<i>Slc5a1</i>	Sodium-glucose co-transporter 1 (Sglt1) - primary apical glucose transporter	Mm00451203_M1	Taqman
<i>Slc2a2</i>	Glucose transporter 2 (Glut2) - basolateral bi-directional symporter for glucose/fructose	Mm00446229_M1	Taqman
<i>Slc2a5</i>	Glucose transporter 5 (Glut5) - apical fructose transporter	Mm00600311_M1	Taqman
<i>Slc15a1</i>	Peptide transporter 1 (Pept1) - apical peptide transporter (≥ 3 amino acids)	Mm0451610_M1	Taqman
<i>Slc6a6</i>	Sodium-chloride-dependent taurine transporter	Mm00436909_M1	Taqman
<i>Slc6a19</i>	Sodium-dependent neutral amino acid transporter	Mm01352157_M1	Taqman
<i>CD36</i>	Cluster of differentiation 36 – apical fatty acid transporter	Mm00432403_M1	Taqman
<i>FABP2</i>	Fatty acid binding protein 2 - intracellular fatty acid transporter	Mm_Fabp2_1_SG	SYBR green

5.5.4.1. *Taqman assays*

TaqMan qRT-PCR was performed using EXPRESS One-Step Superscript RT-PCR kits (Invitrogen 11781-200, California, USA) and a 7500 PCR thermocycler instrument (Applied Biosystems 7500 Real-Time PCR System, Thermo Fisher Scientific). Relative transcript expression was calculated relative to the geometric mean transcript expression of housekeepers β_2 microglobulin (*B2M*), peptidylprolyl isomerase A (*PPIA*) and hypoxanthine-guanine phosphoribosyl transferase (*HPRT*). Normfinder software (Department of Molecular Medicine, Aarhus University Hospital, Denmark) was used to choose these housekeepers with abundant SI expression that was stable across pregnancy [461]. The final normfinder values for combined *B2M*, *PPIA* and *HPRT* were 0.005 in duodenum, 0.008 in jejunum and 0.002 in ileum.

5.5.4.2. *SYBR green assays*

SYBR green qRT-PCR was performed using QuantiTect SYBR Green RT-PCR kits (Qiagen, Hilden, Germany) and a QuantStudio 7 Flex Real-Time PCR System (Thermo Fisher Scientific). Relative transcript expression was calculated relative to the geometric mean transcript expression of the housekeepers *B2M* and *HPRT*. The final normfinder values for combined *B2M* and *HPRT* were 0.001 in duodenum-ileum and 0.002 in jejunum.

For both methods, a DNase digestion step utilising an ezDNase kit (Invitrogen, SA, Australia) was included in the protocol to eliminate genomic DNA from total RNA. Each assay was performed in triplicate and included no-template controls. Each assay also included a no reverse transcriptase control for all SYBR green primers and the housekeeper *PPIA*. Negative controls were performed by substituting RNA template and reverse transcriptase for RNase-free water. Relative mRNA expression was quantified utilising the delta CT method as previously described [462].

5.5.5. Study 2 – Animals

Female 8-10-week-old C57BL/6 mice and proven-fertile male C57BL/6 mice were sourced from Bioresources. All mice acclimatised for a minimum of 7 days under a 12-hour light cycle (0700-1900 h), were weighed daily and fed *ad libitum* as for Study 1. Following acclimatisation, mice were randomised to mating to generate pregnant animals (n=20) or not mated for age-matched non-pregnant controls (n=20). Females for mating were housed in pairs with a C57BL/6 stud male at 1700 h and checked for the presence of a copulatory plug at 0700 h each morning, which when present was recorded as gestational day 0.5 of pregnancy (GD0.5). Female mice were pair-housed in standard cages for the remainder of the study. As active glucose transport differs by oestrous cycle stage in mice [430], vaginal smears were assessed daily for at least a week to confirm diestrus stage in

non-pregnant mice [446] prior to Ussing experiments. Data from a single non-pregnant mouse and single pregnant mouse were excluded due to technical failure of the Ussing chamber platform, and three mated mice were excluded as they were either not pregnant or at the wrong day of pregnancy when humanely killed.

5.5.6. Study 2 – Ex vivo active glucose transport

Mice at late pregnancy (GD17.5) and non-pregnant diestrus females were humanely killed via cervical dislocation. The abdominal cavity was opened midline and the SI exposed to ice-cold Krebs-Ringer buffer (KRB) fortified with 5 mM glucose. The full length of the SI was then removed and two full-thickness segments (2 most proximal and 2 most distal), each ~1 cm long, from each SI region were collected from randomly chosen SI regions as previously described.[430] To reduce the risk of collecting overlapping tissues from the distal jejunum and proximal ileum, a 1 cm segment was removed from the distal jejunum and proximal ileum segments prior to collection of the tissues to be assessed from the respective regions. Tissue segments from the proximal and distal half of each collected region were mounted between two sliders with an exposed aperture of 0.1 cm² (P2303A, Physiologic Instruments, Reno, AZ, USA) and inserted into Ussing chambers (P2300, Physiologic Instruments, Reno, AZ, USA). Following mounting, all tissues were short-circuited and voltage-clamped to 0 potential difference, after which all tissues were kept under continuous voltage-clamp from time of mounting until the end of each experiment. Acquire and Analyze 2.3 software (Version 2.3.4, Physiologic Instruments, Reno, AZ, USA) was used to obtain measurements of short-circuit current (I_{sc}) for all tissues at 5-second intervals from the start of the equilibration period until the end of each experiment. Tissues from each chosen region were randomised to pre-incubation in the absence or presence of the SGLT-1 inhibitor phlorizin (0.3 mM) for 20 minutes, followed by luminal exposure to a 45 mM glucose challenge. At the end of each experiment, tissue viability was assessed via a luminal sided 0.1 μ M carbachol challenge. Only data from viable tissues which met quality control criteria was included in analysis as previously described.[430]

5.5.7. Statistics

SI weight, body weight and litter size were compared between pregnancy stages by one-way ANOVA. Effects of pregnancy stage (non, early, mid, late), SI region (duodenum, jejunum, ileum) and interactions on SI morphology and nutrient transporter gene expression were analysed using mixed models, treating data from multiple regions from individual mice as repeated measures. Where interactions were present, effects of pregnancy stage were assessed separately within each region by one-way ANOVA. Bonferroni post-hoc tests were used to compare SI regions and pregnancy stages where

a significant overall effect was identified. Active glucose transport data was log-transformed for analysis, and analysed by mixed models for effects of pregnancy (non or late-pregnant), SI region (proximal duodenum, distal duodenum, proximal jejunum, distal jejunum, proximal ileum, distal ileum), phlorizin concentration (0, 0.3 mM) and all interactions. All statistical analyses were performed in SPSS version 28 (IBM Corporation, Armonk, New York, USA). Statistical significance was accepted when $p \leq 0.05$ and all data are presented as mean \pm standard deviation (SD).

5.6. Results

5.6.1. Study 1 - mouse and SI characteristics

Mice did not differ in initial body weight between groups, but by mid-pregnancy were 24-25% heavier than non-pregnant or early-pregnant mice, while late-pregnant mice were 57% heavier than non-pregnant mice (Table 5.2). Litter size was similar in all pregnant groups (Table 5.2). SI wet weight was similar in non-pregnant and early-pregnant mice, but 20% heavier in mid- and late-pregnant mice compared to non-pregnant controls (each $p < 0.001$, Table 5.2).

5.6.2. Study 1 - SI morphology

The length of villi (Fig. 5.1A) differed between pregnancy stage ($p < 0.001$) and between SI regions ($p < 0.001$), with similar effects of pregnancy in each region. Overall, villi were 18% longer in late-pregnant mice ($p < 0.001$) but similar in early- ($p > 0.1$) and mid-pregnant ($p = 0.083$) mice, compared to non-pregnant mice. Villi were longer in the duodenum than jejunum (21% difference, $p < 0.001$) or ileum (96% difference, $p < 0.001$) and 62% longer in jejunum than ileum ($p < 0.001$). Crypt depth (Fig. 5.1B) also differed between regions ($p < 0.001$) but not between pregnancy stages (pregnancy $p = 0.095$; pregnancy*region $p > 0.5$). Crypt depth was similar in the duodenum and jejunum, but crypts were 23% deeper in ileum than duodenum or jejunum (each $p < 0.001$). The thickness of the smooth muscle layer (Fig. 5.1C) differed between regions ($p < 0.001$) but not between pregnancy stages (pregnancy $p > 0.2$; pregnancy*region $p > 0.4$). The smooth muscle layer was thinnest in the jejunum, intermediate in duodenum and thickest in the ileum ($p < 0.05$ for each comparison).

Table 5.2 Study 1 mouse characteristics

	Non-pregnant	Early-pregnancy	Mid-pregnancy	Late-pregnancy	Significance (<i>p</i>)
No. of mice	11	10	10	11	
Gestational age	N/A	GD6.5	GD12.5	GD17.5	
Litter size	0	9.2 ± 0.6	8.6 ± 1.2	7.4 ± 2.7	Nsd
Initial body weight ¹ (g)	21.2 ± 0.7	20.7 ± 0.9	20.9 ± 0.9	20.9 ± 1.4	Nsd
Final body weight ² (g)	22.1 ± 1.1 ^a	22.4 ± 1.1 ^a	27.7 ± 1.8 ^b	34.8 ± 3.5 ^c	< 0.001
SI weight (g)	1.29 ± 0.15 ^a	1.38 ± 0.08 ^a	1.55 ± 0.08 ^b	1.55 ± 0.10 ^b	< 0.001

¹Initial body weight was the average of body weight measures in metabolic cages during the last 48 h of acclimatisation. ²Final body weight was the average of body weight measures in metabolic cages during the 24 h before humane killing. Maternal data, litter size and SI weight were analysed by one-way ANOVA, and Bonferroni comparison used to compare specific pregnancy stages. Data are presented as mean ± SD. Pregnancy stages that do not share a common superscript are different (^{a, b, c} *p* < 0.05). GD, gestational day; Nsd, no significant difference.

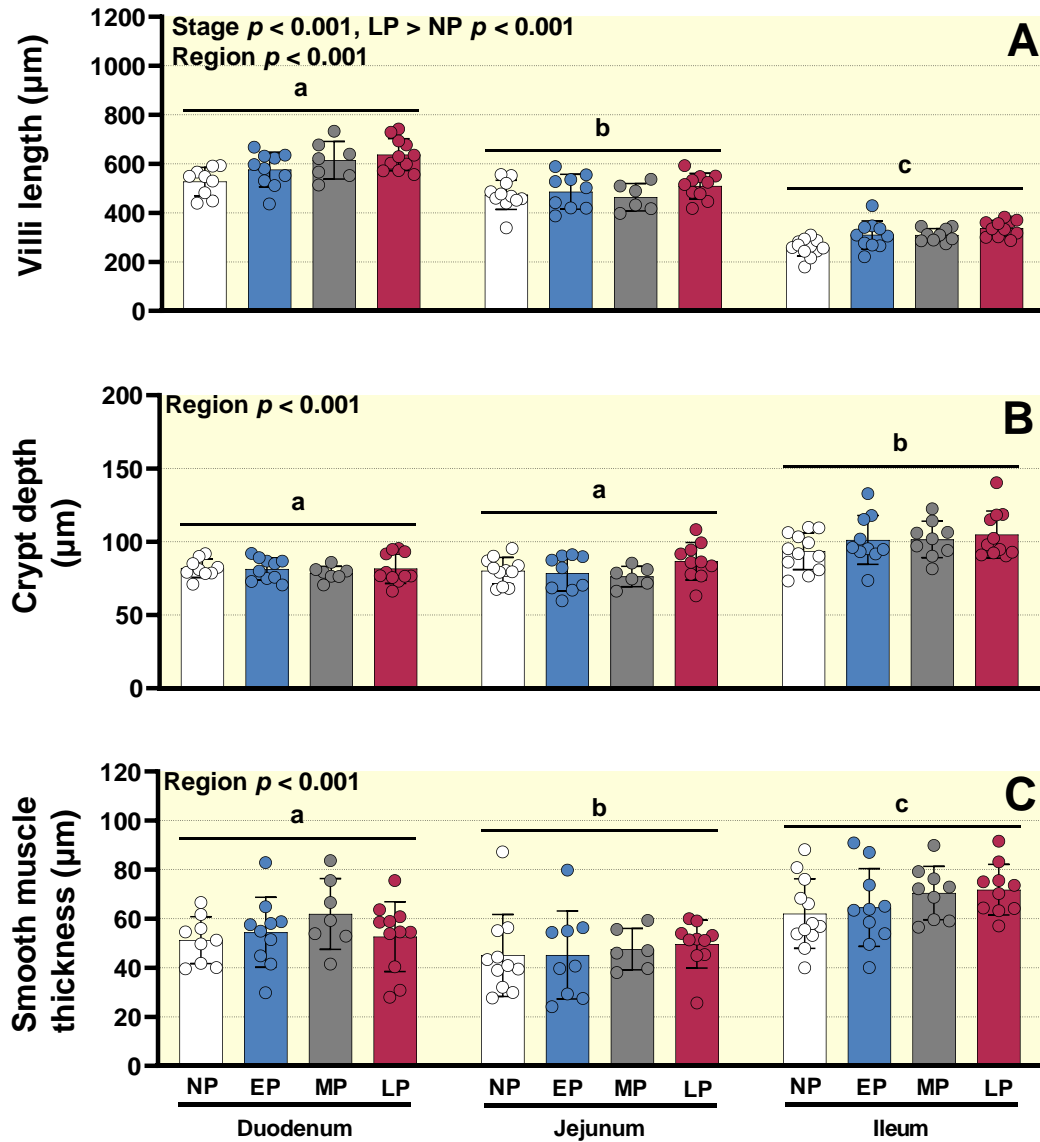


Figure 5.1 Small intestinal (SI) morphology changes with pregnancy and differs between regions. Effects of pregnancy stage and SI region on (A) villi length, (B) crypt depth and (C) smooth muscle thickness in C57BL/6 mice were analysed using mixed models, treating data from multiple regions from individual mice as repeated measures. Bars indicate mean \pm SD, with data for individual animals shown by symbols. $N = 6-12$ mice per pregnancy stage. Overall differences ($p < 0.05$) between SI regions are indicated by superscripts (a, b, c).

5.6.3. Study 1 - Nutrient transporter gene expression

5.6.3.1. *Carbohydrate transporters*

Effects of pregnancy stage on relative expression of *SLC2A5* (Glut5), *SLC2A2* (Glut2) and *SLC5A1* (Sglt1) differed between SI regions (Fig. 5.2A-2C, pregnancy*region interactions each $p < 0.05$). *SLC2A5* expression (Fig. 5.2A) differed by pregnancy stage in the duodenum ($p < 0.05$) and jejunum ($p < 0.01$) but not ileum ($p = 0.07$). Despite an overall effect of pregnancy stage, duodenal *SLC2A5* expression did not differ between pregnancy stages in pair-wise comparisons. In the jejunum, *SLC2A5* expression was 1.7-fold higher in mid-pregnant compared to non-pregnant or late-pregnant groups (Figure 5.2A, each $p = 0.012$). *SLC2A2* expression (Fig. 5.2B) differed by pregnancy stage in the ileum ($p < 0.05$) but not duodenum or jejunum (each $p > 0.1$). In the ileum, *SLC2A2* expression was 2.8-fold higher in late-pregnant compared to non-pregnant mice (Figure 5.2B, $p < 0.05$) but did not differ between other stages in pair-wise comparisons. *SLC5A1* expression (Fig. 5.2C) differed by pregnancy stage in the duodenum ($p < 0.05$) and ileum ($p < 0.01$) but not jejunum. Despite an overall effect of pregnancy stage, duodenal *SLC5A1* expression did not differ between pregnancy stages in pair-wise comparisons. In the ileum, *SLC5A1* expression was 1.7-fold higher in late-pregnant compared to non-pregnant (1.6-fold, $p < 0.05$) or mid-pregnant (1.5-fold, $p < 0.05$) mice (Fig. 5.2C).

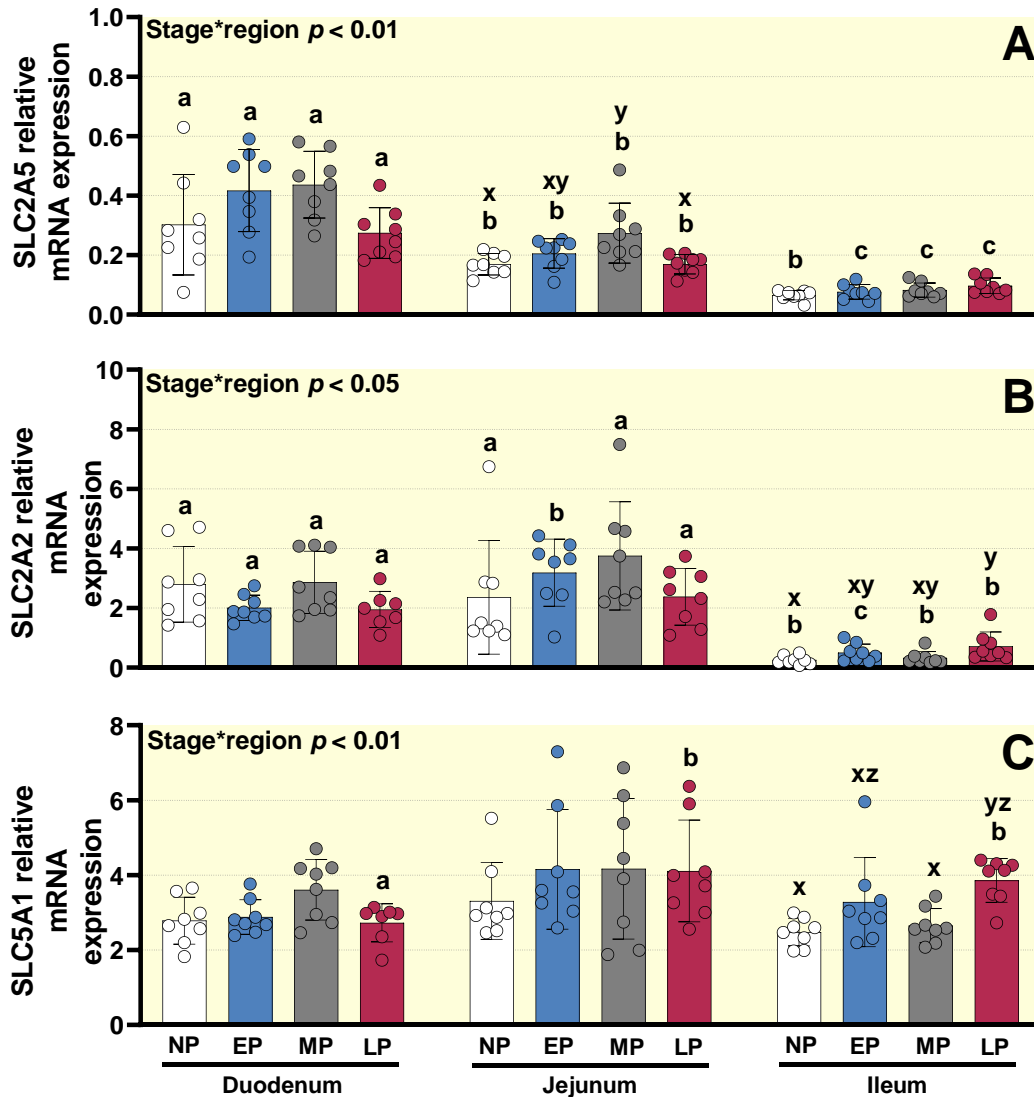


Figure 5.2 Changes in relative transcript expression of carbohydrate transporters SLC2A5, SLC2A2 and SLC5A1 in SI regions across pregnancy compared to non-pregnant controls, normalised to the housekeeper genes B2M, PPIA and HPRT. Transcript expression data was analysed via mixed model, treating data from multiple regions from individual mice as repeated measures. Where interactions were present, effects of pregnancy stage were assessed separately within each SI region, and effects of region were assessed separately within each pregnancy stage, by one-way ANOVA. Bars indicate mean \pm SD, with data for individual animals shown by symbols. $N = 7-8$ mice per pregnancy stage. Differences ($p < 0.05$) between SI regions within each pregnancy stage are indicated by superscripts (a, b, c). Differences ($p < 0.05$) between pregnancy stages within each SI region are indicated by superscripts (x, y, z).

5.6.3.2. *Amino acid transporters*

Relative expression of the neutral amino acid transporter *SLC6A19* (Fig. 5.3A) differed by SI region ($p < 0.001$) and pregnancy stage ($p < 0.01$), and effects of pregnancy stage did not differ between regions (interaction $p > 0.1$). *SLC6A19* expression was 1.6-fold higher in mid-pregnant than late-pregnant mice ($p < 0.01$), while expression in non- and early-pregnant mice did not differ between other stages (Figure 5.3A). *SLC6A19* expression was 1.7- and 1.4-fold higher in jejunum than duodenum or ileum, respectively (each $p < 0.001$). Relative expression of the taurine and β -alanine transporter *SLC6A6* (Fig. 5.3B) differed by SI region ($p < 0.001$) but not by pregnancy stage ($p = 0.07$), and effects of pregnancy stage did not differ between regions (interaction $p > 0.1$). *SLC6A6* expression was 1.4-fold higher in jejunum than duodenum ($p < 0.001$). *SLC6A6* expression in ileum was intermediate and different from both jejunum ($p < 0.01$) and duodenum ($p < 0.05$). Relative expression of peptide transporter 1 (*SLC15A1*, Fig. 5.3C), widely known as Pept1 (di- and tri-peptide transporter), differed by SI region ($p < 0.01$) but not by pregnancy stage ($p > 0.2$). *SLC15A1* expression was 1.9-fold lower in jejunum compared to duodenum or ileum (both $p < 0.05$).

5.6.3.3. *Fatty acid transporters*

Effects of pregnancy stage on relative expression of fatty acid transporters *CD36* and *FABP2* did not differ between regions. Relative expression of *CD36* (Fig. 5.4A) differed by SI region ($p < 0.001$) but not by pregnancy stage ($p > 0.5$). *CD36* expression was 3.1- and 1.8-fold higher in jejunum than ileum or duodenum, respectively (each $p < 0.001$), and was 1.7-fold higher in duodenum than ileum ($p < 0.01$). Relative expression of *FABP2* (Fig. 5.4B) differed by pregnancy stage and region (each $p < 0.001$), and effects of pregnancy stage did not differ between regions (interaction $p > 0.1$). *FABP2* expression was 1.2- to 1.4-fold higher in non-pregnant mice compared to pregnant mice at each stage of pregnancy ($p < 0.05$) and did not differ between early-, mid- or late-pregnant groups. *FABP2* expression was 2.4-fold higher in ileum than duodenum, 1.7-fold higher in ileum than jejunum, and 1.4-fold higher in jejunum than duodenum (each $p < 0.001$).

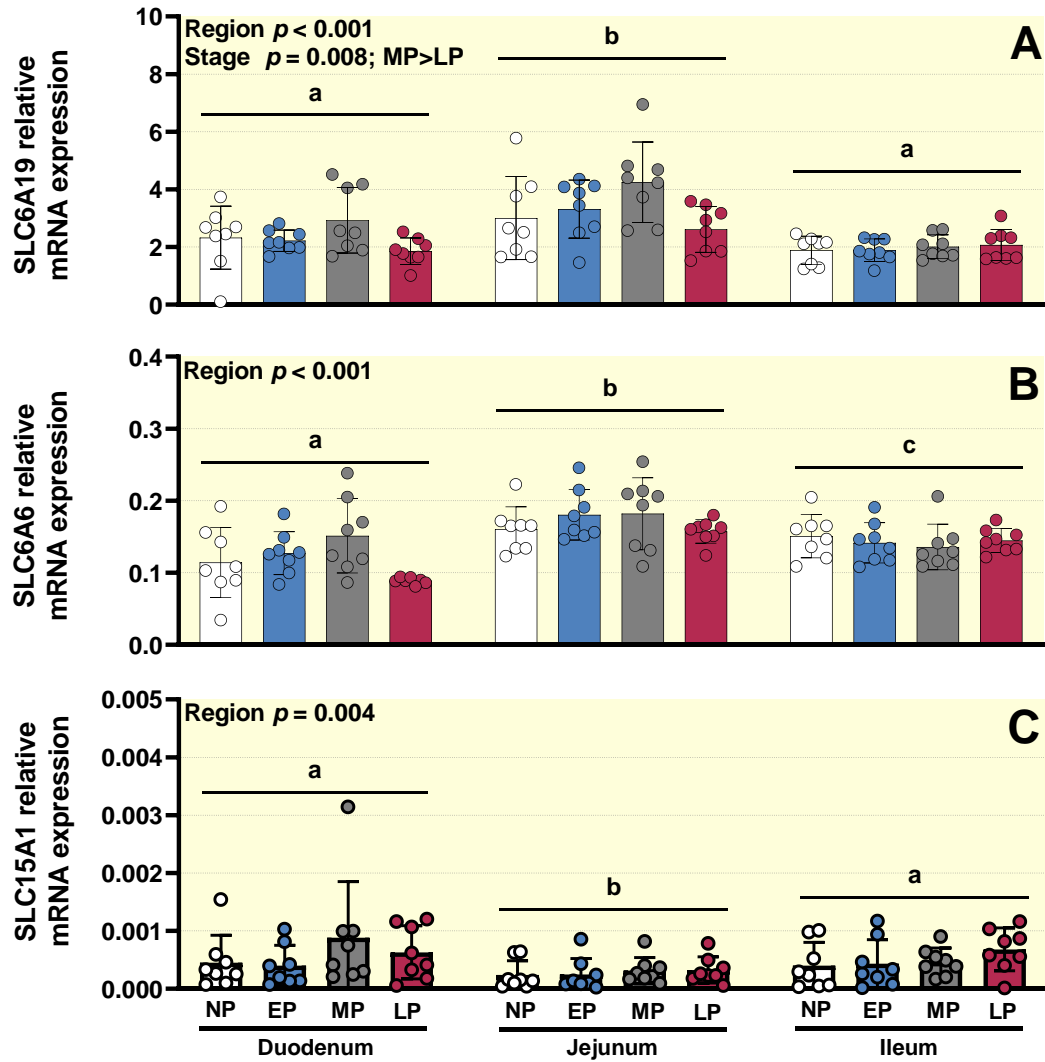


Figure 5.3 Changes in relative transcript expression of amino acid transporters SLC6A16, SLC6A6 and SLC15A1 in SI regions across pregnancy compared to non-pregnant controls, normalised to the housekeeper genes B2M, PPIA and HPRT. Transcript expression data was analysed via mixed model, treating data from multiple regions from individual mice as repeated measures. Bars indicate mean \pm SD, with data for individual animals shown by symbols. $N = 7-8$ mice per pregnancy stage. Overall differences ($p < 0.05$) between SI regions are indicated by superscripts (a, b, c).

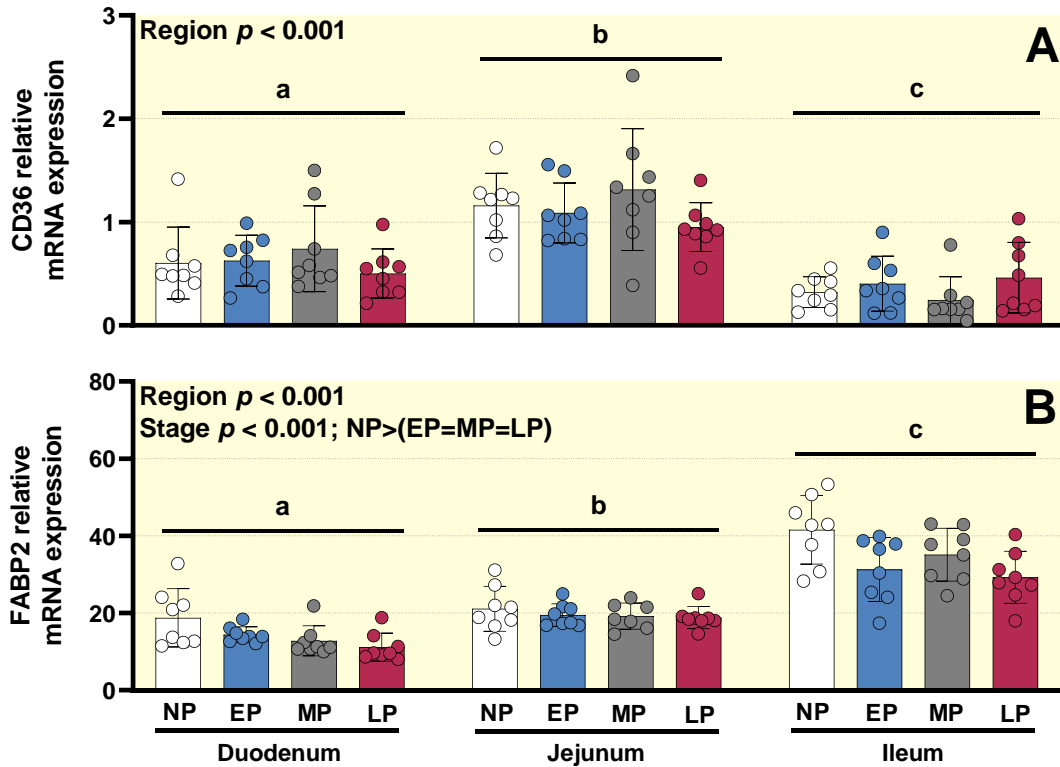


Figure 5.4 Changes in relative transcript expression of fatty acid transporters CD36 and FABP2 in SI regions across pregnancy compared to non-pregnant controls, normalised to the housekeeper genes *B2M*, *PPIA* and *HPRT* for CD36 and *B2M* and *HPRT* for FABP2. Transcript expression data was analysed via mixed model, treating data from multiple regions from individual mice as repeated measures. Bars indicate mean \pm SD, with data for individual animals shown by symbols. $N = 7-8$ mice per pregnancy stage. Overall differences ($p < 0.05$) between SI regions are indicated by superscripts (a, b, c).

5.6.4. Study 2 – mouse characteristics and SI gross morphology

Mice did not differ in initial body weight between groups, while final weights of late-pregnant mice were >50% heavier than non-pregnant mice ($p < 0.001$, Table 5.3). The total SI, duodenum and ileum were each 4-5% longer in late-pregnant than non-pregnant mice (each $p < 0.05$), while jejunum lengths did not differ between these groups (Table 5.3).

5.6.5. Study 2 - Active glucose transport

Active glucose transport (Fig. 5.5A and 5.5B) did not differ between non-pregnant and late-pregnant mice ($p > 0.4$), while effects of the SGLT1 inhibitor phlorizin and SI region were interdependent (interaction: $p < 0.001$). In tissues incubated without phlorizin, glucose-induced ΔI_{sc} differed between SI regions ($p < 0.001$), and was 2.7- to 7.0-fold higher in all other regions compared to the proximal duodenum (all $p < 0.01$). Glucose-induced ΔI_{sc} in the absence of phlorizin were ~2.5-fold higher in distal jejunum and proximal ileum than distal duodenum and distal ileum (all $p < 0.002$), while responses in proximal jejunum were intermediate and not different from any other region except proximal duodenum. Phlorizin inhibited glucose-induced ΔI_{sc} by between 70 and 99% in all regions (each $p < 0.01$). In the presence of phlorizin, glucose responses SI regions ($p < 0.001$), being > 5-fold lower in distal ileum than all other regions except proximal duodenum (all $p \leq 0.031$). Carbachol-induced ΔI_{sc} (Fig. 5.5C and 5.5D) were ~17% lower in late-pregnant than non-pregnant mice ($p < 0.05$), and differed between regions ($p < 0.001$) but were unaffected by phlorizin ($p = 0.084$), with no interactions between factors. Carbachol-induced ΔI_{sc} were ~1.4-fold greater in distal jejunum, proximal ileum and distal ileum than in either duodenal region (each $p < 0.05$), and intermediate in proximal jejunum.

Table 5.3 Study 2 mouse characteristics

	Non-pregnancy	Late-pregnancy	Significance (<i>p</i>)
No. of mice	19	16	
Gestational age	-	GD17.5	NS
Litter size	0	7.4 ± 1.9	NS
Initial body weight ¹ (g)	20.1 ± 1.9	20.0 ± 1.8	NS
Final body weight ² (g)	21.1 ± 1.6	32.0 ± 5.1	< 0.001
SI lengths (cm)			
Total	31.9 ± 1.7	33.3 ± 1.8	< 0.05
Duodenum	7.7 ± 0.5	8.1 ± 0.5	< 0.05
Jejunum	9.5 ± 0.6	9.9 ± 0.8	NS
Ileum	14.7 ± 0.9	15.3 ± 0.7	< 0.05

¹Initial body weight was the body weight recorded at the start of the 7-day acclimatisation period. ²Final body weight was the body weight recorded on the morning of experiments directly prior to humane killing. Data were compared between non-pregnant and pregnant groups by 1-way ANOVA and are presented as mean ± SD. GD, gestational day; NS, not significant.

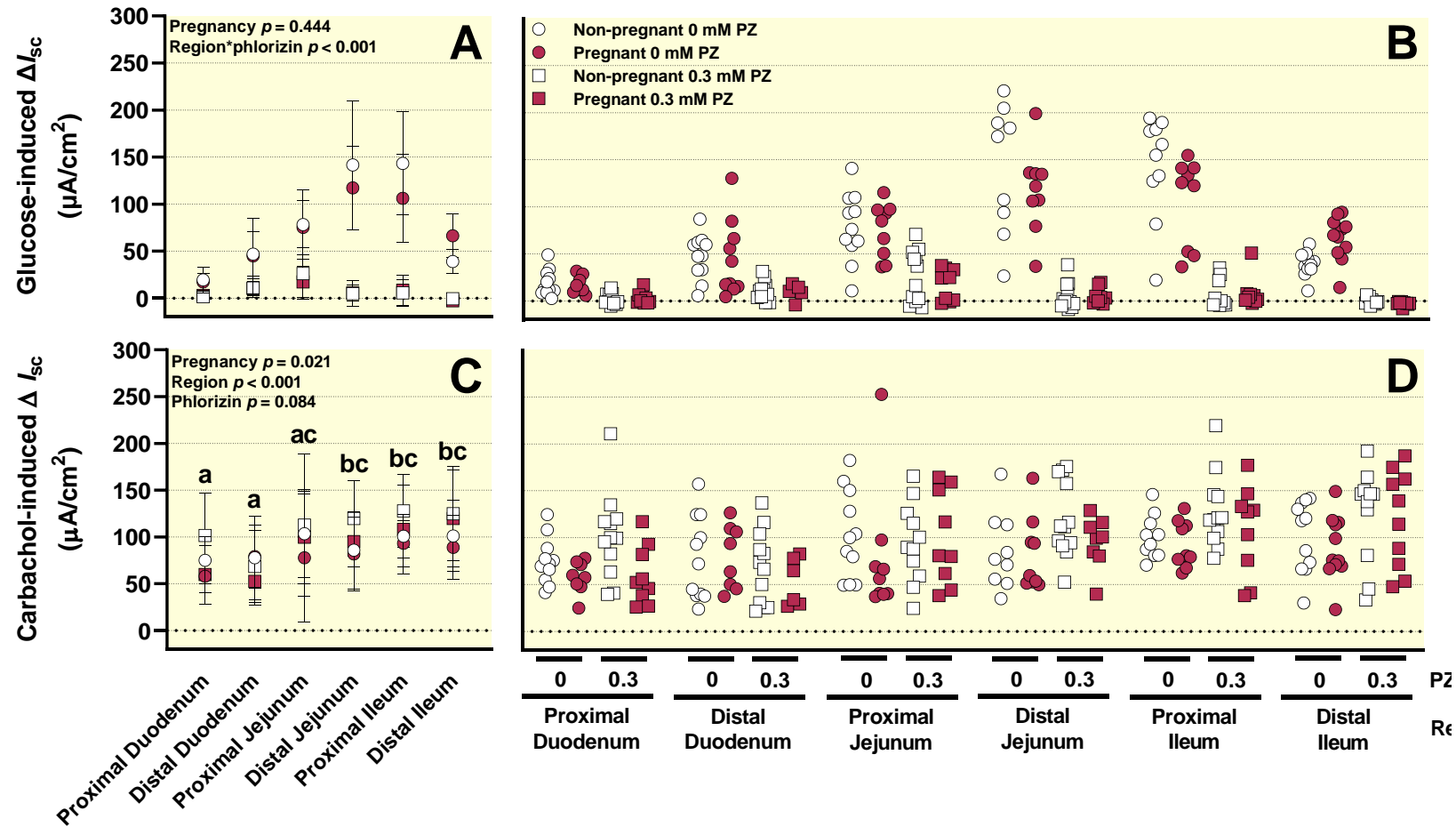


Figure 5.5 Changes in active glucose transport characterised across each SI region in C57BL/5 mice at late-pregnancy vs non-pregnant mice at diestrus. Data was analysed via mixed model, treating data from multiple regions from individual mice as repeated measures and is presented as group mean \pm SD (A & C) and individual values (B & D). $N = 16-19$ mice per pregnancy stage. Overall differences ($p < 0.05$) between SI regions are indicated by superscripts (a, b, c).

5.7. Discussion

The findings of this study support the concept that the SI undergoes macroscopic (length, weight), microscopic (villi morphology) and transcriptional changes in nutrient transporter expression that serve to facilitate increased nutrient uptake in murine pregnancy. These, however, did not enhance active glucose transport per unit area, which was similar within a given SI region irrespective of pregnancy stage, and contrast with previous reports of increased glucose transfer across the SI. Whether other glucose-transport mechanisms change during pregnancy, or effects of pregnancy on glucose transport depend on nutritional status, requires further investigation.

The moderate SI elongation in murine pregnancy was consistent with existing reports in rodents [175, 234, 330], and adds new knowledge that increased SI length arises due to increases in duodenum and ileum length alone. Although a review of gastrointestinal adaptations during pregnancy describes increases in overall SI weight and length and of villi length [5]. These adaptations appear to be variable between studies, SI regions and pregnancy stages. In contrast to our finding that villi were 18% longer in late pregnancy compared to non-pregnant animals, regardless of SI region, unchanged SI villi lengths were reported in pregnant compared to non-pregnant common shrews [179]. Others have reported inconsistent and stage-specific region-specific changes in villi length during rodent pregnancy, which were either increased [175] or unchanged [218] in the duodenum, increased in jejunum [178, 218], and unchanged [175] or decreased [178, 218] in the ileum. Likewise, variable changes in crypt depth and smooth muscle thickness have been reported between studies. Although these parameters were unchanged in the present study, others have reported region- and stage-specific crypt elongation and thickening of the smooth muscle layer with pregnancy progression in mice [178] and rats [218]. Together, the elongation of the entire SI and its villi that we observed was expected to expand SI surface area, although it was not possible to assess this directly in the current study. However, a single report on internal surface areas of SI regions in shrews, calculated from SI size, villi length and density, showed no change before lactation, when duodenal internal surface area increased [179].

To the best of our knowledge, this study is the first to map macronutrient transporter transcript expression across the SI during pregnancy. We found expression of glucose transporters *Sglt1* and *Glut2* was augmented only in the ileum in mice at late-pregnancy, with no changes observed earlier in pregnancy or in other SI regions. This lack of change in duodenal *Sglt1* expression contrasts with the only report of pregnancy-related SI carbohydrate transporter expression in rodents, which assessed only duodenum and reported a 1.5-fold higher *Sglt1* expression in duodenal mucosa of late- compared to non-pregnant rats [223]. The reasons for these differential responses are unclear, since animals were fed a standard chow and were

unfasted in both studies, although since the timing of tissue collection was not stated in the former study [223], it is possible that pregnancy-related changes differ with the circadian cycle. Indeed, we have reported that increases in food intake and meal size during late pregnancy occurred mostly during the light phase in mice [53]. Our finding of similar jejunal *Sglt1* expression in pregnant and non-pregnant mice may indicate that jejunal capacity for carbohydrate uptake is near maximal in non-pregnant mice, and not capable of further upregulation. In non-pregnant rodents and humans, the final stages of carbohydrate digestion to produce simple sugars occur primarily in the duodenum, whilst the majority of glucose uptake occurs in the upper two-thirds of the jejunum [155, 463]. Together with greater food intake during pregnancy, a ceiling on jejunal glucose uptake could increase ileal exposure to glucose. Increased exposure may then drive the 1.5-fold and 1.8-fold increases in ileal *Sglt1* and *Glut2* expression, respectively, increasing ileal capacity for carbohydrate absorption relative to the non-pregnant state. This is consistent with the hypothesis that the ileum acts as a functional reserve for nutrient absorption capacity [343]. It is important to note that the current study did not assess concurrent changes in mucosal carbohydrate transporter protein abundance. Thus, in the absence of protein abundance data, we cannot draw definitive conclusions regarding changes in carbohydrate transport capacity based on changes in transcript expression alone, especially considering the regulatory step involved in the translocation of SGLT-1 protein to the plasma membrane essential for glucose uptake [211, 464]. Carbohydrate absorption over a greater proportion of the SI could also extend the duration of carbohydrate absorption to sustain circulating blood glucose after each meal. This, in turn, could support placental glucose uptake and delivery to the fetus, which occurs down a concentration gradient [36]. In addition, increased ileal glucose may activate the ileal brake, triggering release of GLP-1 and PYY which act to slow upper SI motility [465]. Consistent with this hypothesis, fed concentrations of circulating GLP-1 were ~4-fold higher in mid- than non-pregnant rats, associated with gut hypertrophy but not satiety [234]. Reduced satiety actions of GLP-1 may reflect the downregulation of central and peripheral satiety pathways during pregnancy where food intake increases 20-30% by late pregnancy in rodents [59]. Independent of satiety-related actions, increased GLP-1 secretion and subsequent activation of the ileal brake may extend gut transit time in late-pregnancy, as reported in women [314] and rodents [308], increasing nutrient absorption capacity.

Impacts of pregnancy on SI amino acid uptake are not well characterised, although glycine absorption was 20% higher in late- compared to non-pregnant mice [459]. Glycine uptake is mediated by proton-coupled amino acid transporter 1 (PAT1, [158]), so it is possible that expression of this transporter may change at the transcript and/or protein level during pregnancy, however, this was not measured in the present study. In the current study,

expression of amino acid transporter transcripts, specifically *SLC6A19*, *SLC6A6* and *SLC15A1*, were similar across pregnancy stages and SI regions. Consistent with the similarity in transcript expression of the neutral amino acid (including leucine) transporter *SLC6A19* across pregnancy, another study reported no changes in the absorption of leucine in mid- compared to non-pregnant Albino rats [175].

Expression of apical fatty acid transporter *CD36* transcripts did not differ between pregnancy stages or SI regions in the present study. In contrast, expression of the intracellular transporter *FABP2* declined in the duodenum and ileum as pregnancy progressed. *FABP2* traffics fatty acids to the endoplasmic reticulum for export into the circulation [159], and decreased *FABP2* expression would likely reduce fatty acid supply from the SI, although uptake of fatty acids by the SI has not been reported in pregnancy. It is possible that fatty acids are diverted for use as energy sources within epithelial cells during pregnancy. This may be required to support SI growth, notably in late pregnancy [252, 324], and would also reduce SI demand for glucose as an energy source, protecting glucose supply to the circulation to support conceptus development. Consistent with the pattern of carbohydrate transporter expression, fatty acid transporter expression was also unchanged in the jejunum during pregnancy.

Region-specific gains in SI length, villi elongation and expression of glucose transporters led us to expect augmented SI glucose transport in mice at late pregnancy, which we therefore measured by Ussing chamber methodology [430]. However, *ex vivo* active glucose transport across isolated SI segments was similar in late- and non-pregnant mice, and increased ileal *Sglt1* and *Glut2* transcription did not equate to functional gains in glucose transport. The absence of enhanced glucose transport in pregnancy in our study contrasts with studies using SI perfusion or everted sac methodology, in which glucose transfer across the epithelium was ~20-30% higher in late-pregnant compared to non-pregnant rodents [231, 232]. This difference between studies may reflect our measure of active SGLT1-mediated glucose transport, rather than overall glucose transfer, and suggests that increases in passive glucose transport and/or reduced SI tissue metabolism of glucose may occur during pregnancy. Alternatively, it is possible that GLUT2 may play a greater role in glucose transport during pregnancy, since ileal expression was higher in late pregnancy, and GLUT2-mediated glucose transport does not generate current, which is the outcome detected by the Ussing chamber methodology. There is some, albeit controversial, evidence for translocation of GLUT2 from the basal to apical membrane in extreme physiological states, including a cohort study of morbidly obese women [210]. Whether this occurs in healthy pregnancies has not been assessed. Finally, differences between studies may also reflect different nutritional status of the rodents, which were fasted for 4-24 hours before tissue collection or perfusion in past studies [231, 232, 245], but had unrestricted access to food in the present study. SGLT1

expression is upregulated by luminal glucose, and therefore transcription may already be upregulated in non-pregnant as well as pregnant animals in the present study. It is possible that differential SGLT1 activity between pregnant and non-pregnant animals may be evident on fasting, and may contribute to higher glucose transport reported during pregnancy [231, 232, 245]. Thus, the potential for changes in glucose transport during pregnancy requires further investigation, and are likely to vary with nutritional state. We recognise that mechanisms other than intestinal nutrient delivery contribute to increased glucose availability during pregnancy, in support of fetal and maternal requirements. In addition to decreased insulin sensitivity of maternal peripheral tissues in the second half of pregnancy [466, 467], glucose availability is maintained by increased hepatic endogenous glucose production which is 30% and 60% higher in late pregnancy in women [468] and rats [469], respectively.

5.8. Conclusion

Our study has provided fundamental insight into SI region and pregnancy-stage specific adaptations in anatomy and nutrient transporter transcription expression in mice. Increases in SI weight by mid-pregnancy likely reflect elongation of duodenum and ileum. Elongation of villi by late pregnancy occurred independent of SI region, and would be expected to increase the surface area for nutrient absorption. Upregulation of carbohydrate transporter expression was seen primarily in ileum, where it may act in concert with gains in passive absorption (increased surface area) to support fetal development and the deposition of maternal reserves. Unexpectedly, given the anatomical and molecular changes, active SGLT1-mediated glucose transport per unit area was not greater in late-pregnant than age-matched non-pregnant mice. Increased nutrient demand during pregnancy may therefore be met largely through SI expansion or changes in SI motility, although contributions of other nutrient transport mechanisms require evaluation. Precise knowledge of the adaptations will inform future research that optimises nutritional and dietary support during human pregnancy, improves pregnancy outcomes, and safeguards fetal development and the future health of the mother and newborn.

6. CHAPTER 6: GENERAL DISCUSSION

6.1. Introduction

The requirement for energy and nutrient provisioning increases throughout pregnancy due to greater maternal and fetal demand and the need to deposit adipose tissue to support lactation post parturition [5]. Maternal food intake increases in humans [4, 49, 50] and rodents [14, 51] to satisfy these demands, particularly during the latter stages of pregnancy, when fetal growth and development is rapid. The small intestine (SI) possesses a high degree of anatomical and functional plasticity and is capable of rapidly adapting to changing nutrient demands under physiological conditions, including pregnancy [5]. Despite this capacity, it is unclear if, or how, the SI adapts throughout pregnancy, and the timing and nature of any such SI adaptations remain poorly characterised and understood.

To gain a comprehensive overview of the current state of knowledge regarding determinants of nutrient absorption and adaptive changes of the gastrointestinal tract throughout pregnancy, and to help inform experiments described in this thesis, a scoping review was undertaken. Early results from this review informed experiments to map SI anatomy as well as expression of macronutrient transporter transcripts throughout pregnancy in mice. I then optimised and validated Ussing chamber methodology to precisely determine region-specific changes in *ex vivo* SI active glucose transport across the oestrous cycle in C57BL/6 mice and subsequently applied this method to compare non-pregnant and late-stage pregnancy mice. An overall summary of the work presented in this thesis is shown in figure 6.1.

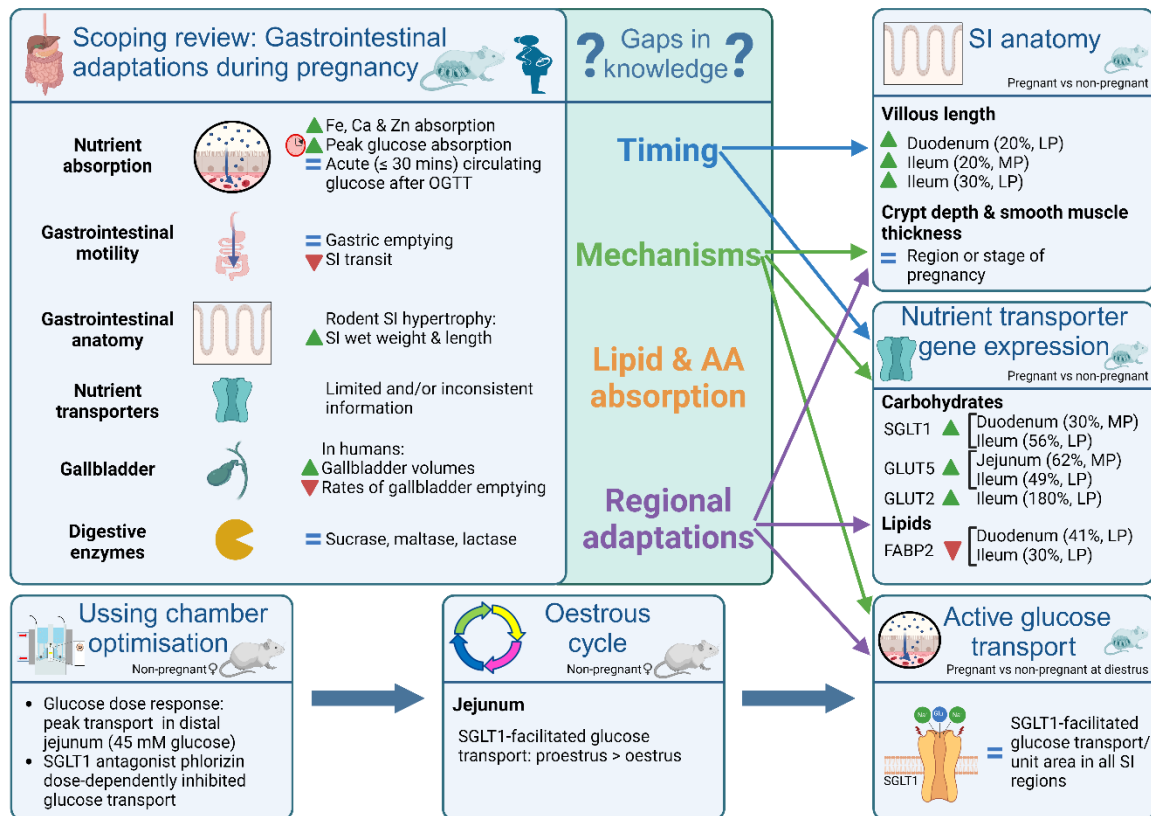


Figure 6.1 Graphical overview of the results of studies presented in this thesis. Green and red triangles indicate increases and decreases compared to non-pregnant control values. Blue equal sign indicates no change compared to non-pregnant control values. Figure created using Biorender.com.

Chapter 3 details findings of the scoping review which highlight a lack of primary data in support of some of the widely accepted concepts regarding anatomical, molecular, and to a lesser extent, functional adaptations of the SI throughout pregnancy in monogastric mammals. Importantly, precise data on the progression of these adaptations across pregnancy are lacking, particularly in early and mid-pregnancy; this is concerning, given the sensitivity of the uterine environment to nutrition [470]. Furthermore, the implantation and embryonic periods encompass critically important periods of fetal growth and development that greatly influence overall pregnancy success [471]. Therefore, further studies which investigate SI adaptations during early- and mid-pregnancy are clearly warranted. Our review showed that most knowledge regarding anatomical, molecular and functional adaptations in the SI during pregnancy in monogastric mammals is derived from rodents and humans. Although the use of model organisms such as rodents is common practice due to practical advantages such as a short gestation period, their use comes with limitations. An example of this limitation is the exceedingly low rate of success in translating successful findings of new cancer drug therapies from rodents to humans (<8%, [472]). Although animal studies provide invaluable sources of *in vivo* information, these often fail to accurately model human physiology, carcinogenesis and disease progression, and safety and efficacy data must be generated in different species,

including a large animal or primate before proceeding to human trials [472]. It is also important to note that humans and rodents differ considerably in rate of fetal growth and fetal to maternal weight ratio [14, 20, 53, 380, 381], and as such, differences in demand for GI/SI adaptation and nutrient provisioning. While animal studies report changes in gross SI anatomy together with limited data on changes in SI nutrient transporter expression and function, these provide little to no mechanistic insight to aid in the identification of signalling pathways and potential therapeutic targets to optimise management of maternal nutrition and gestational weight gain in humans. Moreover, human studies in healthy volunteers exclusively report functional changes in the SI due to the inability to perform invasive experiments to characterise changes in SI anatomy and molecular expression. Interestingly, although changes in direct and indirect carbohydrate uptake are reported in the SI of rodents *in vivo*, corresponding changes in lipid and amino acid uptake, and expression of their associated transporters, are surprisingly understudied. Furthermore, no studies have examined expression of amino acid transporters and potential changes across any pregnancy stage or SI region. In contrast, changes in uptake of key micronutrients such as iron, calcium and zinc are widely reported in rodents, and to a lesser extent in humans, predominantly during late-pregnancy. In summary, the scoping review found a significant lack of primary data regarding determinants of GIT nutrient absorption, and identified major gaps in knowledge on determinants of GIT micronutrient and macronutrient absorption throughout pregnancy in monogastric mammals. Therefore, to address one of the identified major gaps in knowledge, I developed a technique to interrogate *ex vivo* glucose transport in SI regions during pregnancy.

It is well established that food intake changes throughout the course of the human menstrual cycle [473], which is likely due, in part, to fluctuating concentrations of circulating sex steroid hormones such as estrogen and progesterone. Despite this knowledge, no previous studies have specifically investigated the effects of the oestrous cycle on region-specific macronutrient uptake in the SI. A single study has reported significantly lower blood glucose responses to a 50 g OGTT during the follicular compared to the luteal phase of the menstrual cycle in healthy women [432]. However, a major limitation of methods used to study postprandial glycaemic responses in pregnancy are the unknown variables of tissue utilisation, hepatic first-pass clearance, and placental uptake during pregnancy. The only method to obtain an accurate overview of changes in first-point glucose absorption by the SI is to sample the portal vein. However, this method is invasive, and not ethically or practically feasible to use in healthy human volunteers and challenging in small animals such as mice. This constraint further highlights the urgent need to develop new experimental methods to interrogate changes in SI nutrient absorption *in vivo*.

Chapter 4 describes *ex vivo* studies which optimised and validated Ussing chamber methodology in mice, as well as experiments that established a region-specific and physiological glucose dose-response to *ex-vivo* luminal glucose challenges in SI isolated tissue segments. This study was performed to determine the relative contribution of SGLT1 to glucose transport across each SI region, and to validate the efficacy of the SGLT1 inhibitor phlorizin. To help inform the concentration of glucose challenges to be performed in subsequent studies, the responses to 5, 10, 25 and 45 mM glucose challenges were characterised within each SI-region. Next, the suitability of using DMSO as a solvent, and the efficacy of the SGLT1 antagonist phlorizin were evaluated across concentrations. Once optimised, I studied SGLT1-dependent *ex vivo* glucose transport in the jejunum (the region of peak nutrient uptake) in *ad libitum* fed mice at different stages of the oestrous cycle. I discovered that SGLT1-dependent glucose transport was oestrous cycle stage dependent, and lower at oestrus (follicular phase) compared to proestrus (luteal phase) in corroboration of human OGTT data [432]. Due to the extremely limited evidence currently available in humans and rodents, further studies are needed to fully interrogate how circulating sex steroid, satiety and/or appetite regulating factors regulate the adaptive response of the SI to changing energy intake. In addition, to account for changes in both active and passive glucose uptake, future *in vivo* studies in rodents or small mammals should consider portal vein sampling combined with non-metabolisable glucose analogues to bypass factors which directly affect blood glucose concentrations, such as tissue utilisation and hepatic first pass clearance. Following successful optimisation of the Ussing chamber method that demonstrated glucose uptake varied by SI region and oestrous cycle stage, I then applied this method to interrogate changes in region-specific glucose uptake in the SI during pregnancy.

Prior to work presented in this thesis, reports on changes in SI regional anatomy in rodents throughout pregnancy were limited [175, 423, 425], as reviewed in Chapter 3. Moreover, none of those studies investigated concurrent changes in SI anatomy, nutrient transporter expression and function. Findings from studies presented in Chapter 5 support the concept that the SI undergoes anatomical and molecular adaptations to enhance nutrient uptake capacity during pregnancy. This is not surprising considering the increase in nutritional requirements of both mother and fetus [4, 14, 49-51], with glucose the primary substrate used during cellular respiration. Interestingly, despite observing concurrent anatomical and molecular adaptations, SGLT1-dependent glucose transport per unit of area did not differ in any SI region between non- and late-pregnant mice. As most dietary carbohydrates are digested to monosaccharides by brush border enzymes prior to absorption, beginning in the proximal duodenum [155, 156], we expected this region to be the first to adapt to increased maternal and fetal substrate needs. Indeed, we observed both greater duodenal villous length

and upregulated duodenal expression of SGLT1 transcript in late- compared to non-pregnant mice. These adaptations stand to increase capacity for glucose uptake and delivery into circulation. Interestingly, while villous length and SGLT-1 changes were seen also in the ileum, none of these occurred in the jejunum in late- compared to non-pregnant mice, and despite SGLT1-dependent glucose transport patterns in each region being consistent with those observed in Chapter 4, active glucose uptake in all regions was similar in non- and late-pregnant mice. We speculate that the jejunum operates at a ceiling of glucose uptake capacity sufficient to meet the pregnancy demands of glucose absorption, in concert with positive changes in duodenal and ileal anatomy and augmented SGLT1 transcript and/or protein expression.

There are two other important determinants of the rate at which nutrients are absorbed by the SI; the rate of gastric emptying, which tightly regulates SI nutrient exposure, and transit-slowing actions of the 'ileal brake', which is triggered by ileal nutrients and mediated by L cell-released GLP-1 and PYY [182]. Together these mechanisms govern the period nutrients are present and exposed to the SI epithelium. The rate of liquid and solid gastric emptying in humans and rodents, and activity of SI brush border carbohydrase enzymes sucrase, lactase and maltase in rodents, generally do not change during pregnancy, yet SI motility is unequivocally slower towards the end of pregnancy (Chapter 3). Slower SI motility would serve to increase the amount of time available for nutrient absorption, negating the need for further adaptations to increase capacity. Given that fewer nutrients would be expected to reach the ileal brake trigger point in pregnancy, we speculate that nutrient-evoked feedback is, instead, augmented in the proximal SI in late pregnancy to slow motility to fully complete glucose absorption. There is also evidence from studies in rodents which suggests that satiety signalling is dampened towards the end of pregnancy, which would allow for bigger meal sizes and more frequent feeding bouts [59].

In summary, although we observed anatomical and molecular adaptations expected to increase glucose uptake capacity, we did not observe an increase in *ex vivo* active glucose transport per unit area across any SI region between late- and non-pregnant mice. Due to the limited and contradictory evidence available, additional *in vivo* studies, ideally utilising ligated loops, are required to interrogate changes in SI region-specific glucose uptake.

As pregnancy-related changes in fatty acid transport have not previously been reported in the SI in pregnancy, an interesting finding in Chapter 5 was our first documentation that *FABP2* transcripts were downregulated in the duodenum and ileum at late-pregnancy. *FABP2* traffics fatty acids to the endoplasmic reticulum prior to release to the circulation [159], and if this change occurs at protein level, could indicate a preference to sequester fatty acids in SI

enterocytes in pregnancy, potentially as a fuel to meet the energetic requirements of augmented glucose uptake and delivery to the circulation. This is best exemplified in colonocytes, which utilise SCFAs as their primary metabolic substrate [474, 475]. Further studies are required to explore this concept, including a focus on FABP1, which traffics fatty acids to the mitochondria to undergo lipid oxidation which yields energy for in-cell use [159].

6.2. Strengths, weaknesses and limitations of studies presented in this thesis

The molecular and functional studies within this thesis are novel, and my in-depth examination of pregnancy adaptations in mice provides fundamental new knowledge not permissible in humans due to ethical limitations. Indeed, no studies of similar scope have been reported in rodents or humans. There are, however, limitations in the use of mice, such as a significantly shorter length of gestation and litter size difference. The latter increases maternal load resulting in disproportionately higher maternal food intake, weight gain, nutrient and energy requirements compared to human pregnancy [17, 53]. Another major difference between humans and mice is the level of physical activity during pregnancy, which acutely declines from as early as gestational day 1 in mice [14, 476], compared to a gradual decline in humans concurrent with a gradual increase in sedentary activity [477, 478]. As such, caution needs to be exercised when interpreting results from rodent studies, and their translation to human pregnancy.

Due to the similar gross SI anatomy between humans and mice, it is possible to interrogate changes in SI anatomy under similar physiological conditions. Importantly, the expression and function of major nutrient transporter transcripts and proteins is largely homologous between humans and mice [212, 479]. This allows functional studies to interrogate regional changes in active and passive nutrient transport during different states of nutrient demand, i.e., over the course of the reproductive cycle and pregnancy, with high relevance to humans. Furthermore, my optimisation of Ussing chamber methodology provides for future studies aimed to interrogate changes in region-specific transport and SI absorption of individual nutrients under different states of altered nutrient demand, such as pregnancy.

There are limits to the studies presented in Chapter 5, including the lack of protein quantification to confirm pregnancy changes seen in expression of nutrient transporter transcripts. This data is essential to gain insights into protein localisation and abundance which is required to fully interpret Ussing chamber data presented in Chapter 5. Furthermore, based on our histology and PCR findings that changes in SI anatomy and molecular expression occurred towards the end of pregnancy in mice, the Chapter 5 Ussing chamber study only examined SI changes at late-pregnancy compared to non-pregnancy. Additional studies are

also required to determine whether passive and facilitated diffusion routes of glucose absorption and transport are altered in pregnancy. In addition, despite our finding of elevated SGLT1 transcript expression in the duodenum and ileum of pregnant mice (Chapter 5), it is important to note that SGLT1 transcripts undergo post-transcriptional stabilisation via polyadenylation, which could increase protein without change at transcript level [480], which demands further investigation. In Chapter 4 Ussing chamber studies only the jejunum was used to determine oestrous cycle-stage effects on glucose transport, as the region where the majority of nutrient uptake occurs [158, 204]. Future studies should be undertaken to determine whether the duodenum and ileum undergo similar changes in active glucose transport as observed in the jejunum. There is also limited and inconsistent evidence regarding the timing of changes in expression of transporters involved in uptake of micronutrients such as calcium, potassium and zinc (Chapter 3). Therefore, future studies are required to investigate how changes in expression of specific transporters may correlate with periods of increased demand of specific nutrients during early- and mid-pregnancy. Future studies could also investigate changes in single cell expression of nutrient transporters changes across the different cell types which comprise the SI epithelium, in response to changes in demand of specific nutrients such as calcium.

Lastly, the Ussing chamber studies in Chapters 4 and 5 investigated changes in active glucose transport, and future studies will be required to interrogate changes in the absorption of other macronutrients such as lipids and amino acids during pregnancy; the former has only been reported once, in rats [258].

6.3. Conclusion

In summary, data presented in this thesis provide a contemporary and authoritative overview of knowledge regarding SI changes in nutrient absorption and its determinants during pregnancy, whilst identifying major gaps in existing knowledge to inform future research. Such research may ultimately help us better understand how determinants of SI nutrient absorption change during complicated pregnancies and how to potentially avoid or better manage such conditions and complications by better managing maternal nutrition. These include pregnancies exposed to maternal malnutrition, previous surgical procedures such as bariatric surgery or pathologies such as gestational diabetes mellitus and preeclampsia.

My thesis findings support the concept that the maternal SI adapts during pregnancy to augment nutrient absorption in support of increased maternal energy and nutrient requirements throughout pregnancy, however the precise mechanisms underlying these adaptations remain to be fully elucidated. This thesis also outlines optimised Ussing chamber methodology used to provide the first direct evidence of SI active glucose transport changes

during the oestrous cycle in mice, which corroborate past (non-invasive) clinical findings. SI active glucose transport was unchanged across pregnancy stages, despite anatomical and molecular adaptations in late-pregnant mice, warranting investigation of passive and facilitated diffusion routes of glucose absorption in pregnancy.

References

1. Goldstein RF, Abell SK, Ranasinha S, Misso M, Boyle JA, Black MH, Li N, Hu G, Corrado F, Rode L, Kim YJ, Haugen M, Song WO, Kim MH, Bogaerts A, Devlieger R, Chung JH, Teede HJ. Association of gestational weight gain with maternal and infant outcomes: a systematic review and meta-analysis. *JAMA*. 2017;317:2207-25.
2. Goldstein RF, Abell SK, Ranasinha S, Misso ML, Boyle JA, Harrison CL, Black MH, Li N, Hu G, Corrado F, Hegaard H, Kim YJ, Haugen M, Song WO, Kim MH, Bogaerts A, Devlieger R, Chung JH, Teede HJ. Gestational weight gain across continents and ethnicity: systematic review and meta-analysis of maternal and infant outcomes in more than one million women. *BMC Med*. 2018;16:153.
3. Odhiambo JF, Pankey CL, Ghnenis AB, Ford SP. A review of maternal nutrition during pregnancy and impact on the offspring through development: evidence from animal models of over- and undernutrition. *Int J Environ Res Public Health*. 2020;17:6926.
4. Champion ML, Harper LM. Gestational weight gain: update on outcomes and Interventions. *Curr Diab Rep*. 2020;20:11.
5. Astbury S, Mostyn A, Symonds ME, Bell RC. Nutrient availability, the microbiome, and intestinal transport during pregnancy. *Appl Physiol Nutr Metab*. 2015;40:1100-6.
6. Florman HM, Fissore RA. Chapter 4 - Fertilization in mammals. In: Plant TM, Zeleznik AJ, editors. *Knobil and Neill's Physiology of Reproduction (Fourth Edition)*. San Diego: Academic Press; 2015. 149-96.
7. Ramathal C, Reijo Pera RA, Chavez SL. Chapter 6 - Preimplantation embryo development and primordial germ cell lineage specification. In: Plant TM, Zeleznik AJ, editors. *Knobil and Neill's Physiology of Reproduction (Fourth Edition)*. San Diego: Academic Press; 2015. 233-65.
8. Zhang S, Lin H, Kong S, Wang S, Wang H, Wang H, Armant DR. Physiological and molecular determinants of embryo implantation. *Mol Aspects Med*. 2013;34:939-80.
9. Moore KL, Persaud TVN, Torchia MG. *The developing human: clinically oriented embryology (Ninth Edition)*. Philadelphia, Pennsylvania: Saunders/Elsevier; 2013.
10. Murray SA, Morgan JL, Kane C, Sharma Y, Heffner CS, Lake J, Donahue LR. Mouse gestation length is genetically determined. *PLoS One*. 2010;5:e12418.
11. Pugh SJ, Ortega-Villa AM, Grobman W, Hinkle SN, Newman RB, Hediger M, Grewal J, Wing DA, Albert PS, Grantz KL. Longitudinal changes in maternal anthropometry in relation to neonatal anthropometry. *Public Health Nutr*. 2019;22:797-804.
12. Thompson JM, Irgens LM, Skjaerven R, Rasmussen S. Placenta weight percentile curves for singleton deliveries. *BJOG*. 2007;114:715-20.
13. Mu J, Adamson SL. Developmental changes in hemodynamics of uterine artery, utero- and umbilicoplacental, and vitelline circulations in mouse throughout gestation. *Am J Physiol Heart Circ Physiol*. 2006;291:H1421-8.
14. Ladyman SR, Carter KM, Grattan DR. Energy homeostasis and running wheel activity during pregnancy in the mouse. *Physiol Behav*. 2018;194:83-94.
15. Erkadius E, Morgan TO, Di Nicolantonio R. Amniotic fluid composition and fetal and placental growth rates in genetically hypertensive and normotensive rats. *Reprod Fertil Dev*. 1995;7:1563-7.
16. Gokulakrishnan G, Estrada IJ, Sosa HA, Fiorotto ML. In utero glucocorticoid exposure reduces fetal skeletal muscle mass in rats independent of effects on maternal nutrition. *Am J Physiol Regul Integr Comp Physiol*. 2012;302:R1143-52.
17. Girard J, Burnol AF, Leturque A, Ferre P. Glucose homeostasis in pregnancy and lactation. *Biochem Soc Trans*. 1987;15:1028-30.
18. Sferruzzi-Perri AN, Vaughan OR, Haro M, Cooper WN, Musial B, Charalambous M, Pestana D, Ayyar S, Ferguson-Smith AC, Burton GJ, Constancia M, Fowden AL. An obesogenic diet during mouse pregnancy modifies maternal nutrient partitioning and the fetal growth trajectory. *FASEB J*. 2013;27:3928-37.

19. Musial B, Vaughan OR, Fernandez-Twinn DS, Voshol P, Ozanne SE, Fowden AL, Sferruzzi-Perri AN. A Western-style obesogenic diet alters maternal metabolic physiology with consequences for fetal nutrient acquisition in mice. *J Physiol*. 2017;595:4875-92.
20. Rasmussen KM. Weight Gain During Pregnancy: Reexamining the Guidelines. Institute of Medicine (US) and National Research Council (US) Committee to Reexamine IOM Pregnancy Weight Guidelines. 2009.
21. Soma-Pillay P, Nelson-Piercy C, Tolppanen H, Mebazaa A. Physiological changes in pregnancy. *Cardiovasc J Afr*. 2016;27:89-94.
22. Kaur H, Muhlhausler BS, Roberts CT, Gatford KL. The growth hormone-insulin like growth factor axis in pregnancy. *J Endocrinol*. 2021:23-39.
23. Goldberg GR, Prentice AM, Coward WA, Davies HL, Murgatroyd PR, Wensing C, Black AE, Harding M, Sawyer M. Longitudinal assessment of energy expenditure in pregnancy by the doubly labeled water method. *Am J Clin Nutr*. 1993;57:494-505.
24. Forsum E, Kabir N, Sadurskis A, Westerterp K. Total energy expenditure of healthy Swedish women during pregnancy and lactation. *Am J Clin Nutr*. 1992;56:334-42.
25. López-Luna P, Maier I, Herrera E. Carcass and tissue fat content in the pregnant rat. *Biol Neonate*. 1991;60:29-38.
26. Cheung KL, Lafayette RA. Renal physiology of pregnancy. *Adv Chronic Kidney Dis*. 2013;20:209-14.
27. Carter AM. Placental oxygen consumption. Part I: in vivo studies - a review. *Placenta*. 2000;21 Suppl A:S31-7.
28. Catalano PM, Huston L, Amini SB, Kalhan SC. Longitudinal changes in glucose metabolism during pregnancy in obese women with normal glucose tolerance and gestational diabetes mellitus. *Am J Obstet Gynecol*. 1999;180:903-16.
29. Catalano PM, Tyzbit ED, Roman NM, Amini SB, Sims EA. Longitudinal changes in insulin release and insulin resistance in nonobese pregnant women. *Am J Obstet Gynecol*. 1991;165:1667-72.
30. Catalano PM, Tyzbit ED, Wolfe RR, Roman NM, Amini SB, Sims EA. Longitudinal changes in basal hepatic glucose production and suppression during insulin infusion in normal pregnant women. *Am J Obstet Gynecol*. 1992;167:913-9.
31. Wong AY, Kulandavelu S, Whiteley KJ, Qu D, Langille BL, Adamson SL. Maternal cardiovascular changes during pregnancy and postpartum in mice. *Am J Physiol Heart Circ Physiol*. 2002;282:H918-25.
32. Kulandavelu S, Qu D, Adamson SL. Cardiovascular function in mice during normal pregnancy and in the absence of endothelial NO synthase. *Hypertension*. 2006;47:1175-82.
33. Wuyts C, Simoens C, Pinto S, Philippaert K, Vennekens R. Continuous glucose monitoring during pregnancy in healthy mice. *Sci Rep*. 2021;11:4450.
34. Musial B, Fernandez-Twinn DS, Vaughan OR, Ozanne SE, Voshol P, Sferruzzi-Perri AN, Fowden AL. Proximity to delivery alters insulin sensitivity and glucose metabolism in pregnant mice. *Diabetes*. 2016;65:851-60.
35. Urison NT, Buffenstein RB. Metabolic and body temperature changes during pregnancy and lactation in the naked mole rat (*Heterocephalus glaber*). *Physiol Zool*. 1995;68:402-20.
36. Dilworth MR, Sibley CP. Review: transport across the placenta of mice and women. *Placenta*. 2013;34 Suppl:S34-9.
37. Burton GJ, Fowden AL, Thornburg KL. Placental origins of chronic disease. *Physiol Rev*. 2016;96:1509-65.
38. Burton GJ, Fowden AL. The placenta: a multifaceted, transient organ. *Philos Trans R Soc Lond B Biol Sci*. 2015;370:20140066.
39. Desforges M, Sibley CP. Placental nutrient supply and fetal growth. *Int J Dev Biol*. 2010;54:377-90.
40. Jansson T. Amino acid transporters in the human placenta. *Pediatr Res*. 2001;49:141-7.

41. Moe AJ. Placental amino acid transport. *Am J Physiol.* 1995;268:C1321-31.
42. Garcia-Santillan JA, Lazo-de-la-Vega-Monroy ML, Rodriguez-Saldaña GC, Solis-Barbosa MA, Corona-Figueroa MA, Gonzalez-Dominguez MI, Gomez-Zapata HM, Malacara JM, Barbosa-Sabanero G. Placental nutrient transporters and maternal fatty acids in SGA, AGA, and LGA newborns from mothers with and without obesity. *Front Cell Dev Biol.* 2022;10:822527.
43. Díaz P, Harris J, Rosario FJ, Powell TL, Jansson T. Increased placental fatty acid transporter 6 and binding protein 3 expression and fetal liver lipid accumulation in a mouse model of obesity in pregnancy. *Am J Physiol Regul Integr Comp Physiol.* 2015;309:R1569-77.
44. Belkacemi L, Bédard I, Simoneau L, Lafond J. Calcium channels, transporters and exchangers in placenta: a review. *Cell Calcium.* 2005;37:1-8.
45. Glazier JD, Atkinson DE, Thornburg KL, Sharpe PT, Edwards D, Boyd RD, Sibley CP. Gestational changes in Ca²⁺ transport across rat placenta and mRNA for calbindin D9K and Ca²⁺-ATPase. *Am J Physiol Renal Physiol.* 1992;263:R930-5.
46. Jansson T, Wennergren M, Illsley NP. Glucose transporter protein expression in human placenta throughout gestation and in intrauterine growth retardation. *J Clin Endocrinol Metab.* 1993;77:1554-62.
47. Stanirowski PJ, Szukiewicz D, Pyzlak M, Abdalla N, Sawicki W, Cendrowski K. Impact of pre-gestational and gestational diabetes mellitus on the expression of glucose transporters GLUT-1, GLUT-4 and GLUT-9 in human term placenta. *Endocrine.* 2017;55:799-808.
48. Kappen C, Kruger C, Jones S, Herion NJ, Salbaum JM. Maternal diet modulates placental nutrient transporter gene expression in a mouse model of diabetic pregnancy. *PLoS One.* 2019;14:e0224754.
49. Kopp-Hoolihan LE, van Loan MD, Wong WW, King JC. Longitudinal assessment of energy balance in well-nourished, pregnant women. *Am J Clin Nutr.* 1999;69:697-704.
50. Lecorguillé M, Camier A, Kadawathagedara M. Weight changes, nutritional intake, food contaminants, and supplements in women of childbearing age, including pregnant women: guidelines for interventions during the perinatal period from the French National College of Midwives. *J Midwifery Womens Health.* 2022;67 Suppl 1:S135-s48.
51. Ladyman SR, Grattan DR. Region-specific reduction in leptin-induced phosphorylation of signal transducer and activator of transcription-3 (STAT3) in the rat hypothalamus is associated with leptin resistance during pregnancy. *Endocrinology.* 2004;145:3704-11.
52. Makarova EN, Kochubei ED, Bazhan NM. Regulation of food consumption during pregnancy and lactation in mice. *Neurosci Behav Physiol.* 2010;40:263-7.
53. Li H, Clarke GS, Christie S, Ladyman SR, Kentish SJ, Young RL, Gatford KL, Page AJ. Pregnancy-related plasticity of gastric vagal afferent signals in mice. *Am J Physiol Gastrointest Liver Physiol.* 2021;320:G183-G92.
54. Wang GH. The changes in the amount of daily food-intake of the albino rat during pregnancy and lactation. *Am J Physiol.* 1925;71:736-41.
55. Morgan B, Winick M. A possible control of food intake during pregnancy in the rat. *Br J Nutr.* 1981;46:29-37.
56. Ludeña MC, Mena MA, Salinas M, Herrera E. Effects of alcohol ingestion in the pregnant rat on daily food intake, offspring growth and metabolic parameters. *Gen Pharmacol.* 1983;14:327-32.
57. Abelenda M, Puerta ML. Inhibition of diet-induced thermogenesis during pregnancy in the rat. *Pflugers Arch.* 1987;409:314-7.
58. Kanarek RB, Schoenfeld PM, Morgane PJ. Maternal malnutrition in the rat: effects on food intake and body weight. *Physiol Behav.* 1986;38:509-15.
59. Clarke GS, Gatford KL, Young RL, Grattan DR, Ladyman SR, Page AJ. Maternal adaptations to food intake across pregnancy: central and peripheral mechanisms. *Obesity.* 2021;29:1813-24.
60. Winther G, Eskelund A, Bay-Richter C, Elfving B, Müller HK, Lund S, Wegener G. Grandmaternal high-fat diet primed anxiety-like behaviour in the second-generation female offspring. *Behav Brain Res.* 2019;359:47-55.

61. Di Gesù CM, Matz LM, Bolding IJ, Fultz R, Hoffman KL, Gammazza AM, Petrosino JF, Buffington SA. Maternal gut microbiota mediate intergenerational effects of high-fat diet on descendant social behavior. *Cell Rep.* 2022;41:111461.
62. Geraghty AA, Lindsay KL, Alberdi G, McAuliffe FM, Gibney ER. Nutrition during pregnancy impacts offspring's epigenetic status - evidence from human and animal studies. *Nutr Metab Insights.* 2015;8:41-7.
63. Enomoto K, Aoki S, Toma R, Fujiwara K, Sakamaki K, Hirahara F. Pregnancy outcomes based on pre-pregnancy body mass index in Japanese women. *PLoS One.* 2016;11:e0157081.
64. Hung TH, Hsieh TT. Pregestational body mass index, gestational weight gain, and risks for adverse pregnancy outcomes among Taiwanese women: a retrospective cohort study. *Taiwan J Obstet Gynecol.* 2016;55:575-81.
65. Johnson J, Clifton RG, Roberts JM, Myatt L, Hauth JC, Spong CY, Varner MW, Wapner RJ, Thorp JM, Jr., Mercer BM, Peaceman AM, Ramin SM, Samuels P, Sciscione A, Harper M, Tolosa JE, Saade G, Sorokin Y. Pregnancy outcomes with weight gain above or below the 2009 Institute of Medicine guidelines. *Obstet Gynecol.* 2013;121:969-75.
66. Herring CM, Bazer FW, Johnson GA, Wu G. Impacts of maternal dietary protein intake on fetal survival, growth, and development. *Exp Biol Med (Maywood).* 2018;243:525-33.
67. Aerts L, Van Assche FA. Taurine and taurine-deficiency in the perinatal period. *J Perinat Med.* 2002;30:281-6.
68. Desoye G, Herrera E. Adipose tissue development and lipid metabolism in the human fetus: the 2020 perspective focusing on maternal diabetes and obesity. *Prog Lipid Res.* 2021;81:101082.
69. Hussain T, Tan B, Murtaza G, Metwally E, Yang H, Kalhoro MS, Kalhoro DH, Chughtai MI, Yin Y. Role of dietary amino acids and nutrient sensing system in pregnancy associated disorders. *Front Pharmacol.* 2020;11:586979.
70. Sebastiani G, Herranz Barbero A, Borrás-Novell C, Alsina Casanova M, Aldecoa-Bilbao V, Andreu-Fernández V, Pascual Tutusaus M, Ferrero Martínez S, Gómez Roig MD, García-Algar O. The effects of vegetarian and vegan diet during pregnancy on the health of mothers and offspring. *Nutrients.* 2019;11.
71. Jain S, Maheshwari A, Jain SK. Maternal nutrition and fetal/infant development. *Clin Perinatol.* 2022;49:313-30.
72. Lee NM, Saha S. Nausea and vomiting of pregnancy. *Gastroenterology clinics of North America.* 2011;40:309-34, vii.
73. Jansen LAW, Nijsten K, Limpens J, van Eekelen R, Koot MH, Grooten IJ, Roseboom TJ, Painter RC. Perinatal outcomes of infants born to mothers with hyperemesis gravidarum: A systematic review and meta-analysis. *European journal of obstetrics, gynecology, and reproductive biology.* 2023;284:30-51.
74. Roberts SB, Paul AA, Cole TJ, Whitehead RG. Seasonal changes in activity, birth weight and lactational performance in rural Gambian women. *Trans R Soc Trop Med Hyg.* 1982;76:668-78.
75. Paul AA, Muller EM, Whitehead RG. The quantitative effects of maternal dietary energy intake on pregnancy and lactation in rural Gambian women. *Trans R Soc Trop Med Hyg.* 1979;73:686-92.
76. Stein AD, Ravelli AC, Lumey LH. Famine, third-trimester pregnancy weight gain, and intrauterine growth: the Dutch famine birth cohort study. *Hum Biol.* 1995;67:135-50.
77. Yarde F, Broekmans FJ, van der Pal-de Bruin KM, Schönbeck Y, te Velde ER, Stein AD, Lumey LH. Prenatal famine, birthweight, reproductive performance and age at menopause: the Dutch hunger winter families study. *Hum Reprod.* 2013;28:3328-36.
78. Zhang H, Qu X, Wang H, Tang K. Early life famine exposure to the Great Chinese Famine in 1959-1961 and subsequent pregnancy loss: a population-based study. *Br J Obstet Gynaecol.* 2020;127:39-45.
79. Ashton B, Hill K, Piazza A, Zeitz R. Famine in China, 1958-61. *Popul Dev Rev.* 1984;10:613-45.

80. Xu MQ, Sun WS, Liu BX, Feng GY, Yu L, Yang L, He G, Sham P, Susser E, St Clair D, He L. Prenatal malnutrition and adult schizophrenia: further evidence from the 1959-1961 Chinese famine. *Schizophr Bull.* 2009;35:568-76.
81. Li Y, Jaddoe VW, Qi L, He Y, Wang D, Lai J, Zhang J, Fu P, Yang X, Hu FB. Exposure to the Chinese famine in early life and the risk of metabolic syndrome in adulthood. *Diabetes Care.* 2011;34:1014-8.
82. Li Y, Jaddoe VW, Qi L, He Y, Lai J, Wang J, Zhang J, Hu Y, Ding EL, Yang X, Hu FB, Ma G. Exposure to the Chinese famine in early life and the risk of hypertension in adulthood. *J Hypertens.* 2011;29:1085-92.
83. Li N, Liu E, Guo J, Pan L, Li B, Wang P, Liu J, Wang Y, Liu G, Baccarelli AA, Hou L, Hu G. Maternal prepregnancy body mass index and gestational weight gain on pregnancy outcomes. *PLoS One.* 2013;8:e82310.
84. Santos S, Voerman E, Amiano P, Barros H, Beilin LJ, Bergström A, Charles MA, Chatzi L, Chevrier C, Chrousos GP, Corpeleijn E, Costa O, Costet N, Crozier S, Devereux G, Doyon M, Eggesbø M, Fantini MP, Farchi S, Forastiere F, Georgiu V, Godfrey KM, Gori D, Grote V, Hanke W, Hertz-Picciotto I, Heude B, Hivert MF, Hryhorczuk D, Huang RC, Inskip H, Karvonen AM, Kenny LC, Koletzko B, Küpers LK, Lagström H, Lehmann I, Magnus P, Majewska R, Mäkelä J, Manios Y, McAuliffe FM, McDonald SW, Mehegan J, Melén E, Mommers M, Morgen CS, Moschonis G, Murray D, C NC, Nohr EA, Nybo Andersen AM, Oken E, Oostvogels A, Pac A, Papadopoulou E, Pekkanen J, Pizzi C, Polanska K, Porta D, Richiardi L, Rifas-Shiman SL, Roeleveld N, Ronfani L, Santos AC, Standl M, Stigum H, Stoltenberg C, Thiering E, Thijs C, Torrent M, Tough SC, Trnovec T, Turner S, van Gelder M, van Rossem L, von Berg A, Vrijheid M, Vrijkotte T, West J, Wijga AH, Wright J, Zvinchuk O, Sørensen T, Lawlor DA, Gaillard R, Jaddoe V. Impact of maternal body mass index and gestational weight gain on pregnancy complications: an individual participant data meta-analysis of European, North American and Australian cohorts. *Br J Obstet Gynaecol.* 2019;126:984-95.
85. Brandão T, de Carvalho Padilha P, Granado Nogueira da Gama S, Leal MdC, Gabriela Pimenta da Silva Araújo R, Cavalcante de Barros D, Esteves Pereira AP, dos Santos K, Belizán JM, Saunders C. Gestational weight gain and adverse maternal outcomes in Brazilian women according to body mass index categories: An analysis of data from the Birth in Brazil survey. *Clin Nutr ESPEN.* 2020;37:114-20.
86. Knight-Agarwal CR, Williams LT, Davis D, Davey R, Cochrane T, Zhang H, Rickwood P. Association of BMI and interpregnancy BMI change with birth outcomes in an Australian obstetric population: a retrospective cohort study. *BMJ Open.* 2016;6:e010667.
87. Jimenez-Chillaron JC, Isganaitis E, Charalambous M, Gesta S, Pentinat-Pelegrin T, Faucette RR, Otis JP, Chow A, Diaz R, Ferguson-Smith A, Patti ME. Intergenerational transmission of glucose intolerance and obesity by in utero undernutrition in mice. *Diabetes.* 2009;58:460-8.
88. Kind KL, Clifton PM, Grant PA, Owens PC, Sohlstrom A, Roberts CT, Robinson JS, Owens JA. Effect of maternal feed restriction during pregnancy on glucose tolerance in the adult guinea pig. *Am J Physiol Regul Integr Comp Physiol.* 2003;284:R140-52.
89. Levay EA, Paolini AG, Govic A, Hazi A, Penman J, Kent S. Anxiety-like behaviour in adult rats perinatally exposed to maternal calorie restriction. *Behav Brain Res.* 2008;191:164-72.
90. Ganguly A, Collis L, Devaskar SU. Placental glucose and amino acid transport in calorie-restricted wild-type and *Glut3* null heterozygous mice. *Endocrinology.* 2012;153:3995-4007.
91. Jimenez-Chillaron JC, Hernandez-Valencia M, Reamer C, Fisher S, Joszi A, Hirshman M, Oge A, Walrond S, Przybyla R, Boozer C, Goodyear LJ, Patti ME. Beta-cell secretory dysfunction in the pathogenesis of low birth weight-associated diabetes: a murine model. *Diabetes.* 2005;54:702-11.
92. Long NM, George LA, Uthlaut AB, Smith DT, Nijland MJ, Nathanielsz PW, Ford SP. Maternal obesity and increased nutrient intake before and during gestation in the ewe results in altered growth, adiposity, and glucose tolerance in adult offspring. *J Anim Sci.* 2010;88:3546-53.

93. Ford SP, Zhang L, Zhu M, Miller MM, Smith DT, Hess BW, Moss GE, Nathanielsz PW, Nijland MJ. Maternal obesity accelerates fetal pancreatic beta-cell but not alpha-cell development in sheep: prenatal consequences. *Am J Physiol Regul Integr Comp Physiol.* 2009;297:R835-43.
94. Zhu MJ, Ma Y, Long NM, Du M, Ford SP. Maternal obesity markedly increases placental fatty acid transporter expression and fetal blood triglycerides at midgestation in the ewe. *Am J Physiol Regul Integr Comp Physiol.* 2010;299:R1224-31.
95. Ma Y, Zhu MJ, Zhang L, Hein SM, Nathanielsz PW, Ford SP. Maternal obesity and overnutrition alter fetal growth rate and cotyledonary vascularity and angiogenic factor expression in the ewe. *Am J Physiol Regul Integr Comp Physiol.* 2010;299:R249-58.
96. Rautureau GJP, Morio B, Guibert S, Lefevre C, Perrier J, Alves A, Chauvin MA, Pinteur C, Monet MA, Godet M, Madec AM, Rieusset J, Mey A, Panthu B. Dietary obesity in mice is associated with lipid deposition and metabolic shifts in the lungs sharing features with the liver. *Sci Rep.* 2021;11:8712.
97. Picone O, Laigre P, Fortun-Lamothe L, Archilla C, Peynot N, Ponter AA, Berthelot V, Cordier AG, Duranthon V, Chavatte-Palmer P. Hyperlipidic hypercholesterolemic diet in prepubertal rabbits affects gene expression in the embryo, restricts fetal growth and increases offspring susceptibility to obesity. *Theriogenology.* 2011;75:287-99.
98. Che C, Dudick K, Shoemaker R. Cardiac hypertrophy with obesity is augmented after pregnancy in C57BL/6 mice. *Biol Sex Differ.* 2019;10:59.
99. Zhou P, Guan H, Guo Y, Zhu L, Liu X. Maternal high-fat diet programs renal peroxisomes and activates NLRP3 inflammasome-mediated pyroptosis in the rat fetus. *J Inflamm Res.* 2021;14:5095-110.
100. Şanlı E, Kabaran S. Maternal obesity, maternal overnutrition and fetal programming: effects of epigenetic mechanisms on the development of metabolic disorders. *Current genomics.* 2019;20:419-27.
101. Goławski K, Giermaziak W, Ciebiera M, Wojtyła C. Excessive gestational weight gain and pregnancy outcomes. *J Clin Med.* 2023;12.
102. World Health Organisation. Obesity and overweight fact sheet. 2021 [17-08-2023]; Available from: <https://www.who.int/news-room/fact-sheets/detail/obesity-and-overweight>.
103. Quan W, Zeng M, Jiao Y, Li Y, Xue C, Liu G, Wang Z, Qin F, He Z, Chen J. Western dietary patterns, foods, and risk of gestational diabetes mellitus: a systematic review and meta-analysis of prospective cohort studies. *Adv Nutr.* 2021;12:1353-64.
104. Lim CC, Mahmood T. Obesity in pregnancy. *Best Pract Res Clin Obstet Gynaecol.* 2015;29:309-19.
105. National Center for Health Statistics, Centers for Disease Control and Prevention. Increases in pre-pregnancy obesity: United States, 2016–2019. 2020 [17-08-2023]; Available from: <https://www.cdc.gov/nchs/products/databriefs/db392.htm>.
106. Australian Institute of Health and Welfare. Australia's mothers and babies. Canberra 2023 [17-08-2023]; Available from: <https://www.aihw.gov.au/reports/mothers-babies/australias-mothers-babies>.
107. Shasa DR, Odhiambo JF, Long NM, Tuersunjiang N, Nathanielsz PW, Ford SP. Multigenerational impact of maternal overnutrition/obesity in the sheep on the neonatal leptin surge in granddaughters. *International journal of obesity (2005).* 2015;39:695-701.
108. Long NM, Rule DC, Zhu MJ, Nathanielsz PW, Ford SP. Maternal obesity upregulates fatty acid and glucose transporters and increases expression of enzymes mediating fatty acid biosynthesis in fetal adipose tissue depots. *J Anim Sci.* 2012;90:2201-10.
109. Wesołowska E, Jankowska A, Trafalska E, Kałużny P, Grzesiak M, Dominowska J, Hanke W, Calamandrei G, Polańska K. Sociodemographic, lifestyle, environmental and pregnancy-related determinants of dietary patterns during pregnancy. *Int J Environ Res Public Health.* 2019;16.

110. Toop CR, Muhlhausler BS, O'Dea K, Gentili S. Consumption of sucrose, but not high fructose corn syrup, leads to increased adiposity and dyslipidaemia in the pregnant and lactating rat. *J Dev Orig Health Dis.* 2015;6:38-46.
111. Witek K, Wydra K, Suder A, Filip M. Maternal monosaccharide diets evoke cognitive, locomotor, and emotional disturbances in adolescent and young adult offspring rats. *Front Nutr.* 2023;10:1176213.
112. Mizera J, Kazek G, Niedzielska-Andres E, Pomierny-Chamiolo L. Maternal high-sugar diet results in NMDA receptors abnormalities and cognitive impairment in rat offspring. *FASEB J.* 2021;35:e21547.
113. Krasnow SM, Nguyen ML, Marks DL. Increased maternal fat consumption during pregnancy alters body composition in neonatal mice. *Am J Physiol Endocrinol Metab.* 2011;301:E1243-53.
114. Frias AE, Morgan TK, Evans AE, Rasanen J, Oh KY, Thornburg KL, Grove KL. Maternal high-fat diet disturbs uteroplacental hemodynamics and increases the frequency of stillbirth in a nonhuman primate model of excess nutrition. *Endocrinology.* 2011;152:2456-64.
115. McCurdy CE, Bishop JM, Williams SM, Grayson BE, Smith MS, Friedman JE, Grove KL. Maternal high-fat diet triggers lipotoxicity in the fetal livers of nonhuman primates. *J Clin Invest.* 2009;119:323-35.
116. Kuo K, Roberts VHJ, Gaffney J, Takahashi DL, Morgan T, Lo JO, Stouffer RL, Frias AE. Maternal high-fat diet consumption and chronic hyperandrogenemia are associated with placental dysfunction in female rhesus macaques. *Endocrinology.* 2019;160:1937-49.
117. Matuszewska J, Zalewski T, Klimaszuk A, Ziarniak K, Jurga S, Chmurzynska A, Sliwowska JH. Mothers' cafeteria diet induced sex-specific changes in fat content, metabolic profiles, and inflammation outcomes in rat offspring. *Sci Rep.* 2021;11:18573.
118. Jacobs S, Teixeira DS, Guilherme C, da Rocha CF, Aranda BC, Reis AR, de Souza MA, Franci CR, Sanvitto GL. The impact of maternal consumption of cafeteria diet on reproductive function in the offspring. *Physiol Behav.* 2014;129:280-6.
119. Mousa A, Naqash A, Lim S. Macronutrient and micronutrient intake during pregnancy: an overview of recent evidence. *Nutrients.* 2019;11.
120. Viegas OA, Scott PH, Cole TJ, Mansfield HN, Wharton P, Wharton BA. Dietary protein energy supplementation of pregnant Asian mothers at Sorrento, Birmingham. I: unselective during second and third trimesters. *Br Med J (Clin Res Ed).* 1982;285:589-92.
121. Ross SM, Nel E, Naeye RL. Differing effects of low and high bulk maternal dietary supplements during pregnancy. *Early Hum Dev.* 1985;10:295-302.
122. Viegas OA, Scott PH, Cole TJ, Eaton P, Needham PG, Wharton BA. Dietary protein energy supplementation of pregnant Asian mothers at Sorrento, Birmingham. II: selective during third trimester only. *Br Med J (Clin Res Ed).* 1982;285:592-5.
123. Morgan BLG, Naismith DJ. Effects on the products of conception of protein supplementation of the diets of rats. *J Nutr.* 1977;107:1590-4.
124. Liu N, Dai Z, Zhang Y, Chen J, Yang Y, Wu G, Tso P, Wu Z. Maternal L-proline supplementation enhances fetal survival, placental development, and nutrient transport in mice. *Biol Reprod.* 2019;100:1073-81.
125. Choi W, Kim J, Ko JW, Choi A, Kwon YH. Effects of maternal branched-chain amino acid and alanine supplementation on growth and biomarkers of protein metabolism in dams fed a low-protein diet and their offspring. *Amino Acids.* 2022;54:977-88.
126. Burke BS, Harding VV, Stuart HC. Nutrition studies during pregnancy. IV. Relation of protein content of mother's diet during pregnancy to birth length, birth weight, and condition of infant at birth. *J Pediatr.* 1943;23:506-15.
127. Arnell RE, Goldman DW, Bertucci FJ. Protein deficiencies in pregnancy. *JAMA.* 1945;127:1101-7.
128. Ebbs JH, Tisdall FF, Scott WA. The influence of prenatal diet on the mother and child. *Millbank Q.* 1942;20:35-46.

129. Kirigiti MA, Frazee T, Bennett B, Arik A, Blundell P, Bader L, Bagley J, Frias AE, Sullivan EL, Roberts CT, Jr., Kievit P. Effects of pre- and postnatal protein restriction on maternal and offspring metabolism in the nonhuman primate. *Am J Physiol Regul Integr Comp Physiol*. 2020;318:R929-r39.
130. Schoknecht PA, Newton GR, Weise DE, Pond WG. Protein restriction in early pregnancy alters fetal and placental growth and allantoic fluid proteins in swine. *Theriogenology*. 1994;42:217-26.
131. Atinmo T, Pond WG, Barnes RH. Effect of maternal energy vs. protein restriction on growth and development of progeny in swine. *J Anim Sci*. 1974;39:703-11.
132. Desai M, Crowther NJ, Lucas A, Hales CN. Organ-selective growth in the offspring of protein-restricted mothers. *Br J Nutr*. 1996;76:591-603.
133. Petrik J, Reusens B, Arany E, Remacle C, Coelho C, Hoet JJ, Hill DJ. A low protein diet alters the balance of islet cell replication and apoptosis in the fetal and neonatal rat and is associated with a reduced pancreatic expression of insulin-like growth factor-II. *Endocrinology*. 1999;140:4861-73.
134. Snoeck A, Remacle C, Reusens B, Hoet JJ. Effect of a low protein diet during pregnancy on the fetal rat endocrine pancreas. *Biol Neonate*. 1990;57:107-18.
135. Castro TF, de Matos NA, de Souza ABF, Costa GP, Perucci LO, Talvani A, Cangussú SD, de Menezes RCA, Bezerra FS. Protein restriction during pregnancy affects lung development and promotes oxidative stress and inflammation in C57BL/6 mice offspring. *Nutrition*. 2022;101:111682.
136. Roberts VHJ, Lo JO, Lewandowski KS, Blundell P, Grove KL, Kroenke CD, Sullivan EL, Roberts CT, Jr., Frias AE. Adverse placental perfusion and pregnancy outcomes in a new nonhuman primate model of gestational protein restriction. *Reprod Sci*. 2018;25:110-9.
137. Ferreira LB, Lobo CV, Miranda A, Carvalho BDC, Santos LCD. Dietary patterns during pregnancy and gestational weight gain: a systematic review. *Rev Bras Ginecol Obstet*. 2022;44:540-7.
138. Kinshella MW, Omar S, Scherbinsky K, Vidler M, Magee LA, von Dadelszen P, Moore SE, Elango R. Maternal dietary patterns and pregnancy hypertension in low- and middle-income countries: a systematic review and meta-analysis. *Adv Nutr*. 2021;12:2387-400.
139. Godfrey K, Robinson S, Barker DJ, Osmond C, Cox V. Maternal nutrition in early and late pregnancy in relation to placental and fetal growth. *BMJ (Clinical research ed)*. 1996;312:410-4.
140. Gainfort A, Delahunt A, Killeen SL, O'Reilly SL, Hébert JR, Shivappa N, McAuliffe FM. Energy-adjusted dietary inflammatory index in pregnancy and maternal cardiometabolic health: findings from the ROLO study. *AJOG Glob Rep*. 2023;3:100214.
141. Mitchell AJ, Khambadkone SG, Dunn G, Bagley J, Tamashiro KKK, Fair D, Gustafsson H, Sullivan EL. Maternal Western-style diet reduces social engagement and increases idiosyncratic behavior in Japanese macaque offspring. *Brain Behav Immun*. 2022;105:109-21.
142. Kulhanek D, Abrahante Llorens JE, Buckley L, Tkac I, Rao R, Paulsen ME. Female and male C57BL/6J offspring exposed to maternal obesogenic diet develop altered hypothalamic energy metabolism in adulthood. *Am J Physiol Endocrinol Metab*. 2022;323:E448-e66.
143. Anwer H, Morris MJ, Noble DWA, Nakagawa S, Lagisz M. Transgenerational effects of obesogenic diets in rodents: a meta-analysis. *Obes Rev*. 2022;23:e13342.
144. Wang YW, Yu HR, Tiao MM, Tain YL, Lin IC, Sheen JM, Lin YJ, Chang KA, Chen CC, Tsai CC, Huang LT. Maternal obesity related to high fat diet induces placenta remodeling and gut microbiome shaping that are responsible for fetal liver lipid dysmetabolism. *Front Nutr*. 2021;8:736944.
145. Bazer FW, Spencer TE, Wu G, Cudd TA, Meininger CJ. Maternal nutrition and fetal development. *J Nutr*. 2004;134:2169-72.
146. Cheong JN, Wlodek ME, Moritz KM, Cuffe JS. Programming of maternal and offspring disease: impact of growth restriction, fetal sex and transmission across generations. *J Physiol*. 2016;594:4727-40.
147. Aiken CE, Tarry-Adkins JL, Ozanne SE. Transgenerational effects of maternal diet on metabolic and reproductive ageing. *Mamm Genome*. 2016;27:430-9.
148. Agarwal S, Kovilam O, Agrawal DK. Vitamin D and its impact on maternal-fetal outcomes in pregnancy: a critical review. *Crit Rev Food Sci Nutr*. 2018;58:755-69.

149. Georgieff MK. Iron deficiency in pregnancy. *Am J Obstet Gynecol.* 2020;223:516-24.
150. Santander Ballestín S, Giménez Campos MI, Ballestín Ballestín J, Luesma Bartolomé MJ. Is supplementation with micronutrients still necessary during pregnancy? a review. *Nutrients.* 2021;13.
151. Goonewardene M, Shehata M, Hamad A. Anaemia in pregnancy. *Best Pract Res Clin Obstet Gynaecol.* 2012;26:3-24.
152. Molloy AM, Kirke PN, Brody LC, Scott JM, Mills JL. Effects of folate and vitamin B₁₂ deficiencies during pregnancy on fetal, infant, and child development. *Food Nutr Bull.* 2008;29:S101-11; discussion S12-5.
153. Palawaththa S, Islam RM, Illic D, Rabel K, Lee M, Romero L, Leung XY, Karim MN. Effect of maternal dietary niacin intake on congenital anomalies: a systematic review and meta-analysis. *Eur J Nutr.* 2022;61:1133-42.
154. Farias PM, Marcelino G, Santana LF, de Almeida EB, Guimarães RCA, Pott A, Hiane PA, Freitas KC. Minerals in Pregnancy and Their Impact on Child Growth and Development. *Molecules (Basel, Switzerland).* 2020;25.
155. Volk N, Lacy B. Anatomy and physiology of the small bowel. *Gastrointest Endosc Clin N Am.* 2017;27:1-13.
156. Campbell J, Berry J, Liang Y. Chapter 71 - Anatomy and physiology of the small intestine. *Shackelford's Surgery of the Alimentary Tract (Eighth edition).* Philadelphia: Elsevier; 2019. 817-41.
157. Wilson RL, Stevenson CE. Chapter 56 - Anatomy and physiology of the stomach. In: Yeo CJ, editor. *Shackelford's Surgery of the Alimentary Tract (Eighth Edition).* Philadelphia: Elsevier; 2019. 634-46.
158. Kiela PR, Ghishan FK. Physiology of intestinal absorption and secretion. *Best Pract Res Clin Gastroenterol.* 2016;30:145-59.
159. Ko CW, Qu J, Black DD, Tso P. Regulation of intestinal lipid metabolism: current concepts and relevance to disease. *Nat Rev Gastroenterol Hepatol.* 2020;17:169-83.
160. Shames B. Chapter 68 - Anatomy and physiology of the duodenum. *Shackelford's Surgery of the Alimentary Tract (Eighth edition).* Philadelphia: Elsevier; 2019. 786-803.
161. Nguyen TL, Vieira-Silva S, Liston A, Raes J. How informative is the mouse for human gut microbiota research? *Disease models & mechanisms.* 2015;8:1-16.
162. Moran BJ, Jackson AA. Function of the human colon. *Br J Surg.* 1992;79:1132-7.
163. Lee R, Mezoff EA. Chapter 30 - Anatomy and Physiology of the Small and Large Intestines (Sixth Edition). *Pediatric Gastrointestinal and Liver Disease: Elsevier Inc;* 2021. 308-20.e3.
164. Korbonits M, Goldstone AP, Gueorguiev M, Grossman AB. Ghrelin - a hormone with multiple functions. *Front Neuroendocrinol.* 2004;25:27-68.
165. Mateer SW, Cardona J, Marks E, Goggin BJ, Hua S, Keely S. *Ex vivo* intestinal sacs to assess mucosal permeability in models of gastrointestinal disease. *J Vis Exp.* 2016:e53250.
166. San Roman AK, Shivdasani RA. Boundaries, junctions and transitions in the gastrointestinal tract. *Exp Cell Res.* 2011;317:2711-8.
167. Casteleyn C, Rekecki A, Van der Aa A, Simoens P, Van den Broeck W. Surface area assessment of the murine intestinal tract as a prerequisite for oral dose translation from mouse to man. *Lab Anim.* 2010;44:176-83.
168. Kothari A, Rajagopalan P. The assembly of integrated rat intestinal-hepatocyte cultures. *Bioeng Transl Med.* 2020;5:e10146.
169. Kararli TT. Comparison of the gastrointestinal anatomy, physiology, and biochemistry of humans and commonly used laboratory animals. *Biopharm Drug Dispos.* 1995;16:351-80.
170. Darwich AS, Aslam U, Ashcroft DM, Rostami-Hodjegan A. Meta-analysis of the turnover of intestinal epithelia in preclinical animal species and humans. *Drug Metab Dispos.* 2014;42:2016-22.
171. Davies PS, Dismuke AD, Powell AE, Carroll KH, Wong MH. Wnt-reporter expression pattern in the mouse intestine during homeostasis. *BMC Gastroenterol.* 2008;8:57.
172. Ferguson A, Sutherland A, MacDonald TT, Allan F. Technique for microdissection and measurement in biopsies of human small intestine. *J Clin Pathol.* 1977;30:1068-73.

173. Trbojević-Stanković JB, Milićević NM, Milosević DP, Despotović N, Davidović M, Erceg P, Bojić B, Bojić D, Svorcan P, Protić M, Dapcević B, Miljković MD, Milićević Z. Morphometric study of healthy jejunal and ileal mucosa in adult and aged subjects. *Histol Histopathol.* 2010;25:153-8.
174. Giacosa A. Morphometry of normal duodenal mucosa. *Scand J Gastroenterol Suppl.* 1989;167:10-2.
175. Cripps AW, Williams VJ. The effect of pregnancy and lactation on food intake, gastrointestinal anatomy and the absorptive capacity of the small intestine in the albino rat. *Br J Nutr.* 1975;33:17-32.
176. Viguera RM, Rojas-Castañeda J, Hernández R, Reyes G, Alvarez C. Histological characteristics of the intestinal mucosa of the rat during the first year of life. *Lab Anim.* 1999;33:393-400.
177. Wright NA, Carter J, Irwin M. The measurement of villus cell population size in the mouse small intestine in normal and abnormal states: a comparison of absolute measurements with morphometric estimators in sectioned immersion-fixed material. *Cell Tissue Kinet.* 1989;22:425-50.
178. Sensoy E, Oznurlyu Y. Determination of the changes on the small intestine of pregnant mice by histological, enzyme histochemical, and immunohistochemical methods. *Turk J Gastroenterol.* 2019;30:917-24.
179. Jaroszevska M, Wilczyńska B. Dimensions of surface area of alimentary canal of pregnant and lactating common female shrews. *J Mammal.* 2006;87:589-97.
180. Sun EW, de Fontgalland D, Rabbitt P, Hollington P, Sposato L, Due SL, Wattchow DA, Rayner CK, Deane AM, Young RL, Keating DJ. Mechanisms controlling glucose-induced GLP-1 secretion in human small intestine. *Diabetes.* 2017;66:2144-9.
181. Tack J, Verbeure W, Mori H, Schol J, Van den Houde K, Huang IH, Balsiger L, Broeders B, Colomier E, Scarpellini E, Carbone F. The gastrointestinal tract in hunger and satiety signalling. *United Eur Gastroenterol J.* 2021;9:727-34.
182. Hellström PM, Grybäck P, Jacobsson H. The physiology of gastric emptying. *Best Pract Res Clin Anaesthesiol.* 2006;20:397-407.
183. Levin F, Edholm T, Schmidt PT, Grybäck P, Jacobsson H, Degerblad M, Höybye C, Holst JJ, Rehfeld JF, Hellström PM, Näslund E. Ghrelin stimulates gastric emptying and hunger in normal-weight humans. *J Clin Endocrinol Metab.* 2006;91:3296-302.
184. Masuda Y, Tanaka T, Inomata N, Ohnuma N, Tanaka S, Itoh Z, Hosoda H, Kojima M, Kangawa K. Ghrelin stimulates gastric acid secretion and motility in rats. *Biochem Biophys Res Commun.* 2000;276:905-8.
185. Nunez-Salces M, Li H, Feinle-Bisset C, Young RL, Page AJ. The regulation of gastric ghrelin secretion. *Acta Physiol (Oxf).* 2021;231:e13588.
186. Yu CD, Xu QJ, Chang RB. Vagal sensory neurons and gut-brain signaling. *Curr Opin Neurobiol.* 2020;62:133-40.
187. Wang YB, de Lartigue G, Page AJ. Dissecting the role of subtypes of gastrointestinal vagal afferents. *Front Physiol.* 2020;11:643.
188. Browning KN, Travagli RA. Central nervous system control of gastrointestinal motility and secretion and modulation of gastrointestinal functions. *Compr Physiol.* 2014;4:1339-68.
189. Greenwood-Van Meerveld B, Johnson AC, Grundy D. Gastrointestinal physiology and function. *Handb Exp Pharmacol.* 2017;239:1-16.
190. Lyte M, Cryan JF. *Microbial endocrinology: The microbiota-gut-brain axis in health and disease (First Edition).* New York: Springer New York; 2014.
191. Keohane J, Quigley EM. Functional dyspepsia: the role of visceral hypersensitivity in its pathogenesis. *World J Gastroenterol.* 2006;12:2672-6.
192. Dudzińska E, Grabrucker AM, Kwiatkowski P, Sitarz R, Sienkiewicz M. The importance of visceral hypersensitivity in irritable bowel syndrome - plant metabolites in IBS treatment. *Pharmaceuticals (Basel, Switzerland).* 2023;16.

193. Browning KN, Mendelowitz D. Musings on the wanderer: what's new in our understanding of vago-vagal reflexes?: II. Integration of afferent signaling from the viscera by the nodose ganglia. *Am J Physiol Gastrointest Liver Physiol*. 2003;284:G8-14.
194. Furukawa N, Hatano M, Fukuda H. Glutamnergic vagal afferents may mediate both retching and gastric adaptive relaxation in dogs. *Auton Neurosci*. 2001;93:21-30.
195. Berthoud HR, Powley TL. Vagal afferent innervation of the rat fundic stomach: morphological characterization of the gastric tension receptor. *J Comp Neurol*. 1992;319:261-76.
196. Fox EA, Phillips RJ, Baronowsky EA, Byerly MS, Jones S, Powley TL. Neurotrophin-4 deficient mice have a loss of vagal intraganglionic mechanoreceptors from the small intestine and a disruption of short-term satiety. *J Neurosci*. 2001;21:8602-15.
197. Powley TL, Phillips RJ. Vagal intramuscular array afferents form complexes with interstitial cells of Cajal in gastrointestinal smooth muscle: analogues of muscle spindle organs? *Neuroscience*. 2011;186:188-200.
198. Powley TL, Hudson CN, McAdams JL, Baronowsky EA, Phillips RJ. Vagal intramuscular arrays: the specialized mechanoreceptor arbors that Innervate the smooth muscle layers of the stomach examined in the rat. *J Comp Neurol*. 2016;524:713-37.
199. Berthoud HR, Blackshaw LA, Brookes SJ, Grundy D. Neuroanatomy of extrinsic afferents supplying the gastrointestinal tract. *Neurogastroenterol Motil*. 2004;16 Suppl 1:28-33.
200. Karasov WH, Douglas AE. Comparative digestive physiology. *Compr Physiol*. 2013;3:741-83.
201. Cox S. Energy | Metabolism. In: Caballero B, editor. *Encyclopedia of human nutrition* (Second Edition). Oxford: Elsevier; 2005. 106-14.
202. Kellett GL, Helliwell PA. The diffusive component of intestinal glucose absorption is mediated by the glucose-induced recruitment of GLUT2 to the brush-border membrane. *Biochem J*. 2000;350 Pt 1:155-62.
203. Roder PV, Geillinger KE, Zietek TS, Thorens B, Koepsell H, Daniel H. The role of SGLT1 and GLUT2 in intestinal glucose transport and sensing. *PLoS One*. 2014;9:e89977.
204. Koepsell H. Glucose transporters in the small intestine in health and disease. *Pflugers Arch*. 2020;472:1207-48.
205. Larsen R, Mertz-Nielsen A, Hansen MB, Poulsen SS, Bindlev N. Novel modified Ussing chamber for the study of absorption and secretion in human endoscopic biopsies. *Acta Physiol Scand*. 2001;173:213-22.
206. Puthanmadhom Narayanan S, Linden DR, Peters SA, Desai A, Kuwelker S, O'Brien D, Smyrk TJ, Graham RP, Grover M, Bharucha AE. Duodenal mucosal secretory disturbances in functional dyspepsia. *Neurogastroenterol Motil*. 2021;33:e13955.
207. Kellett GL. The facilitated component of intestinal glucose absorption. *J Physiol*. 2001;531:585-95.
208. Kellett GL, Brot-Laroche E. Apical GLUT2: a major pathway of intestinal sugar absorption. *Diabetes*. 2005;54:3056-62.
209. Kellett GL, Brot-Laroche E, Mace OJ, Leturque A. Sugar absorption in the intestine: the role of GLUT2. *Annu Rev Nutr*. 2008;28:35-54.
210. Ait-Omar A, Monteiro-Sepulveda M, Poitou C, Le Gall M, Cotillard A, Gilet J, Garbin K, Houllier A, Château D, Lacombe A, Veyrie N, Hugol D, Tordjman J, Magnan C, Serradas P, Clément K, Leturque A, Brot-Laroche E. GLUT2 accumulation in enterocyte apical and intracellular membranes: a study in morbidly obese human subjects and ob/ob and high fat-fed mice. *Diabetes*. 2011;60:2598-607.
211. Shirazi-Beechey SP, Moran AW, Batchelor DJ, Daly K, Al-Rammahi M. Glucose sensing and signalling; regulation of intestinal glucose transport. *Proc Nutr Soc*. 2011;70:185-93.
212. Kim HR, Park SW, Cho HJ, Chae KA, Sung JM, Kim JS, Landowski CP, Sun D, Abd El-Aty AM, Amidon GL, Shin HC. Comparative gene expression profiles of intestinal transporters in mice, rats and humans. *Pharmacol Res*. 2007;56:224-36.

213. Uhlén M, Fagerberg L, Hallström BM, Lindskog C, Oksvold P, Mardinoglu A, Sivertsson Å, Kampf C, Sjöstedt E, Asplund A, Olsson I, Edlund K, Lundberg E, Navani S, Szigartyo CA, Odeberg J, Djureinovic D, Takanen JO, Hober S, Alm T, Edqvist PH, Berling H, Tegel H, Mulder J, Rockberg J, Nilsson P, Schwenk JM, Hamsten M, von Feilitzen K, Forsberg M, Persson L, Johansson F, Zwahlen M, von Heijne G, Nielsen J, Pontén F. Proteomics. Tissue-based map of the human proteome. *Science*. 2015;347:1260419.
214. Overduin TS, Page AJ, Young RL, Gatford KL. Adaptations in gastrointestinal nutrient absorption and its determinants during pregnancy in monogastric mammals: a scoping review protocol. *JBIEvid Synth*. 2022;20:640-6.
215. Most J, Dervis S, Haman F, Adamo KB, Redman LM. Energy intake requirements in pregnancy. *Nutrients*. 2019;11:1812.
216. Kiserud T, Piaggio G, Carroli G, Widmer M, Carvalho J, Neerup Jensen L, Giordano D, Cecatti JG, Abdel Aleem H, Talegawkar SA, Benachi A, Diemert A, Tshefu Kitoto A, Thinkhamrop J, Lumbiganon P, Tabor A, Kriplani A, Gonzalez Perez R, Hecher K, Hanson MA, Gülmezoglu AM, Platt LD. The World Health Organization fetal growth charts: a multinational longitudinal study of ultrasound biometric measurements and estimated fetal weight. *PLoS medicine*. 2017;14:e1002220.
217. Cole HH, Hart GH. The effect of pregnancy and lactation on growth in the rat. *Am J Physiol*. 1938;123:589-97.
218. Sabet Sarvestani F, Rahmanifar F, Tamadon A. Histomorphometric changes of small intestine in pregnant rat. *Vet Res Forum*. 2015;6:69-73.
219. Johnson ML, Saffrey MJ, Taylor VJ. Gastrointestinal capacity, gut hormones and appetite change during rat pregnancy and lactation. *Reproduction*. 2019;157:431-43.
220. Bruce LA, Behsudi FM. Progesterone effects on three regional gastrointestinal tissues. *Life Sci*. 1979;25:729-34.
221. Matos JF, Americo MF, Sinzato YK, Volpato GT, Cora LA, Calabresi MF, Oliveira RB, Damasceno DC, Miranda JR. Role of sex hormones in gastrointestinal motility in pregnant and non-pregnant rats. *World J Gastroenterol*. 2016;22:5761-8.
222. Coskun T, Sevinc A, Tevetoglu I, Alican I, Kurtel H, Yegen BC. Delayed gastric emptying in conscious male rats following chronic estrogen and progesterone treatment. *Res Exp Med (Berl)*. 1995;195:49-54.
223. Teerapornpantakit J, Klanchui A, Karoonuthaisiri N, Wongdee K, Charoenphandhu N. Expression of transcripts related to intestinal ion and nutrient absorption in pregnant and lactating rats as determined by custom-designed cDNA microarray. *Mol Cell Biochem*. 2014;391:103-16.
224. Singer AJ, Brandt LJ. Pathophysiology of the gastrointestinal tract during pregnancy. *Am J Gastroenterol*. 1991;86:1695-712.
225. Fudge NJ, Kovacs CS. Pregnancy up-regulates intestinal calcium absorption and skeletal mineralization independently of the vitamin D receptor. *Endocrinology*. 2010;151:886-95.
226. Peters MDJ, Godfrey C, McInerney P, Baldini Soares C, Khalil H, D. P. Chapter 11: Scoping Reviews In: Aromataris E, Munn Z, editors. *Joanna Briggs Institute Reviewer's Manual*. JBI2020. Available from <https://synthesismanual.jbi.global>. <https://doi.org/10.46658/JBIMES-20-12>.
227. Tricco AC, Lillie E, Zarin W, O'Brien KK, Colquhoun H, Levac D, Moher D, Peters MDJ, Horsley T, Weeks L, Hempel S, Akl EA, Chang C, McGowan J, Stewart L, Hartling L, Aldcroft A, Wilson MG, Garrity C, Lewin S, Godfrey CM, Macdonald MT, Langlois EV, Soares-Weiser K, Moriarty J, Clifford T, Tuncalp O, Straus SE. PRISMA Extension for Scoping Reviews (PRISMA-ScR): checklist and explanation. *Ann Intern Med*. 2018;169:467-73.
228. Munn Z, Aromataris E, Tufanaru C, Stern C, Porritt K, Farrow J, Lockwood C, Stephenson M, Moola S, Lizarondo L, McArthur A, Peters M, Pearson A, Jordan Z. The development of software to support multiple systematic review types: the Joanna Briggs Institute System for the Unified Management, Assessment and Review of Information (JBI SUMARI). *Int J Evid Based Healthc*. 2019;17:36-43.

229. Barrett JF, Whittaker PG, Williams JG, Lind T. Absorption of non-haem iron from food during normal pregnancy. *BMJ*. 1994;309:79-82.
230. Batey R, Gallagher N. Effect of iron stores and hysterectomy on iron absorption and distribution in pregnant mice. *Am J Physiol Endocrinol Metab*. 1977;232:E57-61.
231. Larralde J, Fernandez-Otero P, Gonzalez M. Increased active transport of glucose through the intestine during pregnancy. *Nature*. 1966;209:1356-7.
232. Musacchia XJ, Hartner AM. Intestinal absorption of glucose, and blood glucose and hematocrit in pregnant and nonpregnant hamsters. *Proc Soc Exp Biol Med*. 1970;135:307-10.
233. Moore MC, Smith MS, Connolly CC. Pregnancy augments hepatic glucose storage in response to a mixed meal. *Br J Nutr*. 2012;107:493-503.
234. Johnson ML, Saffrey MJ, Taylor VJ. Gastrointestinal capacity, gut hormones and appetite change during rat pregnancy and lactation. *Reproduction*. 2019;157:431-43.
235. Overduin TS, Page AJ, Young RL, Gatford KL. Adaptations in gastrointestinal nutrient absorption and its determinants during pregnancy in monogastric mammals: a scoping review protocol. *JBMEvid Synth*. 2022;20:640-6.
236. Pere MC, Baudelin A, Briggs K, Gilbert M. Hepatic metabolism during fasting-refeeding transition in conscious pregnant rabbits. *Am J Physiol Endocrinol Metab*. 1992;262:E899-905.
237. Campbell DM, Sutherland HW, Pearson DW. Maternal glucose response to a standardized test meal throughout pregnancy and postnatally. *Am J Obstet Gynecol*. 1994;171:143-6.
238. Stanley K, Magides A, Arnot M, Bruce C, Reilly C, McFee A, Fraser R. Delayed gastric emptying as a factor in delayed postprandial glycaemic response in pregnancy. *Br J Obstet Gynaecol*. 1995;102:288-91.
239. Campbell N, Pyke DA, Taylor KW. Oral glucose tolerance tests in pregnant women with potential diabetes, latent diabetes and glycosuria. *J Obstet Gynaecol Br Commonw*. 1971;78:498-504.
240. Gillmer MD, Beard RW, Brooke FM, Oakley NW. Carbohydrate metabolism in pregnancy. Part I. Diurnal plasma glucose profile in normal and diabetic women. *BMJ*. 1975;3:399-402.
241. Hagen A. Blood sugar findings during pregnancy in normals and possible prediabetics. *Diabetes*. 1961;10:438-44.
242. Hornnes PJ, Kühl C. Cortisol and glucose tolerance in normal pregnancy. *Diabetes Metab*. 1984;10:1-6.
243. Kühl C. Glucose metabolism during and after pregnancy in normal and gestational diabetic women. 1. Influence of normal pregnancy on serum glucose and insulin concentration during basal fasting conditions and after a challenge with glucose. *Acta Endocrinol (Copenh)*. 1975;79:709-19.
244. Lind T, Billewicz WZ, Brown G. A serial study of changes occurring in the oral glucose tolerance test during pregnancy. *J Obstet Gynaecol Br Commonw*. 1973;80:1033-9.
245. Amano Y. Changes in the levels of blood glucose during pregnancy in the rat. *Jpn J Pharmacol*. 1967;17:105-14.
246. Moffett RC, Irwin N, Francis JM, Flatt PR. Alterations of glucose-dependent insulinotropic polypeptide and expression of genes involved in mammary gland and adipose tissue lipid metabolism during pregnancy and lactation. *PLoS One*. 2013;8:e78560.
247. Moore MC, Menon R, Coate KC, Gannon M, Smith MS, Farmer B, Williams PE. Diet-induced impaired glucose tolerance and gestational diabetes in the dog. *J Appl Physiol*. 2011;110:458-67.
248. Coltart TM, Jourdan MH. Effects of human pregnancy on glucose and fructose tolerance to a sucrose meal. *J Obstet Gynaecol Br Commonw*. 1972;79:966-9.
249. Zholos AV, Dryn DO, Melnyk MI. General anaesthesia-related complications of gut motility with a focus on cholinergic mechanisms, TRP channels and visceral pain. *Front Physiol*. 2023;14:1174655.
250. Stearns AT, Balakrishnan A, Rhoads DB, Ashley SW, Tavakkolizadeh A. Diurnal expression of the rat intestinal sodium-glucose cotransporter 1 (SGLT1) is independent of local luminal factors. *Surgery*. 2009;145:294-302.

251. Stearns AT, Balakrishnan A, Rhoads DB, Tavakkolizadeh A. Rapid upregulation of sodium-glucose transporter SGLT1 in response to intestinal sweet taste stimulation. *Annals of surgery*. 2010;251:865-71.
252. Craft IL. The influence of pregnancy and lactation on the morphology and absorptive capacity of the rat small intestine. *Clin Sci*. 1970;38:287-95.
253. Prieto RM, Ferrer M, Tur JA. Changes in intestinal alpha-methyl-D-glucoside uptake due to pregnancy and lactation in rats. *Digestion*. 1996;57:16-21.
254. Velayudhan DE, Hossain MM, Stein HH, Nyachoti CM. Standardized ileal digestibility of amino acids in canola meal fed to gestating and lactating sows. *J Anim Sci*. 2019;97:4219-26.
255. Péntzes L, Simon G. Intestinal absorption and turnover of DL-methionine during reproduction in the rat. *Jpn J Physiol*. 1968;18:288-96.
256. Davies NT, Williams RB. The effect of pregnancy and lactation on the absorption of zinc and lysine by the rat duodenum in situ. *Br J Nutr*. 1977;38:417-23.
257. Dugas MC, Hazelwood RL, Lawrence AL. Influence of pregnancy and-or exercise on intestinal transport of amino acids in rats. *Proc Soc Exp Biol Med*. 1970;135:127-31.
258. Argilés J, Herrera E. Appearance of circulating and tissue ¹⁴C-lipids after oral ¹⁴C-tripalmitate administration in the late pregnant rat. *Metab Clin Exp*. 1989;38:104-8.
259. Mainoya JR. Influence of reproductive state on intestinal fluid and ion transport by the rat jejunum, in relation to the possible contribution of prolactin. *J Endocrinol*. 1975;67:351-8.
260. Parry E, Shields R, Turnbull AC. The effect of pregnancy on the colonic absorption of sodium, potassium and water. *J Obstet Gynaecol Br Commonw*. 1970;77:616-9.
261. Kent GN, Price RI, Gutteridge DH, Rosman KJ, Smith M, Allen JR, Hickling CJ, Blakeman SL. The efficiency of intestinal calcium absorption is increased in late pregnancy but not in established lactation. *Calcif Tissue Int*. 1991;48:293-5.
262. Vargas Zapata CL, Donangelo CM, Woodhouse LR, Abrams SA, Spencer EM, King JC. Calcium homeostasis during pregnancy and lactation in Brazilian women with low calcium intakes: a longitudinal study. *Am J Clin Nutr*. 2004;80:417-22.
263. Kostial K, Gruden N, Duraković A, Juvancic V, Simonović I. Reduction in strontium absorption in pregnant, lactating and suckling rats. *Acta Radiol Ther Phys Biol*. 1972;11:277-87.
264. Omi N, Ezawa I. Change in calcium balance and bone mineral density during pregnancy in female rats. *J Nutr Sci Vitaminol (Tokyo)*. 2001;47:195-200.
265. Krishnamra N, Thumchai R, Limlomwongse L. Acute effect of prolactin on the intestinal calcium absorption in normal, pregnant and lactating rats. *Bone Miner*. 1990;11:31-41.
266. Boass A, Toverud SU. Enhanced nonsaturable calcium transport in the jejunum of rats during lactation, but not during pregnancy. *J Bone Miner Res*. 1997;12:1577-83.
267. Toraason M. Calcium flux *in vivo* in the rat duodenum and ileum during pregnancy and lactation. *Am J Physiol Gastrointest Liver Physiol*. 1983;245:G624-7.
268. Boass A, Lovdal JA, Toverud SU. Pregnancy-induced and lactation-induced changes in active intestinal calcium-transport in rats. *Am J Physiol Gastrointest Liver Physiol*. 1992;263:G127-G34.
269. Halloran BP, DeLuca HF. Calcium transport in small intestine during pregnancy and lactation. *Am J Physiol Endocrinol Metab*. 1980;239:E64-8.
270. Ibrahim MM, Thomas ML, Forte LR. Maternal-fetal relationships in the parathyroidectomized rat. Intestinal calcium transport, serum calcium, immunoreactive parathyroid hormone and calcitonin. *Biol Neonate*. 1984;46:89-97.
271. Schachter D, Dowdle EB, Schenker H. Active transport of calcium by the small intestine of the rat. *Am J Physiol*. 1960;198:263-8.
272. Wróbel J, Nagel G. Diurnal variations of active calcium transport in the intestine of pregnant and lactating rat. *Biomedicine*. 1980;33:143-5.
273. Quan-Sheng D, Miller SC. Calcitrophic hormone levels and calcium absorption during pregnancy in rats. *Am J Physiol Endocrinol Metab*. 1989;257:E118-23.

274. Charoenphandhu N, Nakkrasae LI, Kraidith K, Teerapornpuntakit J, Thongchote K, Thongon N, Krishnamra N. Two-step stimulation of intestinal Ca²⁺ absorption during lactation by long-term prolactin exposure and suckling-induced prolactin surge. *Am J Physiol Endocrinol Metab.* 2009;297:E609-19.
275. van Dijk JP, van Kreel BK, Heeren JW. Iron metabolism and placental iron transfer in the guinea pig. *J Dev Physiol.* 1983;5:195-207.
276. Batey RG, Gallagher ND. Study of the subcellular localization of ⁵⁹Fe and iron-binding proteins in the duodenal mucosa of pregnant and nonpregnant rats. *Gastroenterology.* 1977;73:267-72.
277. Batey RG, Gallagher ND. Role of the placenta in intestinal absorption of iron in pregnant rats. *Gastroenterology.* 1977;72:255-9.
278. Manis JG, Schachter D. Active transport of iron by intestine: effects of oral iron and pregnancy. *Am J Physiol.* 1962;203:81-6.
279. Raja KB, Bjarnason I, Simpson RJ, Peters TJ. In vitro measurement and adaptive response of Fe³⁺ uptake by mouse intestine. *Cell Biochem Funct.* 1987;5:69-76.
280. Uçkan D, Cin S, Dinçer N, Yalçın S, Cavdar A. Oral zinc tolerance test in pregnant women. *J Trace Elem Exp Med.* 2001;14:17-23.
281. Uriu-Hare JY, Walter RM, Jr., Keen CL. ⁶⁵Zinc metabolism is altered during diabetic pregnancy in rats. *J Nutr.* 1992;122:1988-98.
282. Hambidge KM, Miller LV, Mazariegos M, Westcott J, Solomons NW, Raboy V, Kemp JF, Das A, Goco N, Hartwell T, Wright L, Krebs NF. Upregulation of zinc absorption matches increases in physiologic requirements for zinc in women consuming high- or moderate-phytate diets during late pregnancy and early lactation. *J Nutr.* 2017;147:1079-85.
283. Donangelo CM, Zapata CL, Woodhouse LR, Shames DM, Mukherjea R, King JC. Zinc absorption and kinetics during pregnancy and lactation in Brazilian women. *Am J Clin Nutr.* 2005;82:118-24.
284. Fung EB, Ritchie LD, Woodhouse LR, Roehl R, King JC. Zinc absorption in women during pregnancy and lactation: a longitudinal study. *Am J Clin Nutr.* 1997;66:80-8.
285. Brown J, Robertson J, Gallagher N. Humoral regulation of vitamin B₁₂ absorption by pregnant mouse small intestine. *Gastroenterology.* 1977;72:881-8.
286. Hellegers A, Okuda K, Nesbitt RE, Jr., Smith DW, Chow BF. Vitamin B₁₂ absorption in pregnancy and in the newborn. *Am J Clin Nutr.* 1957;5:327-31.
287. Hall CA. Transport of vitamin B₁₂ in man. *Br J Haematol.* 1969;16:429-33.
288. Robertson JA, Gallagher ND. Effect of placental lactogen on the number of intrinsic factor receptors in the pregnant mouse. *Gastroenterology.* 1979;77:511-7.
289. Robertson JA, Gallagher ND. Increased intestinal uptake of cobalamin in pregnancy does not require synthesis of new receptors. *Biochim Biophys Acta.* 1983;757:145-50.
290. Girdwood RH, Delamore IW. Observations on tests of folic acid absorption and clearance. *Scott Med J.* 1961;6:44-59.
291. Landon MJ, Hytten FE. Plasma folate levels following an oral load of folic acid during pregnancy. *J Obstet Gynaecol Br Commonw.* 1972;79:577-83.
292. Swanson CA, Turnlund JR, King JC. Effect of dietary zinc sources and pregnancy on zinc utilization in adult women fed controlled diets. *J Nutr.* 1983;113:2557-67.
293. Hunt JN, Murray FA. Gastric function in pregnancy. *J Obstet Gynaecol Br Emp.* 1958;65:78-83.
294. Zherebak NM, Golovynska JY, Stepanova LI, Nikitina NS, Beregova T, Gnatko OP. The gastrointestinal motility in rats at first trimester of pregnancy. *Dusunen Adam.* 2018;9:2003-10.
295. Parkman HP, Wang MB, Ryan JP. Decreased electromechanical activity of guinea pig circular muscle during pregnancy. *Gastroenterology.* 1993;105:1306-12.

296. Al-Shboul OA, Al-Rshoud HJ, Al-Dwairi AN, Alqudah MA, Alfaqih MA, Mustafa AG, Jaafar M. Changes in gastric smooth muscle cell contraction during pregnancy: effect of estrogen. *J Pregnancy*. 2019;2019:4302309.
297. Davison JS, Davison MC, Hay DM. Gastric emptying time in late pregnancy and labour. *J Obstet Gynaecol Br Commonw*. 1970;77:37-41.
298. O'Sullivan GM, Sutton AJ, Thompson SA, Carrie LE, Bullingham RE. Noninvasive measurement of gastric emptying in obstetric patients. *Anesth Analg*. 1987;66:505-11.
299. Sandhar BK, Elliott RH, Windram I, Rowbotham DJ. Peripartum changes in gastric emptying. *Anaesthesia*. 1992;47:196-8.
300. Clark JM, Seager SJ. Gastric emptying following premedication with glycopyrrolate or atropine. *Br J Anaesth*. 1983;55:1195-9.
301. Simpson KH, Stakes AF, Miller M. Pregnancy delays paracetamol absorption and gastric emptying in patients undergoing surgery. *Br J Anaesth*. 1988;60:24-7.
302. Macfie AG, Magides AD, Richmond MN, Reilly CS. Gastric emptying in pregnancy. *Br J Anaesth*. 1991;67:54-7.
303. Whitehead EM, Smith M, Dean Y, O'Sullivan G. An evaluation of gastric emptying times in pregnancy and the puerperium. *Anaesthesia*. 1993;48:53-7.
304. Levy DM, Williams OA, Magides AD, Reilly CS. Gastric emptying is delayed at 8-12 weeks' gestation. *Br J Anaesth*. 1994;73:237-8.
305. Rådberg G, Asztély M, Cantor P, Rehfeldt JF, Järnfeldt-Samsioe A, Svanvik J. Gastric and gallbladder emptying in relation to the secretion of cholecystokinin after a meal in late pregnancy. *Digestion*. 1989;42:174-80.
306. Chiloiro M, Darconza G, Piccioli E, De Carne M, Clemente C, Riezzo G. Gastric emptying and orocecal transit time in pregnancy. *J Gastroenterol*. 2001;36:538-43.
307. Chang FY, Lee SD, Yeh GH, Lu CC, Wang PS, Wang SW. Disturbed small intestinal motility in the late rat pregnancy. *Gynecol Obstet Invest*. 1998;45:221-4.
308. Datta U, Sharma RK. Effect of pregnancy and lactation on gastrointestinal motility in rats. *Indian J Physiol Pharmacol*. 1984;28:231-3.
309. Lefebvre RA, Smits GJ. Investigation of the influence of pregnancy on the role of nitric oxide in gastric emptying and non-adrenergic non-cholinergic relaxation in the rat. *Naunyn Schmiedeberg's Arch Pharmacol*. 1998;357:671-6.
310. Ryan JP, Bhojwani A, Wang MB. Effect of pregnancy on gastric motility *in vivo* and *in vitro* in the guinea pig. *Gastroenterology*. 1987;93:29-34.
311. Boyden EA, Rigler LG. Initial emptying time of stomach in primigravidae as related to evacuation of biliary tract. *Exp Biol Med (Maywood)*. 1944;56:200-1.
312. Maes BD, Spitz B, Ghoois YF, Hiele MI, Evenepoel P, Rutgeerts PJ. Gastric emptying in hyperemesis gravidarum and non-dyspeptic pregnancy. *Aliment Pharmacol Ther*. 1999;13:237-43.
313. Parry E, Shields R, Turnbull AC. Transit time in the small intestine in pregnancy. *J Obstet Gynaecol Br Commonw*. 1970;77:900-1.
314. Lawson M, Kern F, Jr., Everson GT. Gastrointestinal transit time in human pregnancy: prolongation in the second and third trimesters followed by postpartum normalization. *Gastroenterology*. 1985;89:996-9.
315. Ryan JP. Effect of pregnancy on intestinal transit: comparison of results using radioactive and non-radioactive test meals. *Life Sci*. 1982;31:2635-40.
316. Chang FY, Lee SD, Yeh GH, Wang PS. Influence of pregnancy and uterine weight on rat gastrointestinal transit. *J Gastroenterol Hepatol*. 1995;10:585-8.
317. Scott LD, Lester R, Van Thiel DH, Wald A. Pregnancy-related changes in small intestinal myoelectric activity in the rat. *Gastroenterology*. 1983;84:301-5.
318. Datta S, Hey VM, Pleuvry BJ. Effects of pregnancy and associated hormones in mouse intestine, *in vivo* and *in vitro*. *Pflugers Arch*. 1974;346:87-95.

319. Scott LD, DeFlora E. Cholinergic responsiveness of intestinal muscle in the pregnant guinea pig. *Life Sci.* 1989;44:503-8.
320. O'Sullivan GM, Bullingham RE. The assessment of gastric acidity and antacid effect in pregnant women by a non-invasive radiotelemetry technique. *Br J Obstet Gynaecol.* 1984;91:973-8.
321. Braverman DZ, Herbet D, Goldstein R, Persitz E, Eylath U, Jacobsohn WZ. Postpartum restoration of pregnancy-induced cholecystoparesis and prolonged intestinal transit time. *J Clin Gastroenterol.* 1988;10:642-6.
322. Szilagyí A, Salomon R, Smith BE, Martin M, Seidman E. Determinants of prolonged oral cecal transit time during late phase pregnancy. *Clin Invest Med.* 1996;19:20-7.
323. Péntzes L. Morphological changes of the rat intestine during reproduction. *Anat Anz.* 1968;122:172-5.
324. Remesar X, Arola L, Palou A, Alemany M. Body and organ size and composition during the breeding cycle of rats (*Rattus norvegicus*). *Lab Anim Sci.* 1981;31:67-70.
325. Ahokas RA, Reynolds SL, Anderson GD, Lipshitz J. Maternal organ distribution of cardiac output in the diet-restricted pregnant rat. *J Nutr.* 1984;114:2262-8.
326. Quick TC, Ong DE. Levels of cellular retinol-binding proteins in the small intestine of rats during pregnancy and lactation. *J Lipid Res.* 1989;30:1049-54.
327. Ardawi MS. The maximal activity of phosphate-dependent glutaminase and glutamine metabolism in late-pregnant and peak-lactating rats. *Biochem J.* 1987;242:75-80.
328. Prieto RM, Ferrer M, Fe JM, Rayo JM, Tur JA. Morphological adaptive changes of small intestinal tract regions due to pregnancy and lactation in rats. *Ann Nutr Metab.* 1994;38:295-300.
329. Younoszai MK, Ranshaw J. Intestinal disaccharidases in the rat: effects of pregnancy and diabetes. *J Nutr.* 1976;106:504-8.
330. Palmer MF, Rolls BA. Activities of some metabolic enzymes in the small intestinal mucosa during pregnancy and lactation in the rat. *J Reprod Fertil.* 1980;60:231-6.
331. Ribeiro TA, Breznik JA, Kennedy KM, Yeo E, Kennelly BKE, Jazwiec PA, Patterson VS, Bellissimo CJ, Anhô FF, Schertzer JD, Bowdish DME, Sloboda DM. Intestinal permeability and peripheral immune cell composition are altered by pregnancy and adiposity at mid- and late-gestation in the mouse. *PloS One.* 2023;18:e0284972.
332. Pelletier G, de Passillé AM, Bernier-Cardou M, Morisset J. Influence of pregnancy, lactation, litter size and diet energy density on the stomach and intestine of sows. *J Nutr.* 1987;117:1759-66.
333. Pond WG, Yen JT, Yen LH. Response of nonpregnant versus pregnant gilts and their fetuses to severe feed restriction. *J Anim Sci.* 1986;63:472-83.
334. Gębczyńska Z, Gębczyński M. Length and weight of the alimentary tract of the root vole. *Acta Theriol.* 1971;16:359-69.
335. Jaroszevska M, Wilczyńska B. Dimensions of surface area of alimentary canal of pregnant and lactating female common shrews. *J Mammal.* 2006;87:589-97.
336. Gohir W, Kennedy KM, Wallace JG, Saoi M, Bellissimo CJ, Britz-McKibbin P, Petrik JJ, Surette MG, Sloboda DM. High-fat diet intake modulates maternal intestinal adaptations to pregnancy and results in placental hypoxia, as well as altered fetal gut barrier proteins and immune markers. *J Physiol.* 2019;597:3029-51.
337. Peeters LL, Grutters G, Martin CB, Jr. Distribution of cardiac output in the unstressed pregnant guinea pig. *Am J Obstet Gynecol.* 1980;138:1177-84.
338. Crean GP, Rumsey RD. Hyperplasia of the gastric mucosa during pregnancy and lactation in the rat. *J Physiol.* 1971;215:181-97.
339. Prieto RM, Ferrer M, Rayó JM, Tur JA. Disaccharidase activities in pregnant and lactating rats. *Comp Biochem Physiol A Physiol.* 1994;109:741-7.
340. Péntzes L, Noble RC, Regius O. Morphometric changes in the duodenal microvillous surface area of the non-pregnant, pregnant and lactating female rat. *Acta Morphol Neerl Scand.* 1988;26:9-17.

341. Péntzes L, Regius O. Changes in the intestinal microvillous surface area during reproduction and ageing in the female rat. *J Anat.* 1985;140:389-96.
342. Péntzes L, Kranz D, Kretschmar K, Rosenthal V, Januschke D, Krämer M, Regius O. Alterations in the intestinal microvillous surface area during the whole life span of the female rat ileum. *Z Alternsforsch.* 1988;43:251-8.
343. Burdett K, Reek C. Adaptation of the small intestine during pregnancy and lactation in the rat. *Biochem J.* 1979;184:245-51.
344. Jolicoeur L, Asselin J, Morisset J. Trophic effects of gestation and lactation on rat duodenum. *Biomed Res (Tokyo).* 1981;2:113-8.
345. Bailey CJ, Conlon JM, Flatt PR. Effect of ovarian hormones, pregnancy and lactation on somatostatin and substance P in the alimentary tract of mice. *J Endocrinol.* 1989;122:645-50.
346. Kirksey A, Tabacchi MH. Pyridoxine deficiency and iron metabolism in the pregnant rat: maternal responses. *J Nutr.* 1967;93:229-40.
347. Mottino AD, Hoffman T, Jennes L, Cao J, Vore M. Expression of multidrug resistance-associated protein 2 in small intestine from pregnant and postpartum rats. *Am J Physiol Gastrointest Liver Physiol.* 2001;280:G1261-73.
348. Dudley MA, Shulman RJ, Reeds PJ, Rosenberger JN, Putman M, Johnston PK, Perkinson JS, Nichols BL. Developmental changes in lactase-phlorizin hydrolase precursor isoforms in the rat. *J Pediatr Gastroenterol Nutr.* 1992;15:260-9.
349. Dawson PA, Karpen SJ. Intestinal transport and metabolism of bile acids. *J Lipid Res.* 2015;56:1085-99.
350. Ovadia C, Perdonés-Montero A, Spagou K, Smith A, Sarafian MH, Gomez-Romero M, Bellafante E, Clarke LCD, Sadiq F, Nikolova V, Mitchell A, Dixon PH, Santa-Pinter N, Wahlström A, Abu-Hayyeh S, Walters JRF, Marschall HU, Holmes E, Marchesi JR, Williamson C. Enhanced microbial bile acid deconjugation and impaired ileal uptake in pregnancy repress intestinal regulation of bile acid synthesis. *Hepatology.* 2019;70:276-93.
351. Mottino AD, Hoffman T, Dawson PA, Luquita MG, Monti JA, Sánchez Pozzi EJ, Catania VA, Cao J, Vore M. Increased expression of ileal apical sodium-dependent bile acid transporter in postpartum rats. *Am J Physiol Gastrointest Liver Physiol.* 2002;282:G41-50.
352. Diaz de Barboza G, Guizzardi S, Tolosa de Talamoni N. Molecular aspects of intestinal calcium absorption. *World J Gastroenterol.* 2015;21:7142-54.
353. Van Cromphaut SJ, Rummens K, Stockmans I, Van Herck E, Dijcks FA, Ederveen AG, Carmeliet P, Verhaeghe J, Bouillon R, Carmeliet G. Intestinal calcium transporter genes are upregulated by estrogens and the reproductive cycle through vitamin D receptor-independent mechanisms. *J Bone Miner Res.* 2003;18:1725-36.
354. Peshin J, Ornoy A, Menczel J. Transplacental effects of thyrocalcitonin on intestinal calcium-binding protein, alkaline phosphatase activity and ossification of long bones in rat fetuses. *Isr J Med Sci.* 1976;12:248-56.
355. Delorme AC, Marche P, Garel JM. Vitamin D-dependent calcium-binding protein. Changes during gestation, prenatal and postnatal development in rats. *J Dev Physiol.* 1979;1:181-94.
356. Leazer TM, Liu Y, Klaassen CD. Cadmium absorption and its relationship to divalent metal transporter-1 in the pregnant rat. *Toxicol Appl Pharmacol.* 2002;185:18-24.
357. Millard KN, Frazer DM, Wilkins SJ, Anderson GJ. Changes in the expression of intestinal iron transport and hepatic regulatory molecules explain the enhanced iron absorption associated with pregnancy in the rat. *Gut.* 2004;53:655-60.
358. Balesaria S, Hanif R, Salama MF, Raja K, Bayele HK, McArdle H, Srai SK. Fetal iron levels are regulated by maternal and fetal Hfe genotype and dietary iron. *Haematologica.* 2012;97:661-9.
359. Lane DJ, Bae DH, Merlot AM, Sahni S, Richardson DR. Duodenal cytochrome b (DCYTB) in iron metabolism: an update on function and regulation. *Nutrients.* 2015;7:2274-96.
360. Mazgaj R, Lipiński P, Edison ES, Bednarz A, Staroń R, Haberkiewicz O, Lenartowicz M, Smuda E, Jończy A, Starzyński RR. Marginally reduced maternal hepatic and splenic ferroportin under severe

- nutritional iron deficiency in pregnancy maintains systemic iron supply. *Am J Hematol.* 2021;96:659-70.
361. Liuzzi JP, Bobo JA, Cui L, McMahon RJ, Cousins RJ. Zinc transporters 1, 2 and 4 are differentially expressed and localized in rats during pregnancy and lactation. *J Nutr.* 2003;133:342-51.
362. Dawson PA, Rakoczy J, Simmons DG. Placental, renal, and ileal sulfate transporter gene expression in mouse gestation. *Biol Reprod.* 2012;87:43.
363. West CA, Welling PA, West DA, Jr., Coleman RA, Cheng KY, Chen C, DuBose TD, Jr., Verlander JW, Baylis C, Gumz ML. Renal and colonic potassium transporters in the pregnant rat. *Am J Physiol Renal Physiol.* 2018;314:F251-9.
364. Gao G, Liu SY, Wang HJ, Zhang TW, Yu P, Duan XL, Zhao SE, Chang YZ. Effects of pregnancy and lactation on iron metabolism in rats. *BioMed Res Int.* 2015;2015:105325.
365. Zhu Y, Goff JP, Reinhardt TA, Horst RL. Pregnancy and lactation increase vitamin D-dependent intestinal membrane calcium adenosine triphosphatase and calcium binding protein messenger ribonucleic acid expression. *Endocrinology.* 1998;139:3520-4.
366. Krisinger J, Dann JL, Applegarth O, Currie WD, Jeung EB, Staun M, Leung PC. Calbindin-D9k gene expression during the perinatal period in the rat: correlation to estrogen receptor expression in uterus. *Mol Cell Endocrinol.* 1993;97:61-9.
367. Bruns ME, Fausto A, Avioli LV. Placental calcium binding protein in rats. Apparent identity with vitamin D-dependent calcium binding protein from rat intestine. *J Biol Chem.* 1978;253:3186-90.
368. Rummens K, van Cromphaut SJ, Carmeliet G, van Herck E, van Bree R, Stockmans I, Bouillon R, Verhaeghe J. Pregnancy in mice lacking the vitamin D receptor: normal maternal skeletal response, but fetal hypomineralization rescued by maternal calcium supplementation. *Pediatr Res.* 2003;54:466-73.
369. Gerdes B. The rate of emptying of the human gall bladder in pregnancy. *Am J Obstet Gynecol.* 1938;36:358-9.
370. Everson GT, McKinley C, Lawson M, Johnson M, Kern F, Jr. Gallbladder function in the human female: effect of the ovulatory cycle, pregnancy, and contraceptive steroids. *Gastroenterology.* 1982;82:711-9.
371. Kern F, Jr., Everson GT, DeMark B, McKinley C, Showalter R, Erfling W, Braverman DZ, Szczepanik-van Leeuwen P, Klein PD. Biliary lipids, bile acids, and gallbladder function in the human female. Effects of pregnancy and the ovulatory cycle. *J Clin Invest.* 1981;68:1229-42.
372. Braverman DZ, Johnson ML, Kern F, Jr. Effects of pregnancy and contraceptive steroids on gallbladder function. *N Engl J Med.* 1980;302:362-4.
373. Go VL, Hofmann AF, Summerskill WH. Pancreozymin bioassay in man based on pancreatic enzyme secretion: potency of specific amino acids and other digestive products. *J Clin Invest.* 1970;49:1558-64.
374. Oyesola TO, Oluwole FS, Oyesola OA. Effects of *Croton Pendliciflous* methanolic extract on intestinal enzymes and protein content in pregnant rats. *Res J Med Plant.* 2009;3:141-5.
375. Takeuchi K, Okabe S. Factors related to gastric hypersecretion during pregnancy and lactation in rats. *Dig Dis Sci.* 1984;29:248-55.
376. Chen TS, Yeh GH, Pu HF, Doong ML, Lu CC, Liu SR, Young TK, Ho LT, Chang FY, Wang PS. Gastric inhibitory polypeptide and gastric acid secretion in pregnant rats. *Placenta.* 1995;16:85-92.
377. Clark DH. Gastric acid secretion in dogs during pregnancy and lactation. *Scott Med J.* 1957;2:392-5.
378. Rolls BA, Henschel MJ, Palmer MF. The effects of pregnancy and lactation on the activities of trypsin and alpha-chymotrypsin in the rat pancreas. *Br J Nutr.* 1979;41:573-8.
379. Villard L, Bates CJ. Carotene dioxygenase (EC 1.13.11.21) activity in rat intestine: effects of vitamin A deficiency and of pregnancy. *Br J Nutr.* 1986;56:115-22.

380. Brambell FWR. Reproduction in the common shrew (*Sorex araneus Linnæus*). I. The oestrous cycle of the female. *Philos Trans R Soc Lond B*. 1935;225:1-49.
381. Gatford KL, Boyce JM, Blackmore K, Smits RJ, Campbell RG, Owens PC. Long-term, but not short-term, treatment with somatotropin during pregnancy in underfed pigs increases the body size of progeny at birth. *J Anim Sci*. 2004;82:93-101.
382. Gatford KL, Smits RJ, Collins CL, Argent C, De Blasio MJ, Roberts CT, Nottle MB, Kind KL, Owens JA. Maternal responses to daily maternal porcine somatotropin injections during early-mid pregnancy or early-late pregnancy in sows and gilts. *J Anim Sci*. 2010;88:1365-78.
383. Kiely ME, McCarthy EK, Hennessy A. Iron, iodine and vitamin D deficiencies during pregnancy: epidemiology, risk factors and developmental impacts. *Proc Nutr Soc*. 2021;80:290-302.
384. Neuhouser ML, Beresford SA, Hickok DE, Monsen ER. Absorption of dietary and supplemental folate in women with prior pregnancies with neural tube defects and controls. *J Am Coll Nutr*. 1998;17:625-30.
385. Boddie AM, Dedlow ER, Nackashi JA, Opalko FJ, Kauwell GP, Gregory JF, 3rd, Bailey LB. Folate absorption in women with a history of neural tube defect-affected pregnancy. *Am J Clin Nutr*. 2000;72:154-8.
386. Ferraris RP, Yasharpour S, Lloyd KC, Mirzayan R, Diamond JM. Luminal glucose concentrations in the gut under normal conditions. *Am J Physiol Gastrointest Liver Physiol*. 1990;259:G822-37.
387. Finer LB, Zolna MR. Declines in unintended pregnancy in the United States, 2008-2011. *N Engl J Med*. 2016;374:843-52.
388. Taylor A. ABC of subfertility: extent of the problem. *BMJ*. 2003;327:434-6.
389. Johnson MS, Thomson SC, Speakman JR. Limits to sustained energy intake. I. Lactation in the laboratory mouse *Mus musculus*. *J Exp Biol*. 2001;204:1925-35.
390. Ahokas RA, Reynolds SL, Anderson GD, Lipshitz J. Maternal organ distribution of cardiac output in the diet-restricted pregnant rat. *J Nutr*. 1984;114:2262-8.
391. Amano Y. Changes in the levels of blood glucose during pregnancy in the rat. *Jpn J Pharmacol*. 1967;17:105-14.
392. Ardawi MS. The maximal activity of phosphate-dependent glutaminase and glutamine metabolism in late-pregnant and peak-lactating rats. *Biochem J*. 1987;242:75-80.
393. Barboni E, Mancinelli P, Bitossi U, AR DEG, Micaglio M, Sorbi F, A DIF. Ultrasound evaluation of the stomach and gastric emptying in pregnant women at term: a case-control study. *Minerva Anesthesiol*. 2016;82:543-9.
394. Burdett K, Reek C. Adaptation of the small intestine during pregnancy and lactation in the rat. *Biochem J*. 1979;184:245-51.
395. Chang FY, Lee SD, Yeh GH, Lu CC, Wang PS, Wang SW. Disturbed small intestinal motility in the late rat pregnancy. *Gynecol Obstet Invest*. 1998;45:221-4.
396. Clapp JF, 3rd, Stepanchak W, Tomaselli J, Kortan M, Faneslow S. Portal vein blood flow-effects of pregnancy, gravity, and exercise. *Am J Obstet Gynecol*. 2000;183:167-72.
397. Craft IL. The influence of pregnancy and lactation on the morphology and absorptive capacity of the rat small intestine. *Clin Sci*. 1970;38:287-95.
398. Dawson PA, Rakoczy J, Simmons DG. Placental, renal, and ileal sulfate transporter gene expression in mouse gestation. *Biol Reprod*. 2012;87:43, 1-9.
399. Delorme AC, Marche P, Garel JM. Vitamin D-dependent calcium-binding protein. Changes during gestation, prenatal and postnatal development in rats. *J Dev Physiol*. 1979;1:181-94.
400. Doguer C, Ha JH, Gulec S, Vulpe CD, Anderson GJ, Collins JF. Intestinal hephaestin potentiates iron absorption in weanling, adult, and pregnant mice under physiological conditions. *Blood Adv*. 2017;1:1335-46.
401. Dudley MA, Shulman RJ, Reeds PJ, Rosenberger JN, Putman M, Johnston PK, Perkinson JS, Nichols BL. Developmental changes in lactase-phlorizin hydrolase precursor isoforms in the rat. *J Pediatr Gastroenterol Nutr*. 1992;15:260-9.

402. Dugas MC, Hazelwood RL, Lawrence AL. Influence of pregnancy and-or exercise on intestinal transport of amino acids in rats. *Proc Soc Exp Biol Med.* 1970;135:127-31.
403. Fairweather-Tait SJ, Wright AJ, Williams CM. Zinc metabolism in pregnant and lactating rats and the effect of varying iron: Zn in the diet. *Br J Nutr.* 1984;52:205-13.
404. Gallagher ND, Robertson, J.A, editor. Adaptation of cobalamin absorption in pregnant rats is controlled by placental lactogen. Mechanisms of intestinal absorption, proceedings of the Second International Conference on Intestinal Adaptation; 1981.
405. Gohir W, Kennedy KM, Wallace JG, Saoi M, Bellissimo CJ, Britz-McKibbin P, Petrik JJ, Surette MG, Sloboda DM. High-fat diet intake modulates maternal intestinal adaptations to pregnancy and results in placental hypoxia, as well as altered fetal gut barrier proteins and immune markers. *J Physiol.* 2019;597:3029-51.
406. Kostial K, Gruden N, Duraković A, Juvancic V, Simonović I. Reduction in strontium absorption in pregnant, lactating and suckling rats. *Acta Radiol Ther Phys Biol.* 1972;11:277-87.
407. Krisinger J, Dann JL, Jeung EB, Leung PC. Calbindin-D9k gene expression during pregnancy and lactation in the rat. *Mol Cell Endocrinol.* 1992;88:119-28.
408. Liuzzi JP, Bobo JA, Cui L, McMahan RJ, Cousins RJ. Zinc transporters 1, 2 and 4 are differentially expressed and localized in rats during pregnancy and lactation. *J Nutr.* 2003;133:342-51.
409. Matos JF, Americo MF, Sinzato YK, Volpato GT, Corá LA, Calabresi MF, Oliveira RB, Damasceno DC, Miranda JR. Role of sex hormones in gastrointestinal motility in pregnant and non-pregnant rats. *World J Gastroenterol.* 2016;22:5761-8.
410. Moore MC, Smith MS, Connolly CC. Pregnancy augments hepatic glucose storage in response to a mixed meal. *Br J Nutr.* 2012;107:493-503.
411. Mottino AD, Hoffman T, Jennes L, Cao J, Vore M. Expression of multidrug resistance-associated protein 2 in small intestine from pregnant and postpartum rats. *Am J Physiol Gastrointest Liver Physiol.* 2001;280:G1261-73.
412. Mottino AD, Hoffman T, Dawson PA, Luquita MG, Monti JA, Sánchez Pozzi EJ, Catania VA, Cao J, Vore M. Increased expression of ileal apical sodium-dependent bile acid transporter in postpartum rats. *Am J Physiol Gastrointest Liver Physiol.* 2002;282:G41-50.
413. Musacchia XJ, Hartner AM. Intestinal absorption of glucose, and blood glucose and hematocrit in pregnant and nonpregnant hamsters. *Proc Soc Exp Biol Med.* 1970;135:307-10.
414. Nakai A, Sekiya I, Oya A, Koshino T, Araki T. Assessment of the hepatic arterial and portal venous blood flows during pregnancy with Doppler ultrasonography. *Arch Gynecol Obstet.* 2002;266:25-9.
415. Palmer MF, Rolls BA. Activities of some metabolic enzymes in the small intestinal mucosa during pregnancy and lactation in the rat. *J Reprod Fertil.* 1980;60:231-6.
416. Pelletier G, de Passillé AM, Bernier-Cardou M, Morisset J. Influence of pregnancy, lactation, litter size and diet energy density on the stomach and intestine of sows. *J Nutr.* 1987;117:1759-66.
417. Péntzes L, Simon G. Intestinal absorption and turnover of dl-methionine during reproduction in the rat. *Jpn J Physiol.* 1968;18:288-96.
418. Peters JM, Krijnen CJ, Boyd EM. Role of concepta in the production of hypertrophy and hydration of maternal body organs in the third week of pregnancy in albino rats. *J Reprod Fertil.* 1967;14:235-42.
419. Prieto RM, Ferrer M, Fe JM, Rayó JM, Tur JA. Morphological adaptive changes of small intestinal tract regions due to pregnancy and lactation in rats. *Ann Nutr Metab.* 1994;38:295-300.
420. Remesar X, Arola L, Palou A, Alemany M. Body and organ size and composition during the breeding cycle of rats (*Rattus norvegicus*). *Lab Anim Sci.* 1981;31:67-70.
421. Rolls BA. Dipeptidase activity in the small intestinal mucosa during pregnancy and lactation in the rat. *Br J Nutr.* 1975;33:1-9.
422. Rummens K, van Cromphaut SJ, Carmeliet G, van Herck E, van Bree R, Stockmans I, Bouillon R, Verhaeghe J. Pregnancy in mice lacking the vitamin D receptor: normal maternal skeletal

- response, but fetal hypomineralization rescued by maternal calcium supplementation. *Pediatr Res.* 2003;54:466-73.
423. Sabet Sarvestani F, Rahmanifar F, Tamadon A. Histomorphometric changes of small intestine in pregnant rat. *Vet Res Forum.* 2015;6:69-73.
424. Schachter D, Kowarski, S., Phyllis, R. Active transport of calcium by intestine: studies with a calcium activity electrode. Cuthbert AW, editor. London: Macmillan; 1970.
425. Şensoy E, Öznurlu Y. Determination of the changes on the small intestine of pregnant mice by histological, enzyme histochemical, and immunohistochemical methods. *Turk J Gastroenterol.* 2019;30:917-24.
426. Swanston-Flatt SK, Flatt PR. The effect of pregnancy, ovariectomy and the administration of ethynyl-oestradiol and oestradiol on the intestinal transfer of folic acid in the rat. *Biochem Soc Trans.* 1980;8:589-90.
427. Teerapornpantakit J, Klanchui A, Karoonuthaisiri N, Wongdee K, Charoenphandhu N. Expression of transcripts related to intestinal ion and nutrient absorption in pregnant and lactating rats as determined by custom-designed cDNA microarray. *Mol Cell Biochem.* 2014;391:103-16.
428. Van Cromphaut SJ, Rummens K, Stockmans I, Van Herck E, Dijcks FA, Ederveen AG, Carmeliet P, Verhaeghe J, Bouillon R, Carmeliet G. Intestinal calcium transporter genes are upregulated by estrogens and the reproductive cycle through vitamin D receptor-independent mechanisms. *J Bone Miner Res.* 2003;18:1725-36.
429. Vargas Zapata CL, Donangelo CM, Woodhouse LR, Abrams SA, Spencer EM, King JC. Calcium homeostasis during pregnancy and lactation in Brazilian women with low calcium intakes: a longitudinal study. *Am J Clin Nutr.* 2004;80:417-22.
430. Overduin TS, Wardill HR, Young RL, Page AJ, Gatford KL. Active glucose transport varies by small intestinal region and oestrous cycle stage in mice. *Exp Physiol.* 2023:In press
DOI:10.1113/EP091040
431. Poulsen SB, Fenton RA, Rieg T. Sodium-glucose cotransport. *Curr Opin Nephrol Hypertens.* 2015;24:463-9.
432. Brennan IM, Feltrin KL, Nair NS, Hausken T, Little TJ, Gentilcore D, Wishart JM, Jones KL, Horowitz M, Feinle-Bisset C. Effects of the phases of the menstrual cycle on gastric emptying, glycemia, plasma GLP-1 and insulin, and energy intake in healthy lean women. *Am J Physiol Gastrointest Liver Physiol.* 2009;297:G602-10.
433. Lissner L, Stevens J, Levitsky DA, Rasmussen KM, Strupp BJ. Variation in energy intake during the menstrual cycle: implications for food-intake research. *Am J Clin Nutr.* 1988;48:956-62.
434. Gong EJ, Garrel D, Calloway DH. Menstrual cycle and voluntary food intake. *Am J Clin Nutr.* 1989;49:252-8.
435. Kemnitz JW, Eisele SG, Lindsay KA, Engle MJ, Perelman RH, Farrell PM. Changes in food intake during menstrual cycles and pregnancy of normal and diabetic rhesus monkeys. *Diabetologia.* 1984;26:60-4.
436. Petersen S. The temporal pattern of feeding over the oestrous cycle of the mouse. *Anim Behav.* 1976;24:939-55.
437. Bailey CJ, Matty AJ. Glucose tolerance and plasma insulin of the rat in relation to the oestrous cycle and sex hormones. *Horm Metab Res.* 1972;4:266-70.
438. Drewett RF. The meal patterns of the oestrous cycle and their motivational significance. *Q J Exp Psychol.* 1974;26:489-94.
439. Dimitriadis GD, Maratou E, Kountouri A, Board M, Lambadiari V. Regulation of postabsorptive and postprandial glucose metabolism by insulin-dependent and insulin-independent mechanisms: an integrative approach. *Nutrients.* 2021;13:1-33.
440. Grundy D. Principles and standards for reporting animal experiments in *The Journal of Physiology and Experimental Physiology.* *J Physiol.* 2015;593:2547-9.
441. Percie du Sert N, Hurst V, Ahluwalia A, Alam S, Avey MT, Baker M, Browne WJ, Clark A, Cuthill IC, Dirnagl U, Emerson M, Garner P, Holgate ST, Howells DW, Karp NA, Ladic SE, Lidster K,

- MacCallum CJ, Macleod M, Pearl EJ, Petersen OH, Rawle F, Reynolds P, Rooney K, Sena ES, Silberberg SD, Steckler T, Wurbel H. The ARRIVE guidelines 2.0: Updated guidelines for reporting animal research. *PLoS Biol.* 2020;18:e3000410.
442. National Health and Medical Research Council. Australian Code for the care and use of animals for scientific purposes, 8th Edition Canberra: Australian Government Publishing Service; 2013. 82 p.
443. Wardill HR, Bowen JM, Van Seville YZ, Secombe KR, Collier JK, Ball IA, Logan RM, Gibson RJ. TLR4-dependent claudin-1 internalization and secretagogue-mediated chloride secretion regulate irinotecan-induced diarrhea. *Mol Cancer Ther.* 2016;15:2767-79.
444. Zhong LX, Li XN, Yang GY, Zhang X, Li WX, Zhang QQ, Pan HX, Zhang HH, Zhou MY, Wang YD, Zhang WW, Hu QS, Zhu W, Zhang B. Circadian misalignment alters insulin sensitivity during the light phase and shifts glucose tolerance rhythms in female mice. *PLoS One.* 2019;14:e0225813.
445. Iwashina I, Mochizuki K, Inamochi Y, Goda T. Clock genes regulate the feeding schedule-dependent diurnal rhythm changes in hexose transporter gene expressions through the binding of BMAL1 to the promoter/enhancer and transcribed regions. *J Nutr Biochem.* 2011;22:334-43.
446. Caligioni CS. Assessing reproductive status/stages in mice. *Curr Protoc Neurosci.* 2009;Appendix 4:Appendix 4I.
447. Kroesen AJ, Stockmann M, Ransco C, Schulzke JD, Fromm M, Buhr HJ. Impairment of epithelial transport but not of barrier function in idiopathic pouchitis after ulcerative colitis. *Gut.* 2002;50:821-6.
448. Hardcastle J, Hardcastle PT, Taylor CJ. Loperamide inhibits the enhanced intestinal glucose absorption of cystic fibrosis in vitro. *Pediatr Res.* 1994;35:354-6.
449. Ferraris RP, Yasharpour S, Lloyd KC, Mirzayan R, Diamond JM. Luminal glucose concentrations in the gut under normal conditions. *Am J Physiol.* 1990;259:G822-37.
450. Smith K, Karimian Azari E, LaMoia TE, Hussain T, Vargova V, Karolyi K, Veldhuis PP, Arnoletti JP, de la Fuente SG, Pratley RE, Osborne TF, Kyriazis GA. T1R2 receptor-mediated glucose sensing in the upper intestine potentiates glucose absorption through activation of local regulatory pathways. *Mol Metab.* 2018;17:98-111.
451. Rider AK, Schedl HP, Nokes G, Shining S. Small intestinal glucose transport. Proximal-distal kinetic gradients. *J Gen Physiol.* 1967;50:1173-82.
452. Yoshida A, Takata K, Kasahara T, Aoyagi T, Saito S, Hirano H. Immunohistochemical localization of Na⁺-dependent glucose transporter in the rat digestive tract. *Histochem J.* 1995;27:420-6.
453. Takata K, Kasahara T, Kasahara M, Ezaki O, Hirano H. Immunohistochemical localization of Na⁺-dependent glucose transporter in rat jejunum. *Cell Tissue Res.* 1992;267:3-9.
454. Haase W, Heitmann K, Friese W, Ollig D, Koepsell H. Characterization and histochemical localization of the rat intestinal Na⁺-D-glucose cotransporter by monoclonal antibodies. *Eur J Cell Biol.* 1990;52:297-309.
455. Klinger S, Lange P, Brandt E, Hustedt K, Schröder B, Breves G, Herrmann J. Degree of SGLT1 phosphorylation is associated with but does not determine segment-specific glucose transport features in the porcine small intestines. *Physiol Rep.* 2018;6:1-18.
456. Yoshikawa T, Inoue R, Matsumoto M, Yajima T, Ushida K, Iwanaga T. Comparative expression of hexose transporters (SGLT1, GLUT1, GLUT2 and GLUT5) throughout the mouse gastrointestinal tract. *Histochem Cell Biol.* 2011;135:183-94.
457. Santer R, Hillebrand G, Steinmann B, Schaub J. Intestinal glucose transport: evidence for a membrane traffic-based pathway in humans. *Gastroenterology.* 2003;124:34-9.
458. Singh R, Nagapaul JP, Majumdar S, Chakravarti RN, Dhall GI. Effects of 17 beta-estradiol and progesterone on intestinal digestive and absorptive functions in ovariectomized rats. *Biochem Int.* 1985;10:777-86.
459. Larralde J, Fernandez Otero P. Effect of pregnancy on in vitro intestinal absorption of glucose and glycine. *Rev Esp Fisiol.* 1968;24:49-50.

460. Feldman AT, Wolfe D. Tissue processing and hematoxylin and eosin staining. *Methods Mol Biol.* 2014;1180:31-43.
461. Li H, Kentish SJ, Wittert GA, Page AJ. Apelin modulates murine gastric vagal afferent mechanosensitivity. *Physiol Behav.* 2018;194:466-73.
462. Bookout AL, Mangelsdorf DJ. Quantitative real-time PCR protocol for analysis of nuclear receptor signaling pathways. *Nucl Recept Signal.* 2003;1:e012.
463. Karasov WH. Integrative physiology of transcellular and paracellular intestinal absorption. *J Exp Biol.* 2017;220:2495-501.
464. Shirazi-Beechey SP, Gribble SM, Wood IS, Tarpey PS, Beechey RB, Dyer J, Scott D, Barker PJ. Dietary regulation of the intestinal sodium-dependent glucose cotransporter (SGLT1). *Biochem Soc Trans.* 1994;22:655-8.
465. Holst JJ. The physiology of glucagon-like peptide 1. *Physiol Rev.* 2007;87:1409-39.
466. Lain KY, Catalano PM. Metabolic changes in pregnancy. *Clin Obstet Gynecol.* 2007;50:938-48.
467. Leturque A, Ferré P, Satabin P, Kervran A, Girard J. In vivo insulin resistance during pregnancy in the rat. *Diabetologia.* 1980;19:521-8.
468. Butte NF. Carbohydrate and lipid metabolism in pregnancy: normal compared with gestational diabetes mellitus. *Am J Clin Nutr.* 2000;71:1256s-61s.
469. Einstein FH, Fishman S, Muzumdar RH, Yang XM, Atzmon G, Barzilai N. Accretion of visceral fat and hepatic insulin resistance in pregnant rats. *Am J Physiol Endocrinol Metab.* 2008;294:E451-5.
470. Peral-Sanchez I, Hojeij B, Ojeda DA, Steegers-Theunissen RPM, Willaime-Morawek S. Epigenetics in the uterine environment: how maternal diet and ART may influence the epigenome in the offspring with long-term health consequences. *Genes.* 2021;13.
471. Fleming TP, Lucas ES, Watkins AJ, Eckert JJ. Adaptive responses of the embryo to maternal diet and consequences for post-implantation development. *Reprod Fertil Dev.* 2011;24:35-44.
472. Mak IW, Evaniew N, Ghert M. Lost in translation: animal models and clinical trials in cancer treatment. *Am J Transl Res.* 2014;6:114-8.
473. Rogan MM, Black KE. Dietary energy intake across the menstrual cycle: a narrative review. *Nutr Rev.* 2023;81:869-86.
474. Jørgensen J, Mortensen PB. Utilization of short-chain fatty acids by colonic mucosal tissue strips. A new method of assessing colonic mucosal metabolism. *Scand J Gastroenterol.* 2000;35:659-66.
475. Donohoe DR, Garge N, Zhang X, Sun W, O'Connell TM, Bunker MK, Bultman SJ. The microbiome and butyrate regulate energy metabolism and autophagy in the mammalian colon. *Cell Metab.* 2011;13:517-26.
476. Ladyman SR, Carter KM, Gillett ML, Aung ZK, Grattan DR. A reduction in voluntary physical activity in early pregnancy in mice is mediated by prolactin. *eLife.* 2021;10.
477. Meander L, Lindqvist M, Mogren I, Sandlund J, West CE, Domellöf M. Physical activity and sedentary time during pregnancy and associations with maternal and fetal health outcomes: an epidemiological study. *BMC pregnancy and childbirth.* 2021;21:166.
478. Hegaard HK, Damm P, Hedegaard M, Henriksen TB, Ottesen B, Dykes AK, Kjaergaard H. Sports and leisure time physical activity during pregnancy in nulliparous women. *Maternal and child health journal.* 2011;15:806-13.
479. Herrera-Ruiz D, Wang Q, Gudmundsson OS, Cook TJ, Smith RL, Faria TN, Knipp GT. Spatial expression patterns of peptide transporters in the human and rat gastrointestinal tracts, Caco-2 in vitro cell culture model, and multiple human tissues. *AAPS pharmSci.* 2001;3:E9.
480. Lescale-Matys L, Dyer J, Scott D, Freeman TC, Wright EM, Shirazi-Beechey SP. Regulation of the ovine intestinal Na⁺/glucose co-transporter (SGLT1) is dissociated from mRNA abundance. *Biochem J.* 1993;291:435-40.

APPENDICES

Appendix 1 Adaptations in gastrointestinal nutrient absorption and its determinants during pregnancy in monogastric mammals: a scoping review protocol

SYSTEMATIC REVIEW PROTOCOL

Adaptations in gastrointestinal nutrient absorption and its determinants during pregnancy in monogastric mammals: a scoping review protocol

Teunis Sebastian Overduin^{1,2,3} · Amanda J. Page^{1,2} · Richard L. Young^{1,2} · Kathryn L. Gatford^{1,2,3}

¹Adelaide Medical School, The University of Adelaide, Adelaide, SA, Australia, ²Nutrition, Diabetes and Gut Health, Lifelong Health Theme, South Australian Health and Medical Research Institute, Adelaide, SA, Australia, and ³Robinson Research Institute, The University of Adelaide, Adelaide, SA, Australia

ABSTRACT

Objective: The aim of this review is to characterize the current state of literature and knowledge regarding adaptations of gastrointestinal nutrient absorption, and the determinants of this absorption during pregnancy in monogastric mammals.

Introduction: Energy demands increase significantly during pregnancy due to the metabolic demands associated with placental and fetal growth, and the deposition of fat stores that support postnatal lactation. Previous studies have examined anatomical changes within the small intestine, but have focused on specific pregnancy stages or specific regions of the small intestine. Importantly, little is known about changes in nutrient absorption during pregnancy, and the underlying mechanisms that lead to these changes. An understanding of these adaptations will inform research to improve pregnancy outcomes for both mothers and newborns in the future.

Inclusion criteria: This review will include primary literature that describes gastrointestinal nutrient absorption and/or its determinants during pregnancy in monogastric mammals, including humans and rodents. Only data for normal pregnancies will be included, and models of pathology and illness will be excluded. Studies must include comparisons between pregnant animals at known stages of pregnancy, and non-pregnant controls, or compare animals at different stages of pregnancy.

Methods: The following databases will be searched for literature on this topic: PubMed, Scopus, Web of Science, Embase, MEDLINE, and ProQuest Dissertations and Theses. Evidence screening and selection will be carried out independently by two reviewers, and conflicts will be resolved through discussion with additional members of the review team. Data will be extracted and presented in tables and/or figures, together with a narrative summary.

Keywords: nutrient absorption; nutrient transport; plasticity; pregnancy; small intestine

JBI Evid Synth 2022; 20(2):640–646.

Introduction

Pregnancy represents a period of rapid physiological change in the mother, with multiple systems adapting quickly to meet the demands of the *conceptus*. Physiological adaptations during pregnancy include increased blood volume and cardiac output (both ↑40% in humans), increased consumption of oxygen (↑20% in humans), and an

increased metabolic rate (↑15% in humans).^{1,2} In humans, maternal weight will increase on average between 11.5 and 16 kg throughout gestation.³ This includes a ~3.8 kg fetus,⁴ and ~800 g placenta,⁵ in addition to fat deposits that support lactation following parturition.⁶ In litter-bearing species such as rats and mice, maternal weight gain increases significantly relative to the pre-pregnancy weight, and these species typically double their bodyweight between conception and parturition.^{7–10}

During pregnancy, maternal food intake increases to meet increased nutrient demands.^{11,12} Food intake increases throughout pregnancy by ~10%

Correspondence: Kathryn L. Gatford, kathy.gatford@adelaide.edu.au

The authors declare no conflict of interest.

DOI: 10.11124/JBIES-21-00025

Appendix 2 Active glucose transport varies by intestinal region and oestrous cycle stage in mice



Received: 23 November 2022 | Accepted: 28 February 2023

DOI: 10.1111/EP091040

RESEARCH ARTICLE

EP Experimental Physiology WILEY

Active glucose transport varies by small intestinal region and oestrous cycle stage in mice

T. Sebastian Overduin^{1,2,3} | Hannah R. Wardill^{1,4} | Richard L. Young^{3,5} |
Amanda J. Page^{1,3} | Kathryn L. Gatford^{1,2,3}

¹School of Biomedicine, University of Adelaide, Adelaide, South Australia, Australia

²Robinson Research Institute, University of Adelaide, Adelaide, South Australia, Australia

³Lifelong Health Theme, South Australian Health and Medical Research Institute, Adelaide, South Australia, Australia

⁴Precision Medicine Theme, South Australian Health and Medical Research Institute, Adelaide, South Australia, Australia

⁵Adelaide Medical School, University of Adelaide, Adelaide, South Australia, Australia

Correspondence

Kathryn L. Gatford, School of Biomedicine, The University of Adelaide, SA 5005, Australia.
Email: kathy.gatford@adelaide.edu.au

Funding information

University of Adelaide, Grant/Award Number: Divisional Scholarship; Hospital Research Foundation, Grant/Award Numbers: THRF ID: 2021.81-QA2531

Amanda J. Page and Kathryn L. Gatford are joint senior author.

Handling Editor: Simon Keely

Abstract

Food intake changes across the ovarian cycle in rodents and humans, with a nadir during the pre-ovulatory phase and a peak during the luteal phase. However, it is unknown whether the rate of intestinal glucose absorption also changes. We therefore mounted small intestinal sections from C57BL/6 female mice (8–9 weeks old) in Ussing chambers and measured active *ex vivo* glucose transport via the change in short-circuit current (ΔI_{sc}) induced by glucose. Tissue viability was confirmed by a positive ΔI_{sc} response to 100 μ M carbachol following each experiment. Active glucose transport, assessed after addition of 5, 10, 25 or 45 mM D-glucose to the mucosal chamber, was highest at 45 mM glucose in the distal jejunum compared to duodenum and ileum ($P < 0.01$). Incubation with the sodium–glucose cotransporter 1 (SGLT1) inhibitor phlorizin reduced active glucose transport in a dose-dependent manner in all regions ($P < 0.01$). Active glucose uptake induced by addition of 45 mM glucose to the mucosal chamber in the absence or presence of phlorizin was assessed in jejunum at each oestrous cycle stage ($n = 9–10$ mice per stage). Overall, active glucose uptake was lower at oestrus compared to pro-oestrus ($P = 0.025$). This study establishes an *ex vivo* method to measure region-specific glucose transport in the mouse small intestine. Our results provide the first direct evidence that SGLT1-mediated glucose transport in the jejunum changes across the ovarian cycle. The mechanisms underlying these adaptations in nutrient absorption remain to be elucidated.

KEYWORDS

oestrous cycle, glucose, mouse, SGLT1, small intestine

1 | INTRODUCTION

Digestion and absorption of nutrients occurs within the gastrointestinal tract, where complex organic molecules are progressively digested into smaller and simpler entities as they pass through the tract. Nutrient absorption begins in the duodenum and peaks in the jejunum (Volk & Lacy, 2017). The terminal ileum acts to brake intestinal

motility in the presence of high nutrient concentrations to maximise nutrient uptake in the small intestine (Karasov & Douglas, 2013; Kiela & Ghishan, 2016). The small intestine absorbs nutrients by passive and active transport, the latter via specific nutrient transporters (Kiela & Ghishan, 2016; Volk & Lacy, 2017). For example, active absorption of glucose is facilitated by sodium–glucose cotransporter 1 (SGLT1), a high affinity, low-capacity transmembrane protein located at the brush

This is an open access article under the terms of the [Creative Commons Attribution License](https://creativecommons.org/licenses/by/4.0/), which permits use, distribution and reproduction in any medium, provided the original work is properly cited.

© 2023 The Authors. *Experimental Physiology* published by John Wiley & Sons Ltd on behalf of The Physiological Society.

Experimental Physiology. 2023;108:865–873.

[wileyonlinelibrary.com/journal/eph](https://onlinelibrary.wiley.com/journal/eph) | 865

Appendix 3 Endocrine disruptor compounds – a cause of impaired immune tolerance driving inflammatory disorders of pregnancy?



Endocrine Disruptor Compounds— A Cause of Impaired Immune Tolerance Driving Inflammatory Disorders of Pregnancy?

John E. Schjenken^{1,2†}, Ella S. Green^{1†}, Tenis S. Overduin¹, Chui Yan Mah¹, Darryl L. Russell¹
and Sarah A. Robertson^{1*}

OPEN ACCESS

Edited by:

Carlo Alviggi,
University of Naples Federico II, Italy

Reviewed by:

Padma Murthi,
Monash University, Australia
Gendie Lash,
Guangzhou Medical University, China

*Correspondence:

Sarah A. Robertson
sarah.robertson@adelaide.edu.au

[†]These authors have contributed
equally to this work

Specialty section:

This article was submitted to
Reproduction,
a section of the journal
Frontiers in Endocrinology

Received: 17 September 2020

Accepted: 04 January 2021

Published: 12 April 2021

Citation:

Schjenken JE, Green ES, Overduin TS,
Mah CY, Russell DL and Robertson SA
(2021) Endocrine Disruptor
Compounds—A Cause of
Impaired Immune Tolerance
Driving Inflammatory
Disorders of Pregnancy?
Front. Endocrinol. 12:607539.
doi: 10.3389/fendo.2021.607539

¹ Adelaide Medical School and The Robinson Research Institute, University of Adelaide, Adelaide, SA, Australia, ² Priority Research Centre for Reproductive Sciences, Discipline of Biological Sciences, The Hunter Medical Research Institute, New Lambton Heights and the University of Newcastle, Newcastle, NSW, Australia

Endocrine disrupting compounds (EDCs) are prevalent and ubiquitous in our environment and have substantial potential to compromise human and animal health. Amongst the chronic health conditions associated with EDC exposure, dysregulation of reproductive function in both females and males is prominent. Human epidemiological studies demonstrate links between EDC exposure and infertility, as well as gestational disorders including miscarriage, fetal growth restriction, preeclampsia, and preterm birth. Animal experiments show EDCs administered during gestation, or to either parent prior to conception, can interfere with gamete quality, embryo implantation, and placental and fetal development, with consequences for offspring viability and health. It has been presumed that EDCs operate principally through disrupting hormone-regulated events in reproduction and fetal development, but EDC effects on maternal immune receptivity to pregnancy are also implicated. EDCs can modulate both the innate and adaptive arms of the immune system, to alter inflammatory responses, and interfere with generation of regulatory T (Treg) cells that are critical for pregnancy tolerance. Effects of EDCs on immune cells are complex and likely exerted by both steroid hormone-dependent and hormone-independent pathways. Thus, to better understand how EDCs impact reproduction and pregnancy, it is imperative to consider how immune-mediated mechanisms are affected by EDCs. This review will describe evidence that several EDCs modify elements of the immune response relevant to pregnancy, and will discuss the potential for EDCs to disrupt immune tolerance required for robust placentation and optimal fetal development.

Keywords: endocrine disrupting compounds, reproduction, reproductive immunology, pregnancy, fetal tolerance, developmental origins of health and disease